Analysis of Steady State Vibration for Piecewise Linear Systems Subjected to Periodic Excitation

Tatsuhito AIHARA

2013

Table of Contents

Chapter 1
Introduction

1.1 Problem Statement

The piping in high-temperature chemical plants includes flanges and other protrusions. Some play is intentionally left between supporting members and piping components in order to provide space for thermal expansion, and it is well known that collision vibration occurs between the components (Suzuki et al., 1984). Figure 1.1 shows the steam pipe of a boiler that was subjected to displacement excitation by the Southern Hyogo Prefecture earthquake (JSME, 1996). The diameter of this pipe is about 0.4 m, and the pipe is covered with heat insulating material. The pipe was not fixed to the floor panel in order to allow for thermal deformation. As a result, this pipe collided with the fence and was deformed by the earthquake. On the other hand, in nuclear power plants, guide tubes for reactivity control systems and pressure tube assemblies are housed in a heavy-water-filled cylindrical vessel with a clearance between them. During an earthquake, many guide tubes collide against the pressure tube assemblies, and collision vibration is generated. Therefore, collision vibrations have been analyzed for a long time, from a viewpoint of operational safety in nuclear power plants (Kuroda et al., 1980). As

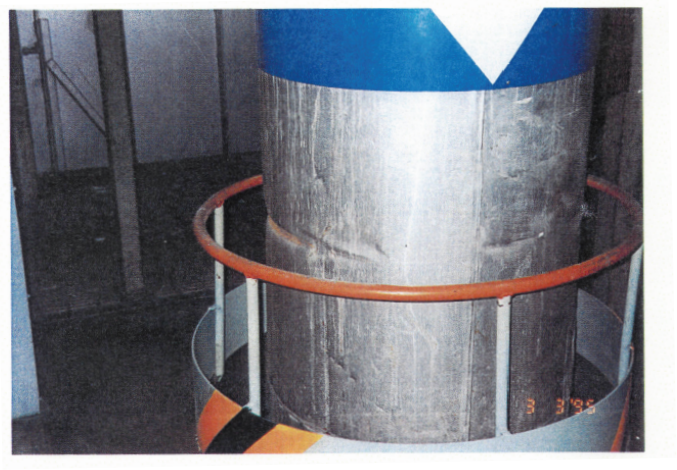

Figure 1.1 Steam pipe of a boiler subjected to displacement excitation by the Southern Hyogo Prefecture earthquake

described above, discussing the safety of the seismic design for collision vibration is critical for power plants.

Structures containing clearances are also regularly encountered in an automobile. For example, the automatic transmission that controls revolution and torque from an engine uses an input shaft supported by a needle roller bearing with a transmission case at the rear end point (Kusamoto et al., 2006). This needle roller bearing consists of several needles as well as a needle holder, with dozens of micrometer-sized clearances between a shaft and a bearing. These clearances decrease frictional losses as well as the possibility of setting. Clearances like these exist not only in a needle roller bearing but also in a ball-type roller bearing, as well as other kinds. Collision vibration occurs between an input shaft and a transmission case because of the fluctuating torque of the engine (Doyle et al., 1982). In recent years, weight reduction has been commonly carried out in the automotive industry in an effort to reduce adverse effects on the environment. A result of the weight reduction is an increase in vehicle interior noise and vibration; therefore, a thorough analysis of collision vibration is required. Collision vibration systems are usually modeled as a nonlinear spring whose characteristics are described by the broken line model in Figure 1.2; these systems are called piecewise linear systems. A piecewise linear system is highly nonlinear, and it is usually difficult to predict the system response using any general analytical solution. If the effects of design parameters such as clearance size and dynamic nonlinearity of the systems are known, the structures can be designed to be safer and more comfortable.

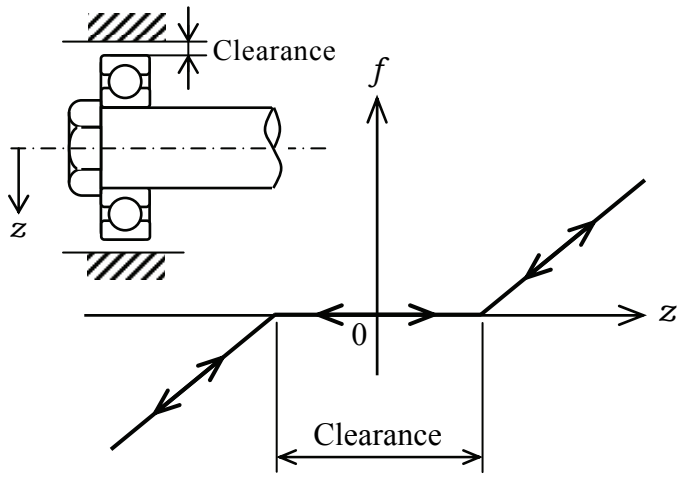

Figure 1.2 Characteristics of piecewise linear systems

1.2 Characteristics of Nonlinear Forced Vibration Systems

In a mass-spring system with a single-degree-of-freedom, if the relation between the restoring force $f(x)$ and the displacement x of a mass is proportional, the spring is called a linear spring and linear vibration occurs. In contrast, if the relationship is not proportional, the spring is called a nonlinear spring and nonlinear vibration occurs. The collision vibration in a piecewise linear system is classified as a nonlinear vibration system. Nonlinear vibration systems exhibit unique phenomena, which are reviewed here.

The resonance curve in a forced vibration system with a nonlinear restoring force tilts toward the right or left depending on whether the system is hardening or softening (Harris et al., 1996). A tilting resonance curve generates "jumping phenomena." As the frequency of exciting vibration initially increases, the amplitude of vibration also increases. However, when the resulting vibration reaches the peak point B shown in Figure 1.3, the amplitude abruptly jumps to the lower branch at point C. Conversely, when the frequency is reduced starting from point D, the amplitude jumps up to point F on the upper curve from point E on the lower curve. Moreover, there is only a single resonance frequency in a single-degree-of-freedom linear system, but this is not the case in a nonlinear system. In a nonlinear vibration system, if the backbone curve of harmonic resonance is expressed as $\omega=\omega_n(a)$, superharmonic vibration $\omega=\omega_n(a)/n$, subharmonic vibration $\omega=\omega_n(a)n$ (Nayfeh et al., 1979), and ultra-subharmonic vibration $\omega=\omega_n(a)(n/m)$ (Yamamoto et al., 1976) can occur. These vibration types are closely interlinked with the stability, and thus, predicting the resulting vibration during the design phase is extremely difficult.

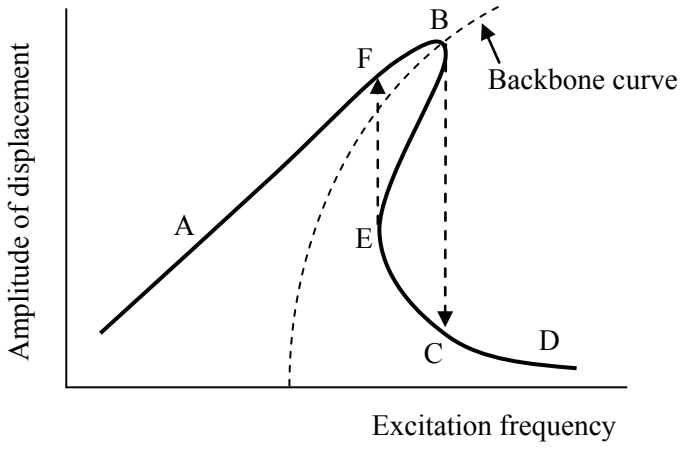

Figure 1.3 Resonance curve for nonlinear systems

1.3 Traditional Theoretical Analysis Methods for Nonlinear Forced Vibration (Harris et al., 1996, JSME, 2007)

Several theoretical analysis methods for nonlinear vibration have been proposed to date. However, in nonlinear vibration systems, a theoretical solution cannot be derived analytically in most cases. Therefore, when theoretically analyzing nonlinear vibration, the nonlinearity of the system is limited to or approximated by a weakly nonlinear model. In the following, the typical analytical methods for nonlinear vibration are introduced. Furthermore, a benchmark for theoretical analysis methods is shown.

(i) Duffing's Method (Iteration Method)

Consider the following nonlinear differential equation:

$$\ddot{x} + ax + bx^3 = F\cos\omega t \tag{1.1}$$

where F is the displacement, ω is the frequency of forced vibration, and t is time. Equation (1.1) is transformed as follows:

$$\ddot{x} + \omega^2 x = (\omega^2 - a)x - bx^3 + F\cos\omega t \tag{1.2}$$

Duffing's method assumes that b and F are small and ω^2 is nearly equal to a. Thus, the right side of Equation (1.2) is approximated by zero, giving the first approximate solution

$$x_1 = A_1\cos\omega t \tag{1.3}$$

Substituting Equation (1.3) into Equation (1.2) gives the following equation:

$$\ddot{x}_2 + \omega^2 x_2 = \{(\omega^2 - a)A_1 - \frac{3bA_1^3}{4} + F\}\cos\omega t - \frac{bA_1{}^3}{4}\cos 3\omega t \tag{1.4}$$

where x_2 is the second approximate solution. Since this problem has a periodic solution, the coefficient of $\cos\omega t$ in Equation (1.4) must be zero, resulting in

$$\omega^2 = a + \frac{3}{4} b A_1{}^2 - F / A_1 \tag{1.5}$$

Thus, the second approximate solution x_2 is obtained as follows:

$$x_2(t) = A_2 \cos \omega t + \frac{b A_1{}^3}{32\omega} \cos 3\omega t \tag{1.6}$$

Here, the coefficient A_2 is considered to be equal to A_1. The second approximate solution x_2 is then given by

$$x_2(t) = A_1 \cos \omega t + \frac{b A_1{}^3}{32\omega} \cos 3\omega t \tag{1.7}$$

(ii) Perturbation Method

The perturbation method is one of the most common methods for analyzing nonlinear vibrations. Consider the following nonlinear differential equation:

$$\ddot{x} + \omega_n^2 x = \varepsilon (F\omega_n^2 \cos \omega t - \omega_n^2 x^3) \tag{1.8}$$

where ε is a parameter with a small value, ω_n is the natural angular frequency, and ω is the angular frequency of forced vibration. A solution x to Equation (1.8) may be expanded in terms of ε:

$$x = x_0(t) + \varepsilon x_1(t) + \varepsilon^2 x_2(t) + \cdots \tag{1.9}$$

Substituting Equation (1.9) into Equation (1.8) and comparing the coefficients with respect to ε on both sides, we get the following equations:

$$\left.\begin{aligned} &\varepsilon^0 : \ddot{x}_0 + x_0 = 0 \\ &\varepsilon^2 : \ddot{x}_1 + x_1 = F\cos\omega t - \frac{\omega^2 - \omega_n^2}{\varepsilon\omega_n^2}\ddot{x}_0 - x_0^3 \\ &\qquad\vdots \end{aligned}\right\} \tag{1.10}$$

A solution to the first equation in Equation (1.10) is assumed as follows:

$$x_0 = a\cos(\omega t + \alpha) \tag{1.11}$$

Substituting Equation (1.11) into the second equation in Equation (1.10) gives the following differential equation:

$$\begin{aligned} \ddot{x}_1 + x_1 = &\left\{F\cos\alpha + (\frac{\omega^2 - \omega_n^2}{\varepsilon\omega_n^2} - \frac{3}{4}a^2)a\right\}\cos(\omega t + \alpha) + F\sin\alpha\sin(\omega t + \alpha) \\ &-\frac{1}{4}a^3\cos 3(\omega t + \alpha) \end{aligned} \tag{1.12}$$

Since this problem has a periodic solution, the coefficients of $\cos(\omega t+\alpha)$ and $\sin(\omega t+\alpha)$ must be zero:

$$F\cos\alpha + \left(\frac{\Omega^2 - \omega_n^2}{\varepsilon\omega_n^2} - \frac{3}{4}a^2\right)a = 0 \tag{1.13}$$

Finally, the displacement a of the resulting vibration is calculated using Equation (1.13).

(iii) Method of Averaging

Consider the following nonlinear differential equation

$$\ddot{x} + \omega_n^2 x = \varepsilon f(x, \dot{x}, \omega t) \tag{1.14}$$

where ε is a with a small value and ω_n is the natural angular frequency. A solution of Equation (1.14) in the case of $\varepsilon = 0$ is assumed as follows:

$$x = a\cos(\omega t + \alpha),\ \dot{x} = -a\omega\sin(\omega t + \alpha) \tag{1.15}$$

where a and α are constants actually, but in the method of averaging, a and α are considered to be functions of time t. Then, differentiating the first equation in Equation (1.15) with respect to t and using the second equation in Equation (1.15), we obtain the following equation:

$$\dot{a}\cos(\omega t + \alpha) - a\dot{\alpha}\sin(\omega t + \alpha) = 0 \tag{1.16}$$

Differentiating the second equation in (1.15) with respect to t gives the following equation:

$$\ddot{x} = -\dot{a}\omega\sin(\omega t + \alpha) - a\omega(\omega + \dot{\alpha})\cos(\omega t + \dot{\alpha}) \tag{1.17}$$

Substituting Equations (1.15) and (1.17) into Equation (1.14) and using Equation (1.16), we have

$$\left.\begin{aligned}\dot{a} &= -\frac{1}{\omega}\left\{\varepsilon f\left(a\cos(\omega t + \alpha), -a\omega\sin(\omega t + \alpha),\ \omega t\right) + \left(\omega^2 - \omega_n^2\right)a\cos(\omega t + \alpha)\right\}\sin(\omega t + \alpha)\\ \dot{\alpha} &= -\frac{1}{a\omega}\left\{\varepsilon f\left(a\cos(\omega t + \alpha), -a\omega\sin(\omega t + \alpha),\ \omega t\right) + \left(\omega^2 - \omega_n^2\right)a\cos(\omega t + \alpha)\right\}\cos(\omega t + \alpha)\end{aligned}\right\} \tag{1.18}$$

Here, $\dot{a}$ and $\dot{\alpha}$ are averaged over one period and substituted into Equation (1.15), yielding an approximate solution for the resulting vibration.

(iv) Method of Harmonic Balance

Consider the following nonlinear differential equation

$$\ddot{x} = f(x, \dot{x}, t) \tag{1.19}$$

where f is a periodic function of t and a smooth function of x and t. It is assumed that a unique solution of Equation (1.19) exists and that it can be differentiated. Then, the solution of Equation (1.19) can be expanded into a Fourier series as follows:

Table 1.1 Benchmark of theoretical analysis methods for nonlinear forced vibration

	Duffing's	Perturbation	Averaging	Harmonic balance
Strong nonlinearity	×	×	×	○
Large exciting force	×	△	○	○
Arbitrary precision	×	△	△	○
Transient response	×	○	○	×

$$x = a_0 + a_1 \cos\theta + a_2 \cos 2\theta + \cdots a_n \cos n\theta + b_1 \sin\theta + b_2 \sin 2\theta + \cdots b_n \sin n\theta \tag{1.20}$$

It is established that the approximate solution converges to the exact solution when $n \to \infty$ (Urabe, 1969). Substituting Equation (1.20) approximated to m^{th} order into Equation (1.19) and balancing coefficients on both sides with respect to the constants for both sine and cosine terms, we obtain nonlinear simultaneous equations as the approximate solution of displacement. Finally, the resulting vibration can be analyzed by numerically solving the nonlinear simultaneous equations. The method of harmonic balance is a suitable computational technique because of the high regularity algorithm. A periodic solution can be obtained with arbitrary precision for a strongly nonlinear system using this method.

Table 1.1 presents the benchmark of the theoretical analysis methods for nonlinear forced vibration systems. The method of harmonic balance can be applied to strong nonlinear vibration systems, and the precision of the solution can be arbitrarily raised through use of this method by increasing the number of terms in the Fourier expansion. This method is mathematically rigorous, and the numerical procedure is reliable. Therefore, in the case of analyzing the steady forced vibration for piecewise linear systems, the method of harmonic balance is considered to be the most appropriate method from among all the methods presented above.

1.4 Previous Research on Steady Forced Vibration for Piecewise Linear Systems

As mentioned in the previous section, the method of harmonic balance is considered to be the most appropriate method for the theoretical analysis of piecewise linear systems. In this section, previous research on piecewise linear systems conducted using theoretical analysis based on harmonic balance is first reviewed. Next, conventional numerical and experimental analyses are introduced.

Maezawa (1960) proposed a Fourier series method based on harmonic balance. This method expands the nonlinear restoring force into a Fourier series, and a nonlinear equation of motion is formally linearized. An exact solution can thus be obtained for piecewise linear systems. Kumano et al (1982) applied the Fourier series method to a mass-spring system with a single-degree-of-freedom excited by a general periodic force function. The main resonance and superharmonic resonances from the second order up to the fourth order were analyzed, and exact solutions were derived. Numerical calculations were also carried out based on the exact solutions and resonance curves were constructed. This analysis neglected damping of the system and the phase lag angle. The waveform of the restoring force was assumed to be symmetric with respect to the maximum point. However, in the superharmonic resonance region, the waveform of the restoring force may have an asymmetrical form. In addition, stability analysis for periodic solutions was not performed. Choi et al. (1988) analyzed the steady forced collision response of a single-degree-of-freedom system with an asymmetrical piecewise linear restoring force. The restoring force was derived using a fast Fourier transformation algorithm, and the method of harmonic balance was applied. The nonlinear simultaneous equations derived by harmonic balance were solved by using a Newton-Raphson iteration method, and periodic solutions were calculated. Furthermore, the periodic solutions were compared with the results of Maezawa's Fourier series method and showed good agreement. This method can obtain periodic solutions more efficiently than the conventional method of harmonic balance. However, in this analysis, forced vibration was limited to a single harmonic wave and the effects of some parameters on the resonance phenomena were not seen. Wong et al. (1991) developed an incremental harmonic balance method that used concepts of the incremental and Newton-Raphson iteration methods. Through application of this method to collision vibration in a mass-spring system with an asymmetrical piecewise linear restoring force, the harmonic,

subharmonic, and superharmonic resonances were analyzed. This analysis considered damping in the system, and stability analysis was also performed. However, only the effect of the amplitude of excitation on the resonance curve was shown. Studies introduced up to this point conducted theoretical analyses for lumped parameter systems with a piecewise linear restoring force. However, only a few theoretical studies have been conducted for distributed parameter systems with a piecewise linear restoring force. Aoki et al. (1995) analyzed the steady forced collision response of a cantilever having an asymmetrical piecewise linear restoring force by the Fourier series method. The main resonance was analyzed and an exact solution was derived. Numerical calculations were also performed based on the exact solution and resonance curves were constructed. The effect of the nonlinearity on the resonance was shown. However, the forced vibration was limited to a single harmonic wave and the collision position was limited to the tip of a beam. Furthermore, the validity of this theoretical method was not investigated and the stability criterion for a periodic solution was not established. As stated above, not all nonlinear resonance phenomena for piecewise linear systems were elucidated by previous studies that performed theoretical analyses.

In recent years, numerical analysis methods have been developed for studying collision vibrations in addition to improving computational speed. A numerical method can be applied to a strong nonlinear system and does not require complex expansions of the equation. If the equation of motion for an analysis system can be obtained, periodic solutions can be calculated numerically. Suzuki et al. (1989) analyzed the steady forced vibration of a piping system with a nonlinear supporting gap subjected to earthquake. The analysis model for the piping system was a mass-spring system with a single-degree-of-freedom and having a piecewise linear symmetric restoring force. The resulting vibration was calculated by a numerical integration method, and the effects of the support stiffness and gap size on the maximum response of the piping system subjected to random excitations were revealed. Furthermore, the results obtained in this analysis were used in realistic design applications. Yoshitake et al. (1995) carried out numerical calculations for collision vibration in a two-degrees-of-freedom system with a clearance that is excited by a forced acceleration. Periodic solutions for harmonic, superharmonic, and ultra-subharmonic resonances were calculated by direct numerical integration and the effectiveness of this method for multiple-degrees-of-freedom systems was shown. It was shown that the resonance curves formed islands when the excitation amplitude was large in the case of

a superharmonic resonance. Hyper-chaos was also observed for the first time in a mechanical system. Wang (1995) analyzed the dynamic response of a single-degree-of-freedom system with an asymmetrical piecewise linear restoring force for harmonic and subharmonic resonances by using a finite element method in the time domain based on Hamilton's weak principle. This method has the advantage that Floquet's stability theory can be easily applied without any special effort, because this method creates a transition matrix for the analysis of stability of small perturbations about the periodic solution as a byproduct. To verify the effectiveness of this method, the results were compared with direct numerical integration and harmonic balance methods, and fairly good agreement was observed. As mentioned above, numerical simulations are effective for nonlinear forced vibration. However, numerical approaches have some disadvantages in comparison to theoretical approaches. Numerical methods can be too expensive to completely clarify the characteristics of the piecewise linear system based on different variables. In the resonance region, multiple-valued responses exist, and trial-and-error processes are needed to obtain all possible periodic solutions by changing the initial conditions. Moreover, for convergence, the time step and initial conditions must be chosen carefully. Therefore, these are not necessarily the best methods.

Experimental analyses have also been performed for piecewise linear systems. Shintani et al. (1998) performed an experimental analysis with the aim of identifying the vibration characteristics in a piping system and also developed an analytical model. This experiment showed that the characteristics of the restoring force can be identified using a cubic equation. Numerical calculations were performed by including experimental parameters in the analysis model. The analytical results were compared with the experimental data and showed good agreement. Maruyama et al. (2006) performed experimental analysis for chaotic vibrations in a cantilever beam colliding with a bar. The collision vibration occurring near the fundamental resonance region when subjected to a lateral periodic acceleration was studied. The resulting chaotic vibration was revealed by using the maximum Lyapunov exponent, a Poincare map, and a waveform in the time domain. Furthermore, the waveform was measured in the time domain, analysis was performed for the principal component. As a result, two regions of chaotic responses were observed near the fundamental resonance frequency, and the contribution of superharmonic vibrations to the chaotic phenomenon was shown.

1.5 Objectives and Scope

As mentioned in the previous section, conventional studies based on theoretical analyses for steady forced vibrations having a piecewise linear restoring force almost always employed a mass-spring system with a single degree of freedom. In these studies, the forced vibration was limited to a single harmonic wave. However, components of structures such as power plant systems are not usually subjected to single harmonic excitation. Rather, they are subjected to a wide variety of simultaneous excitations. In previous studies, the effects of design parameters on the dynamic characteristics were not shown clearly enough. Therefore, conventional theoretical analyses are not sufficient from a practical viewpoint. In numerical analysis, direct numerical integration and finite element methods were applied to the piecewise linear system, but these are not necessarily the best methods for such calculations because of the high calculation times and costs involved. On the other hand, if an exact solution can be obtained theoretically, the influence of various factors on the resonance will be clear and the solution itself will be completely transparent.

This thesis is aimed at clarifying resonance phenomena theoretically for lumped and distributed parameter systems having a piecewise linear restoring force subjected to periodic excitation. A Fourier series method is applied to obtain a theoretical solution for the resulting vibration with no limitations on the exciting forced vibration. The steady state periodic solutions are calculated based on the results of theoretical analysis, and resonance curves are calculated using several design parameters. The effects of each of these parameters on the resonance are numerically examined. Finally, experiments are performed with a real model that corresponds to the analytical model in order to show the validity of the results of theoretical analysis. The thesis is organized as follows:

In chapter 1, the objectives and background for the thesis are described and its composition is shown.

In chapter 2, as an example of lumped parameter systems, the response vibration in a single-degree-of-freedom mass-spring-damper system with an asymmetrical piecewise linear restoring force and excited by a periodic displacement using arbitrary functions is analyzed. In order to clarify harmonic, superharmonic, and subharmonic resonances for the piecewise linear system, the resulting vibrations are analyzed by the Fourier series method. In this analysis, the waveform of the restoring force is not limited to being symmetric around the maximum point

through the introduction of two parameters for every instance of collision, and theoretical solutions are derived. Analysis of the stability criterion is also performed for periodic solutions using a variational equation in order to investigate the consequences of a minute perturbation on the steady state vibration predicted by a periodic solution for the original equation of motion. The steady state periodic solutions are calculated based on the results of a theoretical analysis, and the resonance curves and stability charts are constructed. The calculation results show the effects of the damping ratio, the stiffness of clamped spring, clearance, and the amplitude of forced vibration on the resonance curves. An experiment and a numerical simulation using the fourth-order Runge-Kutta method are also performed to verify the results of the theoretical analysis.

In chapter 3, as an example of distributed parameter systems, the response vibration in an Euler-Bernoulli beam with a symmetrical piecewise linear restoring force excited by periodic displacement with arbitrary functions is analyzed. In this model, the position on the beam that is subjected to the symmetrical piecewise linear restring force can be arbitrarily chosen. In other words, the case of two springs clamped symmetrically at an arbitrary distance above and below the beam and at an arbitrary position along the beam is analyzed. In order to clarify the main resonance of the system, the resulting vibration is analyzed by using the Fourier series method, and a theoretical solution is derived. Calculations are performed based on the theoretical analysis and resonance curves are constructed. The calculation results show the effects of the stiffness of the clamped spring, collision position, clearance, and the amplitude of forced vibration on the resonance curves. An experiment is also carried out to verify the results of the theoretical analysis.

In chapter 4, a stability analysis method is proposed for the periodic steady state solution in an Euler-Bernoulli beam with a symmetrical piecewise linear restoring force excited by a periodic displacement using arbitrary functions. The proposed method employs a variational equation to investigate the consequences of a minute perturbation on the steady state vibration in modal coordinates. These perturbations are added to a periodic solution for the modal equation of motion. Conditional equations for the stability criterion for a periodic steady state solution are shown. Calculations are performed on the basis of the theoretical results, and stability charts are constructed. These charts are then used to examine resonance curves given by the theoretical analysis results, and the stable periodic solutions are distinguished from the

unstable ones. Experiments are also carried out to verify the theoretical analysis results.

In Chapter 5, the conclusions drawn from this study are summarized and future research directions are discussed.

Chapter 2
Analysis of Response Vibration and Stability Criterion in Lumped Parameter Systems

This chapter deals with response vibration in a single-degree-of-freedom mass-spring-damper system as an example of lumped parameter systems with piecewise linear restoring force excited by periodic displacement with arbitrary functions. When the system is subjected to an exciting vibration by displacement, the mass is subjected to piecewise linear restoring force. In order to clarify harmonic, superharmonic and subharmonic resonances for the piecewise linear system, the resulting vibrations are analyzed by the Fourier series method. Figure 2.1 shows the

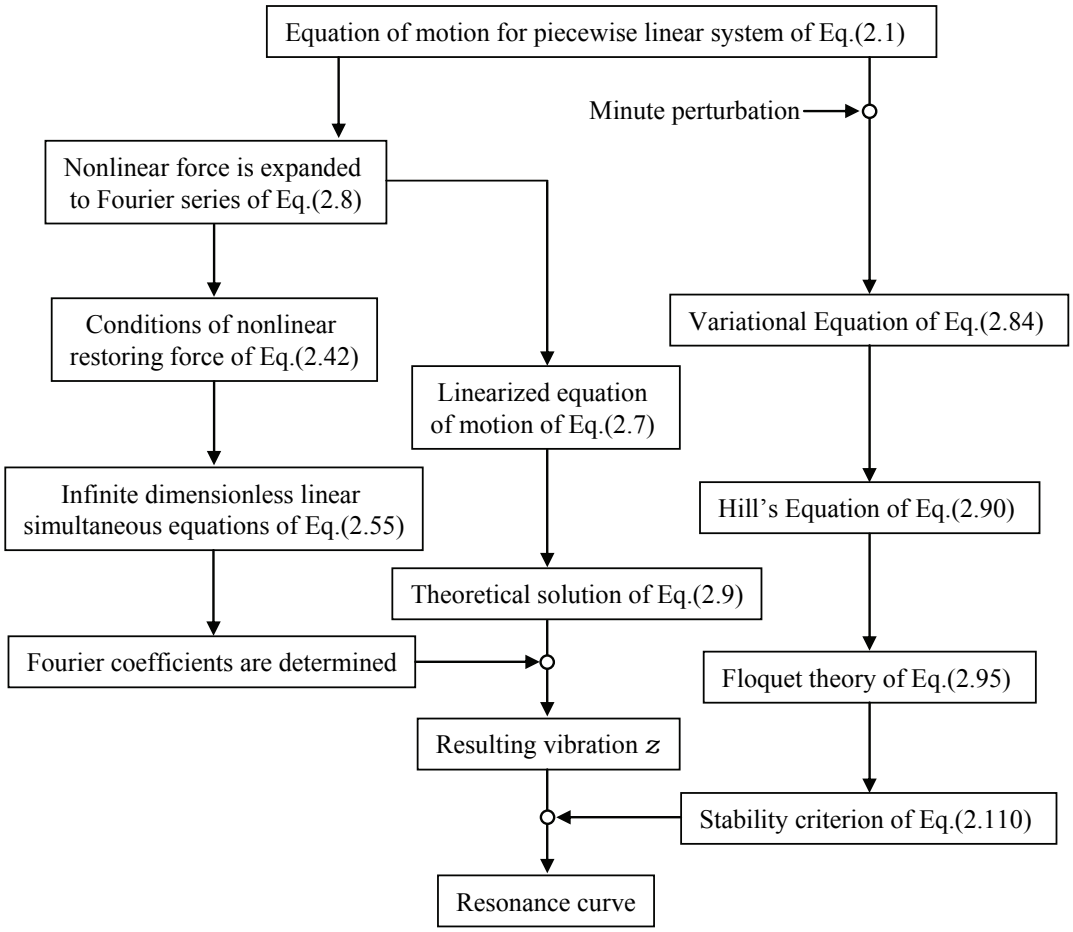

Figure 2.1 Flowchart of theoretical analysis method

fundamental flow of the theoretical analysis method in this chapter. A nonlinear restoring force is expanded to a Fourier series, and an equation of motion is linearized formally. Therefore, a theoretical solution can be obtained. A stability analysis is also carried out for periodic solutions using a variational equation to investigate consequences of a minute perturbation to a steady state vibration predicted by a periodic solution for an original equation of motion. The steady state periodic solutions are calculated based on the theoretical analysis results, and resonance curves and stability charts are constructed. The stability for periodic solutions on the steady state vibration is discussed using stability charts. By using them, stable branches for the resonance curves are distinguished from unstable ones. The theoretical calculation results show the effects of the damping ratio, the stiffness of clamped spring, clearance and the amplitude of forced vibration on the resonance curves. An experiment and a numerical simulation by the fourth order Runge-Kutta method are also carried out to verify the theoretical analysis results. Comparing the theoretical calculation results with the experimental and numerical simulation results, it is shown that they show a fairly good agreement.

2.1 Theoretical Analysis

2.1.1 Analysis of Response Vibration for Harmonic Resonance

Here, the resulting vibration for main resonance is analyzed. The analytical model, shown in Figure 2.2, is a single-degree-of-freedom mass-spring-damper system with piecewise linear restoring force excited by periodic displacement with arbitrary functions.

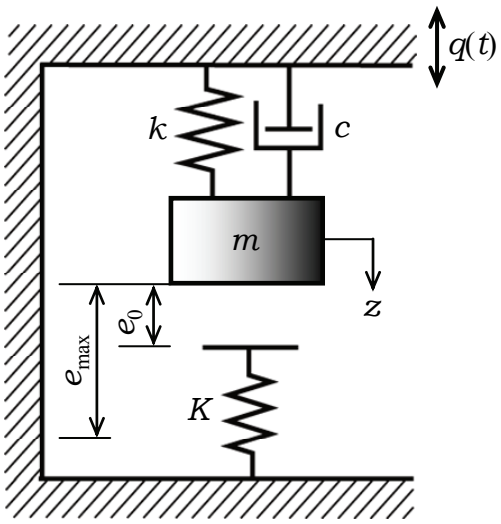

Figure 2.2 Analytical model of steady forced vibration in mass-spring-damper system

(1) Characteristics of System and Equation of Motion

The system to be investigated is a mass-spring-damper system with a single-degree-of-freedom (DOF), consisting of a mass m and a restoring force described by the asymmetrical function $f(z)$ as shown in Figure 2.3. It is excited by the displacement vibration of arbitrary periodic function $q(t)$. If the relative displacement of the mass is z, time is t and the damping coefficient is c, the equation of motion of the system takes the following form:

$$m\frac{d^2z}{dt^2}+c\frac{dz}{dt}+f(z)=-m\frac{d^2q(t)}{dt^2} \tag{2.1}$$

As shown in Figure 2.3, the restoring force of the spring is asymmetrical piecewise linear and expressed as follows:

$$\left.\begin{array}{lll} f(z)=kz & z\le e_0 & \text{Region I} \\ f(z)=kz+K(z-e_0) & e_0\le z\le e_{\max} & \text{Region II} \end{array}\right\} \tag{2.2}$$

where e_0 is the clearance between the mass and the collided spring at initial state and $e_{\max}$ is the maximum resulting displacement. The displacement of the excitation $q(t)$ acting on the system

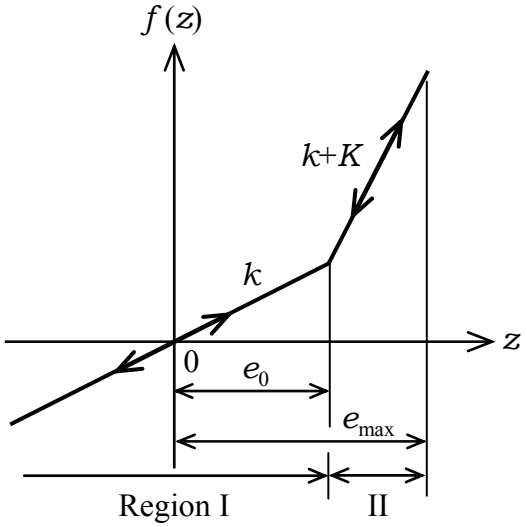

Figure 2.3 Characteristics of restoring force

is assumed to be an arbitrary periodic function and can therefore be expanded into a following Fourier series:

$$q(t) = \frac{f_0}{2} + \sum_{n=1}^{\infty} (f_n \cos n\omega t + g_n \sin n\omega t) \tag{2.3}$$

where ω is the angular frequency and f_0, f_n and g_n are Fourier coefficients.

(2) Fourier Series Method

(i) Fourier Series Solution

When the restoring force is the piecewise linear, the vibration becomes periodic steady state after the transient period and these steady state vibrations can be classified into several types. The vibration mode is defined by the number of times the resulting displacement enters region I from region II: if this transition occurs once, it is called a Type I vibration; if it occurs twice, it is called a Type II vibration. Here, this analysis limits considerations to resulting waves in which the mass strikes and compresses the lower spring (spring constants K) in the nonlinear region only one time each during the main resonance region. Figure 2.4 shows the assumed excitation, the resulting displacement and the solution for the harmonic resonance vibration of the restoring force of the spring. Figure 2.4 (a) shows the periodic displacement excitation acting on the system (solid line: example of rectangular wave excitation; dashed line: fundamental wave). Figure 2.4 (b) shows the resulting displacement of the mass and Figure 2.4 (c) shows the restoring force exerted on the mass during elastic collision with the spring. One cycle of the resulting wave of the relative displacement z is divided into two zones (I, II), as shown in Figure 2.4 (c). These zones correspond to zones I, and II in the restoring force characteristic graph in Figure 2.3. The phase angle θ is introduced here and shown in Figure 2.4 (b) in terms of the portion of the cycle θ_0 and θ_1 (dwell phase angle) spent in contact with the spring. The origin for measuring the phase angle θ is defined from the peak of the resulting waveform. The independent variable of time t is transformed to phase angle θ which is defined as:

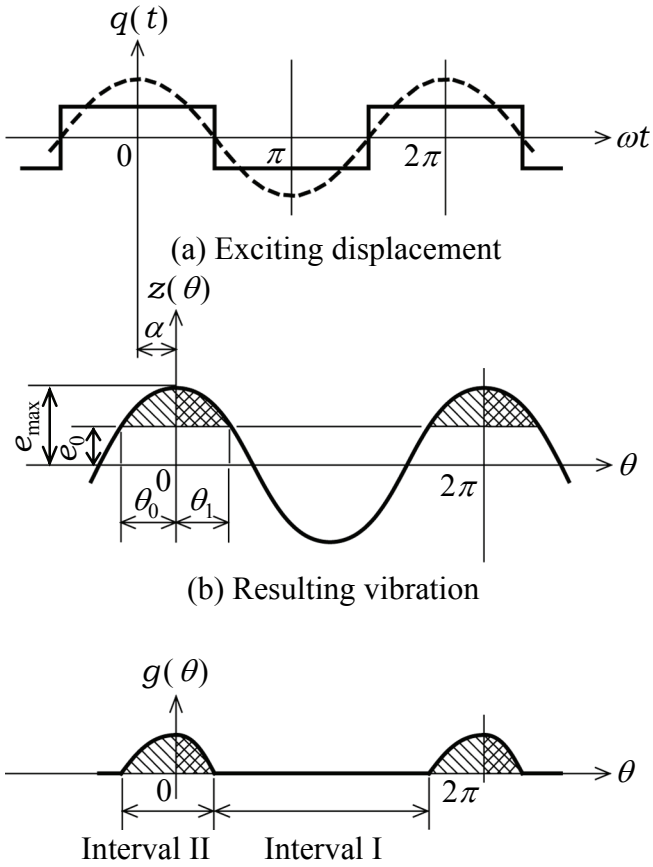

Figure 2.4 Harmonic resonance vibration Type I

$$\theta = \omega t - \alpha \tag{2.4}$$

where α is the phase lag angle, which is currently undefined but will be determined later. Substituting Equation (2.4) into the displacement excitation of arbitrary periodic function $q(t)$ of Equation (2.3) gives the following equation:

$$q(\theta) = \frac{f_0}{2} + \sum_{n=1}^{\infty} \{ f_n \cos n(\theta + \alpha) + g_n \sin n(\theta + \alpha) \} \tag{2.5}$$

Expressing the interval of each region by the phase angle, the interval I corresponds to (θ_1, $2\pi - \theta_0$) and the interval II corresponds to ($-\theta_0, \theta_1$). If the region I in Figiure.2.3 is the standard,

then from the view point of the entire system, the region II is the nonlinear region. Thus, the linear part of the restoring force is kz and the nonlinear part is $K(z-e_0)$. The nonlinear part of the restoring force is expressed by $g(\theta)$, which is expressed as follows:

$$\left.\begin{array}{lll} g(\theta)=0 & ;\ \theta_1 \le \theta \le 2\pi-\theta_0 & :\ \text{Region I} \\ g(\theta)=K(z-e_0) & ;\ \theta_0 \le \theta \le \theta_1 & :\ \text{Region II} \end{array}\right\} \tag{2.6}$$

Regarding this nonlinear part of the restoring force $g(\theta)$ as a virtual external force and subtracting this force from the actual one, the equation of motion of Equation (2.1) is linearized formally as follows:

$$m\omega^2\frac{d^2z}{d\theta^2}+c\omega\frac{dz}{d\theta}+kz=-m\omega^2\frac{d^2q(\theta)}{d\theta^2}-g(\theta) \tag{2.7}$$

When the system reaches steady state, this nonlinear part of the restoring force $g(\theta)$ becomes a periodic function with the period 2π with respect to θ and this periodic function $g(\theta)$ can be expanded into a Fourier series:

$$g(\theta)=\frac{s_0}{2}+\sum_{n=1}^{\infty}(s_n\cos n\theta+t_n\sin n\theta) \tag{2.8}$$

where s_0, s_n and t_n (n=1,2,3$\cdots$) are Fourier coefficients to be determined afterwards.

(ii) Formal Solution of *z*

A formal solution of the equation of motion of Equation (2.7) is also expanded into a Fourier series as follows:

$$z(\theta)=\frac{a_0}{2}+\sum_{n=1}^{\infty}(a_n\cos n\theta+b_n\sin n\theta) \tag{2.9}$$

where a_0, a_n and b_n (n=1,2,3$\cdots$) are Fourier coefficients to be determined afterwards. The first

term on the right side of Equation (2.7) is transformed to

$$-m\omega^2 \frac{d^2 q(\theta)}{d\theta^2} = \sum_{n=1}^{\infty} \left(f_n' \cos n\theta + g_n' \sin n\theta \right) \tag{2.10}$$

where

$$\left.\begin{aligned} f_n' &= kn^2 \Omega^2 \left(f_n \cos n\alpha + g_n \sin n\alpha \right) \\ g_n' &= kn^2 \Omega^2 \left(g_n \cos n\alpha - f_n \sin n\alpha \right) \end{aligned}\right\} \tag{2.11}$$

where Ω is the frequency ratio and expressed as follows:

$$\Omega = \frac{\omega}{\omega_n} = \omega \sqrt{\frac{m}{k}} \tag{2.12}$$

Differentiating the resulting vibration $z(\theta)$ of Equation (2.9) gives the following equations:

$$\left.\begin{aligned} \dot{z}(\theta) &= \sum_{n=1}^{\infty} n \left(-a_n \sin n\theta + b_n \cos n\theta \right) \\ \ddot{z}(\theta) &= -\sum_{n=1}^{\infty} n^2 \left(a_n \cos n\theta + b_n \sin n\theta \right) \end{aligned}\right\} \tag{2.13}$$

Substituting Equation (2.13) into Equation (2.7) gives the following equation:

$$\begin{aligned} &-m\omega^2 \sum_{n=1}^{\infty} n^2 \left(a_n \cos n\theta + b_n \sin n\theta \right) + c\omega \sum_{n=1}^{\infty} n \left(-a_n \sin n\theta + b_n \cos n\theta \right) + \\ &k \left\{ \frac{a_0}{2} + \sum_{n=1}^{\infty} \left(a_n \cos n\theta + b_n \sin n\theta \right) \right\} \\ &= -m\omega^2 \frac{d^2 q(\theta)}{d\theta^2} - g(\theta) \end{aligned} \tag{2.14}$$

The left side of Equation (2.14) is transformed to,

$$\begin{aligned}&\frac{ka_0}{2}+\sum_{n=1}^{\infty}\left[\left\{\left(k-n^2m\omega^2\right)\cdot a_n+nc\omega\cdot b_n\right\}\cdot\cos n\theta+\left\{-nc\omega\cdot a_n+\left(k-n^2m\omega^2\right)\cdot b_n\right\}\cdot\sin n\theta\right]\\&=\frac{ka_0}{2}+\sum_{n=1}^{\infty}\frac{k}{M_n}\left\{\left(\cos n\varphi_n\cdot a_n+\sin n\varphi_n\cdot b_n\right)\cos n\theta+\left(-\sin n\varphi_n\cdot a_n+\cos n\varphi_n\cdot b_n\right)\sin n\theta\right\}\end{aligned} \tag{2.15}$$

where

$$\left.\begin{aligned}&\varphi_n=\tan^{-1}\frac{2n\zeta\Omega}{1-n^2\Omega^2},\\&M_n=\frac{1}{\sqrt{\left(1-n^2\Omega^2\right)^2+(2n\zeta\Omega)^2}},\\&\zeta=\frac{c}{2\sqrt{mk}}\end{aligned}\right\} \tag{2.16}$$

Substituting Equations (2.8), (2.10) and (2.15) into Equation (2.14) gives the following equation:

$$\begin{aligned}&\frac{ka_0}{2}+\sum_{n=1}^{\infty}\frac{k}{M_n}\left\{\left(\cos\varphi_n\cdot a_n+\sin\varphi_n\cdot b_n\right)\cos n\theta+\left(-\sin\varphi_n\cdot a_n+\cos\varphi_n\cdot b_n\right)\sin n\theta\right\}\\&=-\frac{s_0}{2}+\sum_{n=1}^{\infty}\left\{\left(f_n'-s_n\right)\cos n\theta+\left(g_n'-t_n\right)\sin n\theta\right\}\end{aligned} \tag{2.17}$$

Comparing coefficients with respect to $\cos n\theta$ and $\sin n\theta$ of both sides of Equation (2.17) gives the following equations:

$$\left.\begin{aligned}&\frac{s_0}{2}=-\frac{ka_0}{2}\\&s_n=f_n'-k\left\{\left(1-n^2\Omega^2\right)\cdot a_n+2n\zeta\Omega\cdot b_n\right\}\\&t_n=g_n'+k\left\{2n\zeta\Omega\cdot a_n-\left(1-n^2\Omega^2\right)\cdot b_n\right\}\end{aligned}\right\} \tag{2.18}$$

or

$$\left.\begin{aligned} \frac{s_0}{2} &= -\frac{ka_0}{2} \\ s_n &= f' - \frac{k}{M_n}\left(\cos\varphi_n \cdot a_n + \sin\varphi_n \cdot b_n\right) \\ t_n &= g'_n - \frac{k}{M_n}\left(-\sin\varphi_n \cdot a_n + \cos\varphi_n \cdot b_n\right) \end{aligned}\right\} \tag{2.19}$$

(iii)Switching-Over Conditions

The dwell phase angle θ_0 and θ_1 are defined as the portion of the resulting vibration spent in nonlinear zone II. The following expressions show the conditions when the mass enters and leaves the nonlinear region and these conditions are called switching-over conditions:

$$\left.\begin{aligned} \theta &= -\theta_0 \quad ; \quad z(-\theta_0) = e_0 \\ \theta &= \theta_1 \quad ; \quad z(\theta_1) = e_0 \\ \theta &= 0 \quad ; \quad z(0) = e_{\max} \end{aligned}\right\} \tag{2.20}$$

The switching-over conditions concerned to the nonlinear part of the restoring force $g(\theta)$ is shown as follows:

$$\left.\begin{aligned} \theta &= -\theta_0 \quad ; \quad g(-\theta_0) = 0 \\ \theta &= \theta_1 \quad ; \quad g(\theta_1) = 0 \\ \theta &= 0 \quad ; \quad g(0) = K(e_{\max} - e_0) \end{aligned}\right\} \tag{2.21}$$

Afterwards, analysis formulae satisfying the switching-over conditions are derived.

(a) Switching-Over Condition: In the case of $\theta = -\theta_0$

When $\theta = -\theta_0$, the resulting displacement $z(-\theta_0)$ is equal to e_0:

$$\begin{aligned} z(-\theta_0) &= \frac{a_0}{2} + \sum_{n=1}^{\infty}\left(a_n \cos n\theta_0 - b_n \sin n\theta_0\right) = e_0 \\ \therefore \frac{a_0}{2} &= e_0 - \sum_{n=1}^{\infty}\left(a_n \cos n\theta_0 - b_n \sin n\theta_0\right) \end{aligned} \tag{2.22}$$

Thus the resulting vibration containing the dwell phase angle θ_0 is

$$z(\theta) = e_0 + \sum_{n=1}^{\infty} \{ (\cos n\theta - \cos n\theta_0) \cdot a_n + (\sin n\theta + \sin n\theta_0) \cdot b_n \} \tag{2.23}$$

(b) Switching-Over Condition: In the case of $\theta = \theta_1$

When $\theta = \theta_1$, the resulting displacement $z(\theta_1)$ is equal to e_0:

$$\begin{aligned} z(\theta_1) &= \frac{a_0}{2} + \sum_{n=1}^{\infty} (a_n \cos n\theta_1 + b_n \sin n\theta_1) = e_0 \\ \therefore \frac{a_0}{2} &= e_0 - \sum_{n=1}^{\infty} (a_n \cos n\theta_1 + b_n \sin n\theta_1) \end{aligned} \tag{2.24}$$

Thus the resulting vibration containing the dwell phase angle θ_1 is

$$z(\theta) = e_0 + \sum_{n=1}^{\infty} \{ (\cos n\theta - \cos n\theta_1) \cdot a_n + (\sin n\theta - \sin n\theta_1) \cdot b_n \} \tag{2.25}$$

(c) Switching-Over Condition: In the case of $\theta = 0$

When $\theta = 0$, the resulting displacement $z(0)$ is equal to $e_{\max}$:

$$\begin{aligned} z(0) &= \frac{a_0}{2} + \sum_{n=1}^{\infty} a_n = e_{\max} \\ \therefore \frac{a_0}{2} &= e_{\max} - \sum_{n=1}^{\infty} a_n \end{aligned} \tag{2.26}$$

Thus the resulting vibration containing the maximum resulting displacement $e_{\max}$ is

$$z(\theta) = e_{\max} + \sum_{n=1}^{\infty} \{ (\cos n\theta - 1) \cdot a_n + \sin n\theta \cdot b_n \} \tag{2.27}$$

The resulting displacement $z(\theta)$ is expressed as follows corresponding to each of the switching-over conditions:

$$\left.\begin{aligned} z(\theta) &= e_0 + \sum_{n=1}^{\infty}\{(\cos n\theta - \cos n\theta_0)\cdot a_n + (\sin n\theta + \sin n\theta_0)\cdot b_n\} \quad (\text{S.O.C} : \theta = -\theta_0) \\ z(\theta) &= e_0 + \sum_{n=1}^{\infty}\{(\cos n\theta - \cos n\theta_1)\cdot a_n + (\sin n\theta - \sin n\theta_1)\cdot b_n\} \quad (\text{S.O.C} : \theta = \theta_1) \\ z(\theta) &= e_{\max} + \sum_{n=1}^{\infty}\{(\cos n\theta - 1)\cdot a_n + \sin n\theta \cdot b_n\} \quad (\text{S.O.C} : \theta = 0) \end{aligned}\right\} \tag{2.28}$$

(iv) Derivation of Non-dimensional Equations

(a) Non-Dimensional Resulting Vibration and Nonlinear Part of Restoring Force

Dividing Equation (2.9) by e_0 gives the non-dimensional resulting vibration as follows:

$$\frac{z(\theta)}{e_0} = \frac{z}{e_0} = \frac{1}{2}\cdot\frac{a_0}{e_0} + \sum_{n=1}^{\infty}\left(\cos n\theta \cdot \frac{a_n}{e_0} + \sin n\theta \cdot \frac{b_n}{e_0}\right) \tag{2.29}$$

Dividing Equation (2.8) by ke_0 gives the non-dimensional nonlinear part of the restoring force as follows:

$$\frac{g(\theta)}{ke_0} = \frac{1}{2}\cdot\frac{s_0}{ke_0} + \sum_{n=1}^{\infty}\left(\cos n\theta \cdot \frac{s_n}{ke_0} + \sin n\theta \cdot \frac{t_n}{ke_0}\right) \tag{2.30}$$

The coefficients of Equation (2.11) are transformed into the non-dimensional ones by ke_0:

$$\left.\begin{aligned} \frac{f_n'}{ke_0} &= n^2\Omega^2\left(\cos n\alpha \cdot \frac{f_n}{e_0} + \sin n\alpha \cdot \frac{g_n}{e_0}\right) \\ \frac{g_n'}{ke_0} &= n^2\Omega^2\left(\cos n\alpha \cdot \frac{g_n}{e_0} - \sin n\alpha \cdot \frac{f_n}{e_0}\right) \end{aligned}\right\} \tag{2.31}$$

The non-dimensional coefficients are defined as follows:

$$\left.\begin{aligned} u'_n &= \frac{f'_n}{ke_0}\ ,\quad v'_n = \frac{g'_n}{ke_0} \\ s'_0 &= \frac{s_0}{ke_0}\ ,\quad s'_n = \frac{s_n}{ke_0}\ ,\quad t'_n = \frac{t_n}{ke_0} \\ x_0 &= \frac{a_0}{e_0}\ ,\quad x_n = \frac{a_n}{e_0}\ ,\quad y_n = \frac{b_n}{e_0} \end{aligned}\right\} \tag{2.32}$$

For simplicity, substituting the coefficients of Equation (2.32) into Equations (2.29) and (2.30), the non-dimensional resulting vibration and the nonlinear part of the restoring force are expressed as follows:

$$\frac{z}{e_0} = \frac{x_0}{2} + \sum_{n=1}^{\infty}\left(\cos n\theta \cdot x_n + \sin n\theta \cdot y_n\right) \tag{2.33}$$

$$\frac{g(\theta)}{ke_0} = \frac{s'_0}{2} + \sum_{n=1}^{\infty}\left(\cos n\theta \cdot s'_n + \sin n\theta \cdot t'_n\right) \tag{2.34}$$

Similarly, the resulting vibration $z(\theta)$ of Equation (2.28) obtained by using the switching-over conditions are also transformed into the non-dimensional equations:

$$\left.\begin{aligned} \frac{z}{e_0} &= 1 + \sum_{n=1}^{\infty}\left\{\left(\cos n\theta - \cos n\theta_0\right)\cdot x_n + \left(\sin n\theta + \sin n\theta_0\right)\cdot y_n\right\} \quad (\text{S.O.C} : \theta = -\theta_0) \\ \frac{z}{e_0} &= 1 + \sum_{n=1}^{\infty}\left\{\left(\cos n\theta - \cos n\theta_1\right)\cdot x_n + \left(\sin n\theta - \sin n\theta_1\right)\cdot y_n\right\} \quad (\text{S.O.C} : \theta = \theta_1) \\ \frac{z}{e_0} &= \frac{e_{\max}}{e_0} + \sum_{n=1}^{\infty}\left\{\left(\cos n\theta - 1\right)\cdot x_n + \sin n\theta \cdot y_n\right\} \quad (\text{S.O.C} : \theta = 0) \end{aligned}\right\} \tag{2.35}$$

Using Equations (2.19) and (2.32), the Fourier coefficients s'_0, s'_n and t'_n of the nonlinear restoring force can be expressed as follows:

$$\left.\begin{aligned}
\frac{s_0'}{2} &= -\frac{x_0}{2} \\
s_n' &= u_n' - \frac{1}{M_n}\left(\cos\varphi_n \cdot x_n + \sin\varphi_n \cdot y_n\right) \\
&= u_n' - \left\{\left(1 - n^2\Omega^2\right)\cdot x_n + 2n\zeta\Omega \cdot y_n\right\} \\
t_n' &= v_n' - \frac{1}{M_n}\left(-\sin\varphi_n \cdot x_n + \cos\varphi_n \cdot y_n\right) \\
&= v_n' - \left\{-2n\zeta\Omega \cdot x_n + \left(1 - n^2\Omega^2\right)\cdot y_n\right\}
\end{aligned}\right\} \tag{2.36}$$

(b) Non-dimensional Maximum Resulting Displacement

Dividing Equation (2.26) by e_0 gives the following equation:

$$\frac{x_0}{2} = \frac{e_{\max}}{e_0} - \sum_{n=1}^{\infty} x_n \tag{2.37}$$

When θ=0, the nonlinear part of the restoring force of Equation (2.34) is expressed as follows:

$$\frac{g(0)}{ke_0} = \frac{s_0'}{2} + \sum_{n=1}^{\infty} s_n' = \frac{K\left(e_{\max} - e_0\right)}{ke_0} \tag{2.38}$$

Substituting Equations (2.36) and (2.37) into Equation (2.38) gives the following equation:

$$\begin{aligned}
\frac{g(0)}{ke_0} &= \frac{s_0'}{2} + \sum_{n=1}^{\infty} s_n' \\
&= -\frac{x_0}{2} + \sum_{n=1}^{\infty}\left\{ u_n' - \frac{1}{M_n}\left(\cos\varphi_n \cdot x_n + \sin\varphi_n \cdot y_n\right)\right\} \\
&= -\frac{e_{\max}}{e_0} + \sum_{n=1}^{\infty} x_n + \sum_{n=1}^{\infty}\left\{ u_n' - \frac{1}{M_n}\left(\cos\varphi_n \cdot x_n + \sin\varphi_n \cdot y_n\right)\right\} \\
&= \frac{K\left(e_{\max} - e_0\right)}{ke_0}
\end{aligned} \tag{2.39}$$

And thus, the non-dimensional maximum resulting displacement is

$$\begin{aligned}\frac{e_{\max}}{e_0} &= \frac{K}{k+K}+\frac{k}{k+K}\sum_{n=1}^{\infty}\left\{ u_n' + \left(1-\frac{\cos\varphi_n}{M_n}\right)\cdot x_n - \frac{\sin\varphi_n}{M_n}\cdot y_n \right\} \\ &= \frac{K}{k+K}+\frac{k}{k+K}\sum_{n=1}^{\infty}\left(u_n' + n^2\Omega^2\cdot x_n - 2n\zeta\Omega\cdot y_n \right)\end{aligned} \tag{2.40}$$

Substituting Equation (2.40) into Equation (2.37) gives the Fourier coefficient x_0 as follows:

$$x_0 = \frac{2K}{k+K}+\frac{2k}{k+K}\sum_{n=1}^{\infty}\left[u_n' - \left\{\frac{K}{k}+\left(1-n^2\Omega^2\right)\right\}\cdot x_n - 2n\zeta\Omega\cdot y_n \right] \tag{2.41}$$

(3) Determination of Non-Dimensional Fourier Coefficients x_n and y_n

The resulting vibration of Equation (2.33) and the maximum resulting displacement of Equation (2.40) can all be determined by using the non-dimensional Fourier coefficients x_n and y_n (n=1,2,3,$\cdots$). Therefore, once x_n and y_n are known, the resulting vibration and the maximum resulting displacement are determined. The non-dimensional Fourier coefficients must be set to satisfy the piecewise linear characteristics of the nonlinear part of the restoring force. Here, the infinite dimensionless linear simultaneous equations for determining non-dimensional Fourier coefficients are derived by using orthogonality.

(i) Derivation of Infinite Dimensionless Linear Simultaneous Equations

The nonlinear part of the restoring force $g(\theta)$ is

$$\begin{aligned}\frac{g(\theta)}{ke_0} &= \frac{s_0'}{2}+\sum_{n=1}^{\infty}\left(\cos n\theta\cdot s_n' + \sin n\theta\cdot t_n'\right) \\ &= \begin{cases} 0 & : \theta_1 \le \theta \le 2\pi-\theta_0 \quad \text{Interval I} \\ \dfrac{K(z-e_0)}{ke_0} & : -\theta_0 \le \theta \le \theta_1 \quad \text{Interval II} \end{cases}\end{aligned} \tag{2.42}$$

Multiplying the non-dimensional nonlinear part of the restoring force $g(\theta)$ of Equation (2.42) by $\cos m\theta$ (m=1,2,3,$\cdots$) and integrating over the full period (0,2π) gives the following equation:

$$\begin{aligned}\int_{-\theta_0}^{\theta_1}\frac{K(z-e_0)}{ke_0}\cos m\theta d\theta &= \int_{-\theta_0}^{0}\frac{K(z-e_0)}{ke_0}\cos m\theta d\theta + \int_{0}^{\theta_1}\frac{K(z-e_0)}{ke_0}\cos m\theta d\theta \\ &= \pi s'_m \quad (m=1,2,3,\ldots)\end{aligned} \tag{2.43}$$

where the first term on the right side of Equation (2.43) is

$$\begin{aligned}&\int_{-\theta_0}^{0}\frac{K(z-e_0)}{ke_0}\cos m\theta d\theta \quad (m=1,2,3,\ldots) \\ &= \int_{-\theta_0}^{0}\left[\frac{K}{k}\sum_{n=1}^{\infty}\left\{(\cos n\theta-\cos n\theta_0)\cdot x_n+(\sin n\theta+\sin n\theta_0)\cdot y_n\right\}\right]\cos m\theta d\theta \\ &= \frac{K}{k}\sum_{n=1}^{\infty}\left\{x_n\int_{-\theta_0}^{0}(\cos n\theta-\cos n\theta_0)\cos m\theta d\theta + y_n\int_{-\theta_0}^{0}(\sin n\theta+\sin n\theta_0)\cos m\theta d\theta\right\} \\ &= \frac{K}{k}\sum_{n=1}^{\infty}\left\{\frac{1}{2}\frac{\sin(m+n)\theta_0}{m+n}-\frac{1}{2}\frac{\sin(m-n)\theta_0}{m-n}-\frac{\sin m\theta_0\cos n\theta_0}{m}\right\}\cdot x_n \\ &\quad+\frac{K}{k}\sum_{n=1}^{\infty}\left\{-\frac{1}{2}\frac{1-\cos(m+n)\theta_0}{m+n}+\frac{1}{2}\frac{1-\cos(m-n)\theta_0}{m-n}+\frac{\sin m\theta_0\sin n\theta_0}{m}\right\}\cdot y_n\end{aligned} \tag{2.44}$$

Similarly, the second term on the right side of Equation (2.43) is

$$\begin{aligned}&\int_{0}^{\theta_1}\frac{K(z-e_0)}{ke_0}\cos m\theta d\theta \quad (m=1,2,3,\ldots) \\ &= \int_{0}^{\theta_1}\left[\frac{K}{k}\sum_{n=1}^{\infty}\left\{(\cos n\theta-\cos n\theta_1)\cdot x_n+(\sin n\theta-\sin n\theta_1)\cdot y_n\right\}\right]\cos m\theta d\theta \\ &= \frac{K}{k}\sum_{n=1}^{\infty}\left\{x_n\int_{0}^{\theta_1}(\cos n\theta-\cos n\theta_1)\cos m\theta d\theta + y_n\int_{0}^{\theta_1}(\sin n\theta-\sin n\theta_1)\cos m\theta d\theta\right\} \\ &= \frac{K}{k}\sum_{n=1}^{\infty}\left\{\frac{1}{2}\frac{\sin(m+n)\theta_1}{m+n}+\frac{1}{2}\frac{\sin(m-n)\theta_1}{m-n}-\frac{\sin m\theta_1\cos n\theta_1}{m}\right\}\cdot x_n \\ &\quad+\frac{K}{k}\sum_{n=1}^{\infty}\left\{\frac{1}{2}\frac{1-\cos(m+n)\theta_1}{m+n}-\frac{1}{2}\frac{1-\cos(m-n)\theta_1}{m-n}-\frac{\sin m\theta_1\sin n\theta_1}{m}\right\}\cdot y_n\end{aligned} \tag{2.45}$$

Substituting Equations (2.44) and (2.45) into Equation (2.43) gives the following equation:

$$
\begin{aligned}
\int_{-\theta_0}^{\theta_1} \frac{g(\theta)}{ke_0}\cos m\theta d\theta &= \int_{-\theta_0}^{\theta_1} \frac{K(z-e_0)}{ke_0}\cos m\theta d\theta \\
&= \int_{-\theta_0}^{0} \frac{K(z-e_0)}{ke_0}\cos m\theta d\theta + \int_{0}^{\theta_1} \frac{K(z-e_0)}{ke_0}\cos m\theta d\theta \\
&= \frac{K}{k}\sum_{n=1}^{\infty}\left\{ \frac{1}{2}\frac{\sin(m+n)\theta_0}{m+n} + \frac{1}{2}\frac{\sin(m-n)\theta_0}{m-n} - \frac{\sin m\theta_0 \cos n\theta_0}{m} \right\}\cdot x_n \\
&\quad + \frac{K}{k}\sum_{n=1}^{\infty}\left\{ -\frac{1}{2}\frac{1-\cos(m+n)\theta_0}{m+n} + \frac{1}{2}\frac{1-\cos(m-n)\theta_0}{m-n} + \frac{\sin m\theta_0 \sin n\theta_0}{m} \right\}\cdot y_n \\
&\quad + \frac{K}{k}\sum_{n=1}^{\infty}\left\{ \frac{1}{2}\frac{\sin(m+n)\theta_1}{m+n} + \frac{1}{2}\frac{\sin(m-n)\theta_1}{m-n} - \frac{\sin m\theta_1 \cos n\theta_1}{m} \right\}\cdot x_n \\
&\quad + \frac{K}{k}\sum_{n=1}^{\infty}\left\{ \frac{1}{2}\frac{1-\cos(m+n)\theta_1}{m+n} - \frac{1}{2}\frac{1-\cos(m-n)\theta_1}{m-n} - \frac{\sin m\theta_1 \sin n\theta_1}{m} \right\}\cdot y_n \\
&= \pi s'_m \quad (m = 1,2,3,\ldots)
\end{aligned}
\tag{2.46}
$$

Equation (2.46) is simplified as follows:

$$
XMA_m \cdot x_m + \sum_{n=1}^{\infty} XA_{mn} \cdot x_n + YMA_m \cdot y_m + \sum_{n=1}^{\infty} YA_{mn} \cdot y_n = P_m \tag{2.47}
$$

where

$$
\left.
\begin{aligned}
XMA_m &= M_m\left(1 - m^2\Omega^2\right) \\
YMA_m &= M_m(2m\zeta\Omega) \\
XA_{mn} &= M_m\left(\overline{UX0_{mn}} + \overline{UX1_{mn}}\right)/\pi \\
YA_{mn} &= M_m\left(\overline{VY0_{mn}} + \overline{VY1_{mn}}\right)/\pi \\
P_m &= M_m \cdot u'_m \\
\overline{UX0_{mn}}(\theta_0) &= \frac{K}{k}\left\{ \frac{1}{2}\frac{\sin(m+n)\theta_0}{m+n} + \frac{1}{2}\frac{\sin(m-n)\theta_0}{m-n} - \frac{\sin m\theta_0 \cos n\theta_0}{m} \right\} \\
\overline{VY0_{mn}}(\theta_0) &= \frac{K}{k}\left\{ -\frac{1}{2}\frac{1-\cos(m+n)\theta_0}{m+n} + \frac{1}{2}\frac{1-\cos(m-n)\theta_0}{m-n} + \frac{\sin m\theta_0 \sin n\theta_0}{m} \right\} \\
\overline{UX1_{mn}}(\theta_1) &= \frac{K}{k}\left\{ \frac{1}{2}\frac{\sin(m+n)\theta_1}{m+n} + \frac{1}{2}\frac{\sin(m-n)\theta_1}{m-n} - \frac{\sin m\theta_1 \cos n\theta_1}{m} \right\} \\
\overline{VY1_{mn}}(\theta_1) &= \frac{K}{k}\left\{ \frac{1}{2}\frac{1-\cos(m+n)\theta_1}{m+n} - \frac{1}{2}\frac{1-\cos(m-n)\theta_1}{m-n} - \frac{\sin m\theta_1 \sin n\theta_1}{m} \right\}
\end{aligned}
\right\}
\tag{2.48}
$$

In the same manner, multiplying the non-dimensional nonlinear part of the restoring force $g(\theta)$ of Equation (2.42) by $\sin m\theta$ (m=1,2,3,$\cdots$) and integrating over the full period (0,2π) gives the following equation:

$$\begin{aligned}\int_{-\theta_0}^{\theta_1}\frac{K(z-e_0)}{ke_0}\sin m\theta d\theta &= \int_{-\theta_0}^{0}\frac{K(z-e_0)}{ke_0}\sin m\theta d\theta + \int_{0}^{\theta_1}\frac{K(z-e_0)}{ke_0}\sin m\theta d\theta \\ &= \pi t'_m \quad (m=1,2,3,\ldots)\end{aligned} \tag{2.49}$$

where the first term on the right side of Equation (2.49) is

$$\begin{aligned}&\int_{-\theta_0}^{0}\frac{K(z-e_0)}{ke_0}\sin m\theta d\theta \quad (m=1,2,3,\ldots)\\ &=\int_{-\theta_0}^{0}\left[\frac{K}{k}\sum_{n=1}^{\infty}\left\{(\cos n\theta-\cos n\theta_0)\cdot x_n+(\sin n\theta+\sin n\theta_0)\cdot y_n\right\}\right]\sin m\theta d\theta\\ &=\frac{K}{k}\sum_{n=1}^{\infty}\left\{x_n\int_{-\theta_0}^{0}(\cos n\theta-\cos n\theta_0)\sin m\theta d\theta+y_n\int_{-\theta_0}^{0}(\sin n\theta+\sin n\theta_0)\sin m\theta d\theta\right\}\\ &=\frac{K}{k}\sum_{n=1}^{\infty}\left\{-\frac{1}{2}\frac{1-\cos(m+n)\theta_0}{m+n}-\frac{1}{2}\frac{1-\cos(m-n)\theta_0}{m-n}+\frac{(1-\cos m\theta_0)\cos n\theta_0}{m}\right\}\cdot x_n\\ &\quad+\frac{K}{k}\sum_{n=1}^{\infty}\left\{-\frac{1}{2}\frac{\sin(m+n)\theta_0}{m+n}+\frac{1}{2}\frac{\sin(m-n)\theta_0}{m-n}-\frac{(1-\cos m\theta_0)\sin n\theta_0}{m}\right\}\cdot y_n\end{aligned} \tag{2.50}$$

Similarly, the second term on the right side of Equation (2.49) is

$$\begin{aligned}&\int_{0}^{\theta_1}\frac{K(z-e_0)}{ke_0}\sin m\theta d\theta \quad (m=1,2,3,\ldots)\\ &=\int_{0}^{\theta_1}\left[\frac{K}{k}\sum_{n=1}^{\infty}\left\{(\cos n\theta-\cos n\theta_1)\cdot x_n+(\sin n\theta-\sin n\theta_1)\cdot y_n\right\}\right]\sin m\theta d\theta\\ &=\frac{K}{k}\sum_{n=1}^{\infty}\left\{x_n\int_{0}^{\theta_1}(\cos n\theta-\cos n\theta_1)\sin m\theta d\theta+y_n\int_{0}^{\theta_1}(\sin n\theta-\sin n\theta_1)\sin m\theta d\theta\right\}\\ &=\frac{K}{k}\sum_{n=1}^{\infty}\left\{\frac{1}{2}\frac{1-\cos(m+n)\theta_1}{m+n}+\frac{1}{2}\frac{1-\cos(m-n)\theta_1}{m-n}-\frac{(1-\cos m\theta_1)\cos n\theta_1}{m}\right\}\cdot x_n\\ &\quad+\frac{K}{k}\sum_{n=1}^{\infty}\left\{-\frac{1}{2}\frac{\sin(m+n)\theta_1}{m+n}+\frac{1}{2}\frac{\sin(m-n)\theta_1}{m-n}-\frac{(1-\cos m\theta_1)\sin n\theta_1}{m}\right\}\cdot y_n\end{aligned} \tag{2.51}$$

Substituting Equations (2.50) and (2.51) into Equation (2.49) gives the following equation:

$$\begin{aligned}
\int_{-\theta_0}^{\theta_1} \frac{g(\theta)}{ke_0}\sin m\theta d\theta &= \int_{-\theta_0}^{\theta_1} \frac{K(z-e_0)}{ke_0}\sin m\theta d\theta \\
&= \int_{-\theta_0}^{0} \frac{K(z-e_0)}{ke_0}\sin m\theta d\theta + \int_{0}^{\theta_1} \frac{K(z-e_0)}{ke_0}\sin m\theta d\theta \\
&= \frac{K}{k}\sum_{n=1}^{\infty}\left\{ -\frac{1}{2}\frac{1-\cos(m+n)\theta_0}{m+n} - \frac{1}{2}\frac{1-\cos(m-n)\theta_0}{m-n} + \frac{(1-\cos m\theta_0)\cos n\theta_0}{m} \right\}\cdot x_n \\
&\quad + \frac{K}{k}\sum_{n=1}^{\infty}\left\{ -\frac{1}{2}\frac{\sin(m+n)\theta_0}{m+n} + \frac{1}{2}\frac{\sin(m-n)\theta_0}{m-n} - \frac{(1-\cos m\theta_0)\sin n\theta_0}{m} \right\}\cdot y_n \\
&\quad + \frac{K}{k}\sum_{n=1}^{\infty}\left\{ \frac{1}{2}\frac{1-\cos(m+n)\theta_1}{m+n} + \frac{1}{2}\frac{1-\cos(m-n)\theta_1}{m-n} - \frac{(1-\cos m\theta_1)\cos n\theta_1}{m} \right\}\cdot x_n \\
&\quad + \frac{K}{k}\sum_{n=1}^{\infty}\left\{ -\frac{1}{2}\frac{\sin(m+n)\theta_1}{m+n} + \frac{1}{2}\frac{\sin(m-n)\theta_1}{m-n} - \frac{(1-\cos m\theta_1)\sin n\theta_1}{m} \right\}\cdot y_n \\
&= \pi t'_m \quad (m = 1,2,3,\ldots)
\end{aligned} \tag{2.52}$$

Equation (2.52) is simplified as follows:

$$XMB_m \cdot x_m + \sum_{n=1}^{\infty} XB_{mn} \cdot x_n + YMB_m \cdot y_m + \sum_{n=1}^{\infty} YB_{mn} \cdot y_n = Q_m \tag{2.53}$$

where

$$
\left.
\begin{aligned}
&XMB_m = M_m\left(-2m\zeta\Omega\right)\\
&YMB_m = M_m\left(1-m^2\Omega^2\right)\\
&XB_{mn} = M_m\left(\ \overline{\overline{UX0_{mn}}}+\overline{\overline{UX1_{mn}}}\ \right)\Big/\pi\\
&YA_{mn} = M_m\left(\ \overline{\overline{VY0_{mn}}}+\overline{\overline{VY1_{mn}}}\ \right)\Big/\pi\\
&Q_m = M_m\cdot v'_m\\
&\overline{\overline{UX0_{mn}}}(\theta_0)=\frac{K}{k}\left\{-\frac{1}{2}\frac{1-\cos(m+n)\theta_0}{m+n}-\frac{1}{2}\frac{1-\cos(m-n)\theta_0}{m-n}+\frac{(1-\cos m\theta_0)\cos n\theta_0}{m}\right\}\\
&\overline{\overline{VY0_{mn}}}(\theta_0)=\frac{K}{k}\left\{-\frac{1}{2}\frac{\sin(m+n)\theta_0}{m+n}+\frac{1}{2}\frac{\sin(m-n)\theta_0}{m-n}-\frac{(1-\cos m\theta_0)\sin n\theta_0}{m}\right\}\\
&\overline{\overline{UX1_{mn}}}(\theta_1)=\frac{K}{k}\left\{\frac{1}{2}\frac{1-\cos(m+n)\theta_1}{m+n}+\frac{1}{2}\frac{1-\cos(m-n)\theta_1}{m-n}-\frac{(1-\cos m\theta_1)\cos n\theta_1}{m}\right\}\\
&\overline{\overline{VY1_{mn}}}(\theta_1)=\frac{K}{k}\left\{-\frac{1}{2}\frac{\sin(m+n)\theta_1}{m+n}+\frac{1}{2}\frac{\sin(m-n)\theta_1}{m-n}-\frac{(1-\cos m\theta_1)\sin n\theta_1}{m}\right\}
\end{aligned}
\right\} \qquad (2.54)
$$

Thus, the infinite dimensionless linear simultaneous equations for determining the non-dimensional Fourier coefficients x_n and y_n are obtained by Equations (2.47) and (2.53):

$$
\left.
\begin{aligned}
&XMA_m\cdot x_m+\sum_{n=1}^{\infty}XA_{mn}\cdot x_n+YMA_m\cdot y_m+\sum_{n=1}^{\infty}YA_{mn}\cdot y_n=P_m\\
&XMB_m\cdot x_m+\sum_{n=1}^{\infty}XB_{mn}\cdot x_n+YMB_m\cdot y_m+\sum_{n=1}^{\infty}YB_{mn}\cdot y_n=Q_m
\end{aligned}
\right\} \qquad (2.55)
$$

(ii) Determination of Parameters (Ω, α, θ_0, θ_1)

The coefficients XMA_m, XA_{mn},$\cdots Q_m$ of Equation (2.55) contain four parameters (Ω, α, θ_0, θ_1). Therefore substituting four parameters into the infinite dimensionless linear simultaneous equations of Equation (2.55) and solving, the non-dimensional Fourier coefficients x_n and y_n can be obtained. Here, the equations for determining the four parameters are derived.

(a) Characteristic of Restoring Force

Integrating the non-dimensional nonlinear part of the restoring force $g(\theta)$ of Equation (2.42) over the full period $(0,2\pi)$ gives the following equation:

$$\begin{aligned}\int_0^{2\pi}\frac{g(\theta)}{ke_0}d\theta &= \int_{-\theta_0}^{\theta_1}\frac{g(\theta)}{ke_0}d\theta \\ &= \int_{-\theta_0}^{\theta_1}\frac{K(z-e_0)}{ke_0}d\theta \\ &= \int_{-\theta_0}^{0}\frac{K(z-e_0)}{ke_0}d\theta+\int_0^{\theta_1}\frac{K(z-e_0)}{ke_0}d\theta \\ &= \pi s_0'\end{aligned} \tag{2.56}$$

Expanding the right side of Equation (2.56) gives the following equation:

$$\begin{aligned}&\int_{-\theta_0}^{0}\frac{K(z-e_0)}{ke_0}d\theta+\int_0^{\theta_1}\frac{K(z-e_0)}{ke_0}d\theta \\ &=\int_{-\theta_0}^{0}\left[\frac{K}{k}\sum_{n=1}^{\infty}\left\{\left(\cos n\theta-\cos n\theta_0\right)\cdot x_n+\left(\sin n\theta+\sin n\theta_0\right)\cdot y_n\right\}\right]d\theta \\ &\quad+\int_0^{\theta_1}\left[\frac{K}{k}\sum_{n=1}^{\infty}\left\{\left(\cos n\theta-\cos n\theta_1\right)x_n+\left(\sin n\theta-\sin n\theta_1\right)y_n\right\}\right]d\theta \\ &=\frac{K}{k}\sum_{n=1}^{\infty}\left\{x_n\int_{-\theta_0}^{0}\left(\cos n\theta-\cos n\theta_0\right)d\theta+y_n\int_{-\theta_0}^{0}\left(\sin n\theta+\sin n\theta_0\right)d\theta\right\} \\ &\quad+\frac{K}{k}\sum_{n=1}^{\infty}\left\{x_n\int_0^{\theta_1}\left(\cos n\theta-\cos n\theta_1\right)d\theta+y_n\int_0^{\theta_1}\left(\sin n\theta-\sin n\theta_1\right)d\theta\right\} \\ &=\frac{K}{k}\sum_{n=1}^{\infty}\left\{\left(\frac{\sin n\theta_0}{n}-\theta_0\cdot\cos n\theta_0\right)\cdot x_n+\left(-\frac{1-\cos n\theta_0}{n}+\theta_0\cdot\sin n\theta_0\right)\cdot y_n\right\} \\ &\quad+\frac{K}{k}\sum_{n=1}^{\infty}\left\{\left(\frac{\sin n\theta_1}{n}-\theta_1\cdot\cos n\theta_1\right)\cdot x_n+\left(\frac{1-\cos n\theta_1}{n}-\theta_1\cdot\sin n\theta_1\right)\cdot y_n\right\}\end{aligned} \tag{2.57}$$

Equation (2.57) is simplified as follows:

$$\sum_{n=1}^{\infty}XC_n\cdot x_n+\sum_{n=1}^{\infty}YC_n\cdot y_n=RC+\sum_{n=1}^{\infty}RC_n \tag{2.58}$$

where

$$\left.\begin{aligned}
XC_n &= \frac{1}{2\pi}\frac{K}{k}\left\{\left(\frac{\sin n\theta_0}{n}-\theta_0\cos n\theta_0\right)+\left(\frac{\sin n\theta_1}{n}-\theta_1\cos n\theta_1\right)\right\}-\frac{k}{k+K}\left\{\frac{K}{k}+\left(1-n^2\Omega^2\right)\right\}\\
YC_n &= \frac{1}{2\pi}\frac{K}{k}\left\{\left(-\frac{1-\cos n\theta_0}{n}+\theta_0\sin n\theta_0\right)+\left(\frac{1-\cos n\theta_1}{n}-\theta_1\sin n\theta_1\right)\right\}-\frac{k}{k+K}\left(2n\zeta\Omega\right)\\
RC &= -\frac{K}{k+K}\\
RC_n &= -\frac{k}{k+K}\sum_{n=1}^{\infty}u'_n
\end{aligned}\right\} \qquad (2.59)$$

And thus, the infinite dimensionless linear simultaneous equations are obtained by Equations (2.55) and (2.58) as follows:

$$\left.\begin{aligned}
&\sum_{n=1}^{\infty}XC_n\cdot x_n+\sum_{n=1}^{\infty}YC_n\cdot y_n=RC+\sum_{n=1}^{\infty}RC_n\\
&XMA_m\cdot x_m+\sum_{n=1}^{\infty}XA_{mn}\cdot x_n+YMA_m\cdot y_m+\sum_{n=1}^{\infty}YA_{mn}\cdot y_n=P_m\\
&XMB_m\cdot x_m+\sum_{n=1}^{\infty}XB_{mn}\cdot x_n+YMB_m\cdot y_m+\sum_{n=1}^{\infty}YB_{mn}\cdot y_n=Q_m
\end{aligned}\right\} \qquad (2.60)$$

The coefficient determinant of Equation (2.60) is expressed as follows:

$$\begin{aligned}
\triangle_C &= \triangle_C(\,\Omega\,,\,\alpha\,,\,\theta_0\,,\,\theta_1\,)\\
&= \begin{vmatrix}
XC_1 & XC_2 & \cdots & YC_1 & YC_2 & \cdots & -\left(RC+\sum_{n=1}^{\infty}RC_n\right)\\
XMA_1+XA_{11} & XA_{12} & \cdots & YMA_1+YA_{11} & YA_{12} & \cdots & -P_1\\
XA_{21} & XMA_2+XA_{22} & \cdots & YA_{21} & YMA_2+YA_{22} & \cdots & -P_2\\
\vdots & \vdots & & \vdots & \vdots & & \vdots\\
XMB_1+XB_{11} & XB_{12} & \cdots & YMB_1+YB_{11} & YB_{12} & \cdots & -Q_1\\
XB_{21} & XMB_2+XB_{22} & \cdots & YB_{21} & YMB_2+YB_{22} & \cdots & -Q_2\\
\vdots & \vdots & & \vdots & \vdots & & \vdots
\end{vmatrix}
\end{aligned} \qquad (2.61)$$

(b) Characteristic of Restoring Force in the Interval I

The nonlinear part of the restoring force $g(\theta)$ is equal to zero at the interval I:

$$\begin{aligned}\int_{\theta_1}^{2\pi-\theta_0}\frac{g(\theta)}{ke_0}d\theta &= \int_{\theta_1}^{2\pi-\theta_0}\left\{\frac{s_0'}{2}+\sum_{n=1}^{\infty}\left(\cos n\theta\cdot s_n'+\sin n\theta\cdot t_n'\right)\right\}d\theta \\ &= \left(2\pi-\theta_0-\theta_1\right)\cdot\frac{s_0'}{2}+\sum_{n=1}^{\infty}\left\{\left(-\frac{\sin n\theta_0+\sin n\theta_1}{n}\right)\cdot s_n'+\left(-\frac{\cos n\theta_0-\cos n\theta_1}{n}\right)\cdot t_n'\right\} \\ &= 0\end{aligned} \tag{2.62}$$

Equation (2.62) is simplified as follows:

$$\sum_{n=1}^{\infty}XD_n\cdot x_n+\sum_{n=1}^{\infty}YD_n\cdot y_n=RD+\sum_{n=1}^{\infty}RD_n \tag{2.63}$$

where

$$\left.\begin{aligned}XD_n &= \left(1-n^2\Omega^2\right)\cdot\left(\frac{\sin n\theta_0+\sin n\theta_1}{n}\right)-\left(2n\zeta\Omega\right)\cdot\left(\frac{\cos n\theta_0-\cos n\theta_1}{n}\right) \\ &\quad+\left(2\pi-\theta_0-\theta_1\right)\cdot\left(\frac{k}{k+K}\right)\cdot\left\{\frac{K}{k}+\left(1-n^2\Omega^2\right)\right\} \\ YD_n &= \left(2n\zeta\Omega\right)\cdot\left(\frac{\sin n\theta_0+\sin n\theta_1}{n}\right)+\left(1-n^2\Omega^2\right)\cdot\left(\frac{\cos n\theta_0-\cos n\theta_1}{n}\right) \\ &\quad+\left(2\pi-\theta_0-\theta_1\right)\cdot\left(\frac{k}{k+K}\right)\cdot\left(2n\zeta\Omega\right) \\ RD &= \left(2\pi-\theta_0-\theta_1\right)\cdot\left(\frac{K}{k+K}\right) \\ RD_n &= \left\{\left(2\pi-\theta_0-\theta_1\right)\cdot\left(\frac{k}{k+K}\right)+\left(\frac{\sin n\theta_0+\sin n\theta_1}{n}\right)\right\}\cdot u_n'+\left(\frac{\cos n\theta_0-\cos n\theta_1}{n}\right)\cdot v_n'\end{aligned}\right\} \tag{2.64}$$

And thus, the infinite dimensionless linear simultaneous equations are obtained by Equations (2.55) and (2.63) as follows:

$$\left.\begin{aligned}&\sum_{n=1}^{\infty}XD_n\cdot x_n+\sum_{n=1}^{\infty}YD_n\cdot y_n=RD+\sum_{n=1}^{\infty}RD_n \\ &XMA_m\cdot x_m+\sum_{n=1}^{\infty}XA_{mn}\cdot x_n+YMA_m\cdot y_m+\sum_{n=1}^{\infty}YA_{mn}\cdot y_n=P_m \\ &XMB_m\cdot x_m+\sum_{n=1}^{\infty}XB_{mn}\cdot x_n+YMB_m\cdot y_m+\sum_{n=1}^{\infty}YB_{mn}\cdot y_n=Q_m\end{aligned}\right\} \tag{2.65}$$

The coefficient determinant of Equation (2.65) is expressed as follows:

$$\begin{aligned}\triangle_D &= \triangle_D(\,\Omega\,,\,\alpha\,,\,\theta_0\,,\,\theta_1\,) \\ &= \begin{vmatrix} XD_1 & XD_2 & \cdots & YD_1 & YD_2 & \cdots & -\left(RD+\sum_{n=1}^{\infty}RD_n\right) \\ XMA_1+XA_{11} & XA_{12} & \cdots & YMA_1+YA_{11} & YA_{12} & \cdots & -P_1 \\ XA_{21} & XMA_2+XA_{22} & \cdots & YA_{21} & YMA_2+YA_{22} & \cdots & -P_2 \\ \vdots & \vdots & & \vdots & \vdots & & \vdots \\ XMB_1+XB_{11} & XB_{12} & \cdots & YMB_1+YB_{11} & YB_{12} & \cdots & -Q_1 \\ XB_{21} & XMB_2+XB_{22} & \cdots & YB_{21} & YMB_2+YB_{22} & \cdots & -Q_2 \\ \vdots & \vdots & & \vdots & \vdots & & \vdots \end{vmatrix}\end{aligned} \tag{2.66}$$

(c) The Switching-Over Condition : In the case of θ=0

When θ=0, the resulting displacement $z(\theta)$ is equal to the maximum $e_{\max}$ and velocity of the mass is equal to zero. Thus, differentiating Equation (2.33) and setting θ=0 gives the following equation:

$$\frac{\dot{z}(\theta)}{e_0}=\frac{d}{d\theta}\left\{\frac{z(\theta)}{e_0}\right\}=\sum_{n=1}^{\infty}n\left(-\sin n0\cdot x_n+\cos n0\cdot y_n\right) \\ =0 \tag{2.67}$$

Equation (2.67) is simplified as follows:

$$\sum_{n=1}^{\infty}XE_n\cdot x_n+\sum_{n=1}^{\infty}YE_n\cdot y_n=0 \tag{2.68}$$

where

$$\left.\begin{aligned} XE_n &= 0 \\ YE_n &= n \end{aligned}\right\} \tag{2.69}$$

And thus, the infinite dimensionless linear simultaneous equations are obtained by Equations

(2.55) and (2.68) as follows:

$$\left.\begin{aligned}
&\sum_{n=1}^{\infty} XE_n \cdot x_n + \sum_{n=1}^{\infty} YE_n \cdot y_n = 0 \\
&XMA_m \cdot x_m + \sum_{n=1}^{\infty} XA_{mn} \cdot x_n + YMA_m \cdot y_m + \sum_{n=1}^{\infty} YA_{mn} \cdot y_n = P_m \\
&XMB_m \cdot x_m + \sum_{n=1}^{\infty} XB_{mn} \cdot x_n + YMB_m \cdot y_m + \sum_{n=1}^{\infty} YB_{mn} \cdot y_n = Q_m
\end{aligned}\right\} \tag{2.70}$$

The coefficient determinant of Equation (2.70) is expressed as follows:

$$\begin{aligned}
\triangle_E &= \triangle_E(\,\Omega\,,\,\alpha\,,\,\theta_0\,,\,\theta_1\,) \\
&= \begin{vmatrix}
XE_1 & XE_2 & \cdots & YE_1 & YE_2 & \cdots & 0 \\
XMA_1 + XA_{11} & XA_{12} & \cdots & YMA_1 + YA_{11} & YA_{12} & \cdots & -P_1 \\
XA_{21} & XMA_2 + XA_{22} & \cdots & YA_{21} & YMA_2 + YA_{22} & \cdots & -P_2 \\
\vdots & \vdots & & \vdots & \vdots & & \vdots \\
XMB_1 + XB_{11} & XB_{12} & \cdots & YMB_1 + YB_{11} & YB_{12} & \cdots & -Q_1 \\
XB_{21} & XMB_2 + XB_{22} & \cdots & YB_{21} & YMB_2 + YB_{22} & \cdots & -Q_2 \\
\vdots & \vdots & & \vdots & \vdots & & \vdots
\end{vmatrix}
\end{aligned} \tag{2.71}$$

(d) The Switching-Over Condition : In the case of $\theta = -\theta_0,\ \theta_1$

The resulting vibration containing the dwell phase angle θ_0 and θ_1 of Equation (2.35) are shown as follows:

$$\left.\begin{aligned}
&\frac{z - e_0}{e_0} = \sum_{n=1}^{\infty} \{(\cos n\theta - \cos n\theta_0)x_n + (\sin n\theta + \sin n\theta_0)y_n\} \quad (\text{S.O.C} : \theta = -\theta_0) \\
&\frac{z - e_0}{e_0} = \sum_{n=1}^{\infty} \{(\cos n\theta - \cos n\theta_1)x_n + (\sin n\theta - \sin n\theta_1)y_n\} \quad (\text{S.O.C} : \theta = \theta_1)
\end{aligned}\right\}$$

Since these equations are equal, the following equation is obtained:

$$\sum_{n=1}^{\infty} \{(\cos n\theta_0 - \cos n\theta_1)x_n - (\sin n\theta_0 + \sin n\theta_1)y_n\} = 0 \tag{2.72}$$

Equation (2.72) is simplified as follows:

$$\sum_{n=1}^{\infty} XF_n \cdot x_n + \sum_{n=1}^{\infty} YF_n \cdot y_n = 0 \tag{2.73}$$

where

$$\left.\begin{aligned} XF_n &= \cos n\theta_0 - \cos n\theta_1 \\ YF_n &= -\sin n\theta_0 - \sin n\theta_1 \end{aligned}\right\} \tag{2.74}$$

And thus, the infinite dimensionless linear simultaneous equations are obtained by Equations (2.55) and (2.73) as follows:

$$\left.\begin{aligned} &\sum_{n=1}^{\infty} XF_n \cdot x_n + \sum_{n=1}^{\infty} YF_n \cdot y_n = 0 \\ &XMA_m \cdot x_m + \sum_{n=1}^{\infty} XA_{mn} \cdot x_n + YMA_m \cdot y_m + \sum_{n=1}^{\infty} YA_{mn} \cdot y_n = P_m \\ &XMB_m \cdot x_m + \sum_{n=1}^{\infty} XB_{mn} \cdot x_n + YMB_m \cdot y_m + \sum_{n=1}^{\infty} YB_{mn} \cdot y_n = Q_m \end{aligned}\right\} \tag{2.75}$$

The coefficient determinant of Equation (2.75) is expressed as follows:

$$\begin{aligned} \triangle_F &= \triangle_F(\,\Omega\,,\,\alpha\,,\,\theta_0\,,\,\theta_1\,) \\ &= \begin{vmatrix} XF_1 & XF_2 & \cdots & YF_1 & YF_2 & \cdots & 0 \\ XMA_1 + XA_{11} & XA_{12} & \cdots & YMA_1 + YA_{11} & YA_{12} & \cdots & -P_1 \\ XA_{21} & XMA_2 + XA_{22} & \cdots & YA_{21} & YMA_2 + YA_{22} & \cdots & -P_2 \\ \vdots & \vdots & & \vdots & \vdots & & \vdots \\ XMB_1 + XB_{11} & XB_{12} & \cdots & YMB_1 + YB_{11} & YB_{12} & \cdots & -Q_1 \\ XB_{21} & XMB_2 + XB_{22} & \cdots & YB_{21} & YMB_2 + YB_{22} & \cdots & -Q_2 \\ \vdots & \vdots & & \vdots & \vdots & & \vdots \end{vmatrix} \end{aligned} \tag{2.76}$$

First, setting value of the coefficient determinants of Equations (2.61), (2.66), (2.71), (2.76) all zero and solving, the four parameters (Ω, α, θ_0, θ_1) can be determined. Next, substituting determined four parameters into the infinite dimensionless linear simultaneous

equations of Equations (2.55) and solving gives the non-dimensional Fourier coefficients x_n and y_n. Finally, the resulting vibration can be calculated by Equation (2.33).

2.1.2 Analysis of Stability Criterion for Harmonic Resonance

Here, stability analysis for periodic solutions of harmonic resonance Type I is carried out. This stability analysis employs a variational equation to investigate consequences of a minute perturbation to a steady forced vibration predicted by a periodic solution for an original equation of motion.

(1) Characteristics of System and Variational Equation

The equation of motion of analytical system is expressed as follows:

$$m\omega^2 \frac{d^2 z}{d\theta^2} + c\omega \frac{dz}{d\theta} + f(z) = -m\omega^2 \frac{d^2}{d\theta^2} q(\theta) \tag{2.77}$$

Substituting the frequency ratio Ω $(=\omega/\omega_n)$ and the damping coefficient ratio ζ $(=c/2\sqrt{mk})$ into Equation (2.77), and the equation of motion is rewritten as follows:

$$\Omega^2 \frac{d^2 z}{d\theta^2} + 2\Omega\zeta \frac{dz}{d\theta} + \frac{f(z)}{k} = -\Omega^2 \frac{d^2 q(\theta)}{d\theta^2} \tag{2.78}$$

Let us now examine whether a periodic solution for a response vibration, as given in the equation of motion of Equation (2.78), is stable when the system reaches steady state. When a minute perturbation is added to the periodic solution $z=z_0(\theta)$, we designate the vibratory displacement $z(\theta)$ and the variation in the vibratory displacement as $x(\theta)$; then, $z=z_0+x$ must satisfy the equation of motion of Equation (2.78):

$$\Omega^2 \frac{d^2}{d\theta^2}(z_0 + x) + 2\Omega\zeta \frac{d}{d\theta}(z_0 + x) + \frac{f(z_0 + x)}{k} = -\Omega^2 \frac{d^2 q(\theta)}{d\theta^2} \tag{2.79}$$

The periodic solution z_0 also satisfies the equation of motion:

$$\Omega^2 \frac{d^2 z_0}{d\theta^2} + 2\Omega\zeta \frac{dz_0}{d\theta} + \frac{f(z_0)}{k} = -\Omega^2 \frac{d^2 q(\theta)}{d\theta^2} \tag{2.80}$$

The restoring force $f(z_0+x)$ of Equation (2.79) is expanded into the following series:

$$f(z_0+x)=f(z_0)+\left\{\frac{d}{dz}f(z)\right\}_{z=z_0}\cdot x+\left\{\frac{d^2}{dz^2}f(z)\right\}_{z=z_0}\cdot\frac{x^2}{2!}+\cdots \tag{2.81}$$

Disregarding the second degree and higher terms of Equation (2.81),

$$f(z_0+x)=f(z_0)+\left\{\frac{d}{dz}f(z)\right\}_{z=z_0}\cdot x \tag{2.82}$$

Substituting Equation (2.82) into Equation (2.79) gives the following equation:

$$\left[\ \Omega^2\frac{d^2x}{d\theta^2}+2\Omega\zeta\frac{dx}{d\theta}+\frac{1}{k}\left\{\frac{d}{dz}f(z)\right\}_{z=z_0}\cdot x\ \right]+\left[\ \Omega^2\frac{d^2z_0}{d\theta^2}+2\Omega\zeta\frac{dz_0}{d\theta}+\frac{f(z_0)}{k}\ \right]=-\Omega^2\frac{d^2q(\theta)}{d\theta^2} \tag{2.83}$$

Substituting (2.80) into Equation (2.83), we obtain the variational equation as follows:

$$\Omega^2\frac{d^2x}{d\theta^2}+2\Omega\zeta\frac{dx}{d\theta}+\frac{1}{k}\left\{\frac{d}{dz}f(z)\right\}_{z=z_0}\cdot x=0 \tag{2.84}$$

(2) Hill's Equation and Stability Criterion

Differentiating the restoring force $f(z)$ of Equation (2.2) with respect to z gives the following equations:

$$\left.\begin{aligned}&\frac{1}{k}\left\{\frac{d}{dz}f(z)\right\}=1 \quad &&:\ \text{Interval I}\ \ (\theta_1\le\theta\le 2\pi-\theta_0)\\&\frac{1}{k}\left\{\frac{d}{dz}f(z)\right\}=1+\frac{K}{k} \quad &&:\ \text{Interval II}\ \ (-\theta_0\le\theta\le\theta_1)\end{aligned}\right\} \tag{2.85}$$

Equation (2.85) is transformed into the following expression by using the step function $\varphi(\theta)$ shown in Figure 2.5:

$$\frac{1}{k}\left\{\frac{d}{dz}f(z)\right\} = 1 + \frac{K}{k}\varphi(\theta) \tag{2.86}$$

where

$$\left.\begin{aligned} &\varphi(\theta) = 0 \quad : \text{Interval I} \quad (\theta_1 \le \theta \le 2\pi - \theta_0) \\ &\varphi(\theta) = 1 \quad : \text{Interval II} \quad (-\theta_0 \le \theta \le \theta_1) \end{aligned}\right\} \tag{2.87}$$

Equation (2.84) is rewritten as follows by using Equation (2.87):

$$\Omega^2 \frac{d^2x}{d\theta^2} + 2\Omega\zeta\frac{dx}{d\theta} + \left\{1 + \frac{K}{k}\varphi(\theta)\right\} \cdot x = 0 \tag{2.88}$$

The variable $\xi(\theta)$ satisfying the following equation is used:

$$\begin{aligned} x(\theta) &= \exp\left(-\frac{\zeta}{\Omega}\theta_\alpha\right) \cdot \exp\left\{-\frac{1}{2}\int\left(\frac{2\zeta}{\Omega}\right)d\theta\right\} \cdot \xi(\theta) \\ &= \exp\left\{-\frac{\zeta}{\Omega}(\theta + \theta_\alpha)\right\} \cdot \xi(\theta) \end{aligned} \tag{2.89}$$

where θ_α is a constant of integration. Substituting Equation (2.89) into Equation (2.88) gives the following equation:

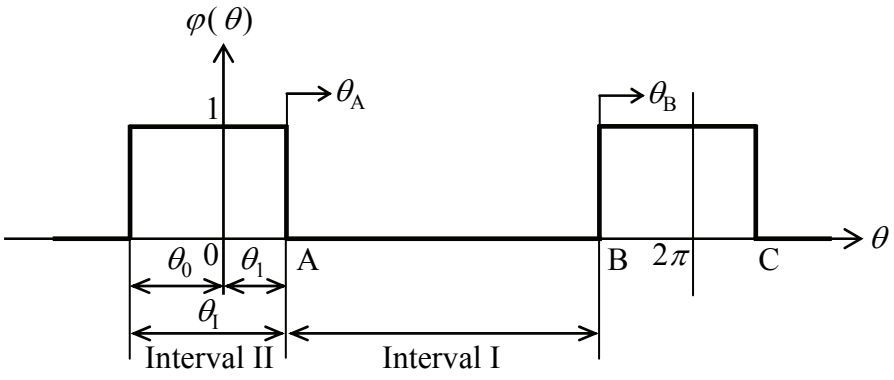

Figure 2.5 Periodic function $\varphi(\theta)$ for Type I

$$\frac{d^2\xi}{d\theta^2} + r(\theta)\cdot\xi = 0 \tag{2.90}$$

where

$$r(\theta) = \left[\frac{1}{\Omega^2}\left\{ 1 + \frac{K}{k}\varphi(\theta) \right\} - \frac{\zeta^2}{\Omega^2} \right] \tag{2.91}$$

Equation (2.90) is a periodic function with the period 2π and called Hill's equation. Equation (2.90) is transformed into the simultaneous equations as follows:

$$\left.\begin{aligned} \frac{d\xi}{d\theta} &= \dot{\xi} \\ \frac{d\dot{\xi}}{d\theta} &= -r(\theta)\xi \end{aligned}\right\} \tag{2.92}$$

Equation (2.92) is transformed into the following expression by using the solution vector $\boldsymbol{\xi}$ and the coefficient matrix **W**.

$$\left.\begin{aligned} &\dot{\boldsymbol{\xi}} = \mathbf{W}\boldsymbol{\xi} \\ &\dot{\boldsymbol{\xi}} = \begin{bmatrix} \dfrac{d\xi}{d\theta} \\ \dfrac{d\dot{\xi}}{d\theta} \end{bmatrix}, \quad \mathbf{W} = \begin{bmatrix} 0 & 1 \\ -r(\theta) & 0 \end{bmatrix}, \boldsymbol{\xi} = \begin{bmatrix} \xi \\ \dot{\xi} \end{bmatrix} \end{aligned}\right\} \tag{2.93}$$

The fundamental solution matrix (Wronski Matrix) for Equation (2.93) is

$$\boldsymbol{\Xi} = \begin{bmatrix} \xi_1 & \xi_2 \\ \dfrac{d\xi_1}{d\theta} & \dfrac{d\xi_2}{d\theta} \end{bmatrix}, \ \det\boldsymbol{\Xi} \neq 0 \tag{2.94}$$

Here, the fundamental period of the periodic solution is *T*, and the following relation can be obtained by Floquet's theorem:

$$\boldsymbol{\Xi}(\theta + T) = \boldsymbol{\Xi}(\theta) \cdot \mathbf{C} \tag{2.95}$$

where **C** is a constant matrix and expressed as follows:

$$\mathbf{C} = \begin{bmatrix} c_{11} & c_{12} \\ c_{21} & c_{22} \end{bmatrix}, \det \mathbf{C} \neq 0 \tag{2.96}$$

The eigenvalues of the matrix **C** of Equation (2.96) are multipliers λ_1 and λ_2. These are the solutions of the following equation:

$$\det[\mathbf{C} - \lambda \mathbf{I}] = \begin{vmatrix} c_{11} - \lambda & c_{12} \\ c_{21} & c_{22} - \lambda \end{vmatrix} = 0 \tag{2.97}$$

Generally, the following equation holds for a fundamental solution matrix of homogenous linear equation (Sato, 1969):

$$\det \boldsymbol{\Xi}(\theta) = \det \boldsymbol{\Xi}(\theta_0) \cdot \exp\left[\int_{\theta_0}^{\theta} \{ \operatorname{tr} \mathbf{W}(s) \} ds \right] \tag{2.98}$$

The unit matrix is chosen to be the initial condition of the fundamental solution matrix:

$$\boldsymbol{\Xi}(\theta_{ini}) = \begin{bmatrix} \xi_1(\theta_{ini}) & \xi_2(\theta_{ini}) \\ \dot{\xi}_1(\theta_{ini}) & \dot{\xi}_2(\theta_{ini}) \end{bmatrix} = \begin{bmatrix} 1 & 0 \\ 0 & 1 \end{bmatrix} = \mathbf{I} \tag{2.99}$$

Summing on-diagonal element of the matrix **W** of Equation (2.93) gives the following equation:

$$\operatorname{tr}[\mathbf{W}] = 0 \tag{2.100}$$

Thus using the equations (2.98) and (2.100),

$$\det \boldsymbol{\Xi}(\theta) = \det \boldsymbol{\Xi}(\theta_{\text{ini}}) = 1 \tag{2.101}$$

By Floquet's theorem of Equation (2.95),

$$\det \boldsymbol{\Xi}(\theta + T) = \det \boldsymbol{\Xi}(\theta) \det \mathbf{C} \tag{2.102}$$

Therefore

$$\det \mathbf{C} = 1 \tag{2.103}$$

Equation (2.95) by Floquet's theorem is transformed as follows:

$$\mathbf{C} = \boldsymbol{\Xi}^{-1}(\theta_{\text{ini}}) \cdot \boldsymbol{\Xi}(\theta_{\text{ini}} + T) = \boldsymbol{\Xi}(\theta_{\text{ini}} + T) = \begin{bmatrix} \xi_1(\theta_{\text{ini}} + T) & \xi_2(\theta_{\text{ini}} + T) \\ \dot{\xi}_1(\theta_{\text{ini}} + T) & \dot{\xi}_2(\theta_{\text{ini}} + T) \end{bmatrix} \tag{2.104}$$

The multipliers λ_1 and λ_2 are derived from Equations (2.97) and (2.104):

$$\left.\begin{aligned} \lambda &= \frac{c_{11} + c_{22}}{2} \pm \sqrt{\left(\frac{c_{11} + c_{22}}{2}\right)^2 - 1} \\ c_{11} &= \xi_1(\theta_{\text{ini}} + T), \quad c_{22} = \dot{\xi}_2(\theta_{\text{ini}} + T) \end{aligned}\right\} \tag{2.105}$$

Summing on-diagonal element of the matrix **C** after the fundamental period gives the following equation:

$$A = c_{11} + c_{22} = \xi_1(\theta_{\text{ini}} + T) + \dot{\xi}_2(\theta_{\text{ini}} + T) \tag{2.106}$$

The product of the two multipliers λ_1 and λ_2 is calculated as follows:

$$\lambda_1 \cdot \lambda_2 = 1 \tag{2.107}$$

In the case where a periodic solution is stable, the multipliers λ_1 and λ_2 satisfy the following

equation:

$$|\lambda_1| \le 1,\ |\lambda_2| \le 1 \tag{2.108}$$

In addition, Equation (2.107) is also considered and the stability criterion is expressed as follows:

$$|\lambda_1| = |\lambda_2| = 1 \tag{2.109}$$

The stability criterion of Equation (2.109) can be rewritten as follows by using *A:*

$$\left.\begin{array}{ll} \text{i)} & |A| > 2 \quad \text{A periodic solution is unstable} \\ \text{ii)} & |A| = 2 \quad \text{A periodic solution is neutral} \\ \text{iii)} & |A| < 2 \quad \text{A periodic solution is stable} \end{array}\right\} \tag{2.110}$$

(3) Expression of Real Number *A*

The stability criterion is set up in the above analysis. Here, the real number *A* of Equation (2.106) is derived by determining the fundamental solutions after the fundamental period. The fundamental solutions for Equation (2.90) can be solved by inosculating method (Maezawa, 1969).

The $r(\theta)$ of Equation (2.91) is the periodic function of 2π period and shown as follows:

$$\begin{aligned} r(\theta) &= r(\theta + T) \\ &= \left[\frac{1}{\Omega^2} \left\{ 1 + \frac{K}{k} \varphi(\theta) \right\} - \frac{\zeta^2}{\Omega^2} \right] \\ &= \left.\begin{array}{ll} {\tau_1}^2 & : \text{Interval I } (\theta_1 \le \theta \le 2\pi - \theta_0) \\ {\tau_2}^2 & : \text{Interval II } (-\theta_0 \le \theta \le \theta_1) \end{array}\right\} \end{aligned} \tag{2.111}$$

where

$$\tau_1 = \frac{\sqrt{1-\zeta^2}}{\Omega} \tag{2.112}$$

$$\tau_2 = \frac{\sqrt{\left(1+\frac{K}{k}\right)-\zeta^2}}{\Omega} \tag{2.113}$$

Transforming Equation (2.89), the variable $\xi(\theta)$ is expressed as follows:

$$\begin{aligned}\xi(\theta) &= \exp\left\{ \frac{\zeta}{\Omega}(\theta+\theta_\alpha) \right\} \cdot x(\theta) \\ &= \exp\{ \eta(\theta+\theta_\alpha) \} \cdot x(\theta)\end{aligned} \tag{2.114}$$

where η is the dimensionless coefficient as follows:

$$\eta = \frac{\zeta}{\Omega} \tag{2.115}$$

Substituting Equation (2.114) into Equation (2.90) gives the following equation:

$$\begin{aligned}\frac{d^2\xi}{d\theta^2} + r(\theta)\cdot\xi &= \exp\{ \eta(\theta+\theta_\alpha) \} \cdot \left[\frac{d^2x}{d\theta^2} + 2\eta\frac{dx}{d\theta} + \frac{1}{\Omega^2}\left\{ 1+\frac{K}{k}\varphi(\theta) \right\} x \right] \\ &= 0\end{aligned} \tag{2.116}$$

where the initial condition of $\xi(\theta)$ is given by Equation (2.99) and that of $x(\theta)$ is calculated as follows:

$$\begin{bmatrix} x_1(0) & \dot{x}_1(0) \\ x_2(0) & \dot{x}_2(0) \end{bmatrix} = \begin{bmatrix} 1 & -\eta \\ 0 & 1 \end{bmatrix} \tag{2.117}$$

(i) In the case of the Fundamental Solution ξ_1

(a) In the interval AB

The Hill's equation of Equation (2.90) is

$$\frac{d^2\xi}{d\theta^2} + \tau_1{}^2\xi = 0 \qquad (\theta_1 \le \theta \le 2\pi - \theta_0) \tag{2.118}$$

Using the independent variable θ_A shown in Figure 2.5, Equation (2.118) is rewritten as follows:

$$\frac{d^2\xi(\theta_A)}{d\theta_A{}^2} + \tau_1{}^2 \cdot \xi(\theta_A) = 0 \qquad (0 \le \theta_A \le 2\pi - \theta_I) \tag{2.119}$$

where

$$\theta_I \equiv \theta_0 + \theta_1 \tag{2.120}$$

Since Equation (2.119) is the second order differential equation, the solution is assumed as follows:

$$\left.\begin{aligned} \xi_1(\theta_A) &= \overline{C_{A1}}\cos\tau_1\theta_A + \overline{S_{A1}}\sin\tau_1\theta_A \\ \dot{\xi}_1(\theta_A) &= \tau_1(-\overline{C_{A1}}\sin\tau_1\theta_A + \overline{S_{A1}}\cos\tau_1\theta_A) \end{aligned}\right\} \tag{2.121}$$

Thus $x_1(\theta_A)$ is expressed as follows:

$$\left.\begin{aligned} x_1(\theta_A) &= \exp(-\eta\theta_A)\cdot\left(\overline{C_{A1}}\cos\tau_1\theta_A + \overline{S_{A1}}\sin\tau_1\theta_A\right) \\ \dot{x}_1(\theta_A) &= -\eta x_1(\theta_A) + \exp(-\eta\theta_A)\cdot\left\{\tau_1\left(-\overline{C_{A1}}\sin\tau_1\theta_A + \overline{S_{A1}}\cos\tau_1\theta_A\right)\right\} \end{aligned}\right\} \tag{2.122}$$

Applying the initial condition of Equation (2.99) to the fundamental solution of Equation (2.121) gives the following equations:

$$\left.\begin{aligned}\xi_1(\theta_A = 0) &= \overline{C_{A1}} = 1 \\ \dot{\xi}_1(\theta_A = 0) &= \tau_1 \overline{S_{A1}} = 0\end{aligned}\right\} \tag{2.123}$$

Thus

$$\overline{C_{A1}} = 1 \quad , \quad \overline{S_{A1}} = 0 \tag{2.124}$$

Substituting Equation (2.124) into Equations (2.121) and (2.122) gives the following equation:

$$\left.\begin{aligned}\xi_1(\theta_A) &= \cos\tau_1\theta_A \\ \dot{\xi}_1(\theta_A) &= -\tau_1 \sin\tau_1\theta_A\end{aligned}\right\} \tag{2.125}$$

$$\left.\begin{aligned}x_1(\theta_A) &= \exp(-\eta\theta_A)\cdot\cos\tau_1\theta_A \\ \dot{x}_1(\theta_A) &= -\eta\cdot x_1(\theta_A) + \exp(-\eta\theta_A)\cdot(-\tau_1\sin\tau_1\theta_A) \\ &= \exp(-\eta\theta_A)\cdot(-\eta\cos\tau_1\theta_A - \tau_1\sin\tau_1\theta_A)\end{aligned}\right\} \tag{2.126}$$

(b) In the interval BC

The Hill's equation of Equation (2.90) is

$$\frac{d^2\xi}{d\theta^2} + {\tau_2}^2\xi = 0 \qquad (2\pi - \theta_0 \le \theta \le 2\pi + \theta_1) \tag{2.127}$$

Using the independent variable θ_B shown in Figure 2.5, Equation (2.127) is rewritten as follows:

$$\frac{d^2\xi(\theta_B)}{d{\theta_B}^2} + {\tau_2}^2\cdot\xi(\theta_B) = 0 \qquad (0 \le \theta_B \le \theta_I) \tag{2.128}$$

Since Equation (2.128) is the second order differential equation, the solution is assumed as follows:

$$\left.\begin{aligned}\xi_1(\theta_B) &= \overline{C_{B1}}\cos\tau_1\theta_B + \overline{S_{B1}}\sin\tau_1\theta_B \\ \dot{\xi}_1(\theta_B) &= \tau_1(-\overline{C_{B1}}\sin\tau_1\theta_B + \overline{S_{B1}}\cos\tau_1\theta_B)\end{aligned}\right\} \tag{2.129}$$

Thus $x_1(\theta_B)$ is expressed as follows:

$$\left.\begin{aligned}x_1(\theta_B) &= \exp\{-\eta(2\pi-\theta_I)\}\cdot\left\{\exp(-\eta\theta_B)\cdot\left(\overline{C_{B1}}\cos\tau_2\theta_B + \overline{S_{B1}}\sin\tau_2\theta_B\right)\right\} \\ \dot{x}_1(\theta_B) &= -\eta\cdot x_1(\theta_B) + \exp\{-\eta(2\pi-\theta_I)\}\cdot\left[\exp(-\eta\theta_B)\cdot\left\{\tau_2\left(-\overline{C_{B1}}\sin\tau_2\theta_B + \overline{S_{B1}}\cos\tau_2\theta_B\right)\right\}\right]\end{aligned}\right\} \tag{2.130}$$

where the relation of the independent variables θ_B and θ_A is

$$\theta_B = 0 \;:\; \theta_A = 2\pi - \theta_I \tag{2.131}$$

Applying the relation of Equation (2.131) to the fundamental solution of Equation (2.129) gives the following equations:

$$\left.\begin{aligned}\xi_1(\theta_B = 0) &= \overline{C_{B1}} \\ &= \xi_1(\theta_A = 2\pi - \theta_I) = \cos\tau_1(2\pi - \theta_I) \\ \dot{\xi}_1(\theta_B = 0) &= \tau_2\overline{S_{B1}} \\ &= \dot{\xi}_1(\theta_A = 2\pi - \theta_I) = -\tau_1\sin\tau_1(2\pi - \theta_I)\end{aligned}\right\} \tag{2.132}$$

Thus

$$\left.\begin{aligned}\overline{C_{B1}} &= \cos\tau_1(2\pi - \theta_I) \\ \overline{S_{B1}} &= -\frac{\tau_1}{\tau_2}\sin\tau_1(2\pi - \theta_I)\end{aligned}\right\} \tag{2.133}$$

Substituting Equation (2.133) into Equation (2.130) gives the following equations:

$$\left.\begin{aligned}x_1(\theta_B) &= \exp(-\eta\theta_B)\cdot\left(\overline{C'_{B1}}\cos\tau_2\theta_B + \overline{S'_{B1}}\sin\tau_2\theta_B\right) \\ \dot{x}_1(\theta_B) &= -\eta\cdot x_1(\theta_B) + \exp(-\eta\theta_B)\cdot\left\{\tau_2\left(-\overline{C'_{B1}}\sin\tau_2\theta_B + \overline{S'_{B1}}\cos\tau_2\theta_B\right)\right\} \\ &= \exp(-\eta\theta_B)\cdot\left\{\left(-\eta\overline{C'_{B1}} + \tau_2\overline{S'_{B1}}\right)\cos\tau_2\theta_B + \left(-\tau_2\overline{C'_{B1}} - \eta\overline{S'_{B1}}\right)\sin\tau_2\theta_B\right\}\end{aligned}\right\} \tag{2.134}$$

where

$$\left.\begin{aligned}\overline{C'_{B1}} &= \exp\{-\eta(2\pi-\theta_{\mathrm{I}})\}\cdot\overline{C_{B1}}\\ \overline{S'_{B1}} &= \exp\{-\eta(2\pi-\theta_{\mathrm{I}})\}\cdot\overline{S_{B1}}\end{aligned}\right\} \tag{2.135}$$

(ii) In the case of the Fundamental Solution ξ_2

(a) In the interval AB

The Hill's equation of Equation (2.90) is

$$\frac{d^2\xi}{d\theta^2}+\tau_1{}^2\xi=0 \qquad (\theta_1\le\theta\le 2\pi-\theta_0) \tag{2.136}$$

Using the independent variable θ_{A} shown in Figure 2.5, Equation (2.136) is rewritten as follows:

$$\frac{d^2\xi(\theta_{\mathrm{A}})}{d\theta_{\mathrm{A}}{}^2}+\tau_1{}^2\cdot\xi(\theta_{\mathrm{A}})=0 \qquad (0\le\theta_{\mathrm{A}}\le 2\pi-\theta_{\mathrm{I}}) \tag{2.137}$$

where

$$\theta_{\mathrm{I}}\equiv\theta_0+\theta_1 \tag{2.138}$$

Since Equation (2.137) is the second order differential equation, the solution is assumed as follows:

$$\left.\begin{aligned}\xi_2(\theta_{\mathrm{A}}) &= \overline{C_{A2}}\cos\tau_1\theta_{\mathrm{A}}+\overline{S_{A2}}\sin\tau_1\theta_{\mathrm{A}}\\ \dot{\xi}_2(\theta_{\mathrm{A}}) &= \tau_1(-\overline{C_{A2}}\sin\tau_1\theta_{\mathrm{A}}+\overline{S_{A2}}\cos\tau_1\theta_{\mathrm{A}})\end{aligned}\right\} \tag{2.139}$$

Thus $x_2(\theta_{\mathrm{A}})$ is expressed as follows:

$$\left.\begin{aligned} x_2(\theta_A) &= \exp(-\eta\theta_A)\cdot\left(\overline{C_{A2}}\cos\tau_1\theta_A + \overline{S_{A2}}\sin\tau_1\theta_A\right) \\ \dot{x}_2(\theta_A) &= -\eta x_2(\theta_A) + \exp(-\eta\theta_A)\cdot\left\{\tau_1\left(-\overline{C_{A2}}\sin\tau_1\theta_A + \overline{S_{A2}}\cos\tau_1\theta_A\right)\right\} \end{aligned}\right\} \tag{2.140}$$

Applying the initial condition of Equation (2.99) to the fundamental solution of Equation (2.139) gives the following equations:

$$\left.\begin{aligned} \xi_1(\theta_A = 0) &= \overline{C_{A2}} = 0 \\ \dot{\xi}_1(\theta_A = 0) &= \tau_1\overline{S_{A2}} = 1 \end{aligned}\right\} \tag{2.141}$$

Thus

$$\overline{C_{A2}} = 0 \quad , \quad \overline{S_{A2}} = \frac{1}{\tau_1} \tag{2.142}$$

Substituting Equation (2.142) into Equations (2.139) and (2.140) gives the following equations:

$$\left.\begin{aligned} \xi_2(\theta_A) &= \frac{1}{\tau_1}\sin\tau_1\theta_A \\ \dot{\xi}_2(\theta_A) &= \cos\tau_1\theta_A \end{aligned}\right\} \tag{2.143}$$

$$\left.\begin{aligned} x_2(\theta_A) &= \exp(-\eta\theta_A)\cdot\left(\frac{1}{\tau_1}\sin\tau_1\theta_A\right) \\ \dot{x}_2(\theta_A) &= -\eta\cdot x_2(\theta_A) + \exp(-\eta\theta_A)\cdot(\cos\tau_1\theta_A) \\ &= \exp(-\eta\theta_A)\cdot\left(-\frac{\eta}{\tau_1}\sin\tau_1\theta_A + \cos\tau_1\theta_A\right) \end{aligned}\right\} \tag{2.144}$$

(b) In the interval BC

The Hill's equation in Equation (2.90) is

$$\frac{d^2\xi}{d\theta^2} + {\tau_2}^2\xi = 0 \qquad (2\pi - \theta_0 \le \theta \le 2\pi + \theta_1) \tag{2.145}$$

Using the independent variable θ_B shown in Figure 2.5, Equation (2.145) is rewritten as follows:

$$\frac{d^2\xi(\theta_B)}{d\theta_B{}^2} + \tau_2{}^2 \cdot \xi(\theta_B) = 0 \qquad (0 \le \theta_B \le \theta_I) \tag{2.146}$$

Since Equation (2.146) is the second order differential equation, the solution assumed in the form:

$$\left.\begin{aligned} \xi_2(\theta_B) &= \overline{C_{B2}} \cos\tau_1\theta_B + \overline{S_{B2}} \sin\tau_1\theta_B \\ \dot{\xi}_2(\theta_B) &= \tau_1(-\overline{C_{B2}} \sin\tau_1\theta_B + \overline{S_{B2}} \cos\tau_1\theta_B) \end{aligned}\right\} \tag{2.147}$$

Thus $x_2(\theta_B)$ is expressed as follows:

$$\left.\begin{aligned} x_2(\theta_B) &= \exp\{-\eta(2\pi-\theta_I)\}\cdot\{\exp(-\eta\theta_B)\cdot(\overline{C_{B2}}\cos\tau_2\theta_B + \overline{S_{B2}}\sin\tau_2\theta_B)\} \\ \dot{x}_2(\theta_B) &= -\eta\cdot x_1(\theta_B) + \exp\{-\eta(2\pi-\theta_I)\}\cdot[\exp(-\eta\theta_B)\cdot\{\tau_2(-\overline{C_{B2}}\sin\tau_2\theta_B + \overline{S_{B2}}\cos\tau_2\theta_B)\}] \end{aligned}\right\} \tag{2.148}$$

where the relation of the independent variables θ_B and θ_A is

$$\theta_B = 0 : \quad \theta_A = 2\pi - \theta_I \tag{2.149}$$

Applying the relation of Equation (2.149) to the fundamental solution of Equation (2.147) gives the following equations:

$$\left.\begin{aligned} \xi_2(\theta_B = 0) &= \overline{C_{B2}} \\ &= \xi_2(\theta_A = 2\pi - \theta_I) = \frac{1}{\tau_1}\sin\tau_1(2\pi - \theta_I) \\ \dot{\xi}_2(\theta_B = 0) &= \tau_2\overline{S_{B2}} \\ &= \dot{\xi}_2(\theta_A = 2\pi - \theta_I) = \cos\tau_1(2\pi - \theta_I) \end{aligned}\right\} \tag{2.150}$$

Thus

$$\left.\begin{aligned}\overline{C_{B2}} &= \frac{1}{\tau_1}\sin\tau_1(2\pi-\theta_{\mathrm{I}}) \\ \overline{S_{B2}} &= \frac{1}{\tau_2}\cos\tau_1(2\pi-\theta_{\mathrm{I}})\end{aligned}\right\} \tag{2.151}$$

Substituting Equation (2.151) into Equation (2.148) gives the following equations:

$$\left.\begin{aligned}x_2(\theta_{\mathrm{B}}) &= \exp(-\eta\theta_{\mathrm{B}})\cdot\left(\overline{C'_{B2}}\cos\tau_2\theta_{\mathrm{B}}+\overline{S'_{B2}}\sin\tau_2\theta_{\mathrm{B}}\right) \\ \dot{x}_2(\theta_{\mathrm{B}}) &= -\eta\cdot x_2(\theta_{\mathrm{B}})+\exp(-\eta\theta_{\mathrm{B}})\cdot\left\{\tau_2\left(-\overline{C'_{B2}}\sin\tau_2\theta_{\mathrm{B}}+\overline{S'_{B2}}\cos\tau_2\theta_{\mathrm{B}}\right)\right\} \\ &= \exp(-\eta\theta_{\mathrm{B}})\cdot\left\{\left(-\eta\overline{C'_{B2}}+\tau_2\overline{S'_{B2}}\right)\cos\tau_2\theta_{\mathrm{B}}+\left(-\tau_2\overline{C'_{B2}}-\eta\overline{S'_{B2}}\right)\sin\tau_2\theta_{\mathrm{B}}\right\}\end{aligned}\right\} \tag{2.152}$$

where

$$\left.\begin{aligned}\overline{C'_{B2}} &= \exp\{-\eta(2\pi-\theta_{\mathrm{I}})\}\cdot\overline{C_{B2}} \\ \overline{S'_{B2}} &= \exp\{-\eta(2\pi-\theta_{\mathrm{I}})\}\cdot\overline{S_{B2}}\end{aligned}\right\} \tag{2.153}$$

Here, the relation of the fundamental solutions $\xi(\theta)$ and $x(\theta)$ is

$$\xi_1(\theta)+\dot{\xi}_2(\theta)=\exp\{\eta(\theta+\theta_\alpha)\}\cdot\{x_1(\theta)+\eta\cdot x_2(\theta)+\dot{x}_2(\theta)\} \tag{2.154}$$

The stability criterion is shown in equation (2.110) and the real number A is expressed as follows:

$$A=\xi_1(2\pi)+\dot{\xi}_2(2\pi) \tag{2.155}$$

Substituting Equation (2.154) into Equation (2.155) and setting $\theta_{\mathrm{A}}=2\pi$, the real number A is expressed as follows:

$$\begin{aligned}A &= \xi_1(\theta_{\mathrm{A}}=2\pi)+\dot{\xi}_2(\theta_{\mathrm{A}}=2\pi) \\ &= \exp\{\eta(\theta_{\mathrm{A}}=2\pi)\}\cdot\{x_1(\theta_{\mathrm{A}}=2\pi)+\eta\cdot x_2(\theta_{\mathrm{A}}=2\pi)+\dot{x}_2(\theta_{\mathrm{A}}=2\pi)\}\end{aligned} \tag{2.156}$$

where the relation of the independent variables θ_{A} and θ_{B} is

$$\theta_A = 2\pi \ : \ \theta_B = \theta_I \tag{2.157}$$

Applying Equation (2.157) to Equation (2.156) gives the real number A as follows:

$$A = \exp\{\eta(\theta_B = \theta_I)\} \cdot \{x_1(\theta_B = \theta_I) + \eta x_2(\theta_B = \theta_I) + \dot{x}_2(\theta_B = \theta_I)\} \tag{2.158}$$

For simplicity, substituting Equations (2.135) and (2.153) into (2.158) gives the following equation:

$$A = \left(\overline{C'_{B1}} + \tau_2 \overline{S'_{B2}}\right)\cos\tau_2\theta_I + \left(\overline{S'_{B1}} - \tau_2 \overline{C'_{B2}}\right)\sin\tau_2\theta_I \tag{2.159}$$

And thus

$$\begin{aligned} |A| &= |\ A(\Omega\ ,\ \zeta\ ,\ K/k\ ,\ \theta_I)\ | \\ &= \left| \left(\overline{C'_{B1}} + \tau_2 \overline{S'_{B2}}\right)\cos\tau_2\theta_I + \left(\overline{S'_{B1}} - \tau_2 \overline{C'_{B2}}\right)\sin\tau_2\theta_I \right| \end{aligned} \tag{2.160}$$

The stability criterion of equation (2.110) is shown as follows:

i) $|A| > 2$ A periodic solution is unstable
ii) $|A| = 2$ A periodic solution is neutral
iii) $|A| < 2$ A periodic solution is stable

2.1.3 Analysis of Response Vibration for Superharmonic Resonance

Here, the resulting vibration for superharmonic resonance Type II is analyzed. The waveform of superharmonic resonance Type II contains two entrances into the nonlinear portions during per cycle of the resulting vibration.

(1) Fourier Series Method

(i) Fourier Series Solution

Figure 2.6 shows the assumed shape of the resonance vibration Type II which enters the nonlinear region II twice per cycle. The resulting displacement z at the mass is considered to be periodic; the response is divided into linear region I, and nonlinear region II. The origin for measuring the phase angle θ is defined from the peak of the resulting waveform. Here, the maximum displacement of the resulting vibration is expressed by $e_{\max}$ and the second maximum displacement is expressed by $e'_{\max}$. Thus, these are satisfied with the following relation:

$$e_{\max} \geq e'_{\max} > e_0 \tag{2.161}$$

The distance between the first peak ($z=e_{\max}$) and the second peak ($z=e'_{\max}$) of the resulting vibration is expressed by the phase angle β and the interval of region II in the second peak is expressed by the phase angle θ_2 and θ_3. In the resonance vibration Type II, the mass collides with the spring two times in per cycle. Thus the nonlinear part of the restoring force $g(\theta)$ is expressed as follows:

$$\left.\begin{array}{lll} g(\theta)=0 & ; \ \theta_1 \leq \theta \leq \beta-\theta_2 \ , \ \beta+\theta_3 \leq \theta \leq 2\pi-\theta_0 & : \ \text{Interval I} \\ g(\theta)=K(z-e_0) & ; \ -\theta_0 \leq \theta \leq \theta_1 \ , \ \beta-\theta_2 \leq \theta \leq \beta+\theta_3 & : \ \text{Interval II} \end{array}\right\} \tag{2.162}$$

(ii)Switching-Over Conditions

The switching-over conditions are expressed as follows:

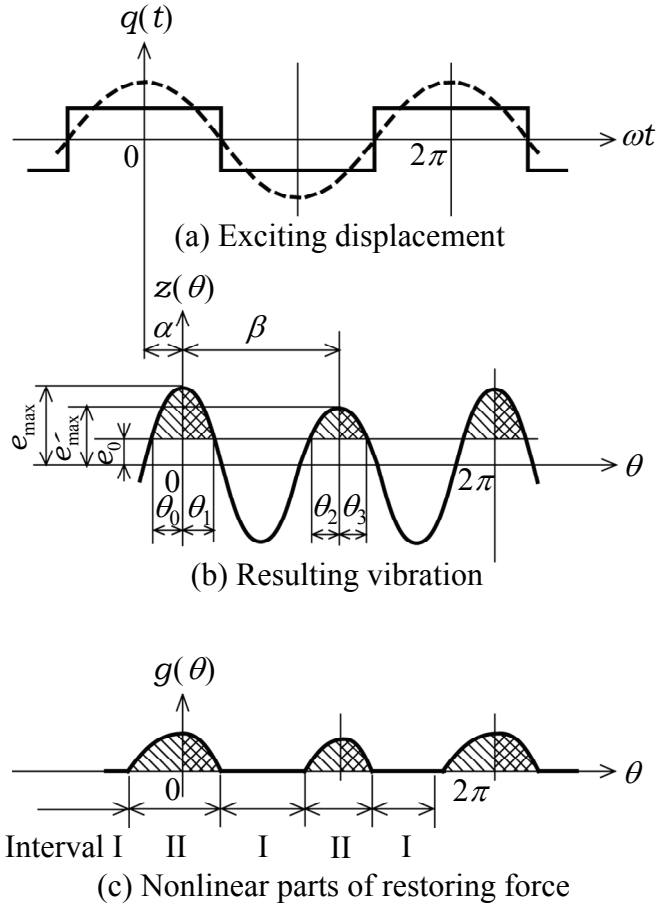

Figure 2.6 Superharmonic resonance vibration TypeII

$$\left.\begin{array}{lll} \theta=-\theta_0 & ; & z(-\theta_0)=e_0 \\ \theta=0 & ; & z(0)=e_{\max} \\ \theta=\theta_1 & ; & z(\theta_1)=e_0 \end{array}\right\}\ \text{TypeI}$$
$$\left.\begin{array}{lll} \theta=\beta-\theta_2 & ; & z(\beta-\theta_2)=e_0 \\ \theta=\beta & ; & z(\beta)=e'_{\max} \\ \theta=\beta+\theta_3 & ; & z(\beta+\theta_3)=e_0 \end{array}\right\}\ \text{TypeII} \qquad (2.163)$$

The switching-over conditions concerned to the nonlinear part of the restoring force $g(\theta)$ is shown as follows:

$$\left.\begin{array}{lll}\theta=-\theta_0 & ; & g(-\theta_0)=0\\ \theta=0 & ; & g(0)=K(e_{\max}-e_0)\\ \theta=\theta_1 & ; & g(\theta_1)=0\end{array}\right\}\ \text{TypeI}$$
$$\left.\begin{array}{lll}\theta=\beta-\theta_2 & ; & g(\beta-\theta_2)=0\\ \theta=\beta & ; & g(\beta)=K(e'_{\max}-e_0)\\ \theta=\beta+\theta_3 & ; & g(\beta+\theta_3)=0\end{array}\right\}\ \text{TypeII} \qquad (2.164)$$

Afterwards, analysis formulae satisfying the switching-over conditions for the resonance vibration Type II are derived. The switching-over conditions for only Type II are expressed as follows:

$$\left.\begin{array}{lll}\theta=\beta-\theta_2 & ; & z(\beta-\theta_2)=e_0\\ \theta=\beta & ; & z(\beta)=e'_{\max}\\ \theta=\beta+\theta_3 & ; & z(\beta+\theta_3)=e_0\end{array}\right\}\ \text{TypeII} \qquad (2.165)$$

(a) Switching-Over Condition: In the case of $\theta=\beta-\theta_2$

When $\theta=\beta-\theta_2$, the resulting displacement $z(\beta-\theta_2)$ is equal to e_0:

$$\begin{aligned} z(\beta-\theta_2)&=\frac{a_0}{2}+\sum_{n=1}^{\infty}\{\,a_n\cos n(\beta-\theta_2)+b_n\sin n(\beta-\theta_2)\,\}=e_0\\ \therefore\ \frac{a_0}{2}&=e_0-\sum_{n=1}^{\infty}\{\,a_n\cos n(\beta-\theta_2)+b_n\sin n(\beta-\theta_2)\,\}\end{aligned} \qquad (2.166)$$

Thus the resulting vibration containing the dwell phase angle θ_2 is

$$z(\theta)=e_0+\sum_{n=1}^{\infty}[\{\cos n\theta-\cos n(\beta-\theta_2)\}\cdot a_n+\{\sin n\theta-\sin n(\beta-\theta_2)\}\cdot b_n] \qquad (2.167)$$

(b) Switching-Over Condition: In the case of $\theta=\beta+\theta_3$

When $\theta=\beta+\theta_3$, the resulting displacement $z(\beta+\theta_3)$ is equal to e_0:

$$z(\beta+\theta_3)=\frac{a_0}{2}+\sum_{n=1}^{\infty}\{\,a_n\cos n(\beta+\theta_3)+b_n\sin n(\beta+\theta_3)\,\}=e_0$$
$$\therefore\ \frac{a_0}{2}=e_0-\sum_{n=1}^{\infty}\{\,a_n\cos n(\beta+\theta_3)+b_n\sin n(\beta+\theta_3)\,\} \tag{2.168}$$

Thus the resulting vibration containing the dwell phase angle θ_3 is

$$z(\theta)=e_0+\sum_{n=1}^{\infty}[\{\cos n\theta-\cos n(\beta+\theta_3)\}\cdot a_n+\{\sin n\theta-\sin n(\beta+\theta_3)\}\cdot b_n] \tag{2.169}$$

(c) Switching-Over Condition: In the case of $\theta=\beta$

When $\theta=\beta$, the resulting displacement $z(\theta=\beta)$ is equal to $e'_{\max}$:

$$z(\beta)=\frac{a_0}{2}+\sum_{n=1}^{\infty}(a_n\cos n\beta+b_n\sin n\beta)=e'_{\max}$$
$$\therefore\ \frac{a_0}{2}=e'_{\max}-\sum_{n=1}^{\infty}(a_n\cos n\beta+b_n\sin n\beta) \tag{2.170}$$

Thus the resulting vibration containing the second maximum resulting displacement $e'_{\max}$ is

$$z(\theta)=e'_{\max}+\sum_{n=1}^{\infty}\{\,(\cos n\theta-\cos n\beta)\cdot a_n+(\sin n\theta-\sin n\beta)\cdot b_n\,\} \tag{2.171}$$

The resulting displacement $z(\theta)$ is expressed as follows corresponding to each of the switching-over conditions:

$$\left.\begin{aligned}
z(\theta)&=e_0+\sum_{n=1}^{\infty}[\,\{\cos n\theta-\cos n(\beta-\theta_2)\}\cdot a_n+\{\sin n\theta-\sin n(\beta-\theta_2)\}\cdot b_n\,]\quad(\text{S.O.C}:\theta=\beta-\theta_2)\\
z(\theta)&=e_0+\sum_{n=1}^{\infty}[\,\{\cos n\theta-\cos n(\beta+\theta_3)\}\cdot a_n+\{\sin n\theta-\sin n(\beta+\theta_3)\}\cdot b_n\,]\quad(\text{S.O.C}:\theta=\beta+\theta_3)\\
z(\theta)&=e'_{\max}+\sum_{n=1}^{\infty}\{\,(\cos n\theta-\cos n\beta)\cdot a_n+(\sin n\theta-\sin n\beta)\cdot b_n\,\}\quad(\text{S.O.C}:\theta=\beta)
\end{aligned}\right\} \tag{2.172}$$

(iii) Derivation of Non-dimensional Equations

(a) Non-Dimensional Resulting Vibration

Dividing Equation (2.172) by clearance e_0, the non-dimensional resulting vibration is

$$\left.\begin{aligned}
\frac{z(\theta)}{e_0} &= 1+\sum_{n=1}^{\infty}\left[\ \left\{\ \cos n\theta-\cos n(\beta-\theta_2)\ \right\}\cdot x_n+\left\{\ \sin n\theta-\sin n(\beta-\theta_2)\ \right\}\cdot y_n\ \right] \quad (\text{S.O.C}:\ \theta=\beta-\theta_2)\\
\frac{z(\theta)}{e_0} &= 1+\sum_{n=1}^{\infty}\left[\ \left\{\ \cos n\theta-\cos n(\beta+\theta_3)\ \right\}\cdot x_n+\left\{\ \sin n\theta-\sin n(\beta+\theta_3)\ \right\}\cdot y_n\ \right] \quad (\text{S.O.C}:\ \theta=\beta+\theta_3)\\
\frac{z(\theta)}{e_0} &= \frac{e'_{\max}}{e_0}+\sum_{n=1}^{\infty}\left\{\ (\cos n\theta-\cos n\beta)\cdot x_n+(\sin n\theta-\sin n\beta)\cdot y_n\ \right\} \quad (\text{S.O.C}:\ \theta=\beta)
\end{aligned}\right\} \tag{2.173}$$

(b) Non-dimensional Second Maximum Resulting Displacement

Dividing Equation (2.170) by e_0 gives the following equation:

$$\frac{x_0}{2}=\frac{e'_{\max}}{e_0}-\sum_{n=1}^{\infty}(x_n\cos n\beta+y_n\sin n\beta) \tag{2.174}$$

When $\theta=\beta$, the nonlinear part of the restoring force of Equation (2.34) is expressed as follows:

$$\frac{g(\beta)}{ke_0}=\frac{s'_0}{2}+\sum_{n=1}^{\infty}(\cos n\beta\cdot s'_n+\sin n\beta\cdot t'_n)=\frac{K(e'_{\max}-e_0)}{ke_0} \tag{2.175}$$

Substituting Equations (2.36) and (2.174) into Equation (2.175) gives the following equation:

$$\begin{aligned}\frac{g(\beta)}{ke_0} &= \frac{s'_0}{2} + \sum_{n=1}^{\infty}\left(\cos n\beta \cdot s'_n + \sin n\beta \cdot t'_n\right) \\ &= -\left\{ \frac{e'_{\max}}{e_0} - \sum_{n=1}^{\infty}\left(\cos n\beta \cdot x_n + \sin n\beta \cdot x_n\right) \right\} \\ &\quad + \sum_{n=1}^{\infty}\cos n\beta \cdot \left[u'_n - \left\{ \left(1 - n^2\Omega^2\right)\cdot x_n + (2n\zeta\Omega)\cdot y_n \right\} \right] \\ &\quad + \sum_{n=1}^{\infty}\sin n\beta \cdot \left[v'_n - \left\{ -(2n\zeta\Omega)\cdot x_n + \left(1 - n^2\Omega^2\right)\cdot y_n \right\} \right] \\ &= \frac{K\left(e'_{\max} - e_0\right)}{ke_0}\end{aligned} \tag{2.176}$$

And thus, the non-dimensional second maximum resulting displacement is

$$\begin{aligned}\frac{e'_{\max}}{e_0} &= \frac{K}{k+K} + \frac{k}{k+K}\sum_{n=1}^{\infty}\left(\cos n\beta \cdot u'_n + \sin n\beta \cdot v'_n\right) \\ &\quad + \frac{k}{k+K}\sum_{n=1}^{\infty}\left\{ \left(n^2\Omega^2\right)\cdot\cos n\beta + (2n\zeta\Omega)\cdot\sin n\beta \right\}\cdot x_n \\ &\quad + \frac{k}{k+K}\sum_{n=1}^{\infty}\left\{ -(2n\zeta\Omega)\cdot\cos n\beta + \left(n^2\Omega^2\right)\cdot\sin n\beta \right\}\cdot y_n\end{aligned} \tag{2.177}$$

Substituting Equation (2.177) into Equation (2.174) gives the Fourier coefficient x_0 as follows:

$$\begin{aligned}x_0 &= \frac{2K}{k+K} + \frac{2k}{k+K}\sum_{n=1}^{\infty}\left(\cos n\beta \cdot u'_n + \sin n\beta \cdot v'_n\right) \\ &\quad + \frac{2k}{k+K}\sum_{n=1}^{\infty}\left[-\left\{ \frac{K}{k} + \left(1 - n^2\Omega^2\right) \right\}\cdot\cos n\beta + (2n\zeta\Omega)\cdot\sin n\beta \right]\cdot x_n \\ &\quad + \frac{2k}{k+K}\sum_{n=1}^{\infty}\left[-(2n\zeta\Omega)\cdot\cos n\beta - \left\{ \frac{K}{k} + \left(1 - n^2\Omega^2\right) \right\}\cdot\sin n\beta \right]\cdot y_n\end{aligned} \tag{2.178}$$

(2) Determination of Non-Dimensional Fourier Coefficients x_n and y_n

The resulting vibration of Equation (2.33) and the maximum resulting displacement of Equation (2.177) can all be determined using the non-dimensional Fourier coefficients x_n and y_n (n=1,2,3,$\cdots$). Therefore, once x_n and y_n are known, the resulting vibration and the maximum resulting displacement are determined. The non-dimensional Fourier coefficients

must be set to satisfy the piecewise linear characteristics of the nonlinear part of the restoring force. Here, the infinite dimensionless linear simultaneous equations for determining the non-dimensional Fourier coefficients are derived by using orthogonality.

(i) Derivation of Infinite Dimensionless Linear Simultaneous Equations

The nonlinear part of the restoring force $g(\theta)$ is

$$\frac{g(\theta)}{ke_0} = \frac{s'_0}{2} + \sum_{n=1}^{\infty}\left(\cos n\theta \cdot s'_n + \sin n\theta \cdot t'_n\right)$$
$$\left.\begin{array}{rll} & 0 & : \quad \theta_1 \le \theta \le \beta - \theta_2 \ , \ \beta + \theta_3 \le \theta \le 2\pi - \theta_0 \quad \text{Interval I} \\ = & \dfrac{K(z-e_0)}{ke_0} & : \quad -\theta_0 \le \theta \le \theta_1 \ , \ \beta - \theta_2 \le \theta \le \beta + \theta_3 \quad \text{Interval II} \end{array}\right\} \tag{2.179}$$

Multiplying the non-dimensional nonlinear part of the restoring force $g(\theta)$ of Equation (2.179) by $\cos m\theta$ (m=1,2,3,$\cdots$) and integrating over the full period (0,2π) gives the following equation:

$$\begin{aligned} \int_0^{2\pi} \frac{g(\theta)}{ke_0}\cos m\theta d\theta &= \int_{-\theta_0}^{2\pi-\theta_0} \frac{g(\theta)}{ke_0}\cos m\theta d\theta \\ &= \int_{-\theta_0}^{\theta_1} \frac{K(z-e_0)}{ke_0}\cos m\theta d\theta + \int_{\beta-\theta_2}^{\beta+\theta_3} \frac{K(z-e_0)}{ke_0}\cos m\theta d\theta \\ &= \begin{cases} \pi s'_m & (m=n) \\ 0 & (m \ne n) \end{cases} \qquad (m = 1,2,3,\ldots) \end{aligned} \tag{2.180}$$

where the first term on the right side of Equation (2.180) is expressed by using Equation (2.48):

$$\begin{aligned} \int_{-\theta_0}^{\theta_1} \frac{g(\theta)}{ke_0}\cos m\theta d\theta &= \int_{-\theta_0}^{\theta_1} \frac{K(z-e_0)}{ke_0}\cos m\theta d\theta \\ &= \int_{-\theta_0}^{0} \frac{K(z-e_0)}{ke_0}\cos m\theta d\theta + \int_{0}^{\theta_1} \frac{K(z-e_0)}{ke_0}\cos m\theta d\theta \\ &= \sum_{n=1}^{\infty}\left(\overline{UX0}_{mn} + \overline{UX1}_{mn}\right)\cdot x_n + \sum_{n=1}^{\infty}\left(\overline{VY0}_{mn} + \overline{VY1}_{mn}\right)\cdot y_n \end{aligned} \tag{2.181}$$

Moreover, the second term on the right side of Equation (2.180) is expanded as follows:

$$\int_{\beta-\theta_2}^{\beta+\theta_3}\frac{g(\theta)}{ke_0}\cos m\theta d\theta=\int_{\beta-\theta_2}^{\beta+\theta_3}\frac{K(z-e_0)}{ke_0}\cos m\theta d\theta$$

$$=\int_{\beta-\theta_2}^{\beta}\frac{K(z-e_0)}{ke_0}\cos m\theta d\theta+\int_{\beta}^{\beta+\theta_3}\frac{K(z-e_0)}{ke_0}\cos m\theta d\theta$$

$$=\frac{K}{k}\sum_{n=1}^{\infty}\Bigg[\frac{1}{2}\frac{\sin(m+n)\beta-\sin(m+n)(\beta-\theta_2)}{m+n}+\frac{1}{2}\frac{\sin(m-n)\beta-\sin(m-n)(\beta-\theta_2)}{m-n}$$
$$-\frac{\{\sin m\beta-\sin m(\beta-\theta_2)\}\cos n(\beta-\theta_2)}{m}\Bigg]\cdot x_n$$
$$+\frac{K}{k}\sum_{n=1}^{\infty}\Bigg[-\frac{1}{2}\frac{\cos(m+n)\beta-\cos(m+n)(\beta-\theta_2)}{m+n}+\frac{1}{2}\frac{\cos(m-n)\beta-\cos(m-n)(\beta-\theta_2)}{m-n}$$
$$-\frac{\{\sin m\beta-\sin m(\beta-\theta_2)\}\sin n(\beta-\theta_2)}{m}\Bigg]\cdot y_n$$

$$+\frac{K}{k}\sum_{n=1}^{\infty}\Bigg[-\frac{1}{2}\frac{\sin(m+n)\beta-\sin(m+n)(\beta+\theta_3)}{m+n}-\frac{1}{2}\frac{\sin(m-n)\beta-\sin(m-n)(\beta+\theta_3)}{m-n}$$
$$+\frac{\{\sin m\beta-\sin m(\beta+\theta_3)\}\cos n(\beta+\theta_3)}{m}\Bigg]\cdot x_n$$
$$+\frac{K}{k}\sum_{n=1}^{\infty}\Bigg[\frac{1}{2}\frac{\cos(m+n)\beta-\cos(m+n)(\beta+\theta_3)}{m+n}-\frac{1}{2}\frac{\cos(m-n)\beta-\cos(m-n)(\beta+\theta_3)}{m-n}$$
$$+\frac{\{\sin m\beta-\sin m(\beta+\theta_3)\}\sin n(\beta+\theta_3)}{m}\Bigg]\cdot y_n$$

(2.182)

Substituting Equations (2.181) and (2.182) into Equation (2.180) gives the following equation:

$$\begin{aligned}\int_0^{2\pi}\frac{g(\theta)}{ke_0}\cos m\theta d\theta &= \int_{-\theta_0}^{2\pi-\theta_0}\frac{g(\theta)}{ke_0}\cos m\theta d\theta \\ &= \int_{-\theta_0}^{\theta_1}\frac{g(\theta)}{ke_0}\cos m\theta d\theta + \int_{\beta-\theta_2}^{\beta+\theta_3}\frac{g(\theta)}{ke_0}\cos m\theta d\theta \\ &= \int_{-\theta_0}^{\theta_1}\frac{K(z-e_0)}{ke_0}\cos m\theta d\theta + \int_{\beta-\theta_2}^{\beta+\theta_3}\frac{K(z-e_0)}{ke_0}\cos m\theta d\theta \\ &= \int_{-\theta_0}^{0}\frac{K(z-e_0)}{ke_0}\cos m\theta d\theta + \int_{0}^{\theta_1}\frac{K(z-e_0)}{ke_0}\cos m\theta d\theta \\ &\quad + \int_{\beta-\theta_2}^{\beta}\frac{K(z-e_0)}{ke_0}\cos m\theta d\theta + \int_{\beta}^{\beta+\theta_3}\frac{K(z-e_0)}{ke_0}\cos m\theta d\theta \\ &= \sum_{n=1}^{\infty}\left(\overline{UX0}_{mn}+\overline{UX1}_{mn}\right)\cdot x_n + \sum_{n=1}^{\infty}\left(\overline{VY0}_{mn}+\overline{VY1}_{mn}\right)\cdot y_n \\ &\quad + \sum_{n=1}^{\infty}\left(\overline{UX2}_{mn}+\overline{UX3}_{mn}\right)\cdot x_n + \sum_{n=1}^{\infty}\left(\overline{VY2}_{mn}+\overline{VY3}_{mn}\right)\cdot y_n \\ &= \pi s'_m \quad (m=1,2,3,\ldots)\end{aligned} \tag{2.183}$$

Equation (2.183) is simplified as follows:

$$XMA_m\cdot x_m + \sum_{n=1}^{\infty}XA'_{mn}\cdot x_n + YMA_m\cdot y_m + \sum_{n=1}^{\infty}YA'_{mn}\cdot y_n = P_m \tag{2.184}$$

where

$$
\left.
\begin{aligned}
XA'_{mn} &= M_m\left(\overline{UX0}_{mn}+\overline{UX1}_{mn}+\overline{UX2}_{mn}+\overline{UX3}_{mn}\right)/\pi \\
YA'_{mn} &= M_m\left(\overline{VY0}_{mn}+\overline{VY1}_{mn}+\overline{VY2}_{mn}+\overline{VY3}_{mn}\right)/\pi \\
\overline{UX2}_{mn}(\beta,\ \theta_2) &= \frac{K}{k}\left[\ \frac{1}{2}\frac{\sin(m+n)\beta-\sin(m+n)(\beta-\theta_2)}{m+n}+\frac{1}{2}\frac{\sin(m-n)\beta-\sin(m-n)(\beta-\theta_2)}{m-n}\right. \\
&\qquad \left.-\frac{\{\sin m\beta-\sin m(\beta-\theta_2)\}\cos n(\beta-\theta_2)}{m}\ \right] \\
\overline{VY2}_{mn}(\beta,\ \theta_2) &= \frac{K}{k}\left[\ -\frac{1}{2}\frac{\cos(m+n)\beta-\cos(m+n)(\beta-\theta_2)}{m+n}+\frac{1}{2}\frac{\cos(m-n)\beta-\cos(m-n)(\beta-\theta_2)}{m-n}\right. \\
&\qquad \left.-\frac{\{\sin m\beta-\sin m(\beta-\theta_2)\}\sin n(\beta-\theta_2)}{m}\ \right] \\
\overline{UX3}_{mn}(\beta,\ \theta_3) &= \frac{K}{k}\left[\ -\frac{1}{2}\frac{\sin(m+n)\beta-\sin(m+n)(\beta+\theta_3)}{m+n}-\frac{1}{2}\frac{\sin(m-n)\beta-\sin(m-n)(\beta+\theta_3)}{m-n}\right. \\
&\qquad \left.+\frac{\{\sin m\beta-\sin m(\beta+\theta_3)\}\cos n(\beta+\theta_3)}{m}\ \right] \\
\overline{VY3}_{mn}(\beta,\ \theta_3) &= \frac{K}{k}\left[\ \frac{1}{2}\frac{\cos(m+n)\beta-\cos(m+n)(\beta+\theta_3)}{m+n}-\frac{1}{2}\frac{\cos(m-n)\beta-\cos(m-n)(\beta+\theta_3)}{m-n}\right. \\
&\qquad \left.+\frac{\{\sin m\beta-\sin m(\beta+\theta_3)\}\sin n(\beta+\theta_3)}{m}\ \right]
\end{aligned}
\right\}
\tag{2.185}
$$

In the same manner, multiplying the non-dimensional nonlinear part of the restoring force $g(\theta)$ of Equation (2.179) by $\sin m\theta$ (m=1,2,3,$\cdots$) and integrating over the full period (0,2π) gives the following equation:

$$
\begin{aligned}
\int_0^{2\pi}\frac{g(\theta)}{ke_0}\sin m\theta d\theta &= \int_{-\theta_0}^{2\pi-\theta_0}\frac{K(z-e_0)}{ke_0}\sin m\theta d\theta \\
&= \int_{-\theta_0}^{\theta_1}\frac{K(z-e_0)}{ke_0}\sin m\theta d\theta+\int_{\beta-\theta_2}^{\beta+\theta_3}\frac{K(z-e_0)}{ke_0}\sin m\theta d\theta \\
&= \begin{cases}\pi t'_m & (m=n)\\ 0 & (m\neq n)\end{cases}\qquad (m=1,2,3,\ldots)
\end{aligned}
\tag{2.186}
$$

where the first term on the right side of Equation (2.186) is expressed by using Equation (2.54):

$$\begin{aligned}\int_{-\theta_0}^{\theta_1}\frac{g(\theta)}{ke_0}\sin m\theta d\theta &= \int_{-\theta_0}^{\theta_1}\frac{K(z-e_0)}{ke_0}\sin m\theta d\theta \\ &= \int_{-\theta_0}^{0}\frac{K(z-e_0)}{ke_0}\sin m\theta d\theta + \int_{0}^{\theta_1}\frac{K(z-e_0)}{ke_0}\sin m\theta d\theta \\ &= \sum_{n=1}^{\infty}\left(\overline{\overline{UX0}}_{mn} + \overline{\overline{UX1}}_{mn}\right)\cdot x_n + \sum_{n=1}^{\infty}\left(\overline{\overline{VY0}}_{mn} + \overline{\overline{VY1}}_{mn}\right)\cdot y_n\end{aligned} \tag{2.187}$$

Moreover, the second term on the right side of Equation (2.186) is expanded as follows:

$$\begin{aligned}\int_{\beta-\theta_2}^{\beta+\theta_3}\frac{g(\theta)}{ke_0}\sin m\theta d\theta &= \int_{\beta-\theta_2}^{\beta+\theta_3}\frac{K(z-e_0)}{ke_0}\sin m\theta d\theta \\ &= \int_{\beta-\theta_2}^{\beta}\frac{K(z-e_0)}{ke_0}\sin m\theta d\theta + \int_{\beta}^{\beta+\theta_3}\frac{K(z-e_0)}{ke_0}\sin m\theta d\theta \\ &= \frac{K}{k}\sum_{n=1}^{\infty}\Bigg[-\frac{1}{2}\frac{\cos(m+n)\beta-\cos(m+n)(\beta-\theta_2)}{m+n}-\frac{1}{2}\frac{\cos(m-n)\beta-\cos(m-n)(\beta-\theta_2)}{m-n} \\ &\qquad +\frac{\{\cos m\beta-\cos m(\beta-\theta_2)\}\cos n(\beta-\theta_2)}{m}\Bigg]\cdot x_n \\ &\quad +\frac{K}{k}\sum_{n=1}^{\infty}\Bigg[-\frac{1}{2}\frac{\sin(m+n)\beta-\sin(m+n)(\beta-\theta_2)}{m+n}+\frac{1}{2}\frac{\sin(m-n)\beta-\sin(m-n)(\beta-\theta_2)}{m-n} \\ &\qquad +\frac{\{\cos m\beta-\cos m(\beta-\theta_2)\}\sin n(\beta-\theta_2)}{m}\Bigg]\cdot y_n \\ &\quad +\frac{K}{k}\sum_{n=1}^{\infty}\Bigg[\frac{1}{2}\frac{\cos(m+n)\beta-\cos(m+n)(\beta+\theta_3)}{m+n}+\frac{1}{2}\frac{\cos(m-n)\beta-\cos(m-n)(\beta+\theta_3)}{m-n} \\ &\qquad -\frac{\{\cos m\beta-\cos m(\beta+\theta_3)\}\cos n(\beta+\theta_3)}{m}\Bigg]\cdot x_n \\ &\quad +\frac{K}{k}\sum_{n=1}^{\infty}\Bigg[\frac{1}{2}\frac{\sin(m+n)\beta-\sin(m+n)(\beta+\theta_3)}{m+n}-\frac{1}{2}\frac{\sin(m-n)\beta-\sin(m-n)(\beta+\theta_3)}{m-n} \\ &\qquad -\frac{\{\cos m\beta-\cos m(\beta+\theta_3)\}\sin n(\beta+\theta_3)}{m}\Bigg]\cdot y_n\end{aligned} \tag{2.188}$$

Substituting Equations (2.187) and (2.188) into Equation (2.186) gives the following equation:

$$
\begin{aligned}
\int_0^{2\pi} \frac{g(\theta)}{ke_0}\sin m\theta d\theta &= \int_{-\theta_0}^{2\pi-\theta_0} \frac{g(\theta)}{ke_0}\sin m\theta d\theta \\
&= \int_{-\theta_0}^{\theta_1} \frac{g(\theta)}{ke_0}\sin m\theta d\theta + \int_{\beta-\theta_2}^{\beta+\theta_3} \frac{g(\theta)}{ke_0}\sin m\theta d\theta \\
&= \int_{-\theta_0}^{\theta_1} \frac{K(z-e_0)}{ke_0}\sin m\theta d\theta + \int_{\beta-\theta_2}^{\beta+\theta_3} \frac{K(z-e_0)}{ke_0}\sin m\theta d\theta \\
&= \int_{-\theta_0}^{0} \frac{K(z-e_0)}{ke_0}\sin m\theta d\theta + \int_{0}^{\theta_1} \frac{K(z-e_0)}{ke_0}\sin m\theta d\theta \\
&\quad + \int_{\beta-\theta_2}^{\beta} \frac{K(z-e_0)}{ke_0}\sin m\theta d\theta + \int_{\beta}^{\beta+\theta_3} \frac{K(z-e_0)}{ke_0}\sin m\theta d\theta \\
&= \sum_{n=1}^{\infty}\left(\overline{\overline{UX0}}_{mn} + \overline{\overline{UX1}}_{mn} \right)\cdot x_n + \sum_{n=1}^{\infty}\left(\overline{\overline{VY0}}_{mn} + \overline{\overline{VY1}}_{mn} \right)\cdot y_n \\
&\quad + \sum_{n=1}^{\infty}\left(\overline{\overline{UX2}}_{mn} + \overline{\overline{UX3}}_{mn} \right)\cdot x_n + \sum_{n=1}^{\infty}\left(\overline{\overline{VY2}}_{mn} + \overline{\overline{VY3}}_{mn} \right)\cdot y_n \\
&= \pi t'_m \quad (m = 1,2,3,\ldots)
\end{aligned}
\tag{2.189}
$$

Equation (2.189) is simplified as follows:

$$
XMB_m \cdot x_m + \sum_{n=1}^{\infty} XB'_{mn} \cdot x_n + YMB_m \cdot y_m + \sum_{n=1}^{\infty} YB'_{mn} \cdot y_n = Q_m \tag{2.190}
$$

where

$$
\left.
\begin{aligned}
XB'_{mn} &= M_m\left(\overline{\overline{UX0}}_{mn} + \overline{\overline{UX1}}_{mn} + \overline{\overline{UX2}}_{mn} + \overline{\overline{UX3}}_{mn} \right)\Big/\pi \\
YB'_{mn} &= M_m\left(\overline{\overline{VY0}}_{mn} + \overline{\overline{VY1}}_{mn} + \overline{\overline{VY2}}_{mn} + \overline{\overline{VY3}}_{mn} \right)\Big/\pi \\
\overline{\overline{UX2}}_{mn} &= \frac{K}{k}\left[-\frac{\cos 2n\beta - \cos 2n(\beta-\theta_2)}{4n} + \frac{\{\cos n\beta - \cos n(\beta-\theta_2)\}\cos n(\beta-\theta_2)}{n} \right] \\
\overline{\overline{VY2}}_{mn} &= \frac{K}{k}\left[-\frac{\sin 2n\beta - \sin 2n(\beta-\theta_2)}{4n} + \frac{\theta_2}{2} + \frac{\{\cos n\beta - \cos n(\beta-\theta_2)\}\sin n(\beta-\theta_2)}{n} \right] \\
\overline{\overline{UX3}}_{mn} &= \frac{K}{k}\left[\frac{\cos 2n\beta - \cos 2n(\beta+\theta_3)}{4n} - \frac{\{\cos n\beta - \cos n(\beta+\theta_3)\}\cos n(\beta+\theta_3)}{n} \right] \\
\overline{\overline{VY3}}_{mn} &= \frac{K}{k}\left[\frac{\sin 2n\beta - \sin 2n(\beta+\theta_3)}{4n} + \frac{\theta_3}{2} - \frac{\{\cos n\beta - \cos n(\beta+\theta_3)\}\sin n(\beta+\theta_3)}{n} \right]
\end{aligned}
\right\}
\tag{2.191}
$$

Thus, the infinite dimensionless linear simultaneous equations for determining the non-dimensional Fourier coefficients x_n and y_n are obtained by Equations (2.184) and (2.190):

$$\left.\begin{aligned} XMA_m \cdot x_m + \sum_{n=1}^{\infty} XA'_{mn} \cdot x_n + YMA_m \cdot y_m + \sum_{n=1}^{\infty} YA'_{mn} \cdot y_n = P_m \\ XMB_m \cdot x_m + \sum_{n=1}^{\infty} XB'_{mn} \cdot x_n + YMB_m \cdot y_m + \sum_{n=1}^{\infty} YB'_{mn} \cdot y_n = Q_m \end{aligned}\right\} \tag{2.192}$$

(ii) Determination of Parameters (Ω, α, β, θ_0, θ_1, θ_2, θ_3)

The coefficients XMA_m, XA'_{mn},$\cdots Q_m$ of Equation (2.192) contain seven parameters (Ω, α, β, θ_0, θ_1, θ_2, θ_3). In resonance vibration Type I, four coefficient determinants were derived for determining the independent parameters. In Type II, these four coefficient determinants can be obtained in the same manner in Type I. While the independent parameters are three more than Type I, and three coefficient determinants are needed in addition to Type I. Here, these are derived.

(a) Switching-Over Condition : In the case of $\theta=\beta$

When $\theta=\beta$, the resulting displacement $z(\theta)$ is equal to the second maximum $e'_{\max}$ and velocity of the mass is equal to zero. Thus differentiating Equation (2.33) and setting $\theta=\beta$ gives the following equation:

$$\frac{\dot{z}(\theta)}{e_0} = \frac{d}{d\theta}\left\{\frac{z(\theta)}{e_0}\right\} = \sum_{n=1}^{\infty} n\left(-\sin n\beta \cdot x_n + \cos n\beta \cdot y_n\right) = 0 \tag{2.193}$$

Equation (2.193) is simplified as follows:

$$\sum_{n=1}^{\infty} XG_n \cdot x_n + \sum_{n=1}^{\infty} YG_n \cdot y_n = 0 \tag{2.194}$$

where

$$\left.\begin{aligned} XG_n &= n\cdot(-\sin n\beta) \\ YG_n &= n\cdot(\cos n\beta) \end{aligned}\right\} \tag{2.195}$$

And thus, the infinite dimensionless linear simultaneous equations are obtained by Equations (2.192) and (2.194) as follows:

$$\left.\begin{aligned} &\sum_{n=1}^{\infty} XG_n\cdot x_n + \sum_{n=1}^{\infty} YG_n\cdot y_n = 0 \\ &XMA_m\cdot x_m + \sum_{n=1}^{\infty} XA'_{mn}\cdot x_n + YMA_m\cdot y_m + \sum_{n=1}^{\infty} YA'_{mn}\cdot y_n = P_m \\ &XMB_m\cdot x_m + \sum_{n=1}^{\infty} XB'_{mn}\cdot x_n + YMB_m\cdot y_m + \sum_{n=1}^{\infty} YB'_{mn}\cdot y_n = Q_m \end{aligned}\right\} \tag{2.196}$$

The coefficient determinant of Equation (2.196) is expressed as follows:

$$\begin{aligned} \triangle_G &= \triangle_G(\,\Omega\,,\,\alpha\,,\,\theta_0\,,\,\theta_1\,,\,\beta\,,\,\theta_2\,,\,\theta_3\,) \\ &= \begin{vmatrix} XG_1 & XG_2 & \cdots & YG_1 & YG_2 & \cdots & 0 \\ XMA_1+XA'_{11} & XA'_{12} & \cdots & YMA_1+YA'_{11} & YA'_{12} & \cdots & -P_1 \\ XA'_{21} & XMA_2+XA'_{22} & \cdots & YA'_{21} & YMA_2+YA'_{22} & \cdots & -P_2 \\ \vdots & \vdots & & \vdots & \vdots & & \vdots \\ XMB_1+XB'_{11} & XB'_{12} & \cdots & YMB_1+YB'_{11} & YB'_{12} & \cdots & -Q_1 \\ XB'_{21} & XMB_2+XB'_{22} & \cdots & YB'_{21} & YMB_2+YB'_{22} & \cdots & -Q_2 \\ \vdots & \vdots & & \vdots & \vdots & & \vdots \end{vmatrix} \end{aligned} \tag{2.197}$$

(b) Switching-Over Condition : In the case of $\theta=\beta-\theta_2,\ \beta+\theta_3$

The resulting vibration containing the dwell phase angle θ_2 and θ_3 of Equation (2.173) are shown as follows:

$$\left.\begin{aligned} \frac{z-e_0}{e_0} &= \sum_{n=1}^{\infty}\left[\,\{\cos n\theta-\cos n(\beta-\theta_2)\}\cdot x_n+\{\sin n\theta-\sin n(\beta-\theta_2)\}\cdot y_n\,\right]\ (\text{S.O.C}:\ \theta=\beta-\theta_2) \\ \frac{z-e_0}{e_0} &= \sum_{n=1}^{\infty}\left[\,\{\cos n\theta-\cos n(\beta+\theta_3)\}\cdot x_n+\{\sin n\theta-\sin n(\beta+\theta_3)\}\cdot y_n\,\right]\ (\text{S.O.C}:\ \theta=\beta+\theta_3) \end{aligned}\right\}$$

Since these equations are equal, the following equation is obtained:

$$\sum_{n=1}^{\infty}\left[\ \left\{\cos n(\beta-\theta_2)-\cos n(\beta+\theta_3)\right\}\cdot x_n+\left\{\sin n(\beta-\theta_2)-\sin n(\beta+\theta_3)\right\}\cdot y_n\ \right]=0 \tag{2.198}$$

Equation (2.198) is simplified as follows:

$$\sum_{n=1}^{\infty}XH_n\cdot x_n+\sum_{n=1}^{\infty}YH_n\cdot y_n=0 \tag{2.199}$$

where

$$\left.\begin{aligned}XH_n&=\cos n(\beta-\theta_2)-\cos n(\beta+\theta_3)\\YH_n&=\sin n(\beta-\theta_2)-\sin n(\beta+\theta_3)\end{aligned}\right\} \tag{2.200}$$

And thus, the infinite dimensionless linear simultaneous equations are obtained by Equations (2.192) and (2.199) as follows:

$$\left.\begin{aligned}&\sum_{n=1}^{\infty}XH_n\cdot x_n+\sum_{n=1}^{\infty}YH_n\cdot y_n=0\\&XMA_m\cdot x_m+\sum_{n=1}^{\infty}XA'_{mn}\cdot x_n+YMA_m\cdot y_m+\sum_{n=1}^{\infty}YA'_{mn}\cdot y_n=P_m\\&XMB_m\cdot x_m+\sum_{n=1}^{\infty}XB'_{mn}\cdot x_n+YMB_m\cdot y_m+\sum_{n=1}^{\infty}YB'_{mn}\cdot y_n=Q_m\end{aligned}\right\} \tag{2.201}$$

The coefficient determinant of Equation (2.201) is expressed as follows:

$$\triangle_H = \triangle_H(\,\Omega\,,\,\alpha\,,\,\theta_0\,,\,\theta_1\,,\,\beta\,,\,\theta_2\,,\,\theta_3\,)$$

$$= \begin{vmatrix} XH_1 & XH_2 & \cdots & YH_1 & YH_2 & \cdots & 0 \\ XMA_1 + XA'_{11} & XA'_{12} & \cdots & YMA_1 + YA'_{11} & YA'_{12} & \cdots & -P_1 \\ XA'_{21} & XMA_2 + XA'_{22} & \cdots & YA'_{21} & YMA_2 + YA'_{22} & \cdots & -P_2 \\ \vdots & \vdots & & \vdots & \vdots & & \vdots \\ XMB_1 + XB'_{11} & XB'_{12} & \cdots & YMB_1 + YB'_{11} & YB'_{12} & \cdots & -Q_1 \\ XB'_{21} & XMB_2 + XB'_{22} & \cdots & YB'_{21} & YMB_2 + YB'_{22} & \cdots & -Q_2 \\ \vdots & \vdots & & \vdots & \vdots & & \vdots \end{vmatrix}$$

(2.202)

(c) Switching-Over Condition : In the case of $\theta = \theta_1$, $\beta - \theta_2$

The resulting vibration containing the dwell phase angle θ_1 and θ_3 are shown in Equations (2.35) and (2.173):

$$\left.\begin{aligned} \frac{z-e_0}{e_0} &= \sum_{n=1}^{\infty}\{(\cos n\theta - \cos n\theta_1)x_n + (\sin n\theta - \sin n\theta_1)y_n\} \qquad (\text{S.O.C} : \theta = \theta_1) \\ \frac{z-e_0}{e_0} &= \sum_{n=1}^{\infty}[\,\{\cos n\theta - \cos n(\beta-\theta_2)\}\cdot x_n + \{\sin n\theta - \sin n(\beta-\theta_2)\}\cdot y_n\,] \quad (\text{S.O.C} : \theta = \beta - \theta_2) \end{aligned}\right\}$$

Since these equations are equal, the following equation is obtained:

$$\sum_{n=1}^{\infty}[\,\{\cos n\theta_1 - \cos n(\beta-\theta_2)\}\cdot x_n + \{\sin n\theta_1 - \sin n(\beta-\theta_2)\}\cdot y_n\,] = 0 \qquad (2.203)$$

Equation (2.198) is simplified as follows:

$$\sum_{n=1}^{\infty} XI_n \cdot x_n + \sum_{n=1}^{\infty} YI_n \cdot y_n = 0 \qquad (2.204)$$

where

$$\left.\begin{aligned} XI_n &= \cos n\theta_1 - \cos n(\beta - \theta_2) \\ YI_n &= \sin n\theta_1 - \sin n(\beta - \theta_2) \end{aligned}\right\} \tag{2.205}$$

And thus, the infinite dimensionless linear simultaneous equations are obtained by Equations (2.192) and (2.199) as follows:

$$\left.\begin{aligned} &\sum_{n=1}^{\infty} XI_n \cdot x_n + \sum_{n=1}^{\infty} YI_n \cdot y_n = 0 \\ &XMA_m \cdot x_m + \sum_{n=1}^{\infty} XA'_{mn} \cdot x_n + YMA_m \cdot y_m + \sum_{n=1}^{\infty} YA'_{mn} \cdot y_n = P_m \\ &XMB_m \cdot x_m + \sum_{n=1}^{\infty} XB'_{mn} \cdot x_n + YMB_m \cdot y_m + \sum_{n=1}^{\infty} YB'_{mn} \cdot y_n = Q_m \end{aligned}\right\} \tag{2.206}$$

The coefficient determinant of Equation (2.201) is expressed as follows:

$$\begin{aligned} \triangle_I &= \triangle_I(\ \Omega\ ,\ \alpha\ ,\ \theta_0\ ,\ \theta_1\ ,\ \beta\ ,\ \theta_2\ ,\ \theta_3\ ) \\ &= \begin{vmatrix} XI_1 & XI_2 & \cdots & YI_1 & YI_2 & \cdots & 0 \\ XMA_1 + XA'_{11} & XA'_{12} & \cdots & YMA_1 + YA'_{11} & YA'_{12} & \cdots & -P_1 \\ XA'_{21} & XMA_2 + XA'_{22} & \cdots & YA'_{21} & YMA_2 + YA'_{22} & \cdots & -P_2 \\ \vdots & \vdots & & \vdots & \vdots & & \vdots \\ XMB_1 + XB'_{11} & XB'_{12} & \cdots & YMB_1 + YB'_{11} & YB'_{12} & \cdots & -Q_1 \\ XB'_{21} & XMB_2 + XB'_{22} & \cdots & YB'_{21} & YMB_2 + YB'_{22} & \cdots & -Q_2 \\ \vdots & \vdots & & \vdots & \vdots & & \vdots \end{vmatrix} \end{aligned} \tag{2.207}$$

First, setting value of the coefficient determinants in Equations (2.197), (2.202), (2.207) and obtained by using the same conditions in Type I all zero and solving, the seven parameters (Ω, α, β, θ_0, θ_1, θ_2, θ_3) can be determined. Next, substituting determined seven parameters into the infinite dimensionless linear simultaneous equations in Equation (2.192) and solving gives the non-dimensional Fourier coefficients x_n and y_n. Finally, the resulting vibration can be calculated by Equation (2.33).

2.1.4 Analysis of Stability Criterion for Superharmonic Resonance

Here, stability analysis for periodic solutions of superharmonic resonance Type II is carried out. This stability analysis employs a variational equation to investigate consequences of a minute perturbation to a steady forced vibration predicted by a periodic solution for an original equation of motion.

(1) Hill's Equation and Stability Criterion

The restoring force of the analysis system in resonance vibration Type II is expressed as follows:

$$\left.\begin{array}{ll} f(z)=kz & : \text{Interval I} \quad (\theta_1 \le \theta \le \beta-\theta_2\ ,\ \beta+\theta_3 \le \theta \le 2\pi-\theta_0) \\ f(z)=kz+K(z-e_0) & : \text{Interval II} \quad (-\theta_0 \le \theta \le \theta_1\ ,\ \beta-\theta_2 \le \theta \le \beta+\theta_3) \end{array}\right\} \tag{2.208}$$

Differentiating the restoring force $f(z)$ of Equation (2.208) with respect to z gives the following equations:

$$\left.\begin{array}{ll} \dfrac{1}{k}\left\{\dfrac{d}{dz}f(z)\right\}=1 & : \text{Interval I} \quad (\theta_1 \le \theta \le \beta-\theta_2\ ,\ \beta+\theta_3 \le \theta \le 2\pi-\theta_0) \\ \dfrac{1}{k}\left\{\dfrac{d}{dz}f(z)\right\}=1+\dfrac{K}{k} & : \text{Interval II} \quad (-\theta_0 \le \theta \le \theta_1\ ,\ \beta-\theta_2 \le \theta \le \beta+\theta_3) \end{array}\right\} \tag{2.209}$$

Equation (2.209) is transformed into the following expression by using the step function $\varphi(\theta)$ shown in Figure 2.7:

$$\frac{1}{k}\left\{\frac{d}{dz}f(z)\right\}=1+\frac{K}{k}\varphi(\theta) \tag{2.210}$$

where

$$\left.\begin{array}{ll} \varphi(\theta)=0 & : \text{Interval I} \quad (\theta_1 \le \theta \le \beta-\theta_2\ ,\ \beta+\theta_3 \le \theta \le 2\pi-\theta_0) \\ \varphi(\theta)=1 & : \text{Interval II} \quad (-\theta_0 \le \theta \le \theta_1\ ,\ \beta-\theta_2 \le \theta \le \beta+\theta_3) \end{array}\right\} \tag{2.211}$$

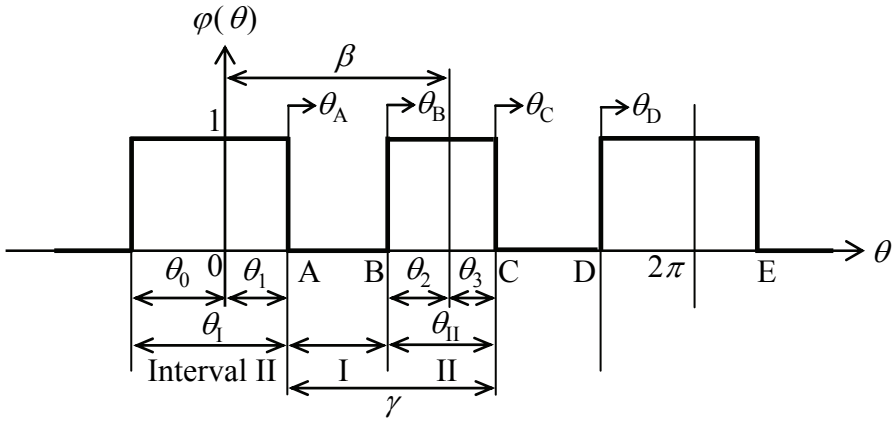

Figure 2.7 Periodic function $\varphi(\theta)$ for Type II

Equation (2.88) is rewritten as follows by using Equation (2.210):

$$\Omega^2 \frac{d^2x}{d\theta^2} + 2\Omega\zeta \frac{dx}{d\theta} + \left\{1 + \frac{K}{k}\varphi(\theta)\right\} \cdot x = 0 \tag{2.212}$$

The variable $\xi(\theta)$ satisfying the following equation is used:

$$\begin{aligned} x(\theta) &= \exp\left(-\frac{\zeta}{\Omega}\theta_\alpha\right) \cdot \exp\left\{-\frac{1}{2}\int\left(\frac{2\zeta}{\Omega}\right)d\theta\right\} \cdot \xi(\theta) \\ &= \exp\left\{-\frac{\zeta}{\Omega}(\theta + \theta_\alpha)\right\} \cdot \xi(\theta) \end{aligned} \tag{2.213}$$

Substituting Equation (2.213) into Equation (2.212) gives the following equation:

$$\frac{d^2\xi}{d\theta^2} + r(\theta) \cdot \xi = 0 \tag{2.214}$$

where

$$r(\theta) = \left[\frac{1}{\Omega^2}\left\{1 + \frac{K}{k}\varphi(\theta)\right\} - \frac{\zeta^2}{\Omega^2} \right] \tag{2.215}$$

(2) Expression of Real Number *A*

The stability criterion is set up in the above analysis. Here, the real number A of Equation (2.106) for superharmonic resonance Type II is derived by determining the fundamental solutions after the fundamental period. The fundamental solutions of Equation (2.214) can be solved by inosculating method.

The $r(\theta)$ of Equation (2.215) is the periodic function of 2π period and shown as follows:

$$\begin{aligned} r(\theta) &= r(\theta+T) \\ &= \left[\frac{1}{\Omega^2}\left\{ 1+\frac{K}{k}\varphi(\theta) \right\} - \frac{\zeta^2}{\Omega^2} \right] \\ &= \left\{ \begin{array}{ll} {\tau_1}^2 = \dfrac{1-\zeta^2}{\Omega^2} & : \text{Interval I} \ \left(\theta_1 \le \theta \le \beta-\theta_2 \ , \ \beta+\theta_3 \le \theta \le 2\pi-\theta_0\right) \\ {\tau_2}^2 = \dfrac{1-\zeta^2}{\Omega^2} + \dfrac{1}{\Omega^2}\cdot\dfrac{K}{k} & : \text{Interval II} \ \left(-\theta_0 \le \theta \le \theta_1 \ , \ \beta-\theta_2 \le \theta \le \beta+\theta_3\right) \end{array} \right\} \end{aligned} \tag{2.216}$$

(i) In the case of the Fundamental Solution ξ_1

(a) In the interval AB

The Hill's equation of Equation (2.214) is

$$\frac{d^2\xi}{d\theta^2} + {\tau_1}^2\xi = 0 \qquad \left(\theta_1 \le \theta \le \beta-\theta_2\right) \tag{2.217}$$

Using the independent variable θ_A shown in Figure 2.7, Equation (2.217) is rewritten as follows:

$$\frac{d^2\xi(\theta_A)}{d{\theta_A}^2} + {\tau_1}^2\cdot\xi(\theta_A) = 0 \qquad \left(0 \le \theta_A \le \gamma-\theta_{II}\right) \tag{2.218}$$

where

$$\theta_{II} \equiv \theta_2+\theta_3 \tag{2.219}$$

$$\gamma \equiv \beta - \theta_1 + \theta_3 \tag{2.220}$$

Since Equation (2.218) is the second order differential equation, the solution assumed in the form:

$$\left.\begin{aligned} \xi_1(\theta_A) &= \overline{\overline{C_{A1}}} \cos\tau_1\theta_A + \overline{\overline{S_{A1}}} \sin\tau_1\theta_A \\ \dot{\xi}_1(\theta_A) &= \tau_1\left(-\overline{\overline{C_{A1}}} \sin\tau_1\theta_A + \overline{\overline{S_{A1}}} \cos\tau_1\theta_A \right) \end{aligned}\right\} \tag{2.221}$$

Thus $x_1(\theta_A)$ is expressed as follows:

$$\left.\begin{aligned} x_1(\theta_A) &= \exp(-\eta\theta_A)\cdot\left(\overline{\overline{C_{A1}}} \cos\tau_1\theta_A + \overline{\overline{S_{A1}}} \sin\tau_1\theta_A \right) \\ \dot{x}_1(\theta_A) &= -\eta\cdot x_1(\theta_A) + \exp(-\eta\theta_A)\cdot\left\{ \tau_1\left(-\overline{\overline{C_{A1}}} \sin\tau_1\theta_A + \overline{\overline{S_{A2}}} \cos\tau_1\theta_A \right) \right\} \end{aligned}\right\} \tag{2.222}$$

Applying the initial condition of Equation (2.99) to the fundamental solution of Equation (2.221) give the following equations:

$$\left.\begin{aligned} \xi_1(\theta_A = 0) &= \overline{\overline{C_{A1}}} = 1 \\ \dot{\xi}_1(\theta_A = 0) &= \tau_1 \overline{\overline{S_{A1}}} = 0 \end{aligned}\right\} \tag{2.223}$$

Thus

$$\overline{\overline{C_{A1}}} = 1 \quad , \quad \overline{\overline{S_{A1}}} = 0 \tag{2.224}$$

Substituting Equation (2.224) into Equations (2.221) and (2.222) gives the following equations:

$$\left.\begin{aligned} \xi_1(\theta_A) &= \cos\tau_1\theta_A \\ \dot{\xi}_1(\theta_A) &= -\tau_1 \sin\tau_1\theta_A \end{aligned}\right\} \tag{2.225}$$

$$\left.\begin{aligned} x_1(\theta_A) &= \exp(-\eta\theta_A)\cdot\cos\tau_1\theta_A \\ \dot{x}_1(\theta_A) &= -\eta\cdot x_1(\theta_A)+\exp(-\eta\theta_A)\cdot(-\tau_1\sin\tau_1\theta_A) \\ &= \exp(-\eta\theta_A)\cdot(-\eta\cos\tau_1\theta_A-\tau_1\sin\tau_1\theta_A) \end{aligned}\right\} \tag{2.226}$$

(b) In the interval BC

The Hill's equation of Equation (2.214) is

$$\frac{d^2\xi}{d\theta^2}+{\tau_2}^2\xi=0 \qquad (\beta-\theta_2\le\theta\le\beta+\theta_3) \tag{2.227}$$

Using the independent variable θ_B shown in Figure 2.7, Equation (2.227) is rewritten as follows:

$$\frac{d^2\xi(\theta_B)}{d{\theta_B}^2}+{\tau_2}^2\cdot\xi(\theta_B)=0 \qquad (0\le\theta_B\le\theta_{II}) \tag{2.228}$$

Since Equation (2.228) is the second order differential equation, the solution assumed in the form:

$$\left.\begin{aligned} \xi_1(\theta_B) &= \overline{\overline{C_{B1}}}\cos\tau_2\theta_B+\overline{\overline{S_{B1}}}\sin\tau_2\theta_B \\ \dot{\xi}_1(\theta_B) &= \tau_2\left(-\overline{\overline{C_{B1}}}\sin\tau_2\theta_B+\overline{\overline{S_{B1}}}\cos\tau_2\theta_B\right) \end{aligned}\right\} \tag{2.229}$$

Thus $x_1(\theta_B)$ is expressed as follows:

$$\left.\begin{aligned} x_1(\theta_B) &= \exp\{-\eta(\gamma-\theta_{II})\}\cdot\left\{\exp(-\eta\theta_B)\cdot\left(\overline{\overline{C_{B1}}}\cos\tau_2\theta_B+\overline{\overline{S_{B1}}}\sin\tau_2\theta_B\right)\right\} \\ \dot{x}_1(\theta_B) &= -\eta\cdot x_1(\theta_B)+\exp\{-\eta(\gamma-\theta_{II})\}\cdot\left[\exp(-\eta\theta_B)\cdot\left\{\tau_2\left(-\overline{\overline{C_{B1}}}\sin\tau_2\theta_B+\overline{\overline{S_{B1}}}\cos\tau_2\theta_B\right)\right\}\right] \end{aligned}\right\} \tag{2.230}$$

where the relation of the independent variables θ_B and θ_A is

$$\theta_B=0: \quad \theta_A=\gamma-\theta_{II} \tag{2.231}$$

Applying the relation of Equation (2.231) to the fundamental solution of Equation (2.229) gives the following equations:

$$\left.\begin{aligned}\xi_1(\theta_{\mathrm{B}}=0)&=\overline{\overline{C_{B1}}}\\&=\xi_1(\theta_{\mathrm{A}}=\gamma-\theta_{\mathrm{II}})=\cos\tau_1(\gamma-\theta_{\mathrm{II}})\\\dot{\xi}_1(\theta_{\mathrm{B}}=0)&=\tau_2\overline{\overline{S_{B1}}}\\&=\dot{\xi}_1(\theta_{\mathrm{A}}=\gamma-\theta_{\mathrm{II}})=-\tau_1\sin\tau_1(\gamma-\theta_{\mathrm{II}})\end{aligned}\right\} \tag{2.232}$$

Thus

$$\left.\begin{aligned}\overline{\overline{C_{B1}}}&=\cos\tau_1(\gamma-\theta_{\mathrm{II}})\\\overline{\overline{S_{B1}}}&=-\frac{\tau_1}{\tau_2}\sin\tau_1(\gamma-\theta_{\mathrm{II}})\end{aligned}\right\} \tag{2.233}$$

Substituting Equation (2.233) into Equation (2.230) gives the following equations:

$$\left.\begin{aligned}x_1(\theta_{\mathrm{B}})&=\exp(-\eta\theta_{\mathrm{B}})\cdot\left(\ \overline{\overline{C'_{B1}}}\cos\tau_2\theta_{\mathrm{B}}+\overline{\overline{S'_{B1}}}\sin\tau_2\theta_{\mathrm{B}}\ \right)\\\dot{x}_1(\theta_{\mathrm{B}})&=-\eta\cdot x_1(\theta_{\mathrm{B}})+\exp(-\eta\theta_{\mathrm{B}})\cdot\left\{\ \tau_2\left(\ -\overline{\overline{C'_{B1}}}\sin\tau_2\theta_{\mathrm{B}}+\overline{\overline{S'_{B1}}}\cos\tau_2\theta_{\mathrm{B}}\ \right)\right\}\\&=\exp(-\eta\theta_{\mathrm{B}})\cdot\left\{\left(\ -\eta\overline{\overline{C'_{B1}}}+\tau_2\overline{\overline{S'_{B1}}}\ \right)\cos\tau_2\theta_{\mathrm{B}}+\left(\ -\tau_2\overline{\overline{C'_{B1}}}-\eta\overline{\overline{S'_{B1}}}\ \right)\sin\tau_2\theta_{\mathrm{B}}\right\}\end{aligned}\right\} \tag{2.234}$$

where

$$\left.\begin{aligned}\overline{\overline{C'_{B1}}}&=\exp\{-\eta(\gamma-\theta_{\mathrm{II}})\}\cdot\overline{\overline{C_{B1}}}\\\overline{\overline{S'_{B1}}}&=\exp\{-\eta(\gamma-\theta_{\mathrm{II}})\}\cdot\overline{\overline{S_{B1}}}\end{aligned}\right\} \tag{2.235}$$

(c) In the interval CD

The Hill's equation of Equation (2.214) is

$$\frac{d^2\xi}{d\theta^2} + {\tau_1}^2\xi = 0 \qquad (\beta + \theta_3 \le \theta \le 2\pi - \theta_0) \tag{2.236}$$

Using the independent variable θ_C shown in Figure 2.7, Equation (2.236) is rewritten as follows:

$$\frac{d^2\xi(\theta_C)}{d{\theta_C}^2} + {\tau_1}^2 \cdot \xi(\theta_C) = 0 \qquad (0 \le \theta_C \le 2\pi - \gamma - \theta_I) \tag{2.237}$$

Since Equation (2.237) is the second order differential equation, the solution assumed in the form:

$$\left.\begin{aligned} \xi_1(\theta_C) &= \overline{\overline{C_{C1}}} \cos\tau_1\theta_C + \overline{\overline{S_{C1}}} \sin\tau_1\theta_C \\ \dot{\xi}_1(\theta_C) &= \tau_1\left(-\overline{\overline{C_{C1}}} \sin\tau_1\theta_C + \overline{\overline{S_{C1}}} \cos\tau_1\theta_C \right) \end{aligned}\right\} \tag{2.238}$$

Thus $x_1(\theta_C)$ is expressed as follows:

$$\left.\begin{aligned} x_1(\theta_C) &= \exp(-\eta\gamma)\cdot\exp(-\eta\theta_C)\cdot\left(\overline{\overline{C_{C1}}} \cos\tau_1\theta_C + \overline{\overline{S_{C1}}} \sin\tau_1\theta_C \right) \\ \dot{x}_1(\theta_C) &= -\eta\cdot x_1(\theta_C) + \exp(-\eta\theta_C)\cdot\left[\exp(-\eta\theta_C)\cdot\left\{ \tau_1\left(-\overline{\overline{C_{C1}}} \sin\tau_1\theta_C + \overline{\overline{S_{C1}}} \cos\tau_1\theta_C \right) \right\} \right] \end{aligned}\right\} \tag{2.239}$$

where the relation of the independent variables θ_C and θ_B is

$$\theta_C = 0 : \quad \theta_B = \theta_{II} \tag{2.240}$$

Applying the relation of Equation (2.240) to the fundamental solution of Equation (2.238) gives the following equations:

$$\left.\begin{aligned}\xi_1(\theta_C=0)&=\overline{\overline{C_{C1}}}\\&=\xi_1(\theta_B=\theta_{II})=\overline{\overline{C_{B1}}}\cos\tau_2\theta_{II}+\overline{\overline{S_{B1}}}\sin\tau_2\theta_{II}\\\dot{\xi}_1(\theta_C=0)&=\tau_1\overline{\overline{S_{C1}}}\\&=\dot{\xi}_1(\theta_B=\theta_{II})=\tau_2\left(-\overline{\overline{C_{B1}}}\sin\tau_2\theta_{II}+\overline{\overline{S_{B1}}}\cos\tau_2\theta_{II}\right)\end{aligned}\right\} \tag{2.241}$$

Thus

$$\left.\begin{aligned}\overline{\overline{C_{C1}}}&=\overline{\overline{C_{B1}}}\cos\tau_2\theta_{II}+\overline{\overline{S_{B1}}}\sin\tau_2\theta_{II}\\\overline{\overline{S_{C1}}}&=\frac{\tau_2}{\tau_1}\left(-\overline{\overline{C_{B1}}}\sin\tau_2\theta_{II}+\overline{\overline{S_{B1}}}\cos\tau_2\theta_{II}\right)\end{aligned}\right\} \tag{2.242}$$

Substituting Equation (2.242) into Equation (2.239) gives the following equation:

$$\left.\begin{aligned}x_1(\theta_C)&=\exp(-\eta\theta_C)\cdot\left(\overline{\overline{C'_{C1}}}\cos\tau_2\theta_C+\overline{\overline{S'_{C1}}}\sin\tau_2\theta_C\right)\\\dot{x}_1(\theta_C)&=-\eta\cdot x_1(\theta_C)+\exp(-\eta\theta_C)\cdot\left\{\tau_2\left(-\overline{\overline{C'_{C1}}}\sin\tau_2\theta_C+\overline{\overline{S'_{C1}}}\cos\tau_2\theta_C\right)\right\}\\&=\exp(-\eta\theta_C)\cdot\left\{\left(-\eta\overline{\overline{C'_{C1}}}+\tau_2\overline{\overline{S'_{C1}}}\right)\cos\tau_2\theta_C+\left(-\tau_2\overline{\overline{C'_{C1}}}-\eta\overline{\overline{S'_{C1}}}\right)\sin\tau_2\theta_C\right\}\end{aligned}\right\} \tag{2.243}$$

where

$$\left.\begin{aligned}\overline{\overline{C'_{C1}}}&=\exp(-\eta\gamma)\cdot\overline{\overline{C_{C1}}}\\\overline{\overline{S'_{C1}}}&=\exp(-\eta\gamma)\cdot\overline{\overline{S_{C1}}}\end{aligned}\right\} \tag{2.244}$$

(d) In the interval DE

The Hill's equation of Equation (2.214) is

$$\frac{d^2\xi}{d\theta^2}+{\tau_2}^2\xi=0\qquad(2\pi-\theta_0\le\theta\le2\pi+\theta_1) \tag{2.245}$$

Using the independent variable θ_D shown in Figure 2.7, Equation (2.245) is rewritten as follows:

$$\frac{d^2\xi(\theta_D)}{d\theta_D{}^2}+\tau_2{}^2\cdot\xi(\theta_D)=0 \qquad (0\le\theta_D\le\theta_I) \tag{2.246}$$

Since Equation (2.246) is the second order differential equation, the solution assumed in the form:

$$\left.\begin{aligned}\xi_1(\theta_D)&=\overline{\overline{C_{D1}}}\cos\tau_2\theta_D+\overline{\overline{S_{D1}}}\sin\tau_2\theta_D\\ \dot{\xi}_1(\theta_D)&=\tau_2\left(-\overline{\overline{C_{D1}}}\sin\tau_2\theta_D+\overline{\overline{S_{D1}}}\cos\tau_2\theta_D\right)\end{aligned}\right\} \tag{2.247}$$

Thus $x_1(\theta_D)$ is expressed as follows:

$$\left.\begin{aligned}x_1(\theta_D)&=\exp\{-\eta(2\pi-\theta_I)\}\cdot\left\{\exp(-\eta\theta_D)\cdot\left(\overline{\overline{C_{D1}}}\cos\tau_2\theta_D+\overline{\overline{S_{D1}}}\sin\tau_2\theta_D\right)\right\}\\ \dot{x}_1(\theta_D)&=-\eta\cdot x_1(\theta_D)+\exp\{-\eta(2\pi-\theta_I)\}\cdot\left[\exp(-\eta\theta_D)\cdot\left\{\tau_2\left(-\overline{\overline{C_{D1}}}\sin\tau_2\theta_D+\overline{\overline{S_{D1}}}\cos\tau_2\theta_D\right)\right\}\right]\end{aligned}\right\} \tag{2.248}$$

where the relation of the independent variables θ_D and θ_C is

$$\theta_D=0\ :\ \ \theta_C=2\pi-\gamma-\theta_I \tag{2.249}$$

Applying the relation of Equation (2.249) to the fundamental solution of Equation (2.247) gives the following equations:

$$\left.\begin{aligned}\xi_1(\theta_D=0)&=\overline{\overline{C_{D1}}}\\ &=\xi_1(\theta_C=2\pi-\gamma-\theta_I)\\ &=\overline{\overline{C_{C1}}}\cos\tau_1(2\pi-\gamma-\theta_I)+\overline{\overline{S_{C1}}}\sin\tau_1(2\pi-\gamma-\theta_I)\\ \dot{\xi}_1(\theta_D=0)&=\tau_2\overline{\overline{S_{D1}}}\\ &=\dot{\xi}_1(\theta_C=2\pi-\gamma-\theta_I)\\ &=\tau_1\left\{-\overline{\overline{C_{C1}}}\sin\tau_1(2\pi-\gamma-\theta_I)+\overline{\overline{S_{C2}}}\cos\tau_1(2\pi-\gamma-\theta_I)\right\}\end{aligned}\right\} \tag{2.250}$$

Thus

$$\left.\begin{aligned}\overline{\overline{C_{D1}}} &= \overline{\overline{C_{C1}}}\cos\tau_1(2\pi-\gamma-\theta_{\mathrm{I}})+\overline{\overline{S_{C1}}}\sin\tau_1(2\pi-\gamma-\theta_{\mathrm{I}})\\ \overline{\overline{S_{D1}}} &= \frac{\tau_1}{\tau_2}\left\{-\overline{\overline{C_{C1}}}\sin\tau_1(2\pi-\gamma-\theta_{\mathrm{I}})+\overline{\overline{S_{C1}}}\cos\tau_1(2\pi-\gamma-\theta_{\mathrm{I}})\right\}\end{aligned}\right\} \tag{2.251}$$

Substituting (2.251) into Equation (2.248) gives the following equations:

$$\left.\begin{aligned}x_1(\theta_{\mathrm{D}}) &= \exp(-\eta\theta_{\mathrm{D}})\cdot\left(\overline{\overline{C'_{D1}}}\cos\tau_2\theta_{\mathrm{D}}+\overline{\overline{S'_{D1}}}\sin\tau_2\theta_{\mathrm{D}}\right)\\ \dot{x}_1(\theta_{\mathrm{D}}) &= -\eta\cdot x_1(\theta_{\mathrm{D}})+\exp(-\eta\theta_{\mathrm{D}})\cdot\left\{\tau_2\left(-\overline{\overline{C'_{D1}}}\sin\tau_2\theta_{\mathrm{D}}+\overline{\overline{S'_{D1}}}\cos\tau_2\theta_{\mathrm{D}}\right)\right\}\\ &= \exp(-\eta\theta_{\mathrm{D}})\cdot\left\{\left(-\eta\overline{\overline{C'_{D1}}}+\tau_2\overline{\overline{S'_{D1}}}\right)\cos\tau_2\theta_{\mathrm{D}}+\left(-\tau_2\overline{\overline{C'_{D1}}}-\eta\overline{\overline{S'_{D1}}}\right)\sin\tau_2\theta_{\mathrm{D}}\right\}\end{aligned}\right\} \tag{2.252}$$

where

$$\left.\begin{aligned}\overline{\overline{C'_{D1}}} &= \exp\{-\eta(2\pi-\theta_{\mathrm{I}})\}\cdot\overline{\overline{C_{D1}}}\\ \overline{\overline{S'_{D1}}} &= \exp\{-\eta(2\pi-\theta_{\mathrm{I}})\}\cdot\overline{\overline{S_{D1}}}\end{aligned}\right\} \tag{2.253}$$

(ii) In the case of the Fundamental Solution ξ_2

(a) In the interval AB

The Hill's equation of Equation (2.214) is

$$\frac{d^2\xi}{d\theta^2}+\tau_1{}^2\xi=0 \qquad (\theta_1\le\theta\le\beta-\theta_2) \tag{2.254}$$

Using the independent variable θ_{A} shown in Figure 2.7, Equation (2.254) is rewritten as follows:

$$\frac{d^2\xi(\theta_{\mathrm{A}})}{d\theta_{\mathrm{A}}{}^2}+\tau_1{}^2\cdot\xi(\theta_{\mathrm{A}})=0 \qquad (0\le\theta_{\mathrm{A}}\le\gamma-\theta_{\mathrm{II}}) \tag{2.255}$$

where

$$\theta_{\mathrm{II}}\equiv\theta_2+\theta_3 \tag{2.256}$$

$$\gamma \equiv \beta - \theta_1 + \theta_3 \tag{2.257}$$

Since Equation (2.255) is the second order differential equation, the solution assumed in the form:

$$\left.\begin{aligned} \xi_2(\theta_A) &= \overline{\overline{C_{A2}}} \cos\tau_1\theta_A + \overline{\overline{S_{A2}}} \sin\tau_1\theta_A \\ \dot{\xi}_2(\theta_A) &= \tau_1\left(-\overline{\overline{C_{A2}}} \sin\tau_1\theta_A + \overline{\overline{S_{A2}}} \cos\tau_1\theta_A \right) \end{aligned}\right\} \tag{2.258}$$

Thus $x_2(\theta_A)$ is expressed as follows:

$$\left.\begin{aligned} x_2(\theta_A) &= \exp(-\eta\theta_A)\cdot\left(\overline{\overline{C_{A2}}} \cos\tau_1\theta_A + \overline{\overline{S_{A2}}} \sin\tau_1\theta_A \right) \\ \dot{x}_2(\theta_A) &= -\eta\cdot x_2(\theta_A) + \exp(-\eta\theta_A)\cdot\left\{ \tau_1\left(-\overline{\overline{C_{A2}}} \sin\tau_1\theta_A + \overline{\overline{S_{A2}}} \cos\tau_1\theta_A \right) \right\} \end{aligned}\right\} \tag{2.259}$$

Applying the initial condition of Equation (2.99) to the fundamental solution of Equation (2.258) gives the following equations:

$$\left.\begin{aligned} \xi_2(\theta_A = 0) &= \overline{\overline{C_{A2}}} = 0 \\ \dot{\xi}_2(\theta_A = 0) &= \tau_1 \overline{\overline{S_{A2}}} = 1 \end{aligned}\right\} \tag{2.260}$$

Thus

$$\overline{\overline{C_{A2}}} = 0 \quad , \quad \overline{\overline{S_{A2}}} = \frac{1}{\tau_1} \tag{2.261}$$

Substituting (2.261) into Equations (2.258) and (2.259) gives the following equations:

$$\left.\begin{aligned} \xi_2(\theta_A) &= \frac{1}{\tau_1} \sin\tau_1\theta_A \\ \dot{\xi}_2(\theta_A) &= \cos\tau_1\theta_A \end{aligned}\right\} \tag{2.262}$$

$$\left.\begin{aligned} x_2(\theta_A) &= \exp(-\eta\theta_A)\cdot\left(\frac{1}{\tau_1}\sin\tau_1\theta_A\right) \\ \dot{x}_2(\theta_A) &= -\eta\cdot x_2(\theta_A)+\exp(-\eta\theta_A)\cdot(\cos\tau_1\theta_A) \\ &= \exp(-\eta\theta_A)\cdot\left(-\frac{\eta}{\tau_1}\sin\tau_1\theta_A+\tau_1\cos\tau_1\theta_A\right) \end{aligned}\right\} \tag{2.263}$$

(b) In the interval BC

The Hill's equation of Equation (2.214) is

$$\frac{d^2\xi}{d\theta^2}+{\tau_2}^2\xi=0 \qquad (\beta-\theta_2\le\theta\le\beta+\theta_3) \tag{2.264}$$

Using the independent variable θ_B shown in Figure 2.7, Equation (2.264) is rewritten as follows:

$$\frac{d^2\xi(\theta_B)}{d{\theta_B}^2}+{\tau_2}^2\cdot\xi(\theta_B)=0 \qquad (0\le\theta_B\le\theta_{II}) \tag{2.265}$$

Since Equation (2.265) is the second order differential equation, the solution assumed in the form:

$$\left.\begin{aligned} \xi_2(\theta_B) &= \overline{\overline{C_{B2}}}\cos\tau_2\theta_B+\overline{\overline{S_{B2}}}\sin\tau_2\theta_B \\ \dot{\xi}_2(\theta_B) &= \tau_2\left(-\overline{\overline{C_{B2}}}\sin\tau_2\theta_B+\overline{\overline{S_{B2}}}\cos\tau_2\theta_B\right) \end{aligned}\right\} \tag{2.266}$$

Thus $x_2(\theta_B)$ is expressed as follows:

$$\left.\begin{aligned} x_2(\theta_B) &= \exp\{-\eta(\gamma-\theta_{II})\}\cdot\left\{\exp(-\eta\theta_B)\cdot\left(\overline{\overline{C_{B2}}}\cos\tau_2\theta_B+\overline{\overline{S_{B2}}}\sin\tau_2\theta_B\right)\right\} \\ \dot{x}_2(\theta_B) &= -\eta\cdot x_1(\theta_B)+\exp\{-\eta(\gamma-\theta_{II})\}\cdot\left[\exp(-\eta\theta_B)\cdot\left\{\tau_2\left(-\overline{\overline{C_{B2}}}\sin\tau_2\theta_B+\overline{\overline{S_{B2}}}\cos\tau_2\theta_B\right)\right\}\right] \end{aligned}\right\} \tag{2.267}$$

where the relation of the independent variables θ_{B} and θ_{A} is

$$\theta_{\mathrm{B}} = 0 \ : \quad \theta_{\mathrm{A}} = \gamma - \theta_{\mathrm{II}} \tag{2.268}$$

Applying the relation of Equation (2.268) to the fundamental solution of Equation (2.266) gives the following equations:

$$\left.\begin{aligned} \xi_2(\theta_{\mathrm{B}}=0) &= \overline{\overline{C_{B2}}} \\ &= \xi_2(\theta_{\mathrm{A}}=\gamma-\theta_{\mathrm{II}}) = \frac{1}{\tau_1}\sin\tau_1(\gamma-\theta_{\mathrm{II}}) \\ \dot{\xi}_2(\theta_{\mathrm{B}}=0) &= \tau_2\overline{\overline{S_{B2}}} \\ &= \dot{\xi}_2(\theta_{\mathrm{A}}=\gamma-\theta_{\mathrm{II}}) = \cos\tau_1(\gamma-\theta_{\mathrm{II}}) \end{aligned}\right\} \tag{2.269}$$

Thus

$$\left.\begin{aligned} \overline{\overline{C_{B2}}} &= \frac{1}{\tau_1}\sin\tau_1(\gamma-\theta_{\mathrm{II}}) \\ \overline{\overline{S_{B2}}} &= \frac{1}{\tau_2}\cos\tau_1(\gamma-\theta_{\mathrm{II}}) \end{aligned}\right\} \tag{2.270}$$

Substituting (2.270) into Equation (2.267) gives the following equations:

$$\left.\begin{aligned} x_2(\theta_{\mathrm{B}}) &= \exp(-\eta\theta_{\mathrm{B}})\cdot\left(\ \overline{\overline{C'_{B2}}}\cos\tau_2\theta_{\mathrm{B}} + \overline{\overline{S'_{B2}}}\sin\tau_2\theta_{\mathrm{B}}\ \right) \\ \dot{x}_2(\theta_{\mathrm{B}}) &= -\eta\cdot x_2(\theta_{\mathrm{B}}) + \exp(-\eta\theta_{\mathrm{B}})\cdot\left\{\ \tau_2\left(\ -\overline{\overline{C'_{B2}}}\sin\tau_2\theta_{\mathrm{B}} + \overline{\overline{S'_{B2}}}\cos\tau_2\theta_{\mathrm{B}}\ \right)\right\} \\ &= \exp(-\eta\theta_{\mathrm{B}})\cdot\left\{\left(\ -\eta\overline{\overline{C'_{B2}}} + \tau_2\overline{\overline{S'_{B2}}}\ \right)\cos\tau_2\theta_{\mathrm{B}} + \left(\ -\tau_2\overline{\overline{C'_{B2}}} - \eta\overline{\overline{S'_{B2}}}\ \right)\sin\tau_2\theta_{\mathrm{B}}\right\} \end{aligned}\right\} \tag{2.271}$$

where

$$\left.\begin{aligned} \overline{\overline{C'_{B2}}} &= \exp\{-\eta(\gamma-\theta_{\mathrm{II}})\}\cdot\overline{\overline{C_{B2}}} \\ \overline{\overline{S'_{B2}}} &= \exp\{-\eta(\gamma-\theta_{\mathrm{II}})\}\cdot\overline{\overline{S_{B2}}} \end{aligned}\right\} \tag{2.272}$$

(c) In the interval CD

The Hill's equation of Equation (2.214) is

$$\frac{d^2\xi}{d\theta^2} + {\tau_1}^2\xi = 0 \qquad (\beta + \theta_3 \le \theta \le 2\pi - \theta_0) \tag{2.273}$$

Using the independent variable θ_C shown in Figure 2.7, Equation (2.273) is rewritten as follows:

$$\frac{d^2\xi(\theta_C)}{d{\theta_C}^2} + {\tau_1}^2 \cdot \xi(\theta_C) = 0 \qquad (0 \le \theta_C \le 2\pi - \gamma - \theta_I) \tag{2.274}$$

Since Equation (2.274) is the second order differential equation, the solution assumed in the form:

$$\left.\begin{aligned} \xi_2(\theta_C) &= \overline{\overline{C_{C2}}}\cos\tau_1\theta_C + \overline{\overline{S_{C2}}}\sin\tau_1\theta_C \\ \dot{\xi}_2(\theta_C) &= \tau_1\left(-\overline{\overline{C_{C2}}}\sin\tau_1\theta_C + \overline{\overline{S_{C2}}}\cos\tau_1\theta_C \right) \end{aligned}\right\} \tag{2.275}$$

Thus $x_2(\theta_C)$ is expressed as follows:

$$\left.\begin{aligned} x_2(\theta_C) &= \exp(-\eta\theta_C)\cdot\left(\overline{\overline{C_{C2}}}\cos\tau_1\theta_C + \overline{\overline{S_{C2}}}\sin\tau_1\theta_C \right) \\ \dot{x}_2(\theta_C) &= -\eta\cdot x_2(\theta_C) + \exp(-\eta\theta_C)\cdot\left\{ \tau_1\left(-\overline{\overline{C_{C2}}}\sin\tau_1\theta_C + \overline{\overline{S_{C2}}}\cos\tau_1\theta_C \right) \right\} \end{aligned}\right\} \tag{2.276}$$

where the relation of the independent variables θ_C and θ_B is

$$\theta_C = 0 : \quad \theta_B = \theta_{II} \tag{2.277}$$

Applying the relation of Equation (2.277) to the fundamental solution of Equation (2.275) gives the following equations:

$$\left.\begin{aligned}
\xi_2(\theta_{\mathrm{C}}=0) &= \overline{\overline{C_{C2}}} \\
&= \xi_2(\theta_{\mathrm{B}}=\theta_{\mathrm{II}}) = \overline{\overline{C_{B2}}}\cos\tau_2\theta_{\mathrm{II}} + \overline{\overline{S_{B2}}}\sin\tau_2\theta_{\mathrm{II}} \\
\dot{\xi}_2(\theta_{\mathrm{C}}=0) &= \tau_1\overline{\overline{S_{C2}}} \\
&= \dot{\xi}_2(\theta_{\mathrm{B}}=\theta_{\mathrm{II}}) = \tau_2\left(-\overline{\overline{C_{B2}}}\sin\tau_2\theta_{\mathrm{II}} + \overline{\overline{S_{B2}}}\cos\tau_2\theta_{\mathrm{II}}\right)
\end{aligned}\right\} \tag{2.278}$$

Thus

$$\left.\begin{aligned}
\overline{\overline{C_{C2}}} &= \overline{\overline{C_{B2}}}\cos\tau_2\theta_{\mathrm{II}} + \overline{\overline{S_{B2}}}\sin\tau_2\theta_{\mathrm{II}} \\
\overline{\overline{S_{C2}}} &= \frac{\tau_2}{\tau_1}\left(-\overline{\overline{C_{B2}}}\sin\tau_2\theta_{\mathrm{II}} + \overline{\overline{S_{B2}}}\cos\tau_2\theta_{\mathrm{II}}\right)
\end{aligned}\right\} \tag{2.279}$$

Substituting (2.279) into Equation (2.276) gives the following equations:

$$\left.\begin{aligned}
x_2(\theta_{\mathrm{C}}) &= \exp(-\eta\theta_{\mathrm{C}})\cdot\left(\overline{\overline{C'_{C2}}}\cos\tau_2\theta_{\mathrm{C}} + \overline{\overline{S'_{C2}}}\sin\tau_2\theta_{\mathrm{C}}\right) \\
\dot{x}_2(\theta_{\mathrm{C}}) &= -\eta\cdot x_2(\theta_{\mathrm{C}}) + \exp(-\eta\theta_{\mathrm{C}})\cdot\left\{\tau_2\left(-\overline{\overline{C'_{C2}}}\sin\tau_2\theta_{\mathrm{C}} + \overline{\overline{S'_{C2}}}\cos\tau_2\theta_{\mathrm{C}}\right)\right\} \\
&= \exp(-\eta\theta_{\mathrm{C}})\cdot\left\{\left(-\eta\overline{\overline{C'_{C2}}} + \tau_2\overline{\overline{S'_{C2}}}\right)\cos\tau_2\theta_{\mathrm{C}} + \left(-\tau_2\overline{\overline{C'_{C2}}} - \eta\overline{\overline{S'_{C2}}}\right)\sin\tau_2\theta_{\mathrm{C}}\right\}
\end{aligned}\right\} \tag{2.280}$$

where

$$\left.\begin{aligned}
\overline{\overline{C'_{C2}}} &= \exp(-\eta\gamma)\cdot\overline{\overline{C_{C2}}} \\
\overline{\overline{S'_{C2}}} &= \exp(-\eta\gamma)\cdot\overline{\overline{S_{C2}}}
\end{aligned}\right\} \tag{2.281}$$

(d) In the interval DE

The Hill's equation of Equation (2.214) is

$$\frac{d^2\xi}{d\theta^2} + {\tau_2}^2\xi = 0 \qquad (2\pi - \theta_0 \le \theta \le 2\pi + \theta_1) \tag{2.282}$$

Using the independent variable θ_{D} shown in Figure 2.7, Equation (2.282) is rewritten as follows:

$$\frac{d^2\xi(\theta_D)}{d\theta_D{}^2}+\tau_2{}^2\cdot\xi(\theta_D)=0 \qquad (0\le\theta_D\le\theta_I) \tag{2.283}$$

Since Equation (2.283) is the second order differential equation, the solution assumed in the form:

$$\left.\begin{aligned}\xi_2(\theta_D)&=\overline{\overline{C_{D2}}}\cos\tau_2\theta_D+\overline{\overline{S_{D2}}}\sin\tau_2\theta_D\\ \dot{\xi}_2(\theta_D)&=\tau_2\left(-\overline{\overline{C_{D2}}}\sin\tau_2\theta_D+\overline{\overline{S_{D2}}}\cos\tau_2\theta_D\right)\end{aligned}\right\} \tag{2.284}$$

Thus $x_2(\theta_D)$ is expressed as follows:

$$\left.\begin{aligned}x_2(\theta_D)&=\exp\{-\eta(2\pi-\theta_I)\}\cdot\left\{\exp(-\eta\theta_D)\cdot\left(\overline{\overline{C_{D2}}}\cos\tau_2\theta_D+\overline{\overline{S_{D2}}}\sin\tau_2\theta_D\right)\right\}\\ \dot{x}_2(\theta_D)&=-\eta\cdot x_2(\theta_D)+\exp\{-\eta(2\pi-\theta_I)\}\cdot\left[\exp(-\eta\theta_D)\cdot\left\{\tau_2\left(-\overline{\overline{C_{D2}}}\sin\tau_2\theta_D+\overline{\overline{S_{D2}}}\cos\tau_2\theta_D\right)\right\}\right]\end{aligned}\right\} \tag{2.285}$$

where the relation of the independent variables θ_D and θ_C is

$$\theta_D=0\ :\ \ \theta_C=2\pi-\gamma-\theta_I \tag{2.286}$$

Applying the relation of Equation (2.286) to the fundamental solution of Equation (2.284) gives the following equations:

$$\left.\begin{aligned}\xi_2(\theta_D=0)&=\overline{\overline{C_{D2}}}\\ &=\xi_2(\theta_C=2\pi-\gamma-\theta_I)\\ &=\overline{\overline{C_{C2}}}\cos\tau_1(2\pi-\gamma-\theta_I)+\overline{\overline{S_{C2}}}\sin\tau_1(2\pi-\gamma-\theta_I)\\ \dot{\xi}_2(\theta_D=0)&=\tau_2\overline{\overline{S_{D2}}}\\ &=\dot{\xi}_2(\theta_C=2\pi-\gamma-\theta_I)\\ &=\tau_1\left\{-\overline{\overline{C_{C2}}}\sin\tau_1(2\pi-\gamma-\theta_I)+\overline{\overline{S_{C2}}}\cos\tau_1(2\pi-\gamma-\theta_I)\right\}\end{aligned}\right\} \tag{2.287}$$

Thus

$$\left.\begin{aligned}\overline{\overline{C_{D2}}} &= \overline{\overline{C_{C2}}}\cos\tau_1(2\pi-\gamma-\theta_{\mathrm{I}})+\overline{\overline{S_{C2}}}\sin\tau_1(2\pi-\gamma-\theta_{\mathrm{I}})\\ \overline{\overline{S_{D2}}} &= \frac{\tau_1}{\tau_2}\left\{-\overline{\overline{C_{C2}}}\sin\tau_1(2\pi-\gamma-\theta_{\mathrm{I}})+\overline{\overline{S_{C2}}}\cos\tau_1(2\pi-\gamma-\theta_{\mathrm{I}})\right\}\end{aligned}\right\} \tag{2.288}$$

Substituting (2.288) into Equation (2.285) gives the following equations:

$$\left.\begin{aligned}x_2(\theta_{\mathrm{D}}) &= \exp(-\eta\theta_{\mathrm{D}})\cdot\left(\overline{\overline{C'_{D2}}}\cos\tau_2\theta_{\mathrm{D}}+\overline{\overline{S'_{D2}}}\sin\tau_2\theta_{\mathrm{D}}\right)\\ \dot{x}_2(\theta_{\mathrm{D}}) &= -\eta\cdot x_2(\theta_{\mathrm{D}})+\exp(-\eta\theta_{\mathrm{D}})\cdot\left\{\tau_2\left(-\overline{\overline{C'_{D2}}}\sin\tau_2\theta_{\mathrm{D}}+\overline{\overline{S'_{D2}}}\cos\tau_2\theta_{\mathrm{D}}\right)\right\}\\ &= \exp(-\eta\theta_{\mathrm{D}})\cdot\left\{\left(-\eta\overline{\overline{C'_{D2}}}+\tau_2\overline{\overline{S'_{D2}}}\right)\cos\tau_2\theta_{\mathrm{D}}+\left(-\tau_2\overline{\overline{C'_{D2}}}-\eta\overline{\overline{S'_{D2}}}\right)\sin\tau_2\theta_{\mathrm{D}}\right\}\end{aligned}\right\} \tag{2.289}$$

where

$$\left.\begin{aligned}\overline{\overline{C'_{D2}}} &= \exp\{-\eta(2\pi-\theta_{\mathrm{I}})\}\cdot\overline{\overline{C_{D2}}}\\ \overline{\overline{S'_{D2}}} &= \exp\{-\eta(2\pi-\theta_{\mathrm{I}})\}\cdot\overline{\overline{S_{D2}}}\end{aligned}\right\} \tag{2.290}$$

Here, the relation of the fundamental solutions $\xi(\theta)$ and $x(\theta)$ is shown in Equation (2.154) as follows:

$$\xi_1(\theta)+\dot{\xi}_2(\theta)=\exp\{\eta(\theta+\theta_\alpha)\}\cdot\{x_1(\theta)+\eta\cdot x_2(\theta)+\dot{x}_2(\theta)\}$$

The stability criterion is shown in equation (2.110) and the real number A is shown in equation (2.155) as follows:

$$A=\xi_1(2\pi)+\dot{\xi}_2(2\pi)$$

The real number A is shown in Equation (2.156) as follows:

$$\begin{aligned}A &= \xi_1(\theta_{\mathrm{A}}=2\pi)+\dot{\xi}_2(\theta_{\mathrm{A}}=2\pi)\\ &= \exp\{\eta(\theta_{\mathrm{A}}=2\pi)\}\cdot\{x_1(\theta_{\mathrm{A}}=2\pi)+\eta\cdot x_2(\theta_{\mathrm{A}}=2\pi)+\dot{x}_2(\theta_{\mathrm{A}}=2\pi)\}\end{aligned}$$

where the relation of the independent variables θ_A and θ_D is

$$\theta_A = 2\pi \quad : \quad \theta_D = \theta_I \tag{2.291}$$

Applying Equation (2.291) to Equation (2.156) gives the real number A as follows:

$$A = \exp\{\eta(\theta_D = \theta_I)\} \cdot \{x_1(\theta_D = \theta_I) + \eta x_2(\theta_D = \theta_I) + \dot{x}_2(\theta_D = \theta_I)\} \tag{2.292}$$

For simplicity, substituting Equations (2.253) and (2.290) into (2.292) gives the following equation:

$$A = \left(\overline{\overline{C'_{D1}}} + \tau_2 \overline{\overline{S'_{D2}}}\right)\cos\tau_2\theta_I + \left(\overline{\overline{S'_{D1}}} - \tau_2 \overline{\overline{C'_{D2}}}\right)\sin\tau_2\theta_I \tag{2.293}$$

And thus

$$\begin{aligned} |A| &= |\ A(\Omega\ ,\ \zeta\ ,\ K/k\ ,\ \gamma\ ,\ \theta_I\ ,\ \theta_{II})\ | \\ &= \left| \left(\overline{\overline{C'_{D1}}} + \tau_2 \overline{\overline{S'_{D2}}}\right)\cos\tau_2\theta_I + \left(\overline{\overline{S'_{D1}}} - \tau_2 \overline{\overline{C'_{D2}}}\right)\sin\tau_2\theta_I \right| \end{aligned} \tag{2.294}$$

The stability criterion is shown in equation (2.110):

i) $|A| > 2$ A periodic solution is unstable
ii) $|A| = 2$ A periodic solution is neutral
iii) $|A| < 2$ A periodic solution is stable

2.1.5 Analysis of Response Vibration for Subharmonic Resonance

Here, the resulting vibration for subharmonic resonance which occurred during two cycles of the exciting vibration is analyzed.

(1) Fourier Series Method

(i) Fourier Series Solution

Figures 2.8 and 2.9 show the assumed excitation, the resulting displacement and the solution for the resonance vibration of the restoring force of the springs for subharmonic resonance vibration Type I and II. The resulting displacement z at the mass is considered to be periodic; the response is divided into the linear region I, and the nonlinear region II. The origin for measuring the phase angle θ is defined from the peak of the resulting waveform. The independent variable of time t is transformed to phase angle θ which is defined as:

$$\theta = (\omega t - \alpha)/2 \tag{2.295}$$

where α is the phase lag angle, which is currently undefined but will be determined later. Substituting Equation (2.295) into the displacement excitation of arbitrary periodic function $q(t)$ gives the following expression:

$$q(\theta) = \frac{f_0}{2} + \sum_{n=1}^{\infty} \{ f_n \cos n(2\theta + \alpha) + g_n \sin n(2\theta + \alpha) \} \tag{2.296}$$

Equation of motion of Equation (2.1) is rewritten by using Equation (2.295) as follows:

$$\frac{m\omega^2}{4}\frac{d^2 z}{d\theta^2} + \frac{c\omega}{2}\frac{dz}{d\theta} + f(z) = -\frac{m\omega^2}{4}\frac{d^2 q(\theta)}{d\theta^2} \tag{2.297}$$

Regarding this nonlinear part of the restoring force $g(\theta)$ as a virtual external force and subtracting this force from the actual one, the equation of motion of Equation (2.297) is linearized formally as follows:

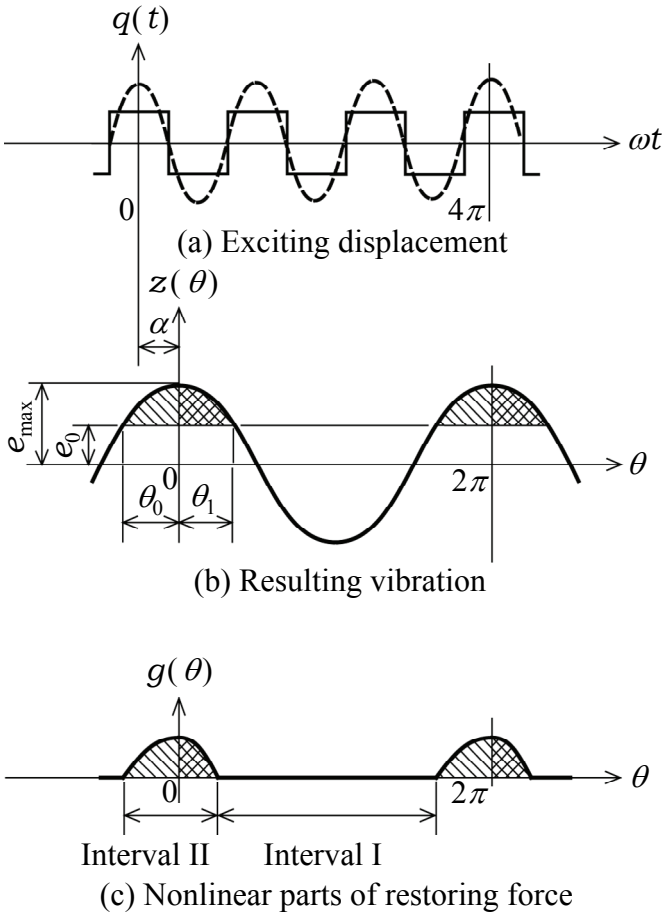

Figure 2.8 1/2nd order subharmonic resonance vibration Type I

$$\frac{m\omega^2}{4}\frac{d^2z}{d\theta^2}+\frac{c\omega}{2}\frac{dz}{d\theta}+kz=-\frac{m\omega^2}{4}\frac{d^2q(\theta)}{d\theta^2}-g(\theta) \tag{2.298}$$

(ii) Formal Solution of z

Substituting the displacement excitation of Equation (2.296) into the first term on the right side of Equation (2.298) gives the following equation:

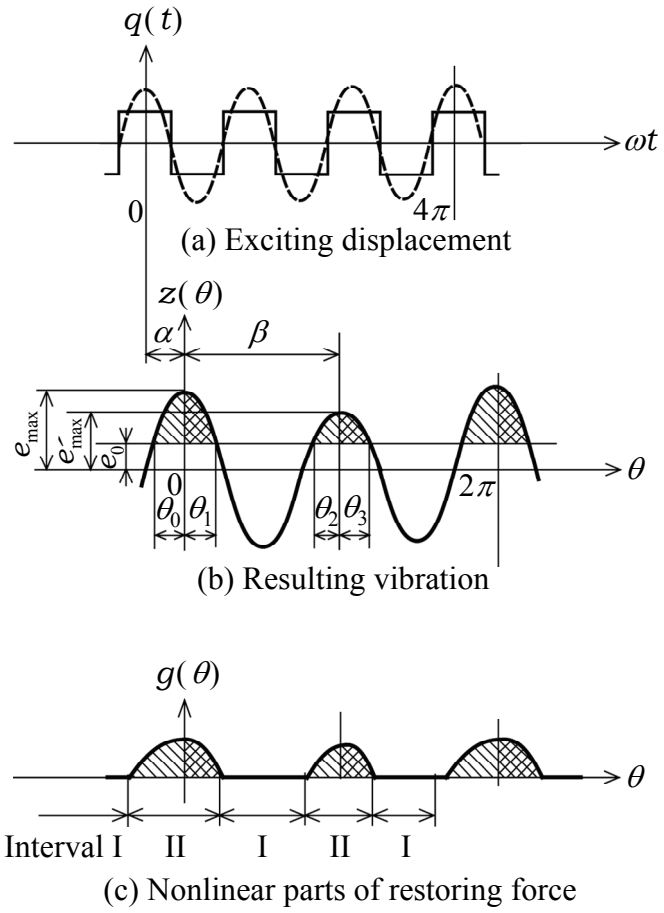

Figure 2.9 1/2nd order subharmonic resonance vibration Type II

$$
\begin{aligned}
-\frac{m\omega^2}{4}\frac{d^2q(\theta)}{d\theta^2} &= m\omega^2\sum_{n=1}^{\infty}n^2\{\, f_n\cos n(2\theta+\alpha)+g_n\sin n(2\theta+\alpha)\,\} \\
&= m\omega^2\sum_{n=1}^{\infty}n^2\{\,(f_n\cos n\alpha+g_n\sin n\alpha)\cos 2n\theta+(g_n\cos n\alpha-f_n\sin n\alpha)\sin 2n\theta\,\} \\
\therefore\ -\frac{m\omega^2}{4}\frac{d^2q(\theta)}{d\theta^2} &= \sum_{n=1}^{\infty}(f_n'\cos 2n\theta+g_n'\sin 2n\theta)
\end{aligned}
\tag{2.299}
$$

where f'_n and g'_n are shown of Equation (2.11) as follows:

$$
\left.
\begin{aligned}
f_n' &= kn^2\Omega^2(f_n\cos n\alpha+g_n\sin n\alpha) \\
g_n' &= kn^2\Omega^2(g_n\cos n\alpha-f_n\sin n\alpha)
\end{aligned}
\right\}\quad (n=1,2,3,\ldots)
$$

The coefficients f''_n and g''_n satisfying follow relations are introduced:

$$\sum_{n=1}^{\infty}\left(f'_n\cos 2n\theta + g'_n \sin 2n\theta\right) = \sum_{n=1}^{\infty}\left(f''_n\cos n\theta + g''_n \sin n\theta\right) \tag{2.300}$$

Thus

$$\left.\begin{aligned} f''_n &= f'_{(n/2)}\cdot\cos^2\left(\frac{n}{2}\pi\right) \\ g''_n &= g'_{(n/2)}\cdot\cos^2\left(\frac{n}{2}\pi\right) \end{aligned}\right\} \quad (n = 1,2,3,\ldots) \tag{2.301}$$

Equation of motion of Equation (2.298) is transformed by using Equation (2.301) as follows:

$$\begin{aligned} \frac{m\omega^2}{4}\frac{d^2z}{d\theta^2} + \frac{c\omega}{2}\frac{dz}{d\theta} + kz &= \sum_{n=1}^{\infty}\left(f''_n\cos n\theta + g''_n\sin n\theta\right) - g(\theta) \\ &= -\frac{s_0}{2} + \sum_{n=1}^{\infty}\left\{\left(f''_n - s_n\right)\cdot\cos n\theta + \left(g''_n - t_n\right)\cdot\sin n\theta\right\} \end{aligned} \tag{2.302}$$

Substituting Equation (2.13) into Equation (2.302) gives the following equation:

$$\begin{aligned} &-\frac{m\omega^2}{4}\sum_{n=1}^{\infty}n^2\left(a_n\cos n\theta + b_n\sin n\theta\right) + \frac{c\omega}{2}\sum_{n=1}^{\infty}n\left(-a_n\sin n\theta + b_n\cos n\theta\right) + \\ &k\left\{\frac{a_0}{2} + \sum_{n=1}^{\infty}\left(a_n\cos n\theta + b_n\sin n\theta\right)\right\} \\ &= -\frac{s_0}{2} + \sum_{n=1}^{\infty}\left\{\left(f''_n - s_n\right)\cdot\cos n\theta + \left(g''_n - t_n\right)\cdot\sin n\theta\right\} \end{aligned} \tag{2.303}$$

Simplifying the left side of Equation (2.303),

$$\frac{ka_0}{2}+\sum_{n=1}^{\infty}\left[\left\{\left(k-\frac{n^2m\omega^2}{4}\right)\cdot a_n+\frac{nc\omega}{2}\cdot b_n\right\}\cdot\cos n\theta+\left\{-\frac{nc\omega}{2}\cdot a_n+\left(k-\frac{n^2m\omega^2}{4}\right)\cdot b_n\right\}\cdot\sin n\theta\right]$$

$$=\frac{ka_0}{2}+\sum_{n=1}^{\infty}\frac{k}{M'_n}\left\{\left(\cos\varphi'_n\cdot a_n+\sin\varphi'_n\cdot b_n\right)\cos n\theta+\left(-\sin\varphi'_n\cdot a_n+\cos\varphi'_n\cdot b_n\right)\sin n\theta\right\} \tag{2.304}$$

where

$$\left.\begin{aligned}M'_n&=\frac{1}{\sqrt{\left(1-\frac{n^2\Omega^2}{4}\right)^2+(n\zeta\Omega)^2}}\\ \varphi'_n&=\tan^{-1}\left(\frac{n\zeta\Omega}{1-n^2\Omega^2/4}\right)\end{aligned}\right\} \tag{2.305}$$

Substituting Equation (2.304) into Equation (2.303) gives the following equation:

$$\begin{aligned}&\frac{ka_0}{2}+\sum_{n=1}^{\infty}\frac{k}{M'_n}\left\{\left(\cos\varphi'_n\cdot a_n+\sin\varphi'_n\cdot b_n\right)\cos n\theta+\left(-\sin\varphi'_n\cdot a_n+\cos\varphi'_n\cdot b_n\right)\sin n\theta\right\}\\ &=-\frac{s_0}{2}+\sum_{n=1}^{\infty}\left\{\left(f''_n-s_n\right)\cos n\theta+\left(g''_n-t_n\right)\sin n\theta\right\}\end{aligned} \tag{2.306}$$

Comparing coefficients with respect to $\cos n\theta$ and $\sin n\theta$ of both sides of Equation (2.306) gives the following equations:

$$\left.\begin{aligned}\frac{s_0}{2}&=-\frac{ka_0}{2}\\ s_n&=f''_n-k\left\{\left(1-\frac{n^2\Omega^2}{4}\right)\cdot a_n+n\zeta\Omega\cdot b_n\right\}\\ t_n&=g''_n+k\left\{n\zeta\Omega\cdot a_n-\left(1-\frac{n^2\Omega^2}{4}\right)\cdot b_n\right\}\end{aligned}\right\} \tag{2.307}$$

(2) Determination of Non-Dimensional Fourier Coefficients x_n and y_n

Superharmonic and harmonic resonances are single period vibration. On the other hand, subharmonic resonance is double period vibration. Analytical equations of single period vibration and double period vibration are the same except the following equations:

Single period vibration [$M_n,\ \varphi_n,\ f'_n,\ g'_n$]

$$\left.\begin{aligned} s_n &= f'_n - \frac{k}{M_n}\left(\cos\varphi_n \cdot a_n + \sin\varphi_n \cdot b_n\right) \\ t_n &= g'_n - \frac{k}{M_n}\left(-\sin\varphi_n \cdot a_n + \cos\varphi_n \cdot b_n\right) \end{aligned}\right\} \left.\begin{aligned} M_n &= \frac{1}{\sqrt{\left(1-n^2\Omega^2\right)^2 + (2n\zeta\Omega)^2}} \\ \varphi_n &= \tan^{-1}\left(\frac{2n\zeta\Omega}{1-n^2\Omega^2}\right) \end{aligned}\right\} \tag{2.308}$$

Double period vibration [$M_n \rightarrow M'_n,\ \varphi_n \rightarrow \varphi'_n\ ,\ f'_n \rightarrow f''_n,\ g'_n \rightarrow g''_n$]

$$\left.\begin{aligned} s_n &= f''_n - \frac{k}{M'_n}\left(\cos\varphi'_n \cdot a_n + \sin\varphi'_n \cdot b_n\right) \\ t_n &= g''_n - \frac{k}{M'_n}\left(-\sin\varphi'_n \cdot a_n + \cos\varphi'_n \cdot b_n\right) \end{aligned}\right\} \left.\begin{aligned} f''_n &= f'_{(n/2)} \cdot \cos^2\left(\frac{n}{2}\pi\right) \\ g''_n &= g'_{(n/2)} \cdot \cos^2\left(\frac{n}{2}\pi\right) \end{aligned}\right\} \left.\begin{aligned} M'_n &= \frac{1}{\sqrt{\left(1-\frac{n^2\Omega^2}{4}\right)^2 + (n\zeta\Omega)^2}} \\ \varphi'_n &= \tan^{-1}\left\{\frac{n\zeta\Omega}{1-\left(n^2\Omega^2/4\right)}\right\} \end{aligned}\right\} \tag{2.309}$$

Substituting coefficients of Equation (2.309) into the analytical equations for harmonic and superharmonic resonance vibrations, we can obtain the resulting vibration for subharmonic resonance Type I and II.

2.1.6 Analysis of Stability Criterion for Subharmonic Resonance

Here, stability analysis for periodic solutions of subharmonic resonance Type I and II is carried out. This stability analysis employs a variational equation to investigate consequences of a minute perturbation to a steady forced vibration predicted by a periodic solution for an original equation of motion.

(1) Characteristics of System and Variational Equation

The equation of motion for double period vibration of Equation (2.297) is expressed as follows:

$$\frac{m\omega^2}{4}\frac{d^2z}{d\theta^2}+\frac{c\omega}{2}\frac{dz}{d\theta}+f(z)=-\frac{m\omega^2}{4}\frac{d^2q(\theta)}{d\theta^2}$$

Substituting the frequency ratio Ω and the damping coefficient ratio ζ into Equation (2.297), the equation of motion is rewritten as follows:

$$\frac{\Omega^2}{4}\frac{d^2z}{d\theta^2}+\Omega\zeta\frac{dz}{d\theta}+\frac{f(z)}{k}=-\frac{\Omega^2}{4}\frac{d^2q(\theta)}{d\theta^2} \tag{2.310}$$

Let us now examine whether a periodic solution for the response vibration, as given in the equation of motion of Equation (2.310), is stable when the system reaches steady state. When a minute perturbation is added to the periodic solution $z=z_0(\theta)$, we designate the vibratory displacement $z(\theta)$ and the variation in the vibratory displacement as $x(\theta)$; then, $z=z_0+x$ must satisfy the equation of motion of Equation (2.310):

$$\frac{\Omega^2}{4}\frac{d^2}{d\theta^2}(z_0+x)+\Omega\zeta\frac{d}{d\theta}(z_0+x)+\frac{f(z_0+x)}{k}=-\frac{\Omega^2}{4}\frac{d^2q(\theta)}{d\theta^2} \tag{2.311}$$

where the periodic solution z_0 also satisfies equation of motion:

$$\frac{\Omega^2}{4}\frac{d^2z_0}{d\theta^2}+\Omega\zeta\frac{dz_0}{d\theta}+\frac{f(z_0)}{k}=-\frac{\Omega^2}{4}\frac{d^2q(\theta)}{d\theta^2} \tag{2.312}$$

Substituting the restoring force $f(z_0+x)$ of Equation (2.82) into Equation (2.311) gives the following equation:

$$\begin{aligned}\left[\ \frac{\Omega^2}{4}\frac{d^2x}{d\theta^2}+\Omega\zeta\frac{dx}{d\theta}+\frac{1}{k}\left\{\frac{d}{dz}f(z)\right\}_{z=z_0}\cdot x\ \right]+\\ +\left[\ \frac{\Omega^2}{4}\frac{d^2z_0}{d\theta^2}+\Omega\zeta\frac{dz_0}{d\theta}+\frac{f(z_0)}{k}\ \right]=-\frac{\Omega^2}{4}\frac{d^2q(\theta)}{d\theta^2}\end{aligned} \tag{2.313}$$

Substituting (2.312) into Equation (2.313), we obtain the variational equation as follows:

$$\frac{\Omega^2}{4}\frac{d^2x}{d\theta^2}+\Omega\zeta\frac{dx}{d\theta}+\frac{1}{k}\left\{\frac{d}{dz}f(z)\right\}_{z=z_0}\cdot x=0 \tag{2.314}$$

(2) Equation of Stability Criterion

The variational equation of Equation (2.314) is rewritten as follows:

$$\Omega'^2\frac{d^2x}{d\theta^2}+2\Omega'\zeta\frac{dx}{d\theta}+\frac{1}{k}\left\{\frac{d}{dz}f(z)\right\}_{z=z_0}\cdot x=0 \tag{2.315}$$

where

$$\Omega'=\frac{\Omega}{2} \tag{2.316}$$

The variational equation for double period vibration of Equation (2.315) is the same equation of Equation (2.84) except for Ω'. Therefore the stability criterion for double period vibration can be obtained by replacing Ω with Ω' for single period vibration.

2.1.7 Calculation

The steady state periodic solutions were calculated based on the theoretical analysis results. The exciting vibrations were chosen as two waves as an example of a periodic excitation with an arbitrary function shown in Figure 2.10.

Single harmonic wave in Figure 2.10(a)

$$q(\theta) = \cos\theta \tag{2.317}$$

Combined wave in Figure 2.10(b)

$$q(\theta) = \cos\theta + \sin 2\theta \tag{2.318}$$

The resulting vibration is expressed by the non-dimensional Fourier coefficients x_n, y_n which can be determined by the infinite dimensionless linear simultaneous equations containing the independent parameters. Therefore if the independent parameters are given, the non-dimensional Fourier coefficients x_n, y_n are determined, and the resulting vibration can be calculated. Here, the calculation method based on the theoretical analysis for harmonic resonance vibration is mentioned. Also superharmonic and subharmonic resonance vibrations can be calculated in the same manner.

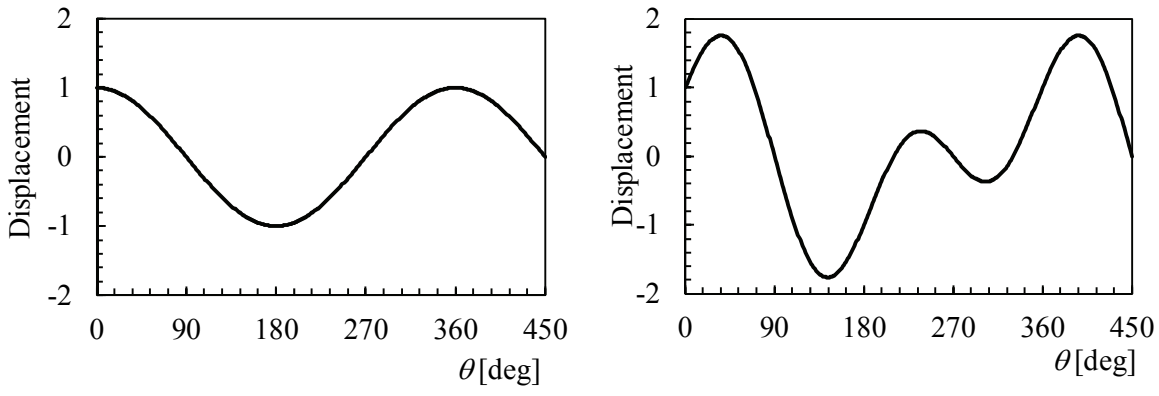

(a) $q(\theta)=\cos\theta$ (b) $q(\theta)=\cos\theta+\sin 2\theta$

Figure 2.10 Displacement excitation

The coefficients XMA_{mn}, XA_{mn}, ⋯ Q_{mn} of the infinite dimensionless linear simultaneous equations of Equation (2.55) contain the independent parameters for the frequency ratio Ω, the phase lag angle α and the dwell phase angle in the nonlinear region II θ_0, θ_1. First, the independent parameters Ω, α θ_0 θ_1 are determined by using the condition that the coefficient determinants of Equations (2.61), (2.66), (2.71) and (2.76) are all zero. Next, substituting the independent parameters into the infinite dimensionless linear simultaneous equations of Equation (2.55) and solving gives the non-dimensional Fourier coefficients x_n, y_n. Finally, substituting the non-dimensional Fourier coefficients into Equation (2.33), the resulting vibration can be calculated. And calculated independent parameters are substituted into Equation (2.160), the real number A is obtained. Thus substituting the real number A into the stability criterion of Equation (2.110), stability of a periodic solution is analyzed. When solving the infinite dimensionless linear simultaneous equations of Equation (2.55), the non-dimensional Fourier coefficients x_n and y_n were performed to the term with n=20 to approximate the response. Figure 2.11 shows the convergence of the non-dimensional Fourier coefficients x_n and y_n for subharmonic vibration Type II. When $n \geqq 19$, x_n and y_n became under 0.001% compared with the first order coefficients x_1 and y_1. Meanwhile, subharmonic resonance vibration Type II is considered to converge slowly compared with the Type I. And thus, term numbers of the non-dimensional Fourier coefficients were calculated up to n=20 in this analysis. Above steps are repeated, resonance curves distinguished from unstable branches are constructed.

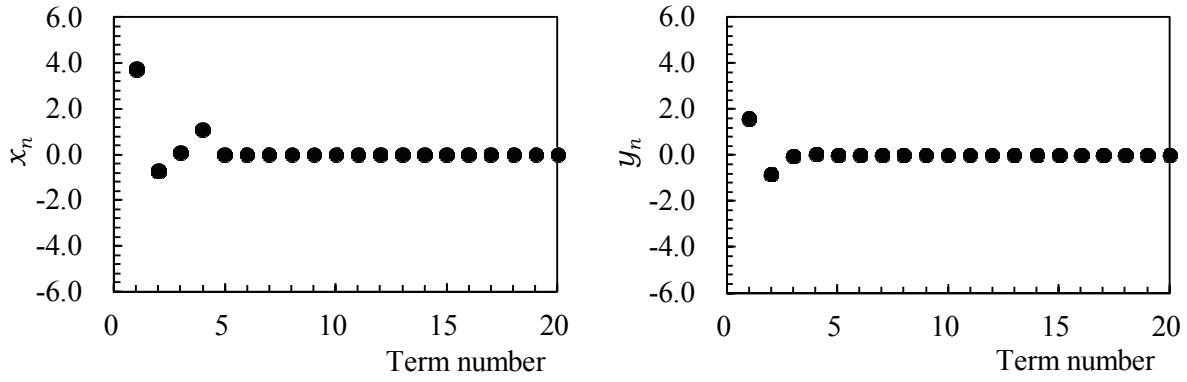

(a) Fourier coefficients x_n (b) Fourier coefficients y_n

Figure 2.11 Convergence of Fourier coefficients for subharmonic vibration Type II

2.2 Experiment

An experimental apparatus was built to embody the analytical model in Figure 2.1 and an experiment was carried out to verify the theoretical analysis results.

Figure 2.12 is a diagram of the apparatus for observing steady state forced vibrations in the mass satisfying the equation of motion of Equation (2.1). Figure 2.13 shows a photograph of experiment equipment overview. Table 2.1 provides properties of coil springs and vibration mass. The test mass ④ was made of steel. The mass was assumed to be a piecewise linear system; to model this, the supporting spring ③ was connected to the mass. Collision spring ⑤ was connected to the frame with the clearance e_0 for mass to create a system with a spring constant that satisfies the property indicated by Figure 2.2. Mass ④ was connected to a linear spring ③ fixed to frame ②. A response vibration occurred under the excitation vibration. Once the displacement of the mass exceeded distance e_0, the mass collided with the collision spring ⑤. At this time, the displacement input vibration caused a reciprocating movement of frame ② on the foundation ① via the linear ball bearing, acting to cause a periodic excitation displacement vibration. A connecting rod ⑦ fixed to the frame ② was connected to the exciting vibrator ⑥. The displacement vibration caused by the exciting vibrator ⑥ was set by the Frequency counter ⑨ connected to the function generator ⑧. The excitation displacement was measured with a laser displacement sensor ⑩ and the resulting vibration was measured

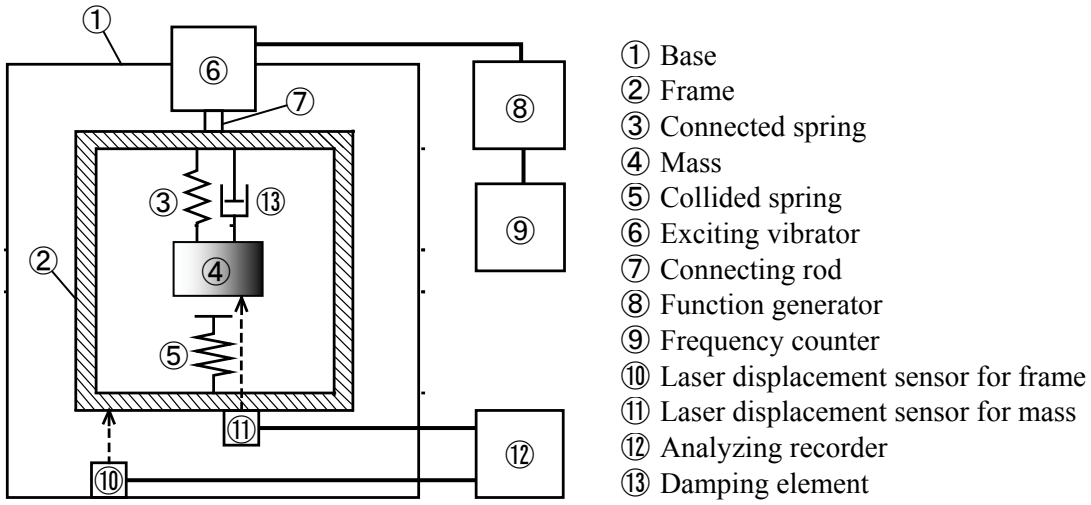

Figure 2.12 Sketch of the experiment apparatus

with another laser displacement sensor ⑪ mounted on the frame. The analog outputs from the sensors were stored on an analyzing recorder ⑫.

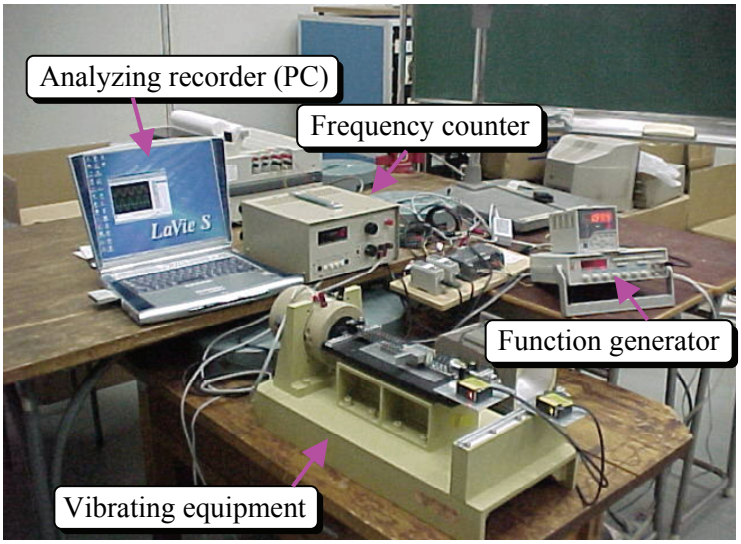

Figure 2.13 Photograph of the experiment apparatus

Table 2.1 Mechanical properties of parts used in experiment

Element	Symbol	Numerical value	
Connected spring constant	k	49 196 1570	[N/m]
Collided spring constant	K	147 588 1570	[N/m]
Mass	m	55×10^{-3} 104×10^{-3}	[kg]
Damping ratio	ζ	0.0534 0.0654	[-]
Clearance	e_0	0.5×10^{-3} 2.0×10^{-3} 3.0×10^{-3}	[m]

2.3 The Results of Theoretical Calculation and Experiment

2.3.1 Comparison of Theoretical Calculation Results with Experimental Results

Figure 2.14 and 2.15 present resonance curves for comparing the theoretical calculation results with the experimental results. The experimental results (△ symbols) and theoretical calculations agreed reasonably well. The ○ symbols in the figure indicate branching points between different types revealed by the calculations. The ● symbols in the figure indicate branching points between stable and unstable resulting vibration.

Figure 2.14 shows the resonance curve for the 2nd order superharmonic resonance vibration. At Ω=0.52-0.56, the superharmonic resonance Type II occurred; the mass contacted the spring twice in each cycle of the mass, which occurred during one cycle of the exciting vibration.

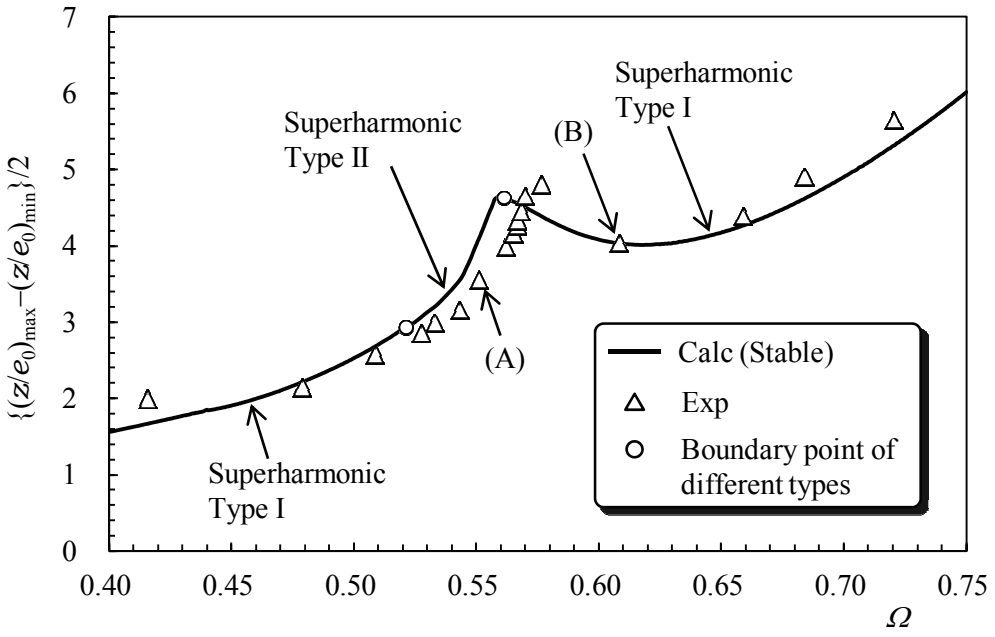

{$q(t)$=4cosωt, ζ=0.0534, K/k=1.0, f_1/e_0=8.0 }

Figure 2.14 Resonance curve of superharmonic vibration for comparing theoretical calculation results with experimental results

Figure 2.15 shows the resonance curve in the region from harmonic to 1/2nd order subharmonic resonances. At Ω=2.05-2.21, the 1/2nd order subharmonic resonance Type II occurred; the mass contacted the spring twice in each cycle of the mass, which occurred during two cycles of the exciting vibration. The results in the physical model showed a jump to the lower line of linear vibrations when the vibration frequency ratio exceeded a value of Ω=2.45 as Ω was being increased. At Ω=2.15-2.85, the resonance curve became triangle-shaped. The harmonic vibration Type I in the triangle-shaped was unstable branch. The experimental results were not in good agreement compared with the calculation ones at large displacement area in the harmonic resonance region. These differences were caused by the precision of identifying damping ratio in the system.

Figures 2.16-2.20 present comparisons of the theoretical calculation results with experimental results for the waveforms of the resulting displacement ratio $z(\theta)/e_0$ and the nonlinear part of the restoring force $g(\theta)/ke_0$ under the excitation $q(\theta)/e_0$ at points A, B, C and D on the resonance curve in Figure 2.15. The waveform, amplitudes and phase lag of these predicted values showed good agreement.

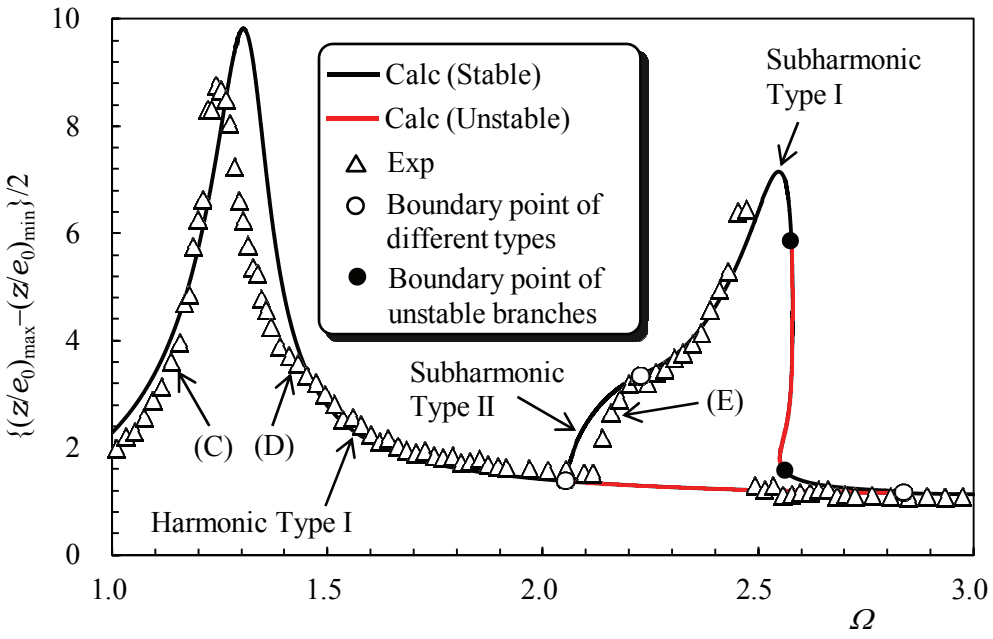

{$q(t)$=cosωt, ζ=0.0654, K/k=3.0, f_1/e_0=1.0 }

Figure 2.15 Resonance curve of harmonic and 1/2nd order subharmonic vibrations for comparing theoretical calculation results with experimental results

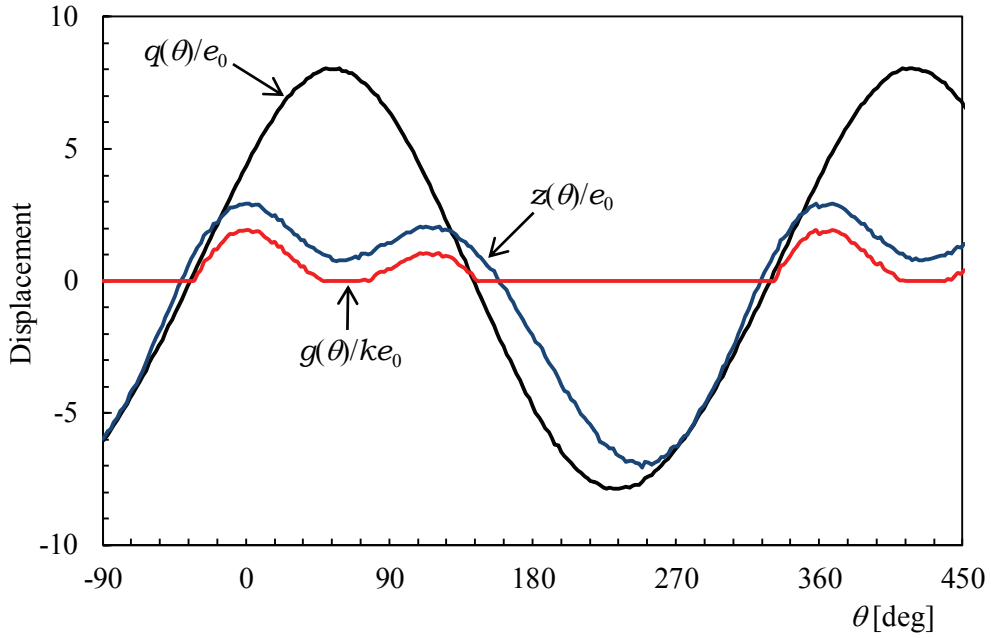

(a) Experimental result

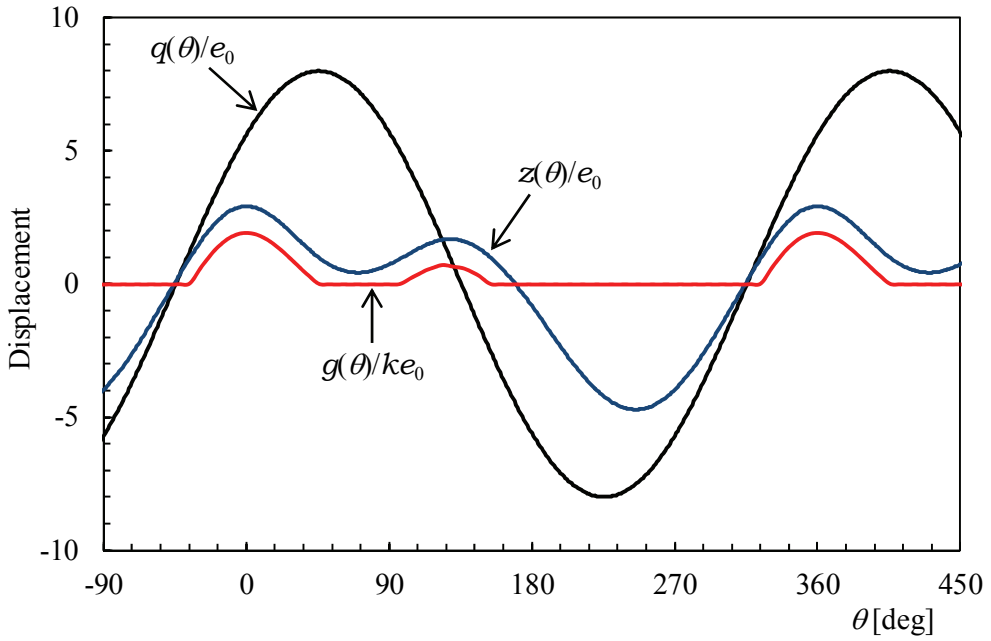

(b) Theoretical calculation result

Figure 2.16 The comparison of experimental result with theoretical calculation result at point A (Ω=0.55) in Figure 2.15

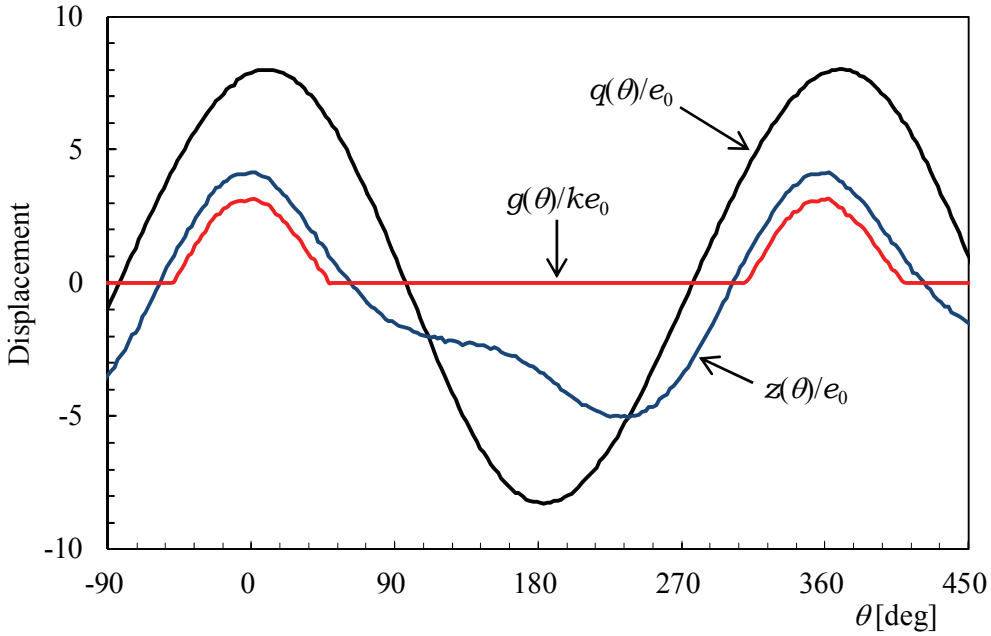

(a) Experimental result

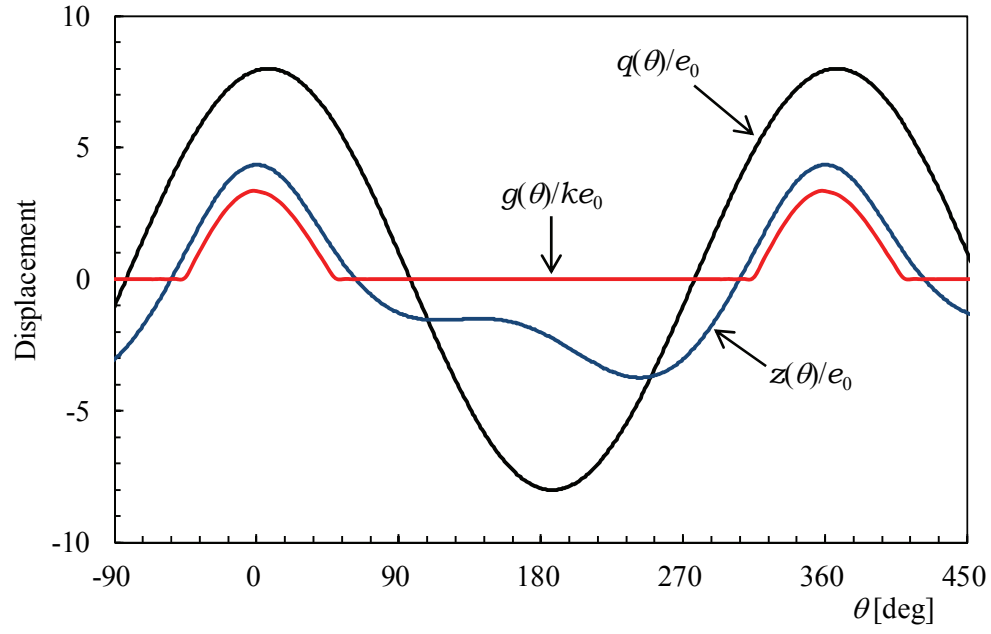

(b) Theoretical calculation result

Figure 2.17 The comparison of experimental result with theoretical calculation result at point B (Ω=0.61) in Figure 2.15

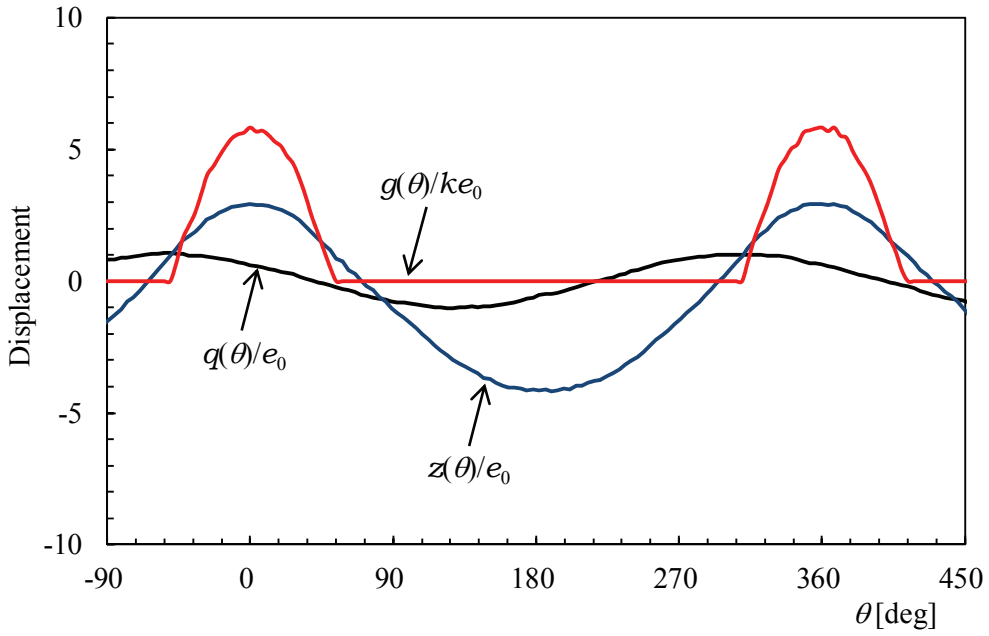

(a) Experimental result

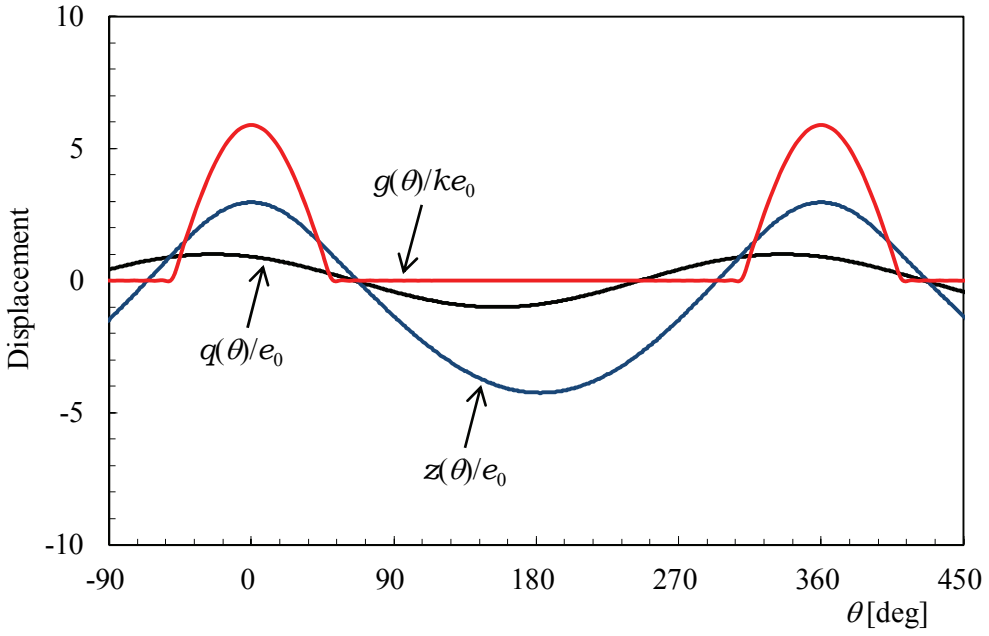

(b) Theoretical calculation result

Figure 2.18 The comparison of experimental result with theoretical calculation result at point C (Ω=1.14) in Figure 2.15

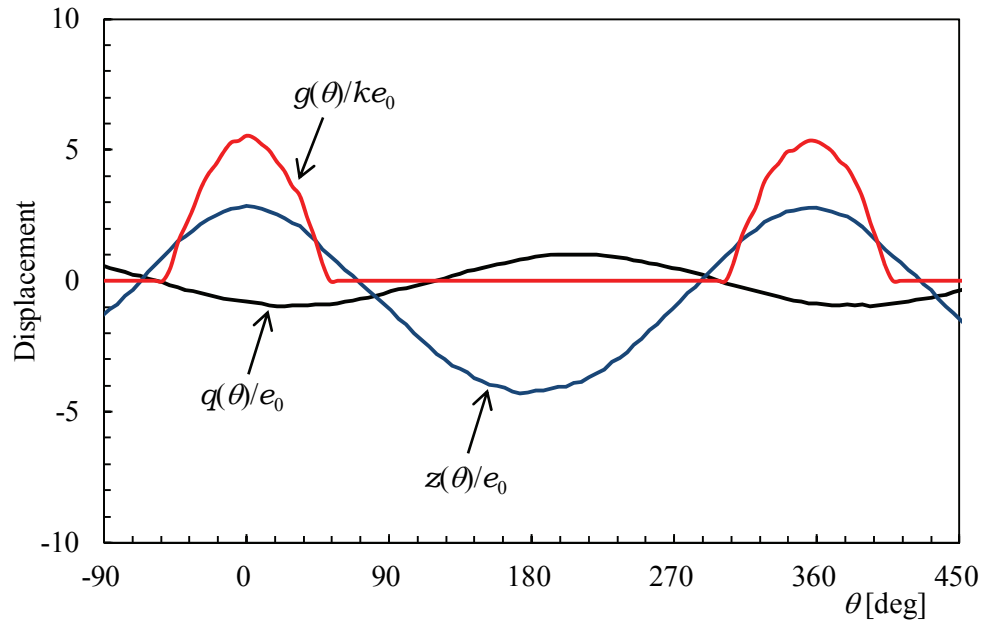

(a) Experimental result

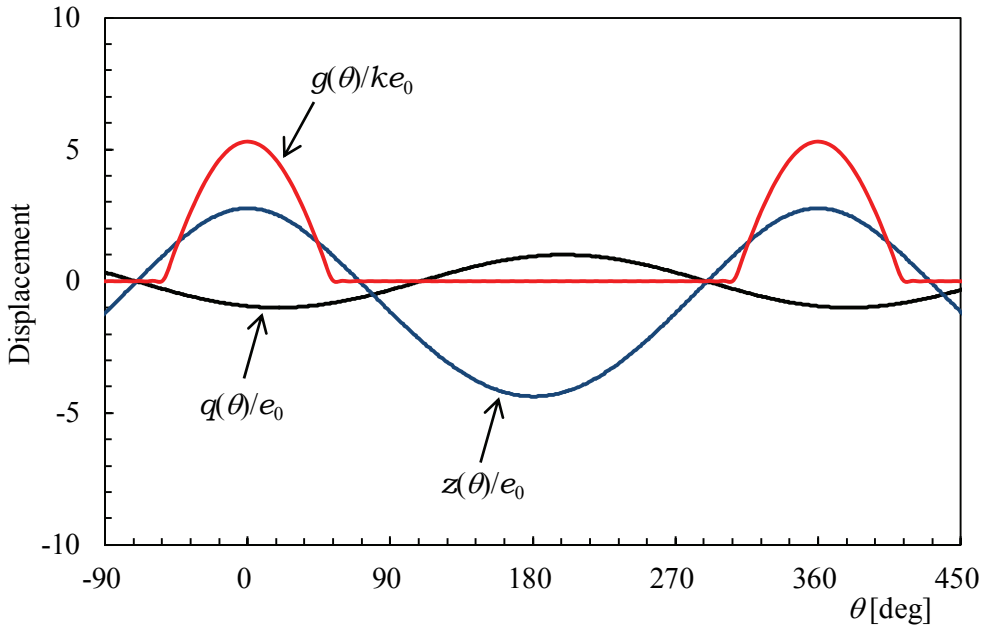

(b) Theoretical calculation result

Figure 2.19 The comparison of experimental result with theoretical calculation result at point D (Ω=1.43) in Figure 2.15

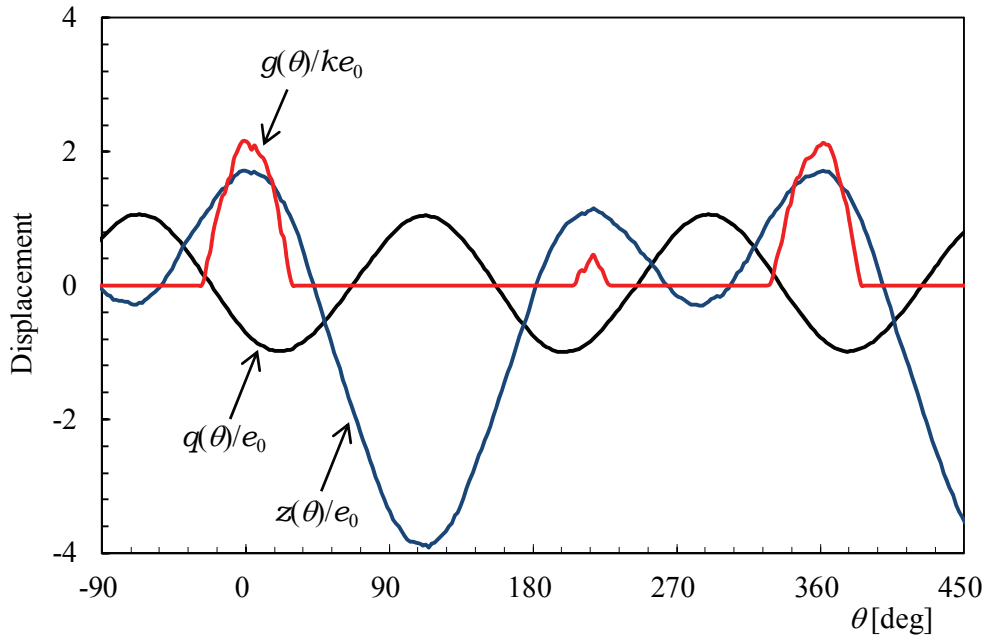

(a) Experimental result

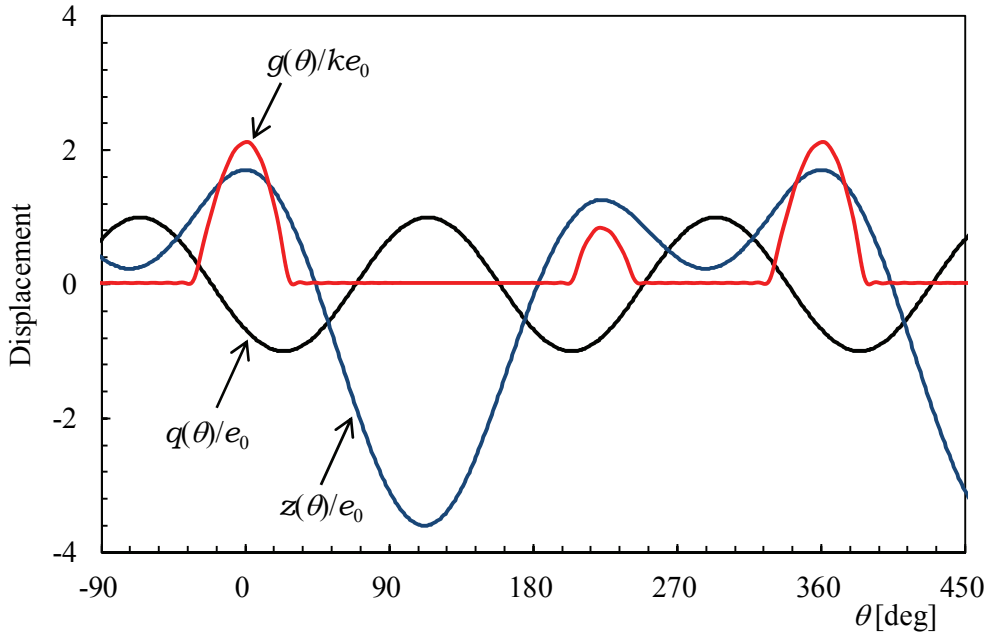

(b) Theoretical calculation result

Figure 2.20 The comparison of experimental result with theoretical calculation result at point E (Ω=2.16) in Figure 2.15

2.3.2 Comparison of Theoretical Calculation Results with Numerical Simulation Results

A numerical simulation was also conducted to verify the theoretical analysis results. Equation of motion (2.1) was directly integrated numerically by using the fourth order Runge-Kutta algorithm.

Figure 2.21 shows the resonance curve for comparing the theoretical calculation results with numerical simulation results. The numerical simulation results (◇ symbols) and calculations agreed reasonably well. The ○ symbols in the figure indicate branching points between different types revealed by the calculations. The ● symbols in the figure indicate branching points between stable and unstable resulting vibration. In theoretical calculations, the 1/2nd order subharmonic resonance Type II resonance occurred at Ω=2.28-2.39; the mass contacted the collided spring twice in each cycle of the mass, which occurred during two cycles of the exciting vibration. A branch of the harmonic resonance bifurcates into harmonic and subharmonic branches at Ω=2.29, and the resonance curve become triangle-shaped at

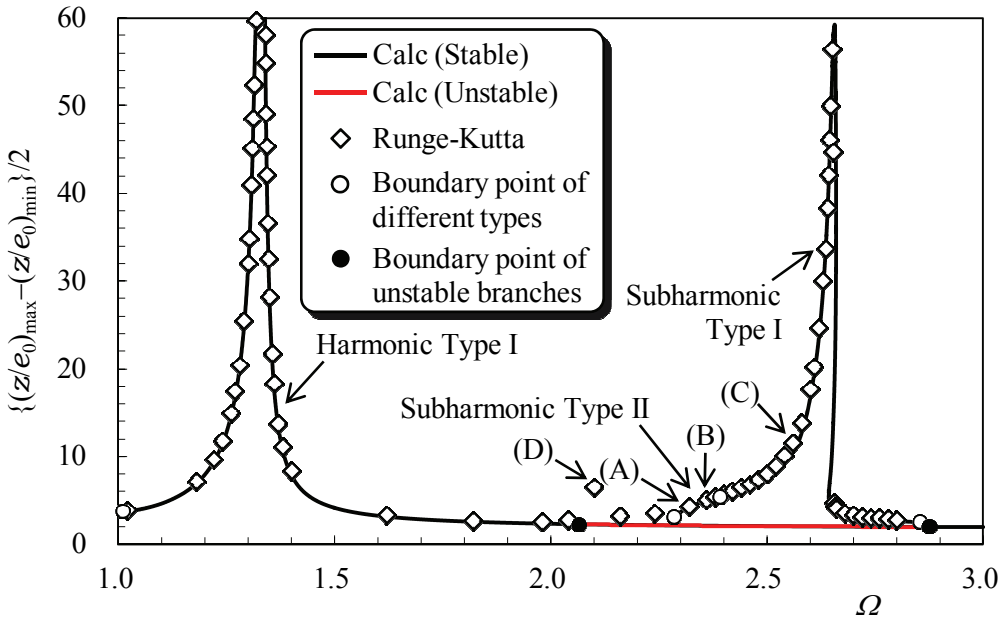

{ $q(t)$=cosω+sin2ωt, ζ=0.01, K/k=3.0, f_1/e_0=1.0}

Figure 2.21 Resonance curve of harmonic and 1/2nd order subharmonic vibrations for comparing theoretical calculation results with numerical simulation results

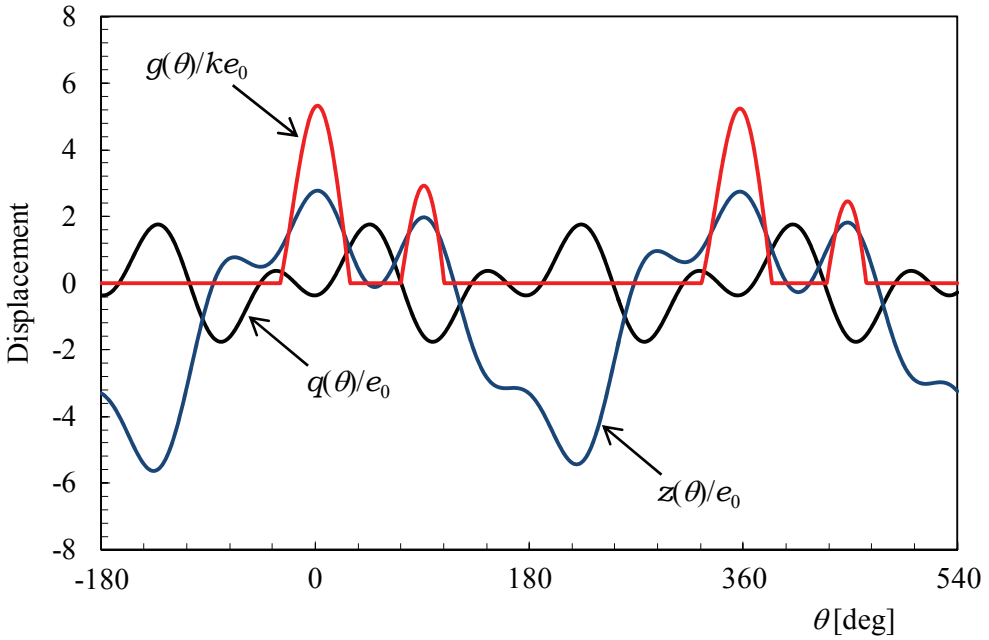

(a) Numerical simulation result

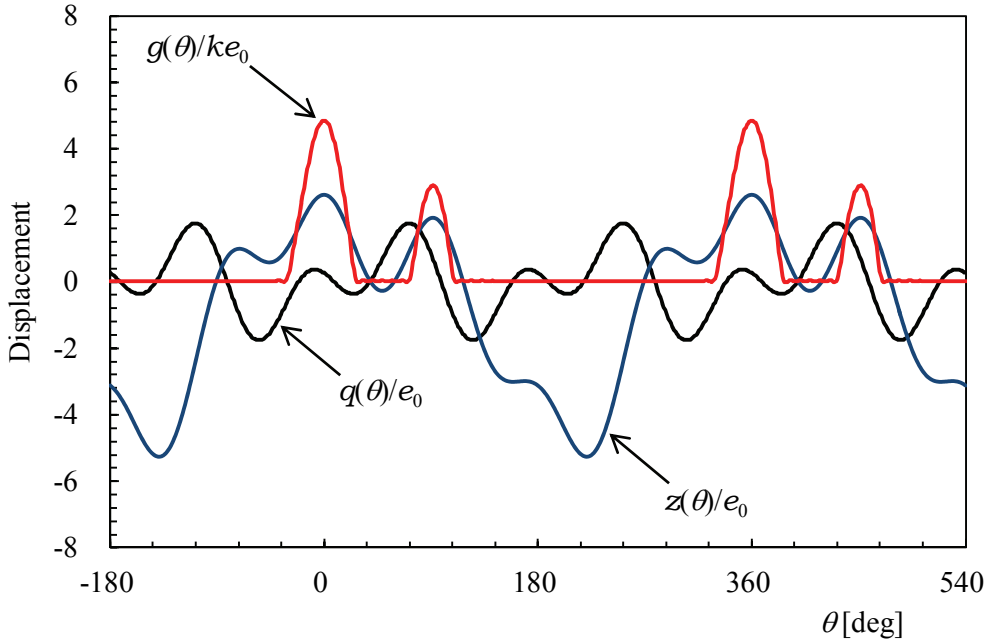

(b) Theoretical calculation result

Figure 2.22 The comparison of numerical simulation result with theoretical calculation result at point A (Ω=2.31) in Figure 2.21

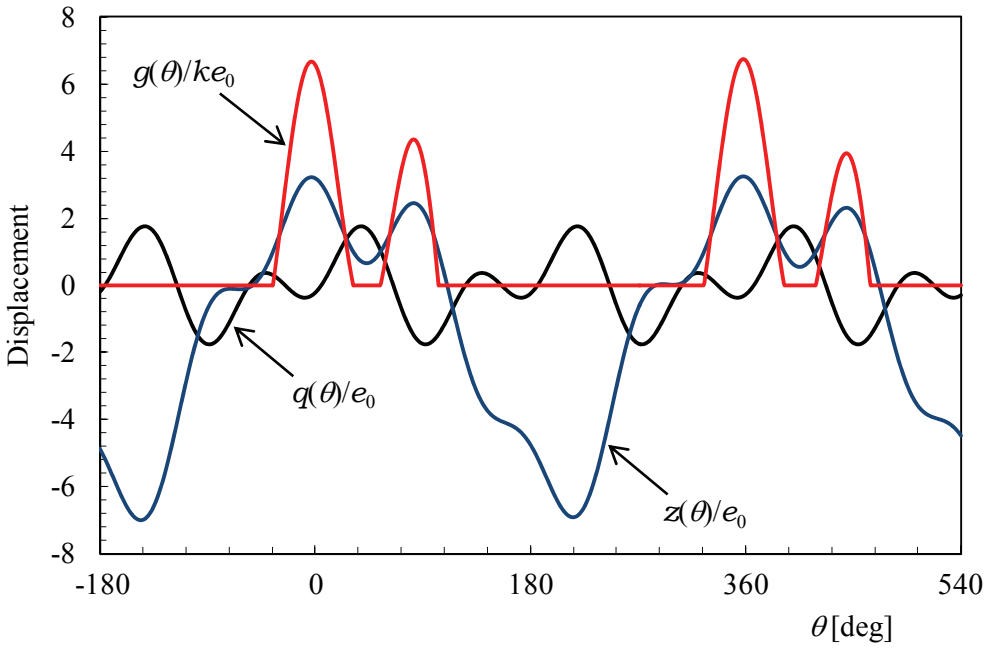

(a) Numerical simulation result

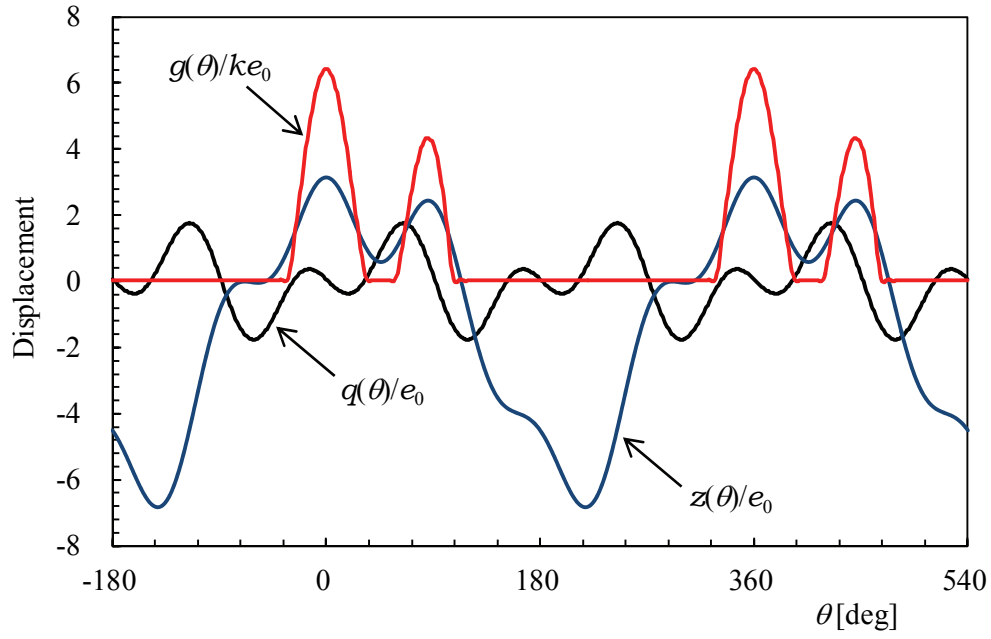

(b) Theoretical calculation result

Figure 2.23 The comparison of numerical simulation result with theoretical calculation result at point B (Ω=2.36) in Figure 2.21

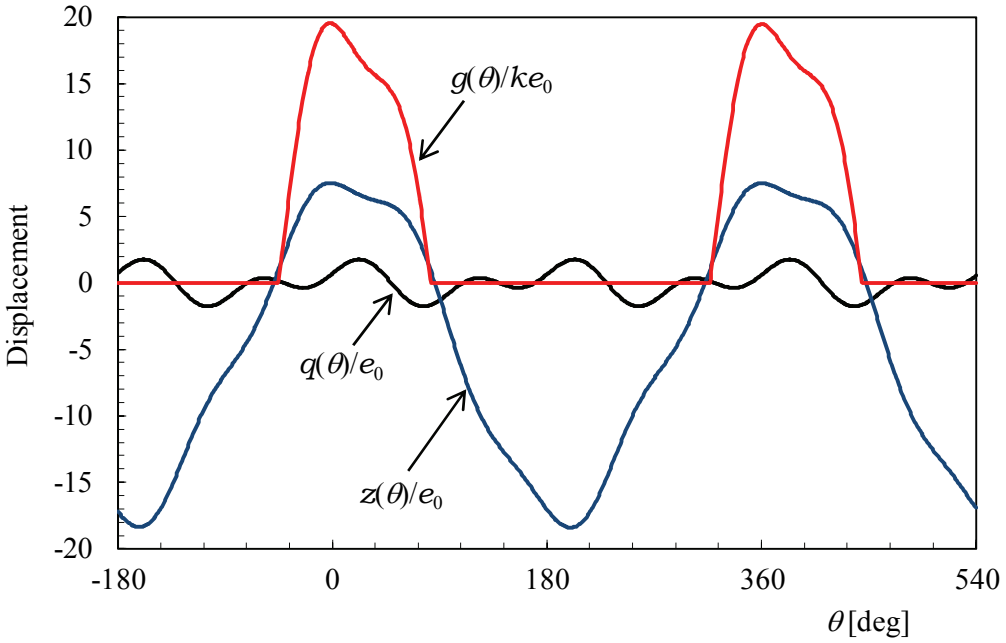

(a) Numerical simulation result

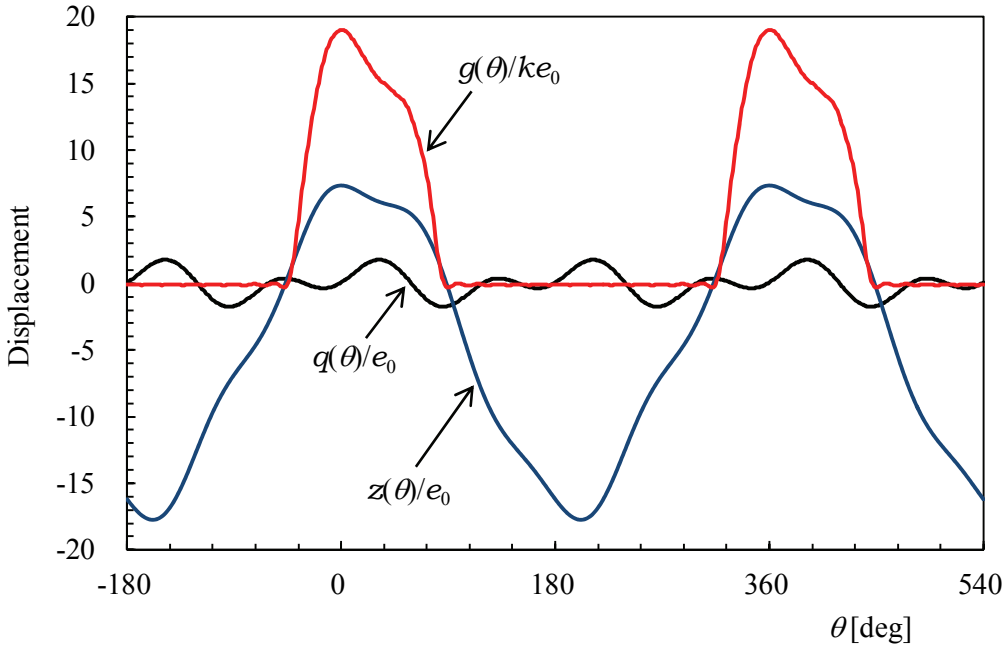

(b) Theoretical calculation result

Figure 2.24 The comparison of numerical simulation result with theoretical calculation result at point C (Ω=2.58) in Figure 2.21

Ω=2.29-2.88. A stable branch is missing at Ω=2.07-2.29. In this region, different resonance vibration Type from assumed Type I and II occurs.

Figures 2.22-2.24 present comparisons of the numerical simulation results with theoretical calculation results for the waveforms of the resulting displacement ratio $z(\theta)/e_0$ and the nonlinear part of the restoring force $g(\theta)/ke_0$ under the excitation $q(\theta)/e_0$ at points A, B and C on the resonance curve in Figure 2.21. The waveforms and amplitudes of these predicted values showed good agreement.

Figure 2.22 and 2.23 present the subharmonic vibration Type II which occurs in the vicinity of the two times frequency ratio and collide to the spring two times in one cycle. The resulting displacement and the nonlinear part of the restoring force in Figure 2.23 are larger than in Figure 2.22. There is a slight difference of the phase lag angle between the numerical simulation results and theoretical calculations. It can be estimated that, in numerical simulation, a numerical error occurs at switching point of the nonlinear restoring force. In subharmonic vibration Type II, the number of transiting switching point is twice as many as vibration Type I. Therefore, numerical error become large and difference of the phase lag angle occurs.

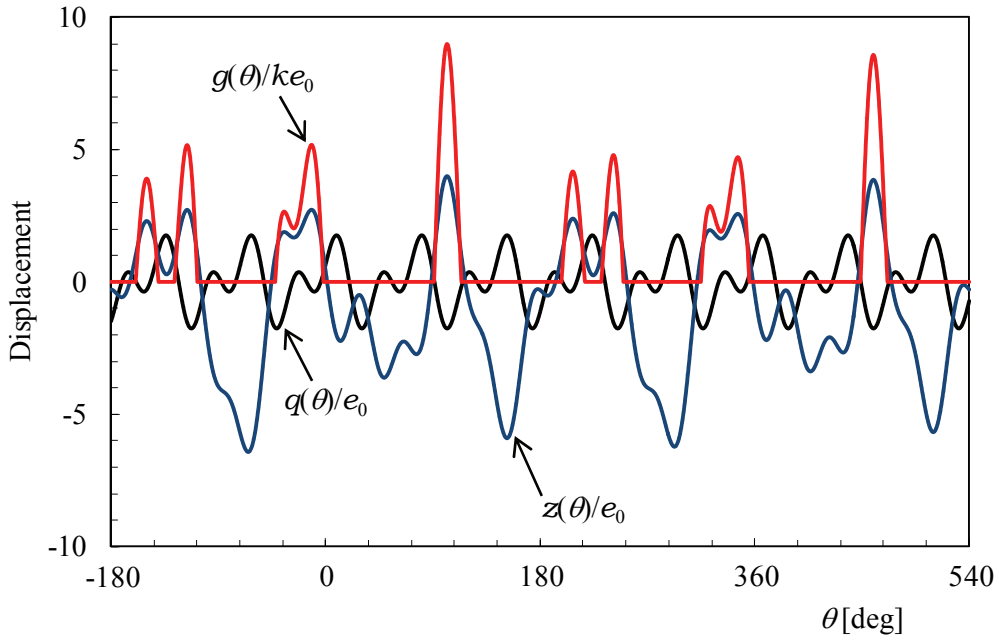

Figure 2.25 Waveforms of displacement excitation, resulting vibration and nonlinear part of restoring force by the Runge-Kutta method at point D in Figure 2.21

Figure 2.24 shows the subharmonic vibration Type I. Comparing the restoring force in Figure 2.23 with 2.24, close two restoring forces in Figure 2.23 grow up and combine, and the subharmonic resonance Type II is transformed into Type I. As a result, the nonlinear part of the restoring force becomes an asymmetrical waveform with respect to the maximum point.

Figures 2.25 shows waveforms of the resulting displacement ratio $z(\theta)/e_0$ and the nonlinear part of restoring force $g(\theta)/ke_0$ under the excitation $q(\theta)/e_0$ by the Runge-Kutta method at point D in Figure 2.21. In this region, the Type IV resonance occurred; the mass contacted the collided spring four times in each cycle of the mass, which occurred during five cycles of the exciting vibration (Ultra-Subharmonic Type IV). In theoretical analysis, resonance vibration Type IV was not considered, therefore stable solutions are missing in this region.

2.3.3 Example of Theoretical Calculations

The steady state periodic solutions were calculated based on the theoretical analysis results in the superhamonic, harmonic and subharmonic resonance region. The calculations were carried out for the combined wave given in Figure 2.9(b), as an example of excitation by a function of arbitrary period. The ○ symbols in the figure indicate boundary points between different vibration types revealed by the calculations. The ● symbols in the figure indicate boundary points between stable and unstable resulting vibration.

Figure 2.26 shows resonance curves obtained by using the damping ratio ζ as a parameter for the 2nd order superharmonic and harmonic resonance vibrations. As ζ increases, the maximum amplitude of the superharmonic and harmonic resonances decreases. In this condition, all periodic solutions are stable.

Figure 2.27 shows resonance curves obtained by the spring constant ratio K/k as a parameter. K/k expresses the magnitude of the nonlinearity of the system; when the resonance curve enters the nonlinear region, it bends, and the greater K/k is, the more the resonance curve

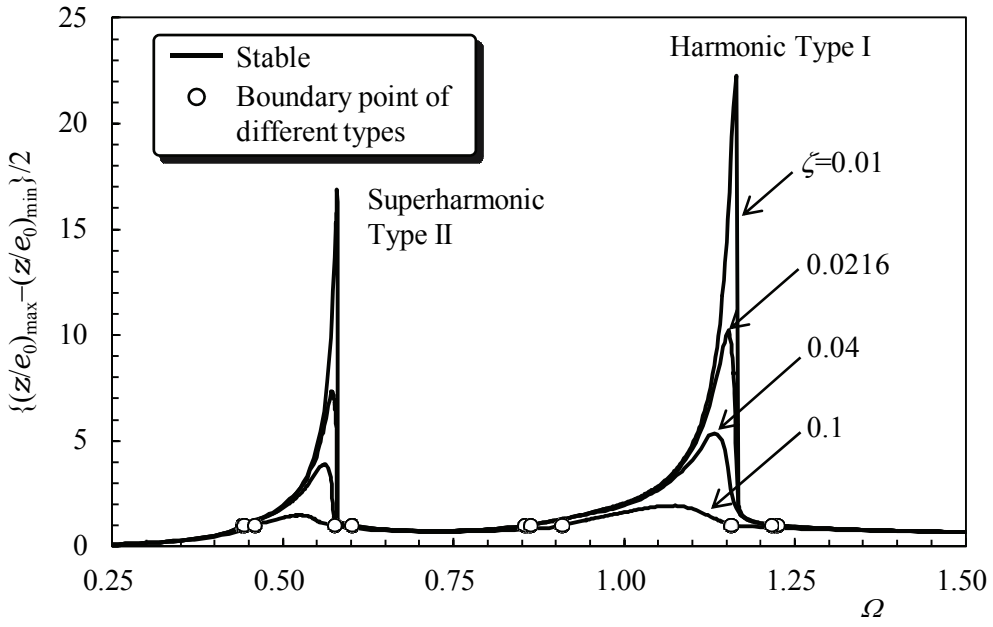

{ $q(t)=\cos\omega t+\sin 2\omega t$, $K/k=1.0$, $f_1/e_0=0.27$}

Figure 2.26 Resonance curves for 2nd order superharmonic and harmonic vibrations in the case where damping ratio ζ is parameter

bends to the right and the maximum amplitude increases. At $K/k \geqq 3$, unstable branches occurred at right side of the resonance curves.

Figure 2.28(a) shows resonance curves in which the excitation amplitude ratio f_1/e_0 has been parameterized. Figure 2.28(b) shows the stability chart to distinguish the stable branches of resonance curves from the unstable ones. This stability chart corresponds to the resonance curves. The numerical results of the chart consist of several insular parts. The "islands" enclosed by the solid lines in the stability chart are unstable regions, while points in the exterior region represent stability. In resonance curves, the greater f_1/e_0 is, the wider the extent of the resonance region, and the lower e_0, the relative width of the linear region (Region I) is, the wider the resonance region. In the cases of f_1/e_0=0.05, 0.2 and 0.32, backbone curves tilt to right towards, and we can estimate that the right branches on the resonance curves are unstable. Exactly, in the stability chart, the portions of the dwell phase angle θ_I for periodic solutions enter into the "islands". At f_1/e_0=0.36, value of θ_I are all outside the 'islands', and thus periodic solutions are all stable.

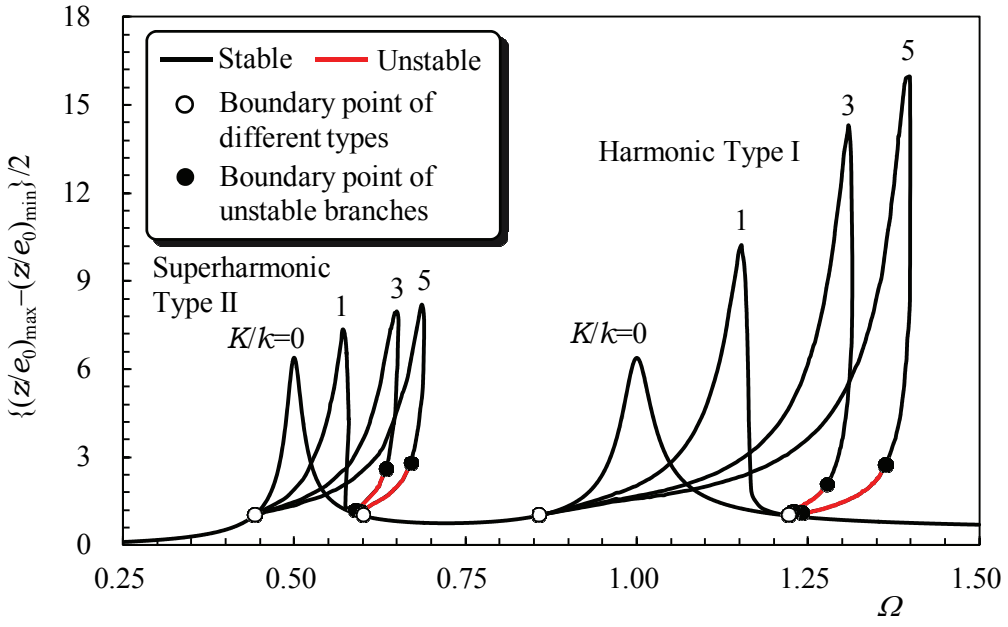

{ $q(t)$=cosωt+sin2ωt, ζ=0.0216, f_1/e_0=0.27}

Figure 2.27 Resonance curves for 2nd order superharmonic and harmonic vibrations in the case where spring constant ratio K/k is parameter

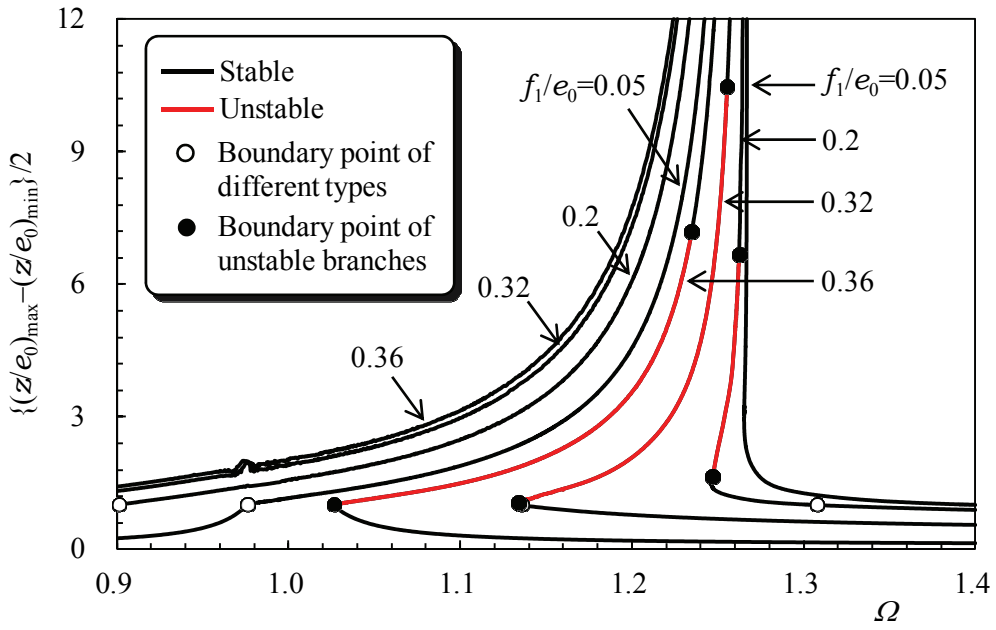

(a) Resonance curves

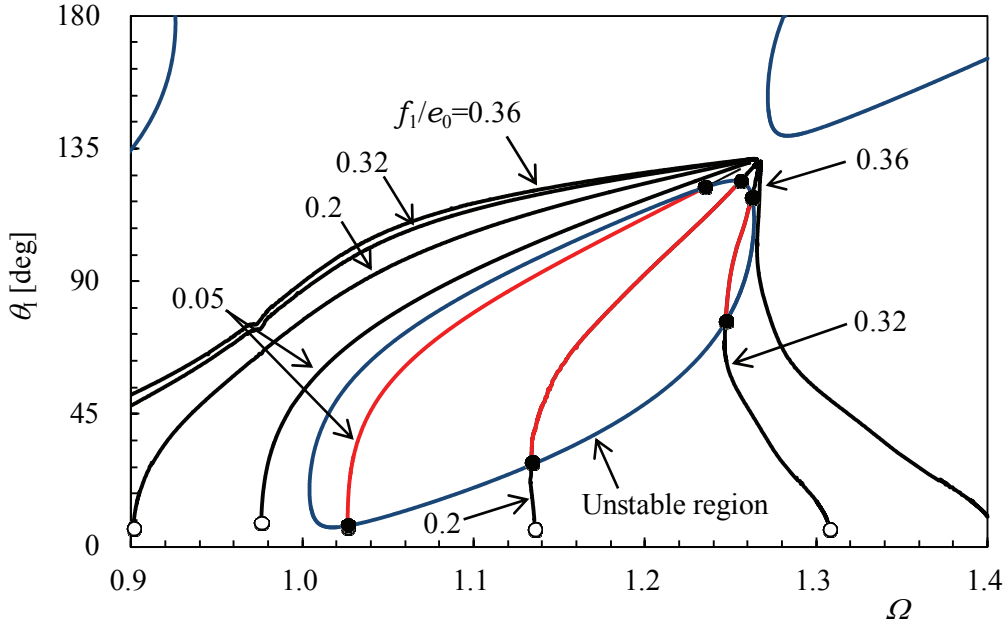

(b) Stability chart

{ $q(t)=\cos\omega t+\sin 2\omega t$, $\zeta=0.001$, $K/k=2.0$}

Figure 2.28 Resonance curves and stability chart for harmonic vibration in the case where f_1/e_0 is parameter

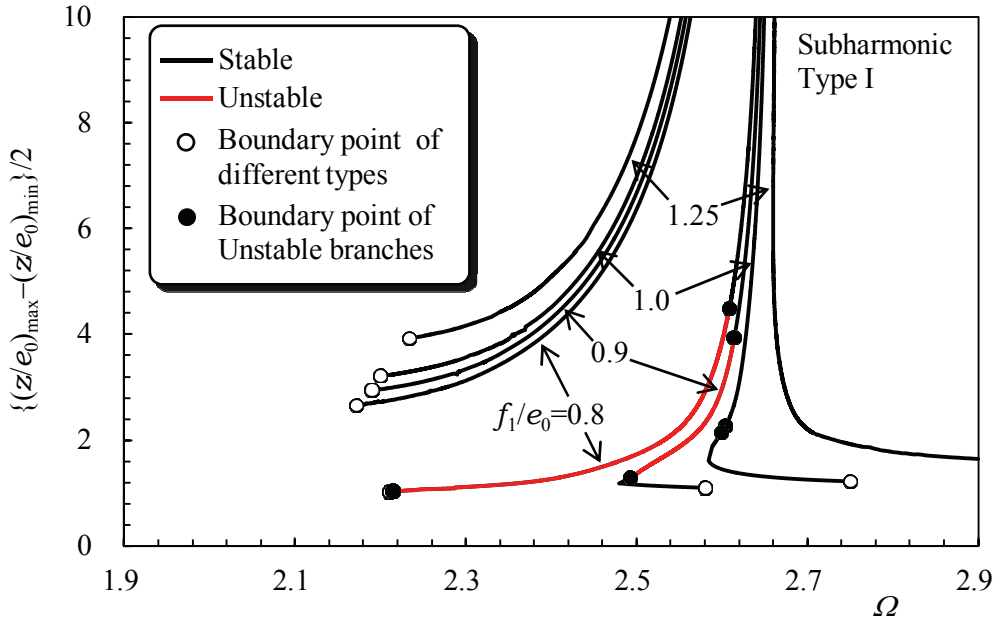

(a) Resonance curves

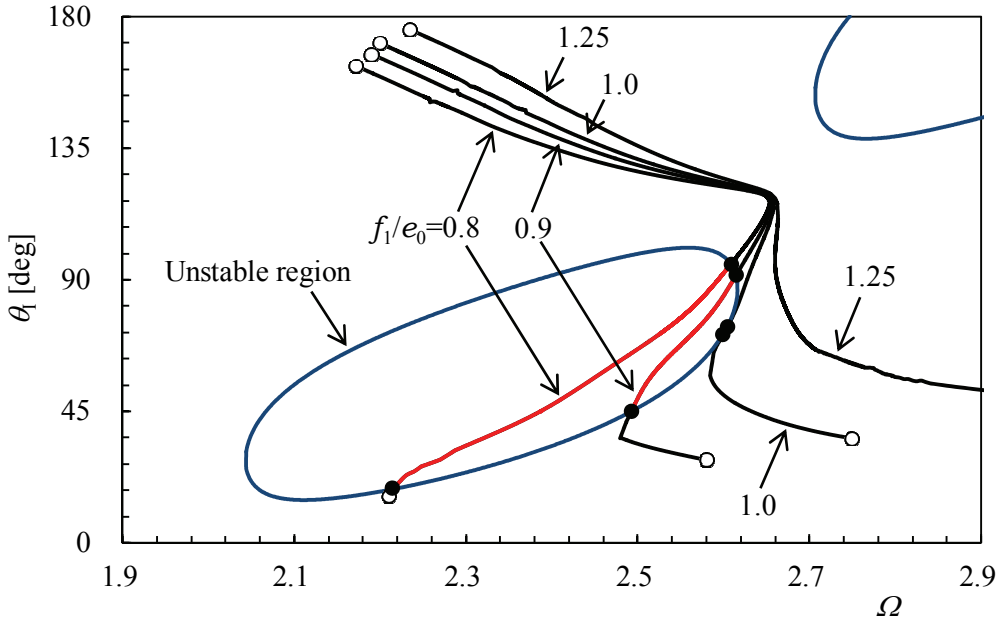

(b) Stability chart

{ $q(t)=\cos\omega t$, $\zeta=0.01$, $K/k=3.0$}

Figure 2.29 Resonance curves and stability chart for 1/2nd order subharmonic vibration in the case where f_1/e_0 is parameter

Figure 2.29(a) shows resonance curves for the subharmonic resonance with the excitation amplitude ratio f_1/e_0 has been parameterized. Figure 2.29(b) shows the stability chart corresponded to the resonance curves. In resonance curves, as f_1/e_0 increases, the resonance region becomes wider and the maximum amplitude increases same as harmonic resonance. In the cases of f_1/e_0=0.8 and 0.9, the potions of θ_1 are in the 'island', and unstable solutions are exist on the right side of the resonance curves. In the cases of f_1/e_0=1.0 and 1.25, all periodic solutions are stable.

Figure 2.30 shows resonance curves for the subharmonic resonance vibration without the stability analysis. Figure (a) shows the resonance curve excited by single harmonic wave [$q(t)=\cos\omega t$]. Figure (b) shows one excited by combined wave [$\cos\omega t+\sin 2\omega t$]. Comparing Figure 2.30(a) with (b), amplitude in Figure (b) is larger than in Figure (a). This is caused by the high harmonic wave of excitation [$\sin 2\omega t$].

Figures 2.31 (a) and (b) show stability charts for the harmonic and subharmonic resonance vibrations in the case of damping ratio ζ=0.

Figure 2.32 shows the stability chart for harmonic resonance vibration obtained by using the damping ratio ζ as parameter. The greater ζ is, the smaller the area of unstable is. In the case of ζ>0.04, the 'islands' are disappeared and all periodic solutions are stable.

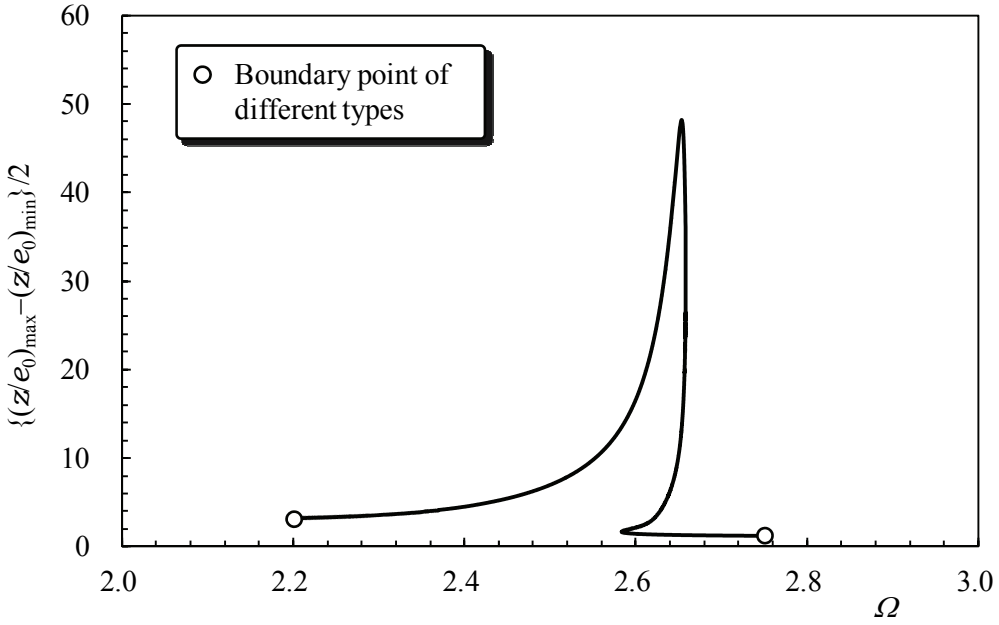

(a) $q(t)=\cos\omega$

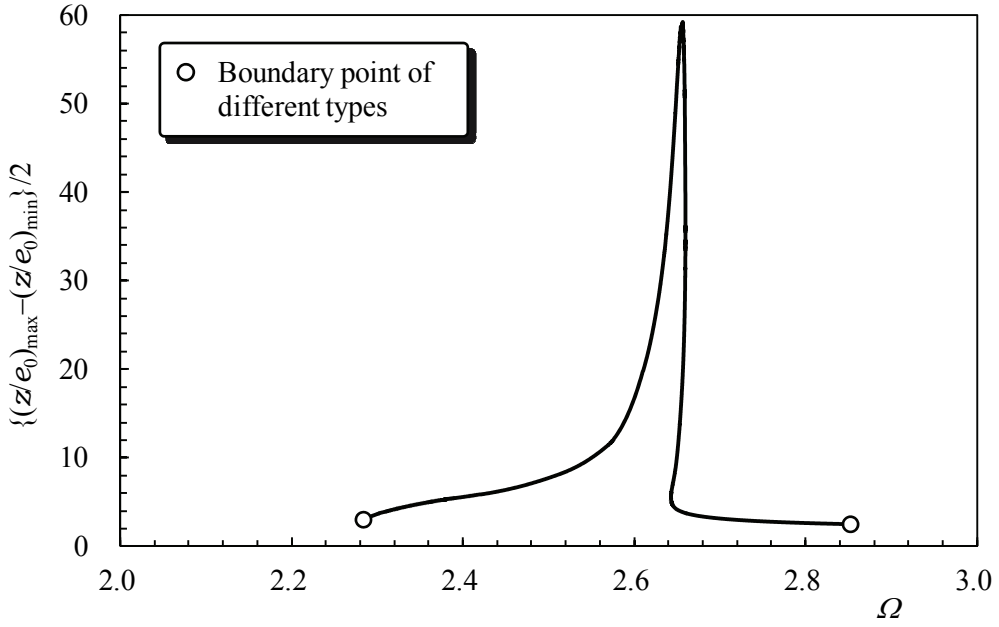

(b) $q(t)=\cos\omega t+\sin 2\omega t$

$\{ f_1/e_0=1.0 , \zeta=0.01, K/k=3.0\}$

Figure 2.30 Resonance curves for 1/2nd order subharmonic vibration subjected to single and combined harmonic excitation

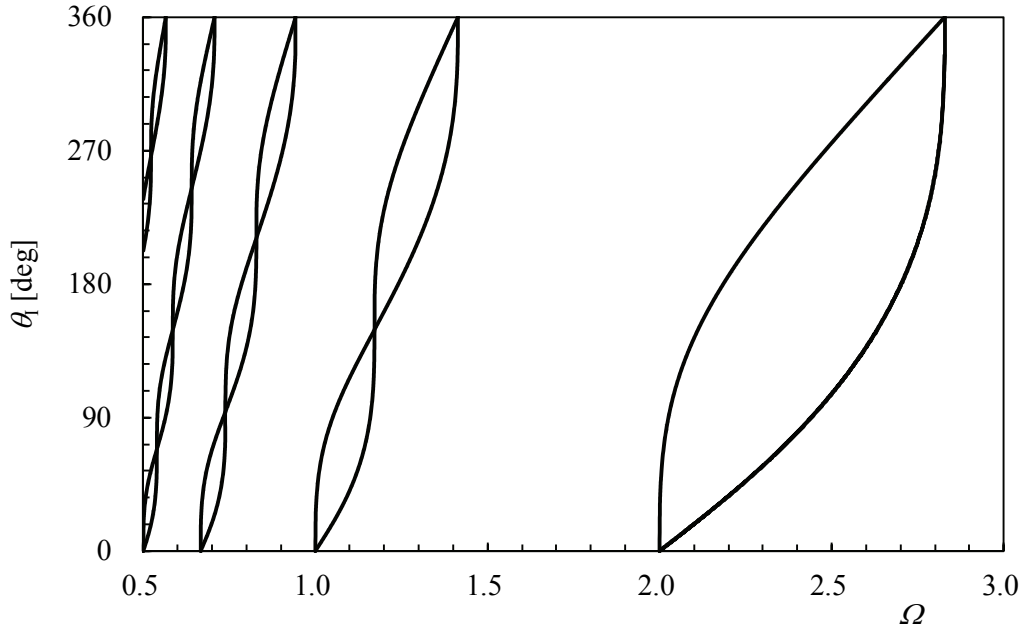

(a) Harmonic vibration

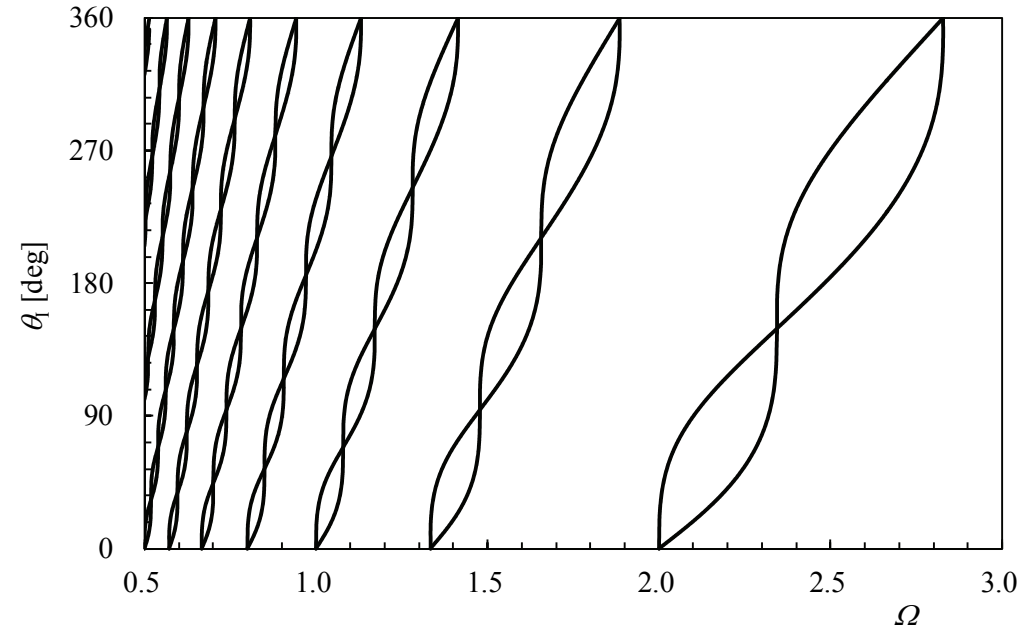

(b) 1/2nd order subharmonic vibration

{ζ=0, K/k=1.0}

Figure2.31 Stability charts for harmonic and 1/2nd order subharmonic vibrations

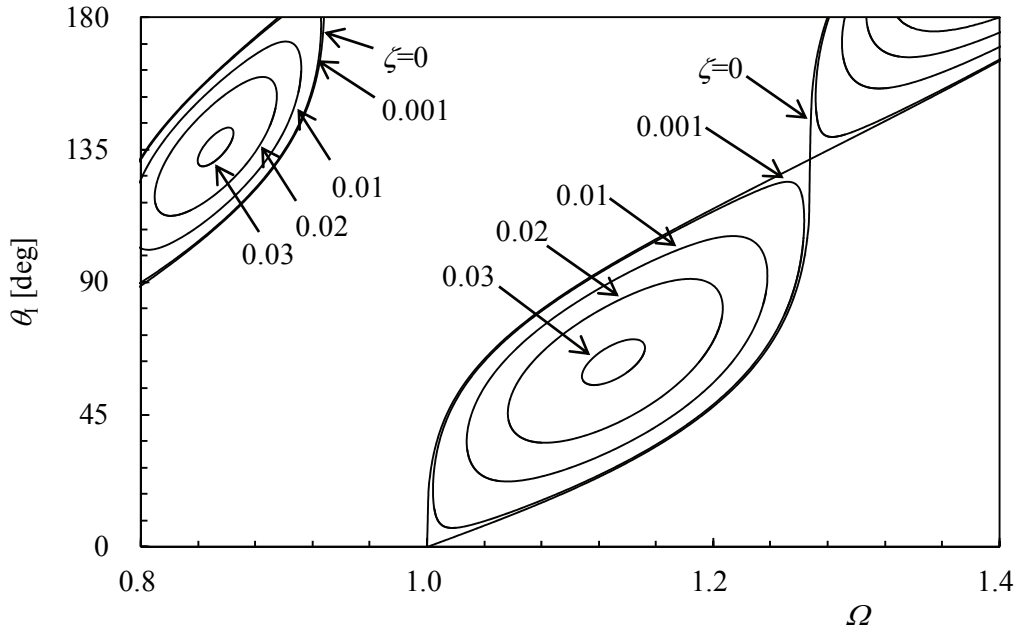

{K/k=2.0}

Figure 2.32 Stability chart for harmonic vibration in the case where ζ is parameter

2.4 Summary

This chapter investigated the resulting vibration and stability of a periodic solution for a mass-spring-damper system as an example of lumped parameter systems with asymmetrical piecewise linear restoring force excited by periodic displacement. The following results were obtained:

(1) An analytical model was constructed of a mass-spring-damper system with a single-degree-of-freedom (DOF) subjected to a periodic excitation and a steady state vibration was analyzed. The analysis assumed the restoring force as an asymmetric piecewise linear system and used the Fourier series method to solve it. Theoretical solutions were derived for the resulting vibration that allows for the harmonic, superharmonic and subharmonic resonances.

(2) The stability of the steady state periodic solutions was investigated with a variational equation. An analytical procedure for examining the effects of minute perturbations on the steady state solution of the original equation of motion was proposed, based on incorporating the variational equation. The stability of the steady state periodic solution was investigated for resonance vibrations Type I and II occurring in the superharmonic , harmonic and subharmonic resonances regions analytically and equations were derived that describe the stability conditions.

(3) Theoretical calculations were performed based on the results of the analysis in (1). The resonance curves were constructed to examine the effects on resonance of several factors: excitation amplitude ratio f_1/e_0, nonlinearity of resulting vibration K/k, damping ratio ζ, resonance curves were also constructed for closer examination of the details of the harmonic, superharmonic and subharmonic resonance regions. The waveform of the resulting vibration and the restoring force of the spring were found.

(4) The stability analysis carried out based on the results of the analysis in (2), and stability charts were constructed. These charts were employed in resonance curves, and stable and unstable branches were distinguished in the resonance curves.

(5) An experiment and a numerical simulation by the fourth order Runge-Kutta method were performed to check the theoretical analysis results for the resonance curve obtained in (3) and (4). The calculation results were shown to agree well with the experimental and numerical simulation results. This analytical method was confirmed to be effective.

(6) It is possible to treat periodic excitations with an arbitrary function in a general manner. Once this analytical method is firmly established, it will be possible to use the procedure in (3) to calculate solutions for resulting vibrations for any magnitude of the parameters in (3).

Chapter 3
Analysis of Response Vibration in Distributed Parameter Systems

This chapter presents basic research on analyzing a steady state vibration arising in an elastic cantilever beam as an example of distributed parameter systems suspended between two springs clamped symmetrically at an arbitrary distance above and below the beam. Thus the beam collides with the supports as it reacted to a periodic displacement excitation with an arbitrary period. The restoring force accompanying the compression of the spring by beam is assumed by a symmetric piecewise linear force. This cantilever model is regularly used as an asymmetrical

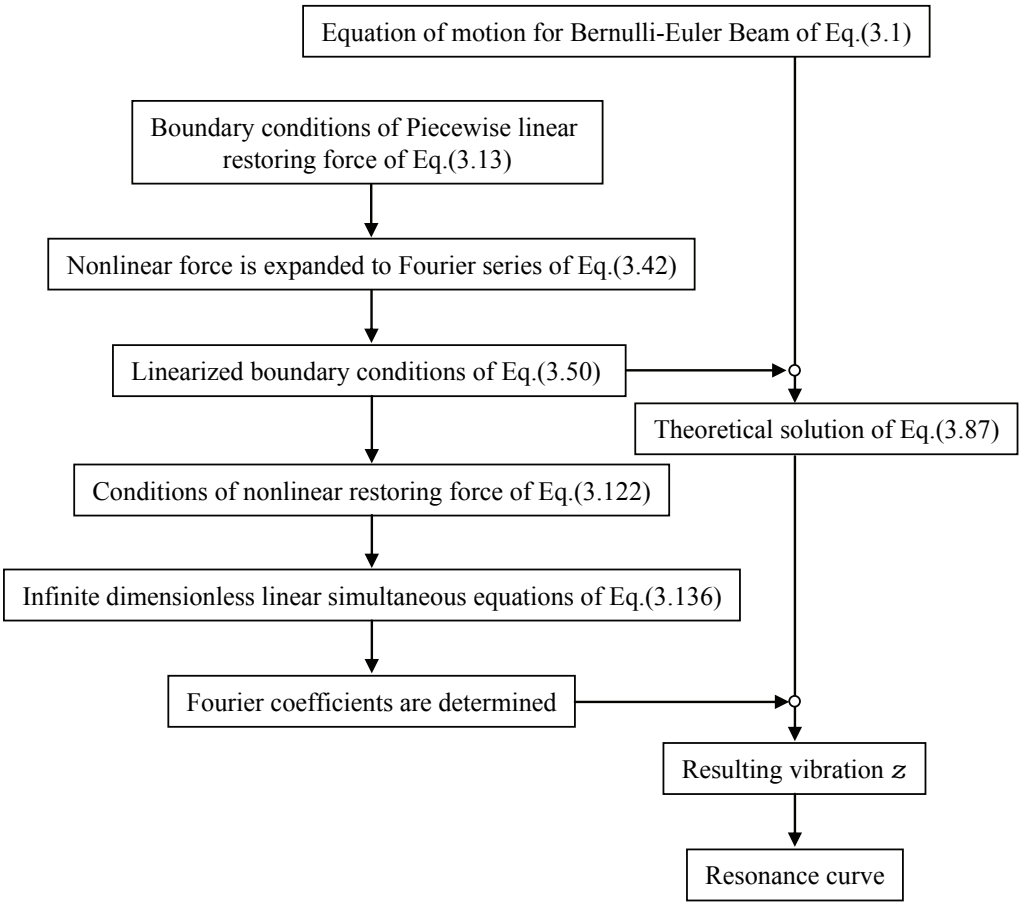

Figure 3.1 Flowchart of theoretical analysis method

structural component. Figure 3.1 shows the fundamental flow of the theoretical analysis method in this chapter. In order to analyze the main resonance for the system, the Fourier series method is applied to obtain a theoretical solution for response vibration. The response waveforms are calculated based on the theoretical results in the main resonance region, resonance curves are generated with parameterized versions of the excitation displacement ratio, the collision position ratio, and the nonlinearity of the restoring force, and the influences of these factors on the resonance curve are examined numerically. An experiment is also conducted with physical conditions matching those used in the simulation; the experimental results are in good agreement with the theoretical predictions, confirming the effectiveness of this analysis.

3.1 Theoretical Analysis

3.1.1 Characteristics of System and Equation of Motion

The system examined in this study is shown in Figure 3.2. It is a cantilever beam (referred to hereafter as "the beam") subjected to elastic collision at an arbitrary point along its span (point collision at $x=a$) with springs clamped to walls located at symmetric distances from the neutral beam position, while subjected to a displacement of a periodic excitation with an arbitrary function $q(t)$. During this vibration, the beam collides elastically with a spring with a spring constant of K at an arbitrary position ($x=a$) along the beam. We consider the beam to consist of two independent bodies on either side of this location: beam I on the side

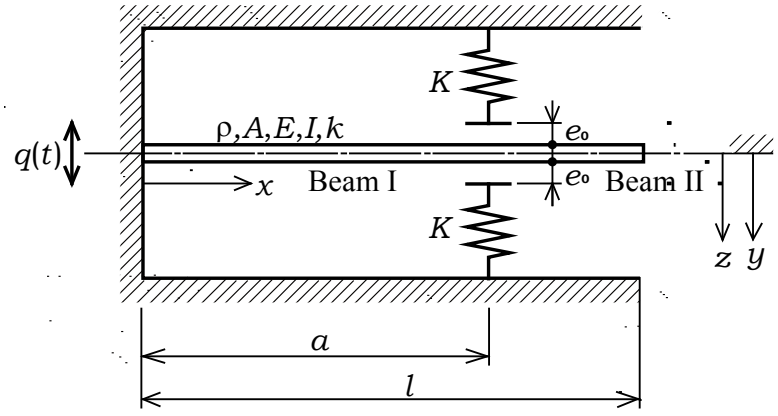

Figure 3.2 Analytical model of steady forced vibration in cantilever beam with clamped springs at arbitrary location

with the fixed end ($0 \le x \le a$) and beam II on the side with the free end ($a \le x \le l$). If the cross-sectional area of the beam is A, the second moment of area is I, the Young's modulus is E, the mass per unit volume is ρ and the absolute displacement of the beam I is y_{I}, then the equation of motion for beam I is given by:

$$\frac{\partial^2 y_{\mathrm{I}}}{\partial t^2} + \frac{EI}{\rho A}\frac{\partial^4 y_{\mathrm{I}}}{\partial x^4} = 0 \tag{3.1}$$

We can calculate the transverse vibration in bending under periodic displacement excitation described by an arbitrary function $q(t)$, the relative displacement of the beam is z_{I}, the following relation is obtained as follows:

$$y_{\mathrm{I}} = z_{\mathrm{I}} + q(t) \tag{3.2}$$

Substituting Equation (3.2) into Equation (3.1) gives the equation of motion for the relative displacement z_{I} as follows:

$$\frac{\partial^2 z_{\mathrm{I}}}{\partial t^2} + \frac{EI}{\rho A}\frac{\partial^4 z_{\mathrm{I}}}{\partial x^4} = -\frac{\partial^2}{\partial t^2} q(t) \tag{3.3}$$

In the same manner, the absolute displacement of the beam II is y_{II} and the relative displacement is z_{II}, the equation of motion for the relative displacement z_{II} is expressed as follows:

$$\frac{\partial^2 z_{\mathrm{II}}}{\partial t^2} + \frac{EI}{\rho A}\frac{\partial^4 z_{\mathrm{II}}}{\partial x^4} = -\frac{\partial^2}{\partial t^2} q(t) \tag{3.4}$$

As shown in Figure 3.3, the restoring force of the spring is symmetric piecewise linear with a dead zone (zone II) at clearance $z = [+e_0, -e_0]$. If zone II is considered as the standard, then zones I and III as an entire system can be considered as the nonlinear regions. The restoring force is expressed as follows:

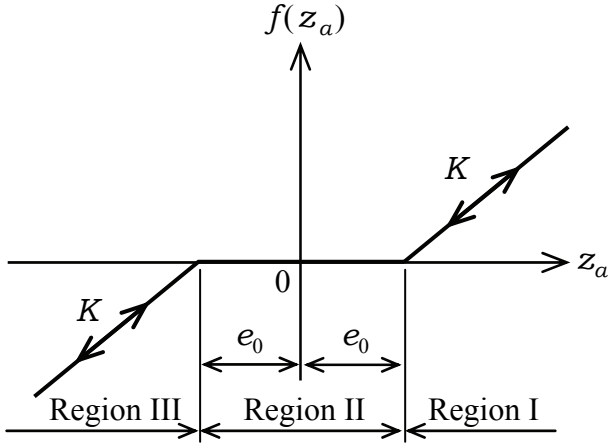

Figure 3.3 Characteristics of restoring force

$$\left.\begin{array}{lll} f(z_a)=K(z_a-e_0), & z_a \geq e_0 & ; \quad \text{Region I} \\ f(z_a)=0, & -e_0 \leq z_a \leq e_0 & ; \quad \text{Region II} \\ f(z_a)=K(z_a+e_0), & z_a \leq -e_0 & ; \quad \text{Region III} \end{array}\right\} \tag{3.5}$$

The boundary conditions for the analytical model shown in Figure 3.2 are set using the following expressions. The subscripts I and II in the expressions indicate values in the corresponding beam number:

$$x=0 : z_{\mathrm{I}}=0 \tag{3.6}$$

$$x=0 : \frac{dz_{\mathrm{I}}}{dx}=0 \tag{3.7}$$

$$x=l : \frac{d^2 z_{\mathrm{II}}}{dx^2}=0 \tag{3.8}$$

$$x=l : \frac{d^3 z_{\mathrm{II}}}{dx^3}=0 \tag{3.9}$$

There is continuity at the boundary point between beam I and II (i.e., the collision position at $x=a$). The continuity conditions are as follows:

$$x = a : z_{\mathrm{I}} = z_{\mathrm{II}} \tag{3.10}$$

$$x = a : \frac{dz_{\mathrm{I}}}{dx} = \frac{dz_{\mathrm{II}}}{dx} \tag{3.11}$$

$$x = a : \frac{d^2 z_{\mathrm{I}}}{dx^2} = \frac{d^2 z_{\mathrm{II}}}{dx^2} \tag{3.12}$$

$$x = a : EI\left(\frac{d^3 z_{\mathrm{I}}}{dx^3} - \frac{d^3 z_{\mathrm{II}}}{dx^3} \right) = f(z_a) \tag{3.13}$$

3.1.2 Fourier Series Method

The displacement of the excitation $q(t)$ acting on the system is assumed to be an arbitrary periodic function and can therefore be expanded into a following complex Fourier series:

$$q(t) = \sum_{n=-\infty}^{\infty} s_n e^{jn\omega t} \tag{3.14}$$

where ω is the angular frequency and s_n is a Fourier coefficient. Substituting Equation (3.14) into Equation (3.3) gives the partial differential equation as follows:

$$\frac{\partial^2 z_{\mathrm{I}}}{\partial t^2} + \frac{EI}{\rho A} \frac{\partial^4 z_{\mathrm{I}}}{\partial x^4} = \sum_{n=-\infty}^{\infty} s_n n^2 \omega^2 e^{jn\omega t} \tag{3.15}$$

The solution $z(x,t)$ of Equation (3.15) is assumed as follows:

$$z(x,t) = V'(x) \cdot T'(t) \tag{3.16}$$

We consider the steady state vibration in this analysis, so the relative beam displacement z is a periodic function of the angular frequency ω. It follows that the time term of the resulting displacement z of Equation (3.16) can be expanded into a following complex Fourier series:

$$T'(t) = \sum_{n=-\infty}^{\infty} r_n e^{jn\omega t} \tag{3.17}$$

where r_n is a Fourier series coefficient to be determined afterwards. Substituting Equation (3.17) into Equation (3.16) and using a relation $V_n(x)=V'_n(x) \cdot r_n$, the relative displacement of response is expressed as follows:

$$z_{\mathrm{I}}(x,t) = \sum_{n=-\infty}^{\infty} V_n(x) e^{jn\omega t} \tag{3.18}$$

In the same manner, the periodic solution of Equation (3.1) is assumed as follows:

$$y_{\mathrm{I}}(x,t) = \sum_{n=-\infty}^{\infty} X_n(x) e^{jn\omega t} \tag{3.19}$$

Substituting the displacement excitation $q(t)$ of Equation (3.14), the absolute displacement $y_{\mathrm{I}}(x,t)$ of Equation (3.19) and the relative displacement $z_{\mathrm{I}}(x,t)$ of Equation (3.18) into Equation (3.2) gives the following equation:

$$\sum_{n=-\infty}^{\infty} \{X_n(x) - V_n(x) - s_n\} e^{jn\omega t} = 0 \tag{3.20}$$

And thus

$$V_n(x) = X_n(x) - s_n \tag{3.21}$$

Substituting Equation (3.18) into Equation (3.15) gives the following equation:

$$\sum_{n=-\infty}^{\infty}\left\{\frac{EI}{\rho A}\frac{\partial^4 V_n(x)}{\partial x^4}-n^2\omega^2 V_n(x)-s_n n^2\omega^2\right\}e^{jn\omega t}=0 \tag{3.22}$$

And thus

$$\frac{EI}{\rho A}\frac{\partial^4 V_n(x)}{\partial x^4}=n^2\omega^2\{V_n(x)+s_n\} \tag{3.23}$$

Substituting Equation (3.21) into Equation (3.23) gives the following ordinary differential equation for the beam I as follows:

$$\frac{d^4 X_n(x)}{dx^4}=\frac{\rho A}{EI}n^2\omega^2 X_n(x) \tag{3.24}$$

In the beam II, the periodic solution is assumed as follows:

$$z_{\mathrm{II}}(x,t)=\sum_{n=-\infty}^{\infty}W_n(x)e^{jn\omega t} \tag{3.25}$$

$$y_{\mathrm{II}}(x,t)=\sum_{n=-\infty}^{\infty}Y_n(x)e^{jn\omega t} \tag{3.26}$$

In the same manner for the beam I, the ordinary differential equation for the beam II can be obtained:

$$\frac{d^4 Y_n(x)}{dx^4}=\frac{\rho A}{EI}n^2\omega^2 Y_n(x) \tag{3.27}$$

$X_n(x)$ and $Y_n(x)$ of equations (3.24) and (3.27) can be expressed as follows by using λ_n:

$$X_n(x)=A_n\cos\lambda_n x+B_n\sin\lambda_n x+C_n\cosh\lambda_n x+D_n\sinh\lambda_n x\quad(n\neq 0) \tag{3.28}$$

$$Y_n(x) = E_n \cos\lambda_n x + F_n \sin\lambda_n x + G_n \cosh\lambda_n x + H_n \sinh\lambda_n x \quad (n \neq 0) \tag{3.29}$$

where the coefficients λ_n are eigenvalues and expressed as follows:

$$\lambda_n^4 = \frac{\rho A}{EI} n^2 \omega^2 \tag{3.30}$$

The A_n, B_n, C_n,$\cdots H_n$ of equations (3.28) and (3.29) are constants to be determined later from the boundary conditions and the continuity ones. The primary angular frequency of a cantilever beam is given by:

$$\omega_1 = \frac{Z_1^2}{l^2}\sqrt{\frac{EI}{\rho A}} \tag{3.31}$$

where

$$Z_1 = 1.875 \tag{3.32}$$

The vibration frequency ratio Ω is

$$\Omega = \frac{\omega}{\omega_1} \tag{3.33}$$

The eigenvalues λ_n are transformed as follows by using Equations (3.30), (3.31) and (3.33):

$$\lambda_n^4 l^4 = Z_1^4 n^2 \Omega^2 \tag{3.34}$$

$$\lambda_n^4 a^4 = \lambda_n^4 l^4 \times \frac{a^4}{l^4} = Z_1^4 n^2 \Omega^2 \times \left(\frac{a}{l}\right)^4 \tag{3.35}$$

Substituting Equation (3.21) into Equation (3.18) gives the resulting vibration z_1 as follows:

$$z_{\mathrm{I}}(x,t)=\sum_{n=-\infty}^{\infty}\{X_n(x)-s_n\}e^{jn\omega t} \tag{3.36}$$

In the same manner, the resulting vibration z_{II} is expressed as follows:

$$z_{\mathrm{II}}(x,t)=\sum_{n=-\infty}^{\infty}\{Y_n(x)-s_n\}e^{jn\omega t} \tag{3.37}$$

We now turn to the situation shown in Figure 3.4, where the restoring force acting on the beam is piecewise linear with a dead zone and consider the waveform of the resulting vibration. This analysis limits considerations to resulting waves in which the beam strikes and compresses the upper and lower springs (both having identical spring constants K) in the nonlinear region only one time each during the main resonance region. Figure 3.4 shows the assumed excitation, the resulting displacement and the solution for the harmonic resonance vibration of the restoring force of the springs. Figure 3.4 (a) shows the periodic displacement excitation acting on the system (solid line: example of rectangular wave excitation; dashed line: fundamental wave). Figure 3.4 (b) shows the resulting beam displacement at the location of the collision with the springs and Figure 3.4 (c) shows the restoring force exerted on the beam during elastic collision with the spring. In order to simplify the analysis, the response waveform is assumed to be approximately axially symmetric about the midpoint of the duration of beam's collision with each of the clamped springs and the maximum or minimum resulting displacement is assumed to occur at those temporal midpoints. One cycle of the resulting wave of the relative displacement z_a at the location of collision with the springs ($x=a$) is divided into three zones (I, II, III), as shown in Figure 3.4 (b) and (c). These zones correspond to zones I, II and III in the restoring force characteristic graph in Figure 3.3. The phase angle θ is introduced here and shown in Figure 3.4 (b) in terms of the portion of the cycle θ_0 (dwell phase angle) spent in contact with one or the other spring. The origin for measuring the phase angle θ is defined from the peak of the resulting waveform. The independent variable of time t is transformed to phase angle θ which is defined as:

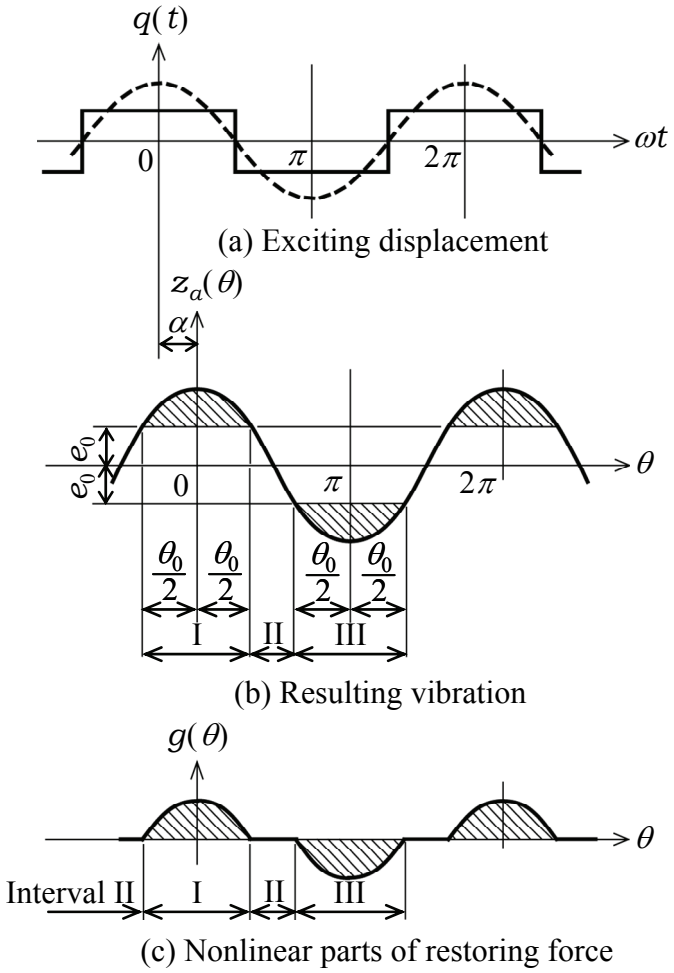

Figure 3.4 Harmonic resonance vibration

$$\theta = \omega t - \alpha \tag{3.38}$$

where α is the phase lag angle, which is currently undefined but will be determined later. Substituting Equation (3.38) into Equations (3.36) and (3.37) gives the resulting vibrations as follows:

Beam I

$$z_{\mathrm{I}}(x,t) = \sum_{n=-\infty}^{\infty} \{X_n(x) - s_n\} e^{jn(\theta+\alpha)} \tag{3.39}$$

Beam II

$$z_{\mathrm{II}}(x,t)=\sum_{n=-\infty}^{\infty}\{Y_n(x)-s_n\}e^{jn(\theta+\alpha)} \tag{3.40}$$

The restoring force $f(z)$ of Equation (3.5) is transformed into $g(\theta)$ by using phase angle:

$$\left.\begin{array}{lll} g(\theta)=K(z_a-e_0), & -\dfrac{\theta_0}{2}\le\theta\le\dfrac{\theta_0}{2} & ;\ \text{Interval I} \\ g(\theta)=0, & \dfrac{\theta_0}{2}\le\theta\le\pi-\dfrac{\theta_0}{2},\ \pi+\dfrac{\theta_0}{2}\le\theta\le 2\pi-\dfrac{\theta_0}{2} & ;\ \text{Interval II} \\ g(\theta)=K(z_a+e_0), & \pi-\dfrac{\theta_0}{2}\le\theta\le\pi+\dfrac{\theta_0}{2} & ;\ \text{Interval III} \end{array}\right\} \tag{3.41}$$

The period of the nonlinear restoring force $g(\theta)$ of Equation (3.41) can be considered to be equal to the period of the resulting vibration waveform. Thus, it can be expanded into a complex Fourier series as follows:

$$g(\theta)=\sum_{n=-\infty}^{\infty}c_n e^{jn\theta} \tag{3.42}$$

3.1.3 Determination of Coefficients

Here, undetermined coefficients of $X_n(x)$ and $Y_n(x)$ of Equations (3.28) and (3.29) are derived by using the boundary conditions of Equations (3.6)-(3.9) and the continuity ones of Equations (3.10)-(3.13). Applying the boundary condition of Equation (3.6) to the resulting vibration of Equation (3.39) gives the following equation:

$$\begin{aligned} &\sum_{n=-\infty}^{\infty}\{X_n(0)-s_n\}\cdot e^{jn(\theta+\alpha)}=0 \\ &\therefore X_n(0)=s_n \end{aligned} \tag{3.43}$$

Applying the boundary condition of Equation (3.7) to the resulting vibration of Equation (3.39) gives the following equation:

$$\sum_{n=-\infty}^{\infty} X_n^{(1)}(0)\cdot e^{jn(\theta+\alpha)} = 0$$
$$\therefore X_n^{(1)}(0) = 0 \tag{3.44}$$

Applying the boundary condition of Equation (3.8) to the resulting vibration of Equation (3.39) gives the following equation:

$$\sum_{n=-\infty}^{\infty} Y_n^{(2)}(l)\cdot e^{jn(\theta+\alpha)} = 0$$
$$\therefore Y_n^{(2)}(l) = 0 \tag{3.45}$$

Applying the boundary condition of Equation (3.9) to the resulting vibration of Equation (3.39) gives the following equation:

$$\sum_{n=-\infty}^{\infty} Y_n^{(3)}(l)\cdot e^{jn(\theta+\alpha)} = 0$$
$$\therefore Y_n^{(3)}(l) = 0 \tag{3.46}$$

Applying the continuity condition of Equation (3.10) to the resulting vibration of Equations (3.39) and (3.40) gives the following equation:

$$\sum_{n=-\infty}^{\infty} \{X_n(a) - s_n\}\cdot e^{jn(\theta+\alpha)} = \sum_{n=-\infty}^{\infty} \{Y_n(a) - s_n\}\cdot e^{jn(\theta+\alpha)}$$
$$\therefore X_n(a) = Y_n(a) \tag{3.47}$$

Applying the continuity condition of Equation (3.11) to the resulting vibration of Equations (3.39) and (3.40) gives the following equation:

$$\sum_{n=-\infty}^{\infty} X_n^{(1)}(a)\cdot e^{jn(\theta+\alpha)} = \sum_{n=-\infty}^{\infty} Y_n^{(1)}(a)\cdot e^{jn(\theta+\alpha)}$$
$$\therefore X_n^{(1)}(a) = Y_n^{(1)}(a) \tag{3.48}$$

Applying the continuity condition of Equation (3.12) to the resulting vibration of Equations (3.39) and (3.40) gives the following equation:

$$\begin{aligned}&\sum_{n=-\infty}^{\infty} X_n^{(2)}(a)\cdot e^{jn(\theta+\alpha)} = \sum_{n=-\infty}^{\infty} Y_n^{(2)}(a)\cdot e^{jn(\theta+\alpha)} \\ &\therefore X_n^{(2)}(a) = Y_n^{(2)}(a)\end{aligned} \tag{3.49}$$

Applying the continuity condition of Equation (3.13) to the resulting vibration of Equation (3.39) and (3.40) gives the following equation:

$$\begin{aligned}&EI\left\{\sum_{n=-\infty}^{\infty} X_n^{(3)}(a)\cdot e^{jn(\theta+\alpha)} - \sum_{n=-\infty}^{\infty} Y_n^{(3)}(a)\cdot e^{jn(\theta+\alpha)}\right\} = \sum_{n=-\infty}^{\infty} c_n e^{jn\theta} \\ &\therefore X_n^{(3)}(a) - Y_n^{(3)}(a) = \frac{c_n}{EIe^{in\alpha}}\end{aligned} \tag{3.50}$$

Using equations (3.28) and (3.43) gives the following equation:

$$\begin{aligned}&X_n(0) = A_n\cos 0 + B_n\sin 0 + C_n\cosh 0 + D_n\sinh 0 = s_n \\ &\therefore C_n = -A_n + s_n\end{aligned} \tag{3.51}$$

Using equations (3.28) and (3.44) gives the following equation:

$$\begin{aligned}&X_n^{(1)}(0) = \left(-A_n\sin 0 + B_n\cos 0 + C_n\sinh 0 + D_n\cosh 0\right)\lambda_n \\ &\therefore D_n = -B_n\end{aligned} \tag{3.52}$$

Substituting Equations (3.51) and (3.52) into Equation (3.28) and differentiating gives the following equations:

$$X_n = A_n\left(\cos\lambda_n x - \cosh\lambda_n x\right) + B_n\left(\sin\lambda_n x - \sinh\lambda_n x\right) + s_n\cosh\lambda_n x \tag{3.53}$$

$$X_n^{(1)} = \left\{-A_n\left(\sin\lambda_n x + \sinh\lambda_n x\right) + B_n\left(\cos\lambda_n x - \cosh\lambda_n x\right) + s_n\sinh\lambda_n x\right\}\lambda_n \tag{3.54}$$

$$X_n^{(2)} = \{-A_n(\cos\lambda_n x + \cosh\lambda_n x) - B_n(\sin\lambda_n x + \sinh\lambda_n x) + s_n \cosh\lambda_n x\}\lambda_n{}^2 \tag{3.55}$$

$$X_n^{(3)} = \{A_n(\sin\lambda_n x - \sinh\lambda_n x) - B_n(\cos\lambda_n x + \cosh\lambda_n x) + s_n \sinh\lambda_n x\}\lambda_n{}^3 \tag{3.56}$$

Differentiating Equation (3.29) gives the following equations:

$$Y_n = E_n \cos\lambda_n x + F_n \sin\lambda_n x + G_n \cosh\lambda_n x + H_n \sinh\lambda_n x \tag{3.57}$$

$$Y_n^{(1)} = \{-E_n \sin\lambda_n x + F_n \cos\lambda_n x + G_n \sinh\lambda_n x + H_n \cosh\lambda_n x\}\lambda_n \tag{3.58}$$

$$Y_n^{(2)} = \{-E_n \cos\lambda_n x - F_n \sin\lambda_n x + G_n \cosh\lambda_n x + H_n \sinh\lambda_n x\}\lambda_n{}^2 \tag{3.59}$$

$$Y_n^{(3)} = \{E_n \sin\lambda_n x - F_n \cos\lambda_n x + G_n \sinh\lambda_n x + H_n \cosh\lambda_n x\}\lambda_n{}^3 \tag{3.60}$$

Applying Equations (3.47)-(3.50) to Equations (3.53)-(3.60), E_n, F_n, G_n, H_n are derived as follows:

$$E_n = A_n - I_n \sin\lambda_n a \tag{3.61}$$

$$F_n = B_n + I_n \cos\lambda_n a \tag{3.62}$$

$$G_n = -A_n + I_n \sinh\lambda_n a + s_n \tag{3.63}$$

$$H_n = -B_n - I_n \cosh\lambda_n a \tag{3.64}$$

where I_n of Equations (3.61)-(3.64) is expressed as follows:

$$I_n = \frac{c_n}{2EI\lambda_n{}^3 e^{in\alpha}} \tag{3.65}$$

Substituting Equations (3.61)-(3.64) into Equation (3.59) and using Equation (3.45) gives the

following equation:

$$\begin{aligned}&-A_n(\cos\lambda_n l+\cosh\lambda_n l)-B_n(\sin\lambda_n l+\sinh\lambda_n l)+s_n\cosh\lambda_n l\\&+I_n(\sin\lambda_n a\cos\lambda_n l-\cos\lambda_n a\sin\lambda_n l+\sinh\lambda_n a\cosh\lambda_n l-\cosh\lambda_n a\sinh\lambda_n l)=0\end{aligned}\tag{3.66}$$

Substituting Equations (3.61)-(3.64) into Equation (3.60) and using Equation (3.46) gives the following equation:

$$\begin{aligned}&A_n(\sin\lambda_n l-\sinh\lambda_n l)-B_n(\cos\lambda_n l+\cosh\lambda_n l)+s_n\sinh\lambda_n l\\&+I_n(-\sin\lambda_n a\sin\lambda_n l-\cos\lambda_n a\cos\lambda_n l+\sinh\lambda_n a\sinh\lambda_n l-\cosh\lambda_n a\cosh\lambda_n l)=0\end{aligned}\tag{3.67}$$

Solving Equations (3.66) and (3.67), the coefficients A_n and B_n are obtained as follows:

$$A_n=\frac{\begin{aligned}&-I_n\begin{pmatrix}\sin\lambda_n a(-1-\cos\lambda_n l\cosh\lambda_n l-\sin\lambda_n l\sinh\lambda_n l)\\+\cos\lambda_n a(\sin\lambda_n l\cosh\lambda_n l-\cos\lambda_n l\sinh\lambda_n l)\\+\sinh\lambda_n a(-1-\cos\lambda_n l\cosh\lambda_n l+\sin\lambda_n l\sinh\lambda_n l)\\+\cosh\lambda_n a(\cos\lambda_n l\sinh\lambda_n l-\sin\lambda_n l\cosh\lambda_n l)\end{pmatrix}+s_n(1+\cos\lambda_n l\cosh\lambda_n l-\sin\lambda_n l\sinh\lambda_n l)\end{aligned}}{2(1+\cos\lambda_n l\cosh\lambda_n l)}\tag{3.68}$$

$$B_n=\frac{\begin{aligned}&I_n\begin{pmatrix}\sin\lambda_n a(-\cos\lambda_n l\sinh\lambda_n l-\sin\lambda_n l\cosh\lambda_n l)\\+\cos\lambda_n a(-1+\sin\lambda_n l\sinh\lambda_n l-\cos\lambda_n l\cosh\lambda_n l)\\+\sinh\lambda_n a(\sin\lambda_n l\cosh\lambda_n l+\cos\lambda_n l\sinh\lambda_n l)\\+\cosh\lambda_n a(-1-\sin\lambda_n l\sinh\lambda_n l-\cos\lambda_n l\cosh\lambda_n l)\end{pmatrix}+s_n(\sin\lambda_n l\cosh\lambda_n l+\cos\lambda_n l\sinh\lambda_n l)\end{aligned}}{2(1+\cos\lambda_n l\cosh\lambda_n l)}\tag{3.69}$$

Substituting coefficients A_n and B_n into Equation (3.53), $X_n(a)$ is expressed as follows:

$$X_n(a)=s_n(N_n+1)+\frac{M_n c_n}{ke^{jn\alpha}}\ (n\neq 0)\tag{3.70}$$

where N_n, M_n and k are constants and expressed as follows:

$$N_n = \frac{1}{2\left(1+\cos\lambda_n l\cosh\lambda_n l\right)} \times \left\{ \begin{array}{l} +\left(\cos\lambda_n a+\cosh\lambda_n a\right)\left(1+\cos\lambda_n l\cosh\lambda_n l\right) \\ -\left(\cos\lambda_n a-\cosh\lambda_n a\right)\sin\lambda_n l\sinh\lambda_n l \\ +\left(\sin\lambda_n a-\sinh\lambda_n a\right)\left(\sin\lambda_n l\cosh\lambda_n l+\cos\lambda_n l\sinh\lambda_n l\right) \end{array} \right\} - 1 \quad (3.71)$$

$$M_n = \frac{3}{\lambda_n^3 l^3}\frac{1}{4\left(1+\cos\lambda_n l\cosh\lambda_n l\right)} \times \left\{ \begin{array}{l} 2\cos\lambda_n a\sin\lambda_n a\sin\lambda_n l\sinh\lambda_n l \\ +2\cos\lambda_n a\sinh\lambda_n a\left(1+\cos\lambda_n l\cosh\lambda_n l-\sin\lambda_n l\sinh\lambda_n l\right) \\ +2\cos\lambda_n a\cosh\lambda_n a\left(-\cos\lambda_n l\sinh\lambda_n l+\sin\lambda_n l\cosh\lambda_n l\right) \\ +2\sin\lambda_n a\cosh\lambda_n a\left(-1-\cos\lambda_n l\cosh\lambda_n l-\sin\lambda_n l\sinh\lambda_n l\right) \\ +2\cosh\lambda_n a\sinh\lambda_n a\sin\lambda_n l\sinh\lambda_n l \\ +2\sin\lambda_n a\sinh\lambda_n a\left(\sin\lambda_n l\cosh\lambda_n l+\cos\lambda_n l\sinh\lambda_n l\right) \\ +\left(\cos^2\lambda_n a-\sin^2\lambda_n a\right)\cos\lambda_n l\sinh\lambda_n l \\ -\left(\cosh^2\lambda_n a+\sinh^2\lambda_n a\right)\sin\lambda_n l\cosh\lambda_n l \\ +\cos\lambda_n l\sinh\lambda_n l-\sin\lambda_n l\cosh\lambda_n l \end{array} \right\} \quad (3.72)$$

$$k = \frac{3EI}{l^3} \quad (3.73)$$

Substituting Equation (3.70) into Equation (3.39) gives the resulting displacement at the collision position ($x=a$) as follows:

$$z_a = \sum_{n=-\infty}^{\infty}\left(s_n N_n e^{jn\alpha} + M_n\frac{c_n}{k}\right)e^{jn\theta} \quad (3.74)$$

Substituting coefficients E_n, F_n, G_n and H_n into Equation (3.57), $Y_n(l)$ is expressed as follows:

$$Y_n(l) = s_n\left(N_n' + 1\right) + \frac{M_n' c_n}{k e^{in\alpha}} \quad (3.75)$$

where N'_n and M'_n are constants and expressed as follows:

$$N'_n = \frac{(\cosh\lambda_n l - 1)(1 - \cos\lambda_n l)}{1 + \cos\lambda_n l \cosh\lambda_n l} \tag{3.76}$$

$$M'_n = \frac{3}{\lambda_n^3 l^3} \frac{1}{4(1 + \cos\lambda_n l \cosh\lambda_n l)} \times \begin{Bmatrix} \sin\lambda_n a\left(-2\cosh\lambda_n l - 2\cos\lambda_n l + \cos^2\lambda_n l \cosh\lambda_n l\right) \\ +\cos\lambda_n a(2\sinh\lambda_n l + 2\sin\lambda_n l - \cos\lambda_n l \sin\lambda_n l \cosh\lambda_n l) \\ +\sinh\lambda_n a\left(2\cos\lambda_n l + 2\cosh\lambda_n l - \cos\lambda_n l \cosh^2\lambda_n l\right) \\ +\cosh\lambda_n a(-2\sin\lambda_n l - 2\sinh\lambda_n l + \cos\lambda_n l \cosh\lambda_n l \sinh\lambda_n l) \end{Bmatrix} \tag{3.77}$$

Substituting Equation (3.75) into Equation (3.40) gives the resulting displacements at tip of the beam ($x=l$) as follows:

$$z_l = \sum_{n=-\infty}^{\infty} \left(s_n N'_n e^{jn\alpha} + M'_n \frac{c_n}{k} \right) e^{jn\theta} \tag{3.78}$$

3.1.4 Changing Complex Fourier Coefficients to Real ones

Here, complex Fourier coefficients in resulting displacements are changed to real ones. By definition of complex Fourier series, the following relations are obtained:

$$\begin{aligned} &f_n = f_{-n}\ ,\ g_n = -g_{-n}\ ,\ g_0 = 0\ ,\ a_n = a_{-n}\ ,\ b_n = -b_{-n}\ ,\ b_0 = 0 \\ &s_n = \frac{f_n - ig_n}{2}\ ,\ c_n = \frac{a_n - ib_n}{2} \end{aligned} \tag{3.79}$$

The eigenvalues λ_n are real number, and thus N_n, M_n, N'_n and M'_n satisfy the following relation:

$$N_n = N_{-n}\ ,\ M_n = M_{-n}\ ,\ N'_n = N'_{-n}\ ,\ M'_n = M'_{-n} \tag{3.80}$$

The complex Fourier coefficients of Equation (3.74) are changed to real number by using Equations (3.79) and (3.80), and the resulting vibration at the collision position z_a is expressed as follows:

$$
\begin{aligned}
z_a &= \sum_{n=-\infty}^{\infty}\left(s_n N_n e^{in\alpha}+\frac{M_n c_n}{k}\right)e^{jn\theta} \\
&= s_0 N_0+\frac{M_0 c_0}{k}+\sum_{n=1}^{\infty}\left[\begin{array}{l}\left(s_n N_n e^{in\alpha}+\dfrac{M_n c_n}{k}\right)(\cos n\theta+i\sin n\theta) \\ +\left\{s_{-n} N_{-n} e^{i(-n)\alpha}+\dfrac{M_{-n} c_{-n}}{k}\right\}\{\cos(-n\theta)+i\sin(-n\theta)\}\end{array}\right] \\
&= s_0 N_0+\frac{M_0 c_0}{k}++\sum_{n=1}^{\infty}\left[\begin{array}{l}\left\{N_n(f_n\cos n\alpha+g_n\sin n\alpha)+M_n\dfrac{a_n}{k}\right\}\cos n\theta \\ +\left\{N_n(g_n\cos n\alpha-f_n\sin n\alpha)+M_n\dfrac{b_n}{k}\right\}\sin n\theta\end{array}\right]
\end{aligned}
\tag{3.81}
$$

Equation (3.81) is simplified as follows:

$$
z_a = s_0 N_0+\frac{M_0 c_0}{k}+\sum_{n=1}^{\infty}\left\{\left(N_n f_n'+M_n\frac{a_n}{k}\right)\cos n\theta+\left(N_n g_n'+M_n\frac{b_n}{k}\right)\sin n\theta\right\} \tag{3.82}
$$

where

$$
\left.\begin{array}{l} f_n' = f_n\cos n\alpha+g_n\sin n\alpha \\ g_n' = g_n\cos n\alpha-f_n\sin n\alpha\end{array}\right\} \tag{3.83}
$$

In this analysis, the resulting wave is assumed to be symmetric and the following relation holds:

$$
z_a(\theta) = -z_a(\pi+\theta) \tag{3.84}
$$

Applying Equation (3.84) to Equation (3.82) gives the following equation:

$$
s_0 N_0+\frac{M_0 c_0}{k}+\sum_{n=2.4.6\cdots}^{\infty}\left\{\left(N_n f_n'+M_n\frac{a_n}{k}\right)\cos n\theta+\left(N_n g_n'+M_n\frac{b_n}{k}\right)\sin n\theta\right\}=0 \tag{3.85}
$$

And thus, the resulting displacements at the collision position ($x=a$) is expressed as follows:

$$z_a = \sum_{n=1,3,5,\cdots}^{\infty} \left\{ \left(N_n f_n' + M_n \frac{a_n}{k} \right) \cos n\theta + \left(N_n g_n' + M_n \frac{b_n}{k} \right) \sin n\theta \right\} \tag{3.86}$$

In the same manner, the resulting displacements at tip of the beam ($x=l$) is derived as follows:

$$z_l = \sum_{n=1,3,5,\cdots}^{\infty} \left\{ \left(N_n' f_n' + M_n' \frac{a_n}{k} \right) \cos n\theta + \left(N_n' g_n' + M_n' \frac{b_n}{k} \right) \sin n\theta \right\} \tag{3.87}$$

3.1.5 Switching-Over Conditions

When the restoring force in collision system is piecewise linear, the vibrations undergo periodic steady state after the transient period, and these steady state vibrations can be occurred several types but, in this chapter analysis is limited to waveforms containing only a single entrance into the nonlinear portions of the restoring force per cycle in the main resonance region. Here, the dwell phase angle θ_0 is defined as the portion of the resulting vibration period spent in nonlinear zones I and III. The following expressions show the conditions at the collision point when the beam enters and leaves the nonlinear regions and these conditions are called switching-over conditions:

$$\theta = \pm \frac{\theta_0}{2} : z_a = e_0 \tag{3.88}$$

$$\theta = \pi \pm \frac{\theta_0}{2} : \ z_a = -e_0 \tag{3.89}$$

In the following theory, above mentioned, the resulting wave is assumed to be symmetric and to satisfy $z(\theta) = -z(\theta + \pi)$. Therefore, only the first half period is considered in the following discussion of the switching-over conditions.

(i) Switching-Over Condition : In the case of $\theta = \theta_0/2$

When $\theta = \theta_0/2$, the resulting displacement $z(\theta_0/2)$ is equal to e_0:

$$e_0 = \sum_{n=1,3,5,\cdots}^{\infty} \left\{ \left(N_n f_n' + M_n \frac{a_n}{k} \right) \cos \frac{n\theta_0}{2} + \left(N_n g_n' + M_n \frac{b_n}{k} \right) \sin \frac{n\theta_0}{2} \right\} \tag{3.90}$$

(ii) Switching-Over Condition : In the case of $\theta = -\theta_0/2$

When $\theta = -\theta_0/2$, the resulting displacement $z(-\theta_0/2)$ is equal to e_0:

$$e_0 = \sum_{n=1,3,5,\cdots}^{\infty} \left\{ \left(N_n f_n' + M_n \frac{a_n}{k} \right) \cos \frac{n\theta_0}{2} - \left(N_n g_n' + M_n \frac{b_n}{k} \right) \sin \frac{n\theta_0}{2} \right\} \tag{3.91}$$

Summing Equation (3.90) and (3.91) gives the following equation:

$$e_0 = \sum_{n=1,3,5,\cdots}^{\infty} \left(N_n f_n' + M_n \frac{a_n}{k} \right) \cos \frac{n\theta_0}{2} \tag{3.92}$$

Subtracting Equation (3.90) from (3.91) gives the following equation:

$$0 = \sum_{n=1,3,5,\cdots}^{\infty} \left(N_n g_n' + M_n \frac{b_n}{k} \right) \sin \frac{n\theta_0}{2} \tag{3.93}$$

3.1.6 Derivation of Non-Dimensional Equations

(1) Non-dimensional resulting Vibration at collision position z_a/e_0

Subtracting Equation (3.92) from Equation (3.86) gives the following equation:

$$z_a - e_0 = \sum_{n=1,3,5,\cdots}^{\infty} \left\{ \left(N_n f_n' + M_n \frac{a_n}{k} \right) \left(\cos n\theta - \cos \frac{n\theta_0}{2} \right) + \left(N_n g_n' + M_n \frac{b_n}{k} \right) \sin n\theta \right\} \tag{3.94}$$

where cosine amplitude of the fundamental wave Γ for the resulting displacement is defined as follows:

$$\Gamma = N_1 f_1' + M_1 \frac{a_1}{k} \tag{3.95}$$

Equation (3.94) is rewritten as follows by using the cosine amplitude of the fundamental wave Γ of Equation (3.95):

$$z_a - e_0 = \Gamma \cdot \sum_{n=1,3,5,\cdots}^{\infty} \left\{ \left(N_n \frac{f_n'}{\Gamma} + M_n \frac{a_n}{k} \right) \left(\cos n\theta - \cos \frac{n\theta_0}{2} \right) + \left(N_n \frac{g_n'}{\Gamma} + M_n \frac{b_n}{k} \right) \sin n\theta \right\} \quad (3.96)$$

The Fourier coefficients of Equation (3.79) are transformed to non-dimensional ones:

$$x_n = \frac{a_n}{k\Gamma}, \quad y_n = \frac{b_n}{k\Gamma} \quad (3.97)$$

And Equation (3.83) is also transformed to non-dimensional one:

$$\left.\begin{aligned} u_n &= \frac{f_n'}{f_1'} = \frac{f_n \cos n\alpha + g_n \sin n\alpha}{f_1 \cos \alpha + g_1 \sin \alpha} \\ v_n &= \frac{g_n'}{f_1'} = \frac{g_n \cos n\alpha - f_n \sin n\alpha}{f_1 \cos \alpha + g_1 \sin \alpha} \end{aligned}\right\} \quad (3.98)$$

Since $g_1=0$, the u_n and v_n are rewritten to following expressions:

$$\left.\begin{aligned} u_n &= \frac{f_n'}{f_1'} = \frac{f_n \cos n\alpha + g_n \sin n\alpha}{f_1 \cos \alpha} \\ v_n &= \frac{g_n'}{f_1'} = \frac{g_n \cos n\alpha - f_n \sin n\alpha}{f_1 \cos \alpha} \end{aligned}\right\} \quad (3.99)$$

The cosine amplitude of the fundamental wave Γ for the resulting displacement is transformed as follows:

$$\frac{f_1'}{\Gamma} = \frac{1 - M_1 x_1}{N_1} \quad (3.100)$$

The resulting vibration at collision position of Equation (3.96) is rewritten as follows by using Equations (3.97), (3.99) and (3.100):

$$z_a - e_0 = \Gamma \cdot \sum_{n=1,3,5,\cdots}^{\infty} \left\{ \begin{array}{r} \left(N_n u_n \dfrac{1-M_1 x_1}{N_1} + M_n x_n \right) \left(\cos n\theta - \cos \dfrac{n\theta_0}{2} \right) \\ + \left(N_n v_n \dfrac{1-M_1 x_1}{N_1} + M_n y_n \right) \sin n\theta \end{array} \right\} \tag{3.101}$$

Dividing Equation (3.86) by Equation (3.92) gives the non-dimensional resulting vibration at collision position as follows:

$$\frac{z_a}{e_0} = \frac{\sum_{n=1,3,5,\cdots}^{\infty} \left\{ \left(N_n f_n' + M_n \dfrac{a_n}{k} \right) \cos n\theta + \left(N_n g_n' + M_n \dfrac{b_n}{k} \right) \sin n\theta \right\}}{\sum_{n=1,3,5,\cdots}^{\infty} \left(N_n f_n' + M_n \dfrac{a_n}{k} \right) \cos \dfrac{n\theta_0}{2}} \tag{3.102}$$

The non-dimensional resulting vibration of Equation (3.102) is simplified by using Equations (3.97), (3.99) and (3.100) as follows:

$$\frac{z_a}{e_0} = \frac{\sum_{n=1,3,5,\cdots}^{\infty} \left\{ \left(N_n u_n \dfrac{1-M_1 x_1}{N_1} + M_n x_n \right) \cos n\theta + \left(N_n v_n \dfrac{1-M_1 x_1}{N_1} + M_n y_n \right) \sin n\theta \right\}}{\sum_{n=1,3,5,\cdots}^{\infty} \left(N_n u_n \dfrac{1-M_1 x_1}{N_1} + M_n x_n \right) \cos \dfrac{n\theta_0}{2}} \tag{3.103}$$

(2) Non-dimensional resulting Vibration at tip of the beam z_l / e_0

Dividing Equation (3.87) by Equation (3.92) gives the non-dimensional resulting vibration at tip of the beam as follows:

$$\frac{z_l}{e_0} = \frac{\sum_{n=1,3,5,\cdots}^{\infty} \left\{ \left(N_n' f_n' + M_n' \dfrac{a_n}{k} \right) \cos n\theta + \left(N_n' g_n' + M_n' \dfrac{b_n}{k} \right) \sin n\theta \right\}}{\sum_{n=1,3,5,\cdots}^{\infty} \left(N_n f_n' + M_n \dfrac{a_n}{k} \right) \cos \dfrac{n\theta_0}{2}} \tag{3.104}$$

The non-dimensional resulting vibration of Equation (3.104) is simplified by using Equation

(3.97), (3.99) and (3.100) as follows:

$$\frac{z_l}{e_0}=\frac{\sum_{n=1,3,5,\cdots}^{\infty}\left\{\left(N'_n u_n\frac{1-M'_1x_1}{N_1}+M_n x_n\right)\cos n\theta+\left(N'_n v_n\frac{1-M'_1x_1}{N_1}+M_n y_n\right)\sin n\theta\right\}}{\sum_{n=1,3,5,\cdots}^{\infty}\left(N_n u_n\frac{1-M_1x_1}{N_1}+M_n x_n\right)\cos\frac{n\theta_0}{2}} \tag{3.105}$$

Using the first equation of Equation (3.99) and Equation (3.100) gives the following equation:

$$f'_n=u_n\Gamma\frac{1-M_1x_1}{N_1} \tag{3.106}$$

Substituting Equation (3.106) into Equation (3.92) gives the cosine amplitude of the fundamental wave Γ as follows:

$$\Gamma=\frac{e_0}{\sum_{n=1,3,5,\cdots}^{\infty}\left(N_n u_n\frac{1-M_1x_1}{N_1}+M_n x_n\right)\cos\frac{n\theta_0}{2}} \tag{3.107}$$

(3) Phase Lag Angle α

Substituting $g_1=0$ into Equations (3.83) gives the following equation:

$$f'_1=f_1\cos\alpha+g_1\sin\alpha=f_1\cos\alpha \tag{3.108}$$

$$g'_1=g_1\cos\alpha-f_1\sin\alpha=-f_1\sin\alpha \tag{3.109}$$

$\cos\alpha$ is expressed as follows by Equations (3.100) and (3.108):

$$\cos\alpha=\frac{\Gamma}{f_1}\frac{1-M_1x_1}{N_1} \tag{3.110}$$

Equation (3.93) is transformed into following expression:

$$N_1 g_1' + M_1 \frac{b_1}{k} = -\sum_{n=3,5,7,\cdots}^{\infty} \left(N_n g_n' + M_n \frac{b_n}{k} \right) \frac{\sin \frac{n\theta_0}{2}}{\sin \frac{\theta_0}{2}} \tag{3.111}$$

Simplifying Equation (3.111) by using Equations (3.97), (3.99) and (3.100), g'_1 is derived as follows:

$$g_1' = -\frac{\Gamma}{N_1} \left\{ M_1 y_1 + \sum_{n=3,5,7,\cdots}^{\infty} \left(N_n \upsilon_n \frac{1 - M_1 x_1}{N_1} + M_n y_n \right) \frac{\sin \frac{n\theta_0}{2}}{\sin \frac{\theta_0}{2}} \right\} \tag{3.112}$$

$\sin\alpha$ is expressed as follows by using Equations (3.109) and (3.112):

$$\sin \alpha = \frac{\Gamma}{f_1 N_1} \left\{ M_1 y_1 + \sum_{n=3,5,7,\cdots}^{\infty} \left(N_n \upsilon_n \frac{1 - M_1 x_1}{N_1} + M_n y_n \right) \frac{\sin \frac{n\theta_0}{2}}{\sin \frac{\theta_0}{2}} \right\} \tag{3.113}$$

Thus, the phase lag angle α is expressed by using Equations (3.110) and (3.113) as follows:

$$\tan \alpha = \frac{\sin \alpha}{\cos \alpha} = \left\{ M_1 y_1 + \sum_{n=3,5,7,\cdots}^{\infty} \left(N_n \upsilon_n \frac{1 - M_1 x_1}{N_1} + M_n y_n \right) \frac{\sin \frac{n\theta_0}{2}}{\sin \frac{\theta_0}{2}} \right\} \Big/ \left(1 - M_1 x_1 \right) \tag{3.114}$$

$$\alpha = \tan^{-1} \left[\left\{ M_1 y_1 + \sum_{n=3,5,7,\cdots}^{\infty} \left(N_n \upsilon_n \frac{1 - M_1 x_1}{N_1} + M_n y_n \right) \frac{\sin \frac{n\theta_0}{2}}{\sin \frac{\theta_0}{2}} \right\} \Big/ \left(1 - M_1 x_1 \right) \right] \tag{3.115}$$

(4) Excitation Amplitude Ratio f_1 / e_0

Dividing Equation (3.110) by e_0 gives the excitation amplitude ratio f_1 / e_0 as follows:

$$\frac{f_1}{e_0} = \frac{1}{\cos\alpha}\frac{\Gamma}{e_0}\frac{1-M_1x_1}{N_1} \tag{3.116}$$

Substituting the cosine amplitude of the fundamental wave Γ of Equation (3.107) into Equation (3.116) gives the excitation amplitude ratio f_1/e_0 as follows:

$$\frac{f_1}{e_0} = \frac{1}{\cos\alpha}\frac{\dfrac{1-M_1x_1}{N_1}}{\displaystyle\sum_{n=1,3,5,\cdots}^{\infty}\left(N_n u_n \frac{1-M_1x_1}{N_1} + M_n x_n\right)\cos\frac{n\theta_0}{2}} \tag{3.117}$$

(5) Non-Dimensional Nonlinear Restoring Force $g(\theta)/k\Gamma$

The restoring force of Equation (3.42) is expressed by a real Fourier series:

$$g(\theta) = \sum_{n=-\infty}^{\infty} c_n e^{in\theta} = \frac{a_0}{2} + \sum_{n=1}^{\infty}\left(a_n\cos n\theta + b_n \sin n\theta\right) \tag{3.118}$$

Dividing Equation (3.118) by $k\Gamma$ and using Equation (3.97), the non-dimensional restoring force is obtained as follows:

$$\frac{g(\theta)}{k\Gamma} = \frac{x_0}{2} + \sum_{n=1}^{\infty}\left(x_n\cos n\theta + y_n \sin n\theta\right) \tag{3.119}$$

In this analysis, above mentioned, the restoring force is assumed to be also symmetric and to satisfy $g(\theta) = -g(\theta+\pi)$. Therefore, the following equation is obtained:

$$\frac{x_0}{2} + \sum_{n=2,4,6,\cdots}^{\infty}\left(x_n\cos n\theta + y_n \sin n\theta\right) = 0 \tag{3.120}$$

And thus, the non-dimensional restoring force is expressed by using Equation (3.120) as follows:

$$\frac{g(\theta)}{k\Gamma} = \sum_{n=1,3,5,\cdots}^{\infty} (x_n \cos n\theta + y_n \sin n\theta) \tag{3.121}$$

3.1.7 Determination of Non-Dimensional Fourier Coefficients x_n and y_n

Equations (3.103), (3.105), (3.107), (3.115), (3.117) and (3.121) can all be determined by three independent parameters Ω, α, θ_0 and non-dimensional Fourier coefficients x_n and y_n. The non-dimensional Fourier coefficients x_n and y_n must be determined such that the condition of piecewise linear characteristics of the nonlinear part of the restoring force is satisfied. In chapter2, the infinite dimensionless linear simultaneous equations with respect to the Fourier coefficients of the resulting vibration were derived. On the other hand, in this chapter, the resulting vibration is explicitly expressed by the Fourier coefficients of the restoring force, and thus the infinite dimensionless linear simultaneous equations with respect to the Fourier coefficients of the restoring force are derived.

The restoring force $g(\theta)$ is

$$\left.\begin{aligned}
&g(\theta) = K(z_a - e_0), && -\frac{\theta_0}{2} \le \theta \le \frac{\theta_0}{2} && ; \quad \text{Interval I} \\
&g(\theta) = 0, && \frac{\theta_0}{2} \le \theta \le \pi - \frac{\theta_0}{2},\ \pi + \frac{\theta_0}{2} \le \theta \le 2\pi - \frac{\theta_0}{2} && ; \quad \text{Interval II} \\
&g(\theta) = K(z_a + e_0), && \pi - \frac{\theta_0}{2} \le \theta \le \pi + \frac{\theta_0}{2} && ; \quad \text{Interval III}
\end{aligned}\right\} \tag{3.122}$$

Dividing Equation (3.122) by $k\Gamma$ gives the non-dimensional restoring force as follows:

$$\left.\begin{aligned}
&\frac{g(\theta)}{k\Gamma} = \frac{K}{k}\frac{(z_a - e_0)}{\Gamma}, && -\frac{\theta_0}{2} \le \theta \le \frac{\theta_0}{2} && ; \quad \text{Interval I} \\
&\frac{g(\theta)}{k\Gamma} = 0, && \frac{\theta_0}{2} \le \theta \le \pi - \frac{\theta_0}{2},\ \pi + \frac{\theta_0}{2} \le \theta \le 2\pi - \frac{\theta_0}{2} && ; \quad \text{Interval II} \\
&\frac{g(\theta)}{k\Gamma} = \frac{K}{k}\frac{(z_a + e_0)}{\Gamma}, && \pi - \frac{\theta_0}{2} \le \theta \le \pi + \frac{\theta_0}{2} && ; \quad \text{Interval III}
\end{aligned}\right\} \tag{3.123}$$

Substituting the resulting displacement of Equation (3.103) and the non-dimensional restoring force of Equation (3.121) into Equation (3.123) gives the following equations:

(i) Interval I

$$\sum_{n=1,3,5,\cdots}^{\infty}\left(x_n\cos n\theta+y_n\sin n\theta\right)$$
$$=\frac{K}{k}\sum_{n=1,3,5,\cdots}^{\infty}\left\{\left(N_n u_n\frac{1-M_1x_1}{N_1}+M_n x_n\right)\left(\cos n\theta-\cos\frac{n\theta_0}{2}\right)+\left(N_n\upsilon_n\frac{1-M_1x_1}{N_1}+M_n y_n\right)\sin n\theta\right\} \tag{3.124}$$

(ii) Interval II

$$\sum_{n=1,3,5,\cdots}^{\infty}\left(x_n\cos n\theta+y_n\sin n\theta\right)=0 \tag{3.125}$$

Multiplying the non-dimensional nonlinear part of the restoring force $g(\theta)$ of Equations (3.124) and (3.125) by $\cos m\theta\,(m=1,3,5,\cdots)$ and integrating over the half period $(-\pi/2,\pi/2)$ gives the following equation:

Left side

$$\int_{-\frac{\pi}{2}}^{\frac{\pi}{2}}\left\{\sum_{n=1,3,5,\cdots}^{\infty}\left(x_n\cos n\theta+y_n\sin n\theta\right)\right\}\cos m\theta\,d\theta=\frac{\pi}{2}x_m \tag{3.126}$$

Right side

$$\int_{-\frac{\theta_0}{2}}^{\frac{\theta_0}{2}}\frac{K}{k}\sum_{n=1,3,5,\cdots}^{\infty}\left\{\begin{array}{c}\left(N_n u_n\dfrac{1-M_1x_1}{N_1}+M_n x_n\right)\left(\cos n\theta-\cos\dfrac{n\theta_0}{2}\right)\\ +\left(N_n\upsilon_n\dfrac{1-M_1x_1}{N_1}+M_n y_n\right)\sin n\theta\end{array}\right\}\cos m\theta\,d\theta$$
$$=\frac{K}{k}\frac{\theta_0}{2}\sum_{n=1,3,5,\cdots}^{\infty}\left(N_n u_n\frac{1-M_1x_1}{N_1}+M_n x_n\right)\left(\frac{\sin\frac{m+n}{2}\theta_0}{\frac{m+n}{2}\theta_0}+\frac{\sin\frac{m-n}{2}\theta_0}{\frac{m-n}{2}\theta_0}-2\cos\frac{n\theta_0}{2}\frac{\sin\frac{m\theta_0}{2}}{\frac{m\theta_0}{2}}\right) \tag{3.127}$$

And thus

$$x_m - \frac{K}{k}\frac{\theta_0}{\pi}\sum_{n=1,3,5,\cdots}^{\infty}\left(M_n x_n - \frac{N_n}{N_1}u_n M_1 x_1\right)\left(\frac{\sin\frac{m+n}{2}\theta_0}{\frac{m+n}{2}\theta_0} + \frac{\sin\frac{m-n}{2}\theta_0}{\frac{m-n}{2}\theta_0} - 2\cos\frac{n\theta_0}{2}\frac{\sin\frac{m\theta_0}{2}}{\frac{m\theta_0}{2}}\right) = \frac{K}{k}\frac{\theta_0}{\pi}\sum_{n=1,3,5,\cdots}^{\infty}\frac{N_n}{N_1}u_n\left(\frac{\sin\frac{m+n}{2}\theta_0}{\frac{m+n}{2}\theta_0} + \frac{\sin\frac{m-n}{2}\theta_0}{\frac{m-n}{2}\theta_0} - 2\cos\frac{n\theta_0}{2}\frac{\sin\frac{m\theta_0}{2}}{\frac{m\theta_0}{2}}\right) \tag{3.128}$$

Equation (3.128) is simplified as follows:

$$x_m - \sum_{n=1,3,5,\cdots}^{\infty}\left(A_{mn}x_n - B_{mn}x_1\right) = \sum_{n=1,3,5,\cdots}^{\infty} I_{mn} \tag{3.129}$$

where

$$\left.\begin{aligned} A_{mn} &= \frac{K}{k}\frac{\theta_0}{\pi}M_n\left(\frac{\sin\frac{m+n}{2}\theta_0}{\frac{m+n}{2}\theta_0} + \frac{\sin\frac{m-n}{2}\theta_0}{\frac{m-n}{2}\theta_0} - 2\cos\frac{n\theta_0}{2}\frac{\sin\frac{m\theta_0}{2}}{\frac{m\theta_0}{2}}\right) \\ I_{mn} &= \frac{N_n}{N_1}\frac{u_n}{M_n}A_{mn},\ B_{mn} = M_1 I_{mn} \end{aligned}\right\} \tag{3.130}$$

In the same manner, multiplying the non-dimensional nonlinear part of the restoring force $g(\theta)$ of Equations (3.124) and (3.125) by $\sin m\theta$ (m=1,3,5,$\cdots$) and integrating over the half period $(-\pi/2, \pi/2)$ gives the following equation:

Left side

$$\int_{-\frac{\pi}{2}}^{\frac{\pi}{2}}\left\{\sum_{n=1,3,5,\cdots}^{\infty}\left(x_n\cos n\theta + y_n\sin n\theta\right)\right\}\sin m\theta d\theta = \frac{\pi}{2}y_m \tag{3.131}$$

Right side

$$\int_{-\frac{\theta_0}{2}}^{\frac{\theta_0}{2}} \frac{K}{k} \sum_{n=1,3,5,\cdots}^{\infty} \left\{ \begin{array}{l} \left(N_n u_n \dfrac{1-M_1 x_1}{N_1} + M_n x_n \right)\left(\cos n\theta - \cos \dfrac{n\theta_0}{2} \right) \\ + \left(N_n \upsilon_n \dfrac{1-M_1 x_1}{N_1} + M_n y_n \right) \sin n\theta \end{array} \right\} \sin m\theta \, d\theta$$
$$= \frac{K}{k} \frac{\theta_0}{2} \sum_{n=1,3,5,\cdots}^{\infty} \left(N_n \upsilon_n \frac{1-M_1 x_1}{N_1} + M_n y_n \right) \left(-\frac{\sin \dfrac{m+n}{2}\theta_0}{\dfrac{m+n}{2}\theta_0} + \frac{\sin \dfrac{m-n}{2}\theta_0}{\dfrac{m+n}{2}\theta_0} \right) \tag{3.132}$$

And thus

$$y_m - \frac{K}{k} \frac{\theta_0}{\pi} \sum_{n=1,3,5,\cdots}^{\infty} \left(M_n y_n - \frac{N_n}{N_1} \upsilon_n M_1 x_1 \right) \left(-\frac{\sin \dfrac{m+n}{2}\theta_0}{\dfrac{m+n}{2}\theta_0} + \frac{\sin \dfrac{m-n}{2}\theta_0}{\dfrac{m+n}{2}\theta_0} \right)$$
$$= \frac{K}{k} \frac{\theta_0}{\pi} \sum_{n=1,3,5,\cdots}^{\infty} \frac{N_n}{N_1} \upsilon_n \left(-\frac{\sin \dfrac{m+n}{2}\theta_0}{\dfrac{m+n}{2}\theta_0} + \frac{\sin \dfrac{m-n}{2}\theta_0}{\dfrac{m+n}{2}\theta_0} \right) \tag{3.133}$$

Equation (3.133) is simplified as follows:

$$y_m - \sum_{n=1,3,5,\cdots}^{\infty} \left(C_{mn} y_n - D_{mn} x_1 \right) = \sum_{n=1,3,5,\cdots}^{\infty} J_{mn} \tag{3.134}$$

where

$$\left. \begin{array}{l} C_{mn} = \dfrac{K}{k} \dfrac{\theta_0}{\pi} M_n \left(-\dfrac{\sin \dfrac{m+n}{2}\theta_0}{\dfrac{m+n}{2}\theta_0} + \dfrac{\sin \dfrac{m-n}{2}\theta_0}{\dfrac{m+n}{2}\theta_0} \right) \\ J_{mn} = \dfrac{N_n}{N_1} \dfrac{\upsilon_n}{M_n} C_{mn} \ , \ D_{mn} = M_1 J_{mn} \end{array} \right\} \tag{3.135}$$

Thus, the infinite dimensionless linear simultaneous equations for determining the non-dimensional Fourier coefficients x_n and y_n are obtained by Equations (3.129) and (3.134):

$$\left.\begin{aligned} x_m - \sum_{n=1,3,5,\cdots}^{\infty}\left(A_{mn}x_n - B_{mn}x_1\right) &= \sum_{n=1,3,5,\cdots}^{\infty} I_{mn} \\ y_m - \sum_{n=1,3,5,\cdots}^{\infty}\left(C_{mn}y_n - D_{mn}x_1\right) &= \sum_{n=1,3,5,\cdots}^{\infty} J_{mn} \end{aligned}\right\} \tag{3.136}$$

3.1.8 Calculation

The steady state periodic solutions were calculated based on the theoretical analysis results. The exciting vibrations were chosen as two waves as an example of a periodic excitation with an arbitrary function shown in Figure 3.5.

Single Harmonic wave in Figure 3.5(a)

$$q(\theta) = \cos\theta \tag{3.137}$$

Combined wave in Figure 3.5(b)

$$q(\theta) = \cos\theta + 0.5\sin 3\theta \tag{3.138}$$

The resulting vibration is expressed by the non-dimensional Fourier coefficients x_n, y_n which are determined by the infinite dimensionless linear simultaneous equations containing the independent parameters. Therefore, if the independent parameters are given, the

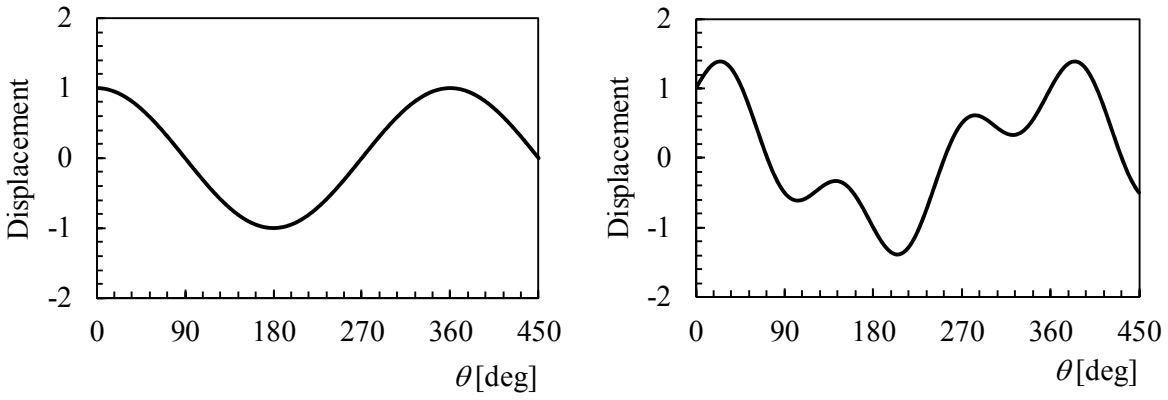

(a) $q(\theta)=\cos\theta$ (b) $q(\theta)=\cos\theta+0.5\sin 3\theta$

Figure 3.5 Displacement excitation

non-dimensional Fourier coefficients x_n, y_n are determined, and the resulting vibration can be calculated. Here, the calculation method based on the theoretical analysis is mentioned.

The coefficients A_{mn}, B_{mn}, C_{mn}, D_{mn}, I_{mn} and J_{mn} of Equation (3.136) contain the independent parameters for the frequency ratio Ω, the phase lag angle α and the dwell phase angle in the nonlinear region I and II θ_0. And thus if the phase lag angle α and the dwell phase angle θ_0 with respect to the objective frequency ratio Ω are given, the infinite dimensionless linear simultaneous equations of Equation (3.136) can be solved. First, substituting the independent parameters Ω, θ_0, α into the infinite dimensionless linear simultaneous equations of Equation (3.136) and solving gives the Fourier coefficients x_n and y_n. Next, substituting the Fourier coefficients x_n and y_n into the phase lag angle α of Equation (3.115) and the excitation amplitude ratio f_1/e_0 of Equation (3.117), these are calculated. If the phase lag angle α substituted into the infinite dimensionless linear simultaneous equations first is equal to the calculated α and calculated the excitation amplitude ratio f_1/e_0 is equal to the objective value, the independent parameters Ω, θ_0 α are adopted as the solution parameters. Finally, determined independent parameters Ω, θ_0 α and the Fourier coefficients x_n, y_n are substituted into Equations (3.103) and (3.105), the resulting vibration can be obtained. In this chapter, independent parameters with respect to the objective frequency ratio Ω are two and waveform of the resulting vibration is assumed to be symmetrical, independent parameters can be obtained by using two equations for the phase lag angle α of Equation (3.115) and the excitation amplitude ratio f_1/e_0 of Equation (3.117). When solving the infinite dimensionless linear simultaneous equations of Equation (3.136), the non-dimensional Fourier coefficients x_n and y_n were performed to the term with n=20 to approximate the response. In chapter2, it was shown that the convergence obtained was satisfactory up to n=20 for vibration Type II. This analysis is limited to harmonic vibration Type I, and the Fourier coefficients converge fast compared with the Type II. Therefore, term numbers of the non-dimensional Fourier coefficients were also calculated up to n=20 in this analysis. Above steps are repeated, resonance curves are constructed.

3.2 Experiment

An experiment was conducted with an apparatus designed to reproduce the analytical model shown in Figure 3.2, in an attempt to verify the theoretical analysis results found in the previous section. Figure 3.6 shows a schematic diagram of the clamped spring collision apparatus that obeys the equation of motion (Equation (3.1)). Figure 3.7 shows a photograph of the experiment apparatus. Table 3.1 shows the dimensions of the sample beam (material: spring steel) and clamped springs.

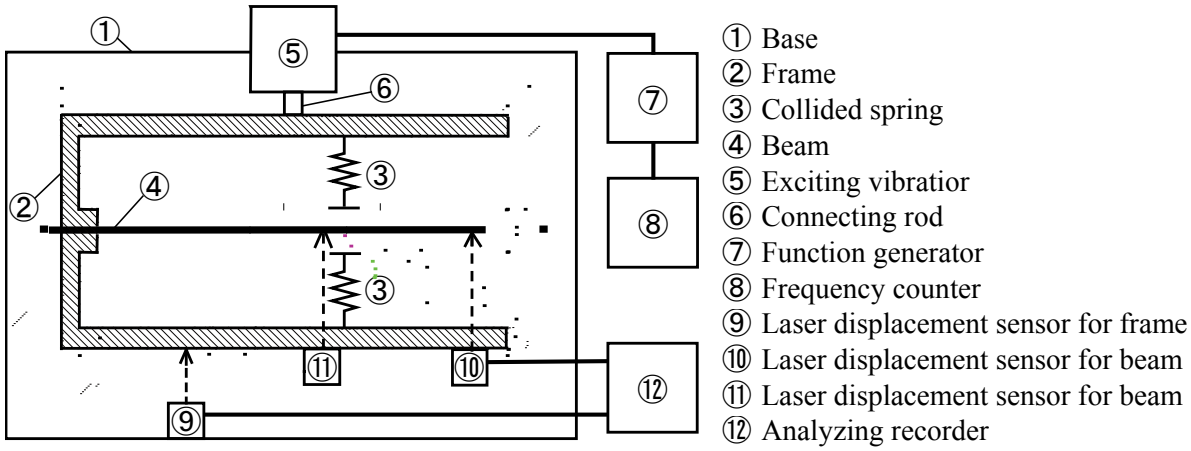

Figure 3.6 Sketch of the experiment apparatus

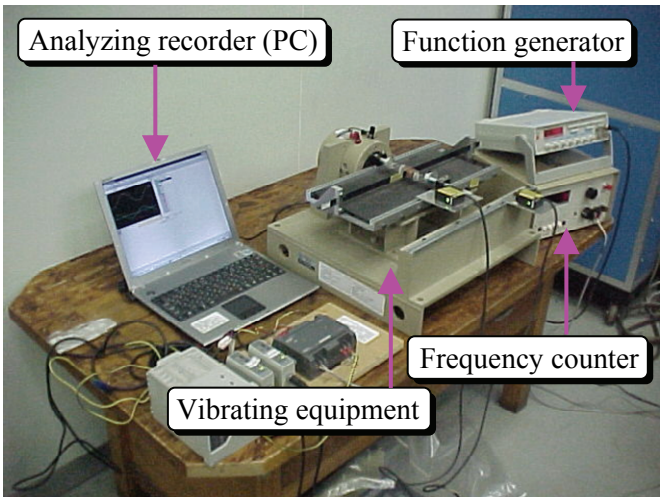

Figure 3.7 Photograph of the experiment apparatus

Table 3.1 Mechanical properties of parts used in experiment

Element	Symbol	Numerical value	
Length of the beam	l	231×10^{-3}	[m]
Cross section of the beam	A	7.87×10^{-6}	[m^2]
Mass of the beam	m	14.1×10^{-3}	[kg]
Density of the beam	ρ	7740	[kg/m^3]
Second moment of area for the beam	I	0.252×10^{-8}	[m^4]
Young's modulus of the beam	E	177×10^{9}	[Pa]
Spring constant of the beam	k	14.7	[N/m]
Clearance	e_0	5.0×10^{-3}	[m]
Collided spring constant	K	24.9	[N/m]

Frame ② of the apparatus holds beam ④ with one end (left) fixed, the other (right) end was free and the collision springs (coiled spring) ③ whose free ends were symmetric at clearance e_0 from beam ④. Beam ④ was excited with a vibration and when the resulting vibration amplitude exceeded clearance e_0, beam ④ elastically collided with springs ③. The excitation was applied to frame ②, which oscillated on a linear ball bearing on top of base ① and transmitted the periodic displacement excitation to beam ④. An exciting vibrator ⑤ fixed to base ① oscillated frame ② through a connecting rod ⑥. The displacement excitation was input by the exciting vibrator ⑤ from a frequency counter ⑧ connected to a function generator ⑦, which was set to generate a cosine excitation. The excitation displacement was observed using a laser displacement sensor ⑨ attached to base ①. The resulting excitations at its tip ($x=l$) and at the collision position ($x=a$) were also observed using laser displacement sensors ⑩, ⑪. The analog outputs of the sensors were recorded using an analyzing recorder ⑫.

3.3 The Results of Theoretical Calculation and Experiment

3.3.1 Comparison of Theoretical Calculation Results with Experimental Results

Figure 3.8 shows resonance curves that compares the theoretically predicted amplitudes at resonance at the collision position ($x=a$) and the tip ($x=l$) excited by the harmonic excitation [$q(t)=\cos\omega t$] in Figure 3.5(a) and the observed amplitudes in the experiment (▲ : $x=l$, △ : $x=a$). These results agreed reasonably well. The resonances curve bended to the right when the amplitude at the collision position ($x=a$) exceeds clearance e_0, bringing the beam into the nonlinear region (marked with ●), exhibiting relatively nonlinear behavior. The results in the physical model showed a jump to the lower line of linear vibrations when the vibration frequency ratio exceeded a value of Ω=1.12 as Ω was being increased. No results were obtained in the nonlinear region in the physical model at higher values of Ω. This is because damping was not considered in the analytical model, while in the physical model there was damping due to air resistance, internal friction in the material and friction at the beam supports. Conversely, when the frequency was reduced, a jump in the opposite direction was

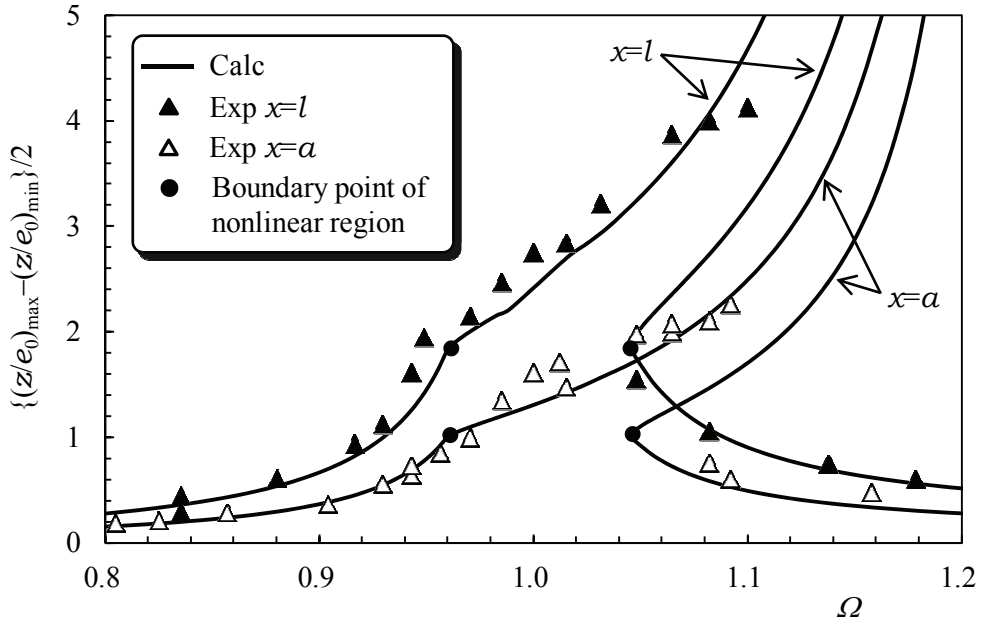

{ $q(t)=\cos\omega t$, a/l=0.67, K/k=1.69, f_1/e_0=0.15 }

Figure 3.8 Resonance curves for comparing theoretical calculation results with experimental results

observed in the neighborhood of Ω=1.05 from the lower line that describes the linear response to the upper line that describes the nonlinear response. These are well-known phenomena in nonlinear vibration studies. This resembled the action of a harden spring. By contrast, the resonance curve at the position of collision along the beam span (a/l=0.67) exhibited a similar trend to the curve describing the beam tip.

3.3.2 Example of Theoretical Calculations

The steady state periodic solutions were calculated based on the theoretical analysis results in the harmonic resonance region. The calculations were carried out for the combined wave given in Figure 3.5(b), as an example of excitation by a function of arbitrary period. The ● symbols indicate the transition point between beam vibration where the amplitude at the collision position is less than the clearance e_0 and the beam vibration where the beam contacts the springs.

Figure 3.9 shows resonance curves obtained by using the excitation amplitude ratio f_1/e_0 as a parameter. Figure 3.9(a) shows dimensionless amplitude at the collision position ($x=a$) and (b) shows at the beam tip ($x=l$). Both Figures 3.9(a) and (b), the greater f_1/e_0 is, the wider the resonance region is; in other words, the lower the relative magnitude of e_0 is, the wider the resonance region is.

Figure 3.10 shows resonance curves obtained by using the collision position ratio a/l as a parameter. Figure 3.10(a) shows the dimensionless amplitude at the collision position ($x=a$) and (b) shows at the beam tip ($x=l$). Both Figures 3.10(a) and (b) show that increasing a/l or bringing the spring collision position closer to the beam tip shifted the gradient of the resonance curves to the right. Low a/l values in Figures 3.10(a) and (b) cause the resonance curves to approach vibration in a linear system. The collision position (●) in Figure 3.10(b) is shifted upward. $a/l=1.0$ implied that the beam tip itself strikes the springs.

Figure 3.11 shows resonance curves obtained by using the nonlinearity of spring constant/beam elasticity K/k as a parameter. Figure 3.11(a) shows dimensionless amplitude at the collision position and Figure 3.11(b) shows at the beam tip. The greater the stiffness of the spring K/k is, the more the curves tilt to the right, and the greater the resulting nonlinearity. $K/k=0$ represented linear behavior, assuming no collision with the spring.

Figure 3.12 shows waveforms at conditions A and B marked in Figure 3.11 comparing the resulting waveforms $z_a(\theta)/e_0$, $z_l(\theta)/e_0$ and the waveform of the restoring force $g(\theta)/k\Gamma$ in the nonlinear region. Points A lie on the left of the resonance curve, so the response is the same phase with respect to the excitation $q(\theta)$. Points B lie on the right of the resonance curve, so the response is about 180º out of phase with the excitation wave.

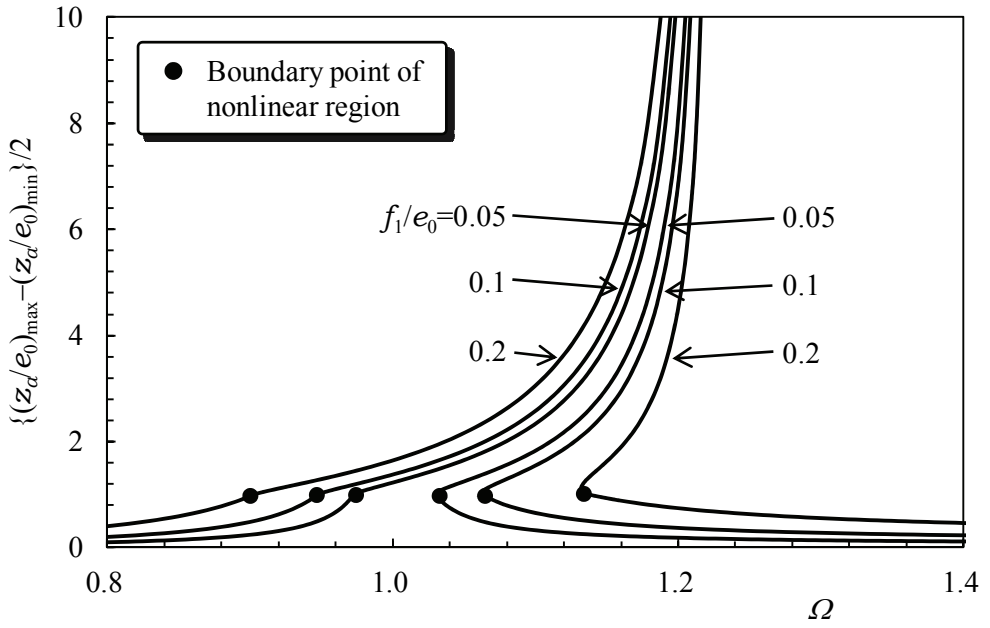

(a) $x=a$

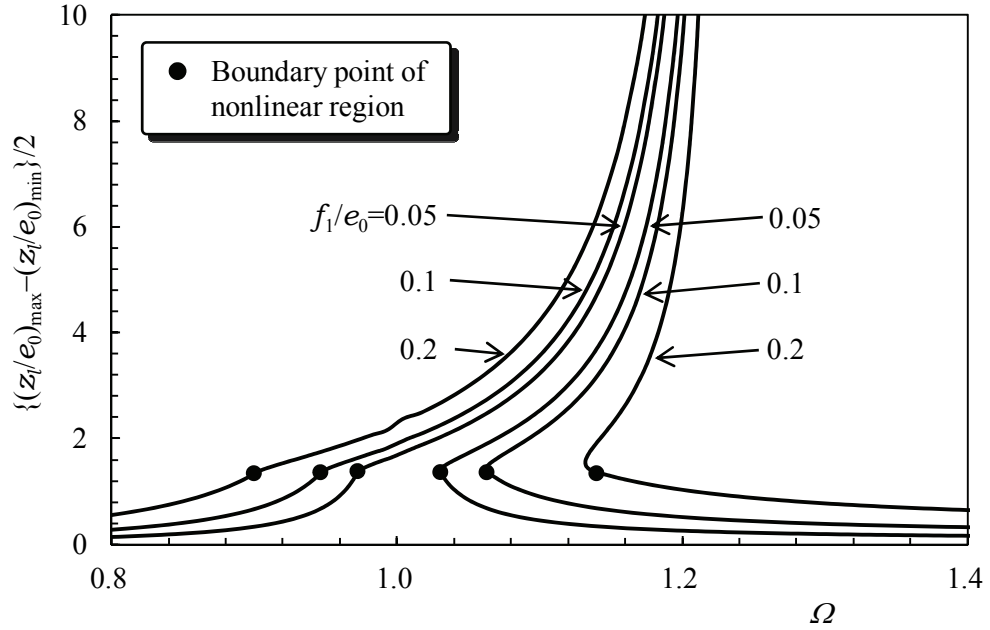

(b) $x=l$

{ $q(t)=\cos\omega t+0.5\sin 3\omega t$, $K/k=1.0$, $a/l=0.8$ }

Figure 3.9 Resonance curves in the case where excitation amplitude ratio f_1/e_0 is parameter

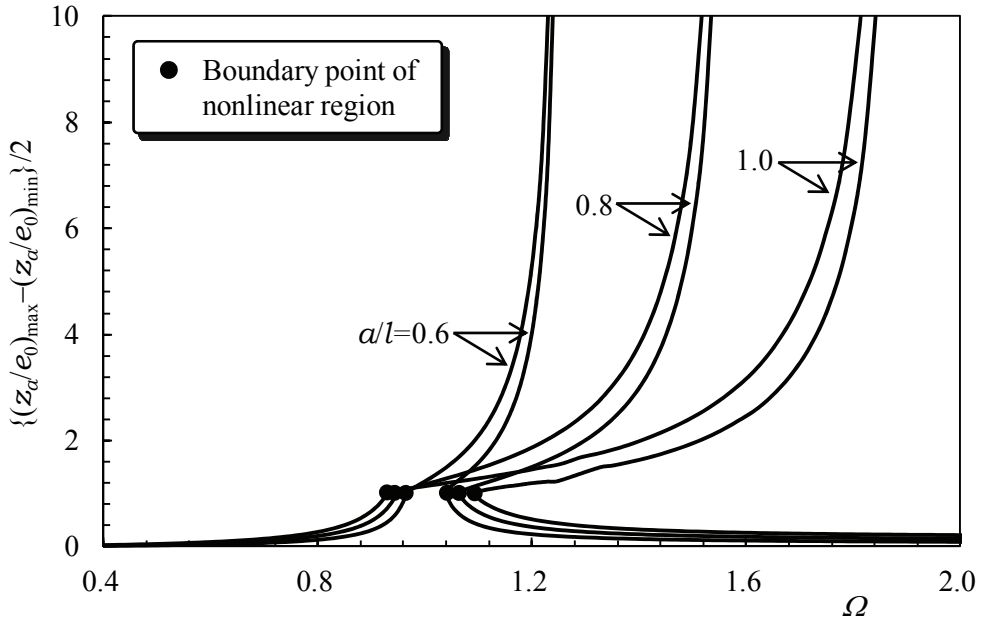

(a) $x=a$

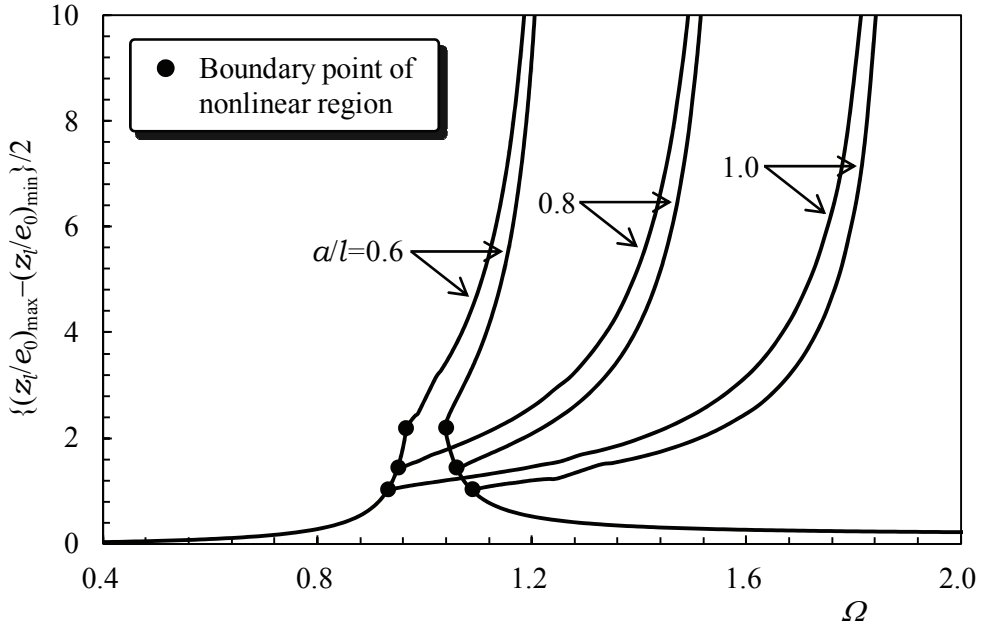

(b) $x=l$

{ $q(t)=\cos\omega t+0.5\sin 3\omega t$, $f_1/e_0=0.1$, $K/k=3.0$}

Figure 3.10 Resonance curves in the case where collision position ratio a/l is parameter

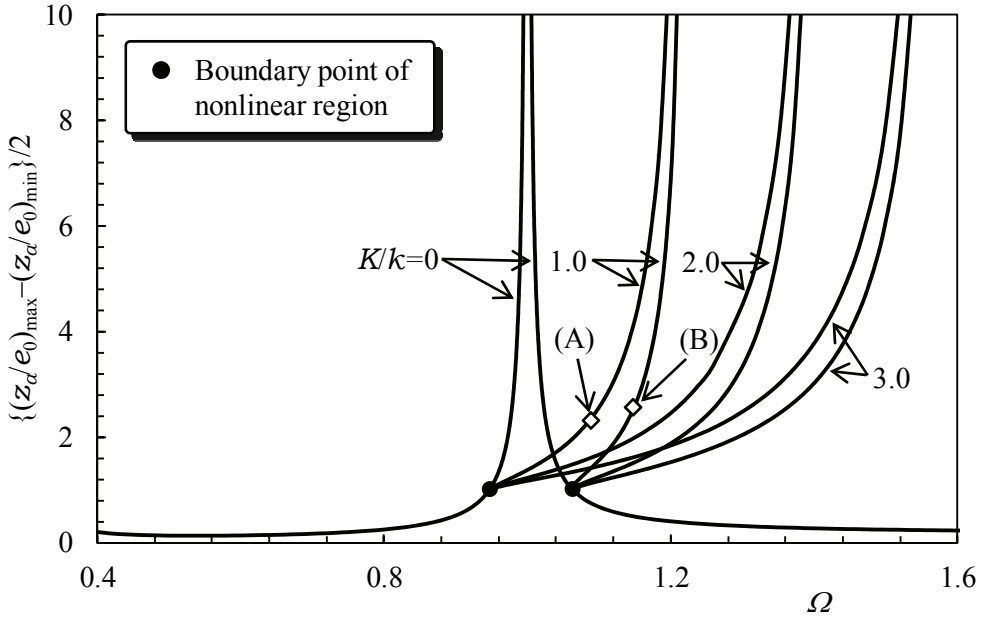

(a) $x=a$

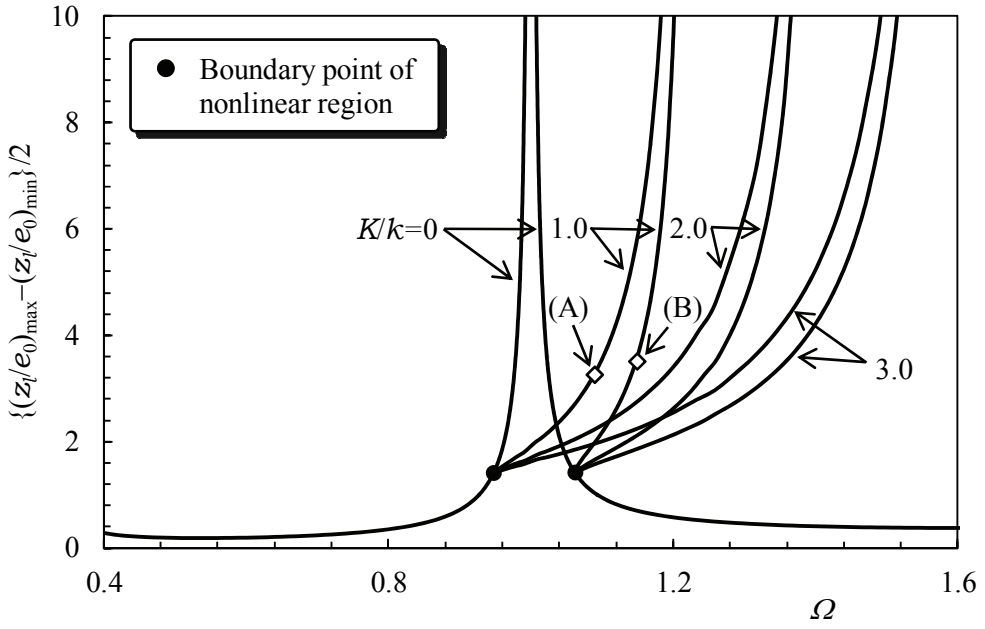

(b) $x=l$

{ $q(t)=\cos\omega t+0.5\sin 3\omega t$, $f_1/e_0=0.1$, $a/l=0.8$ }

Figure 3.11 Resonance curves in the case where spring constant ratio K/k is parameter

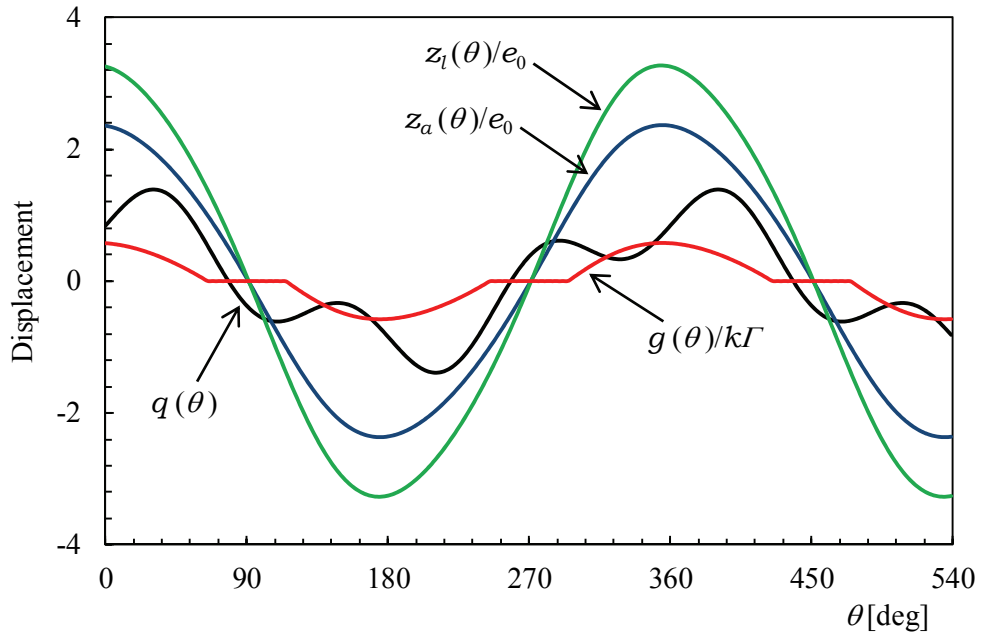

(a) Point A (Ω=1.09)

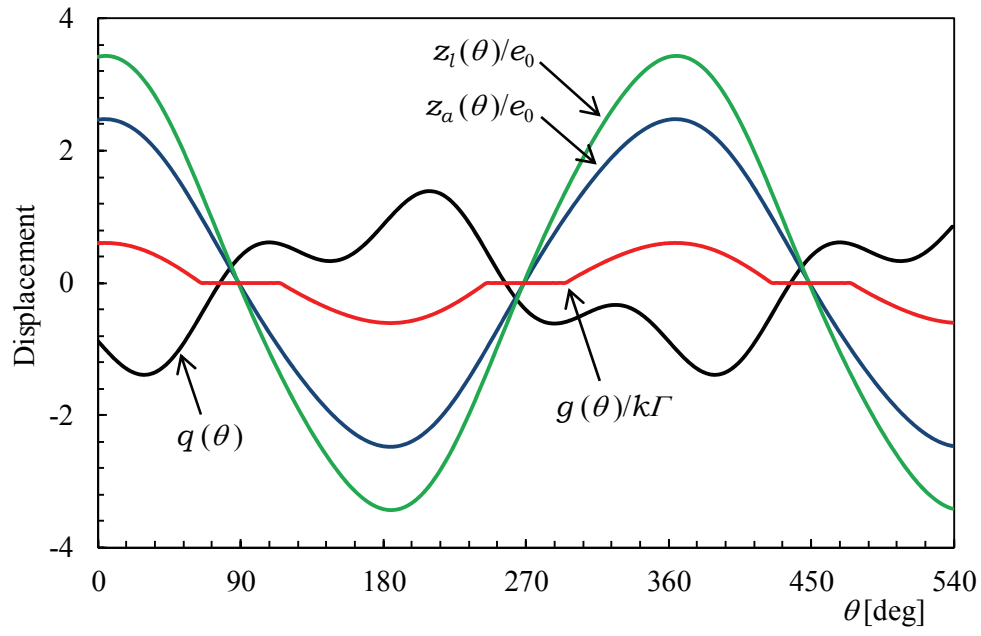

(b) Point B (Ω=1.15)

Figure 3.12 Waveforms of displacement excitation, resulting vibration and nonlinear part of restoring force in Figure 3.11.

3.4 Summary

This chapter investigated the resulting vibration of a cantilever beam as an example of distributed parameter systems with piecewise linear restoring force excited by periodic displacement. The following results were obtained:

(1) An analyzed model consisted of a cantilever beam elastically colliding with clamped springs on both sides, placed at arbitrary locations along the span of the beam. There were symmetric gaps between the rest position of the beam and each spring, leaving a dead zone in the symmetric piecewise linear system. The Fourier series method was employed to examine the steady state vibration resulting from a periodic excitation with an arbitrary function. A theoretical solution was found for the resulting vibration.

(2) A physical model was constructed and subjected to a cosine excitation as an example of periodic excitation with an arbitrary function to verify the results of the analysis conducted in (1) and (2). The experimental results were compared with the analytical results and found to agree with them well.

(3) Theoretical calculations were performed based on the results of the analysis in (1). Parameters were created of the excitation amplitude ratio f_1/e_0, spring collision position ratio a/l and nonlinearity (ratio of spring constants) K/k to produce graphs of resonance curves and the effect of these factors on the resonance curve shape were identified numerically. The resulting vibration waveform of a periodic solution on the resonance curve and the restoring force in the compressed spring were also calculated.

(4) It is possible to treat periodic excitations with an arbitrary function in a general manner. Once this analytical method is firmly established, it will be possible to use the procedure in (3) to calculate solutions for resulting vibrations for any magnitude of the parameters in (3).

Chapter 4
Analysis of Stability Criterion in Distributed Parameter Systems

This chapter deals with stability analysis for a nonlinear vibration in distributed parameter systems excited by periodic displacement with arbitrary functions. A system of steady state forced vibration in a simply-supported-beam connected with a nonlinear spring at midpoint of span is considered. The restoring force is approximated to be a piecewise linear system. For such a system, the beam undergoes a nonlinear vibration when the amplitude is large. Figure 4.1

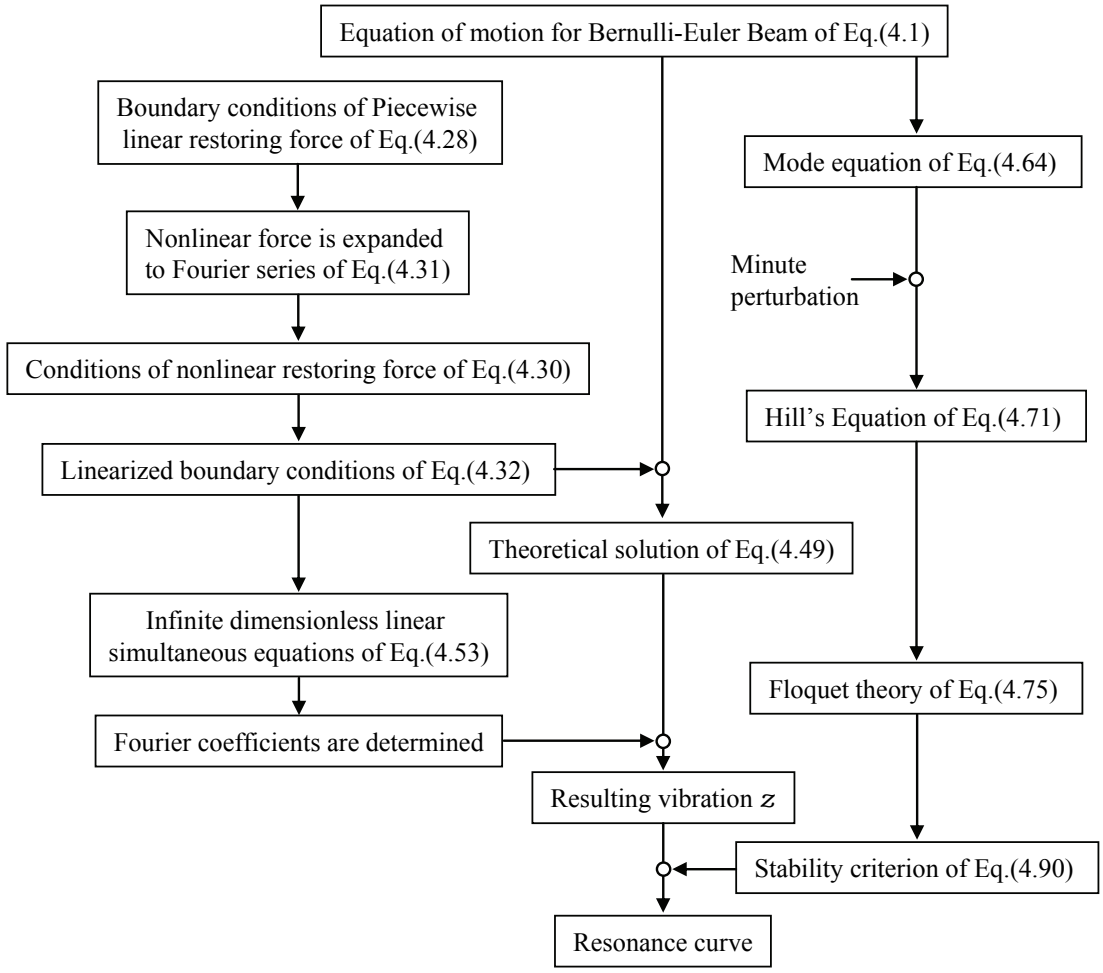

Figure 4.1 Flowchart of theoretical analysis method

shows the fundamental flow of the theoretical analysis method in this chapter. In order to analyze main resonance for the system, the Fourier series method is applied to obtain a theoretical solution for response vibration. The calculations based on the theoretical analysis results are performed to construct the resonance curves. Next, method of stability analysis for distributed parameter systems having a piecewise linear restoring force is proposed. The stability of a periodic solution is analyzed utilizing a variational equation to investigate consequences of a minute perturbation to a steady state vibration in modal coordinate predicted by a periodic solution for modal equation of motion, and stability criterion for a periodic steady state solution are shown. Stability charts for the resulting vibrations are constructed by calculations based on the theoretical analysis results. The stability for periodic solutions on the steady state vibration is discussed by utilizing these charts. By using these charts, the stable branches on the resonance curves are distinguished from the unstable ones. Moreover, in order to clarify the influence of the nonlinearity for stability, the stability chart is also constructed taking the nonlinearity as parameter. The experiments are also carried out to verify the theoretical analysis results.

4.1 Theoretical Analysis

4.1.1 Analysis of Response Vibration

(1) Characteristics of System and Equation of Motion

As shown in Figure 4.2, the vibration considered in this subject is a steady state response of a simply-supported-beam in lateral bending with an additional nonlinear supporting spring (on pin mounts) acting at mid-span. It is excited by a displacement of a periodic excitation with an arbitrary function $q(t)$. The restoring force acting on the beam is the cubic curve indicated by the dotted line in Figure 4.3 and is assumed to be a characteristic of the nonlinear supporting spring (spring constant K). This dotted line is treated by approximating it as a symmetric piecewise linear spring (solid line), combining the spring constant of K_1 between the boundary lines $z_{l/2}=\pm e_0$ with a spring constant of K_1+K_2 outside the boundary line. The straight lines are selected to give equal areas between the dotted line and straight lines below the curve and between the dotted line and straight lines above the curve. Thus, this analysis assumes that the restoring force can be represented by a symmetric piecewise linear function. If Region II in Figure 4.3 is the standard, then from the viewpoint of the entire system, Regions I and II are the

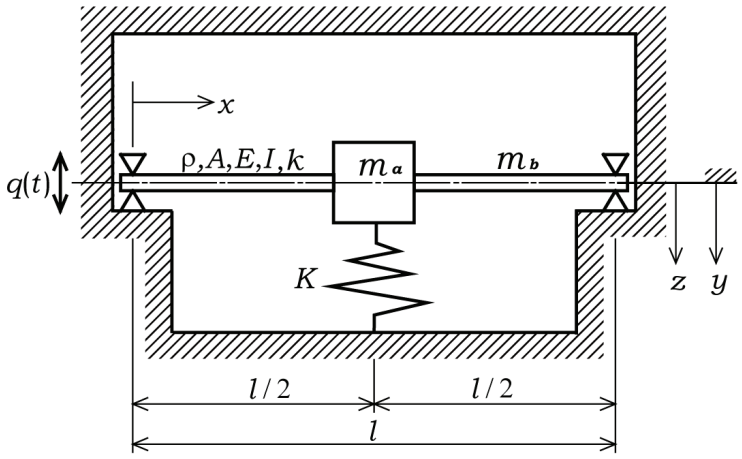

Figure 4.2 Analytical model of steady forced vibration in simply-supported-beam having a nonlinear spring at midpoint of span

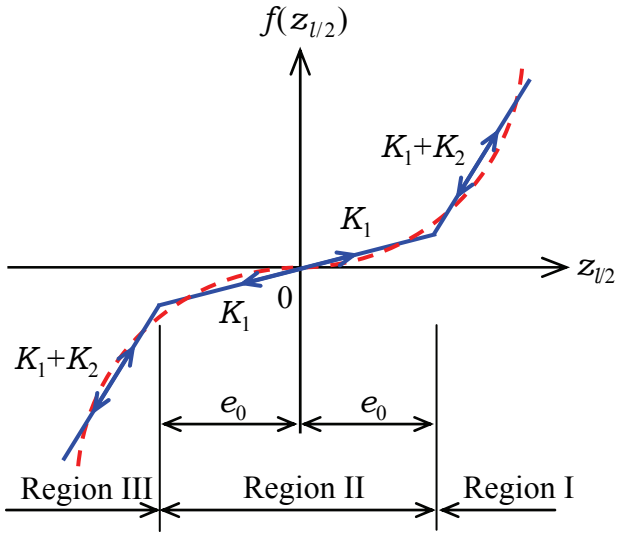

Figure 4.3 Characteristics of restoring force

nonlinear regions. The restoring force is represented by the symmetrical piecewise linear sections on either side of the linear portion. The material of the beam is assumed to be homogenous. If the cross-sectional area of the beam is A, the second moment of area is I, the Young's modulus is E, the mass per unit volume is ρ and the excitation acting to displacement this system is $q(t)$,then the equation of motion for relative displacement z of this system is

given by:

$$\frac{\partial^2 z}{\partial t^2}+\frac{EI}{\rho A}\cdot\frac{\partial^4 z}{\partial x^4}=-\frac{\partial^2 q(t)}{\partial t^2} \tag{4.1}$$

The boundary conditions for the analytical model shown in Figure 4.2 are expressed as follows:

$$x=0\ :\ z=0 \tag{4.2}$$

$$x=0\ :\ \frac{d^2 z}{dx^2}=0 \tag{4.3}$$

$$x=\frac{l}{2}\ :\ 2EI\frac{d^3 z}{dx^3}=m_a\frac{d^2 z}{dt^2}+f(z_{l/2}) \tag{4.4}$$

Analytical model is a simply-supported-beam having an attached mass connected with a nonlinear spring at mid-span. And main resonance is treated in this analysis. Therefore, the first order vibration mode becomes dominant and the following boundary condition is applied:

$$x=\frac{l}{2}\ :\ \frac{dz}{dx}=0 \tag{4.5}$$

$f(z_{l/2})$ of Equation (4.4) is the restoring force applied by the nonlinear supporting spring; the restoring force has the characteristics indicated in Figure 4.3, so these can be expressed in the three regions:

$$\left.\begin{array}{lll} f(z_{l/2})=K_1 z+K_2\left(z_{l/2}-e_0\right) & :z_{l/2}\geq e_0 & :\text{Region I} \\ f(z_{l/2})=K_1 z & :-e_0\leq z_{l/2}\leq e_0 & :\text{Region II} \\ f(z_{l/2})=K_1 z+K_2\left(z_{l/2}+e_0\right) & :z_{l/2}\leq -e_0 & :\text{Region III} \end{array}\right\} \tag{4.6}$$

(2) Fourier Series Method

Let the excitation $q(t)$ acting on the beam have an arbitrary period; then, the real and complex Fourier series can be expanded about $q(t)$:

$$q(t) = \sum_{n=-\infty}^{\infty} s_n e^{jn\omega t} = \frac{f_0}{2} + \sum_{n=1}^{\infty} \left(f_n \cos n\omega t + g_n \sin n\omega t \right) \tag{4.7}$$

where ω is the angular frequency. Substituting Equation (4.7) into Equation (4.1) gives the following equation:

$$\frac{\partial^2 z}{\partial t^2} + \frac{EI}{\rho A} \cdot \frac{\partial^4 z}{\partial x^4} = \sum_{n=-\infty}^{\infty} n^2 \omega^2 s_n e^{jn\omega t} \tag{4.8}$$

The solution $z(x,t)$ for Equation (4.8) is assumed as follows:

$$z(x,t) = W'(x) \cdot T'(t) \tag{4.9}$$

We consider the steady state vibration in this analysis, so the relative beam displacement z is a periodic function of the angular frequency ω. It follows that the time term of the resulting displacement z of Equation (4.9) can be expanded into the following complex Fourier series:

$$T'(t) = \sum_{n=-\infty}^{\infty} r_n e^{jn\omega t} \tag{4.10}$$

where r_n is a Fourier series coefficient to be determined afterwards. Substituting Equation (4.10) into Equation (4.9) and introducing a relation $W_n(x) = W'_n(x) \cdot r_n$ gives the relative displacement of response as follows:

$$z(x,t) = \sum_{n=-\infty}^{\infty} W_n(x) e^{jn\omega t} \tag{4.11}$$

In the same manner, the periodic solution $y(x,t)$ of equation of motion for the absolute displacement is assumed as follows:

$$y(x,t) = \sum_{n=-\infty}^{\infty} X_n(x) e^{jn\omega t} \tag{4.12}$$

Substituting the displacement excitation $q(t)$ of Equation (4.7), the absolute displacement $y(x,t)$ of Equation (4.12) and the relative displacement $z(x,t)$ of Equation (4.11) into the relation $y(x,t)=z(x,t)+q(t)$ gives the following equation:

$$W_n(x) = X_n(x) - s_n \tag{4.13}$$

Substituting Equation (4.11) into Equation (4.8) gives the following equation:

$$\sum_{n=-\infty}^{\infty} \left\{ \frac{EI}{\rho A} \frac{\partial^4 W_n(x)}{\partial x^4} - n^2\omega^2 W_n(x) - n^2\omega^2 s_n \right\} e^{jn\omega t} = 0 \tag{4.14}$$

And thus

$$\frac{EI}{\rho A} \frac{\partial^4 W_n(x)}{\partial x^4} = n^2\omega^2 \{W_n(x) + s_n\} \tag{4.15}$$

Substituting Equation (4.13) into Equation (4.15) gives the following ordinary differential equation as follows:

$$\frac{d^4 X_n(x)}{dx^4} = \frac{\rho A}{EI} n^2\omega^2 X_n(x) \tag{4.16}$$

$X_n(x)$ of equation (4.16) can be expressed as follows by using λ_n:

$$X_n(x) = A_n \cosh \lambda_n x + B_n \sinh \lambda_n x + C_n \cos \lambda_n x + D_n \sin \lambda_n x \qquad (n \neq 0) \tag{4.17}$$

where coefficients λ_n are eigenvalues and expressed as follows:

$$\lambda_n{}^4 = \frac{\rho A}{EI} n^2 \omega^2 \tag{4.18}$$

The A_n, B_n, C_n, and D_n are unknown constants that can be determined by the boundary conditions. The angular frequency ω_i is expressed by:

$$\omega_i = \frac{(\beta_i l)^2}{l^2} \sqrt{\frac{EI}{\rho A}}, \qquad (i = 1,2,3,\cdots) \tag{4.19}$$

where $\beta_i l$ of Equation (4.19) is determined by the mass ratio $\mu(=m_a/m_b)$ and can be calculated by the following frequency equation:

$$\mu\beta_i l = \frac{4}{\tan(\beta_i l/2) - \tanh(\beta_i l/2)} \tag{4.20}$$

Equation (4.18) is transformed into as follows by using the frequency ratio $\Omega(=\omega/\omega_1)$:

$$\lambda_n{}^4 l^4 = (\beta_i l)^4 n^2 \Omega^2 \tag{4.21}$$

Substituting Equation (4.13) into Equation (4.11) gives the resulting vibration $z(x,t)$ as follows:

$$z(x,t) = \sum_{n=-\infty}^{\infty} \{X_n(x) - s_n\} e^{jn\omega t} \tag{4.22}$$

This analysis is limited to waveforms containing only a single entrance into the upper and lower nonlinear portions of the restoring force per cycle in the main resonance region. Figure 4.4 shows the assumed shape of the harmonic resonance vibration caused by the excitation acting on the beam shown in Figure 4.2, by the resulting vibration $z_{l/2}(\theta)$, and by the nonlinear restoring force $g(\theta)$ due to the spring constant K_2 approximated by the piecewise linear

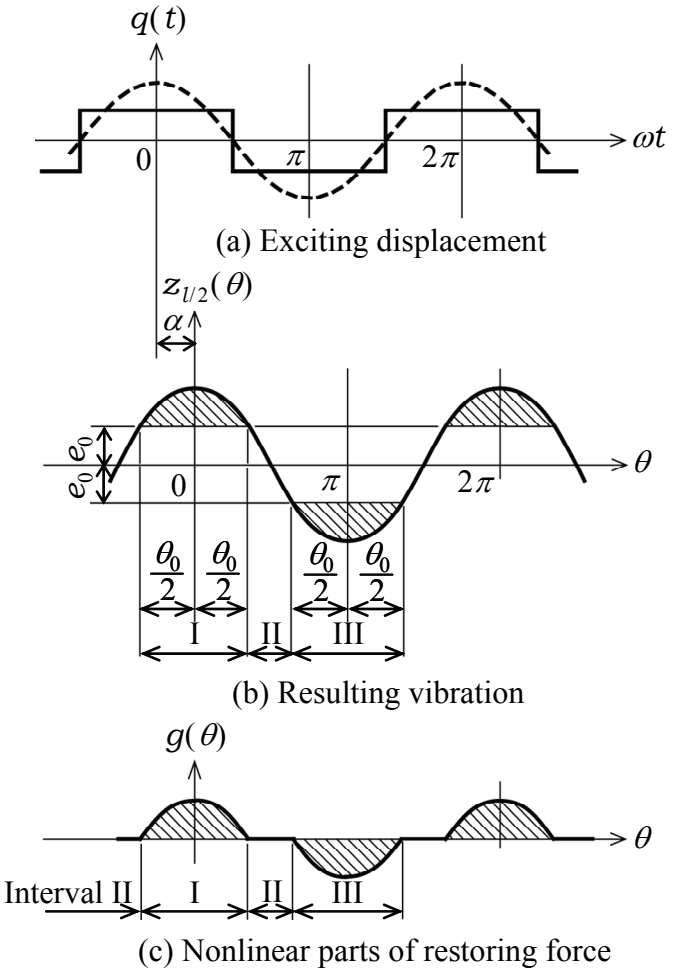

Figure 4.4 Harmonic resonance vibration

system in Figure 4.3. The resulting relative displacement $z_{l/2}$ at the beam midpoint is considered to be periodic; the response is divided into regions I, II, and III, corresponding to the regions shown in Figure 4.3. The origin for measuring the phase angle θ is defined from the peak of the resulting waveform. The independent variable of time t is transformed to phase angle θ, which is defined as:

$$\theta = \omega t - \alpha \tag{4.23}$$

where α is the phase lag angle, which is currently undefined but will be determined later. The displacement can then be expressed as:

$$z(x,\theta) = \sum_{n=-\infty}^{\infty} \{X_n(x) - s_n\} e^{jn(\theta+\alpha)} \tag{4.24}$$

(3) Determination of Coefficients

Here, undefined coefficients of $X_n(x)$ of Equation (4.17) are derived by using boundary conditions. Applying the boundary condition of Equation (4.2) to the resulting vibration of Equation (4.24) gives the following equation:

$$\begin{aligned} &\sum_{n=-\infty}^{\infty} \{X_n(0) - s_n\} e^{jn(\theta+\alpha)} = 0 \\ &\therefore \ X_n(0) = s_n \end{aligned} \tag{4.25}$$

Applying the boundary condition of Equation (4.5) to the resulting vibration of Equation (4.24) gives the following equation:

$$\begin{aligned} &\sum_{n=-\infty}^{\infty} \left\{ \frac{d}{dx} X_n(\tfrac{l}{2}) - 0 \right\} e^{jn(\theta+\alpha)} = 0 \\ &\therefore \ \frac{dX_n(\frac{l}{2})}{dx} = 0 \end{aligned} \tag{4.26}$$

Applying the boundary condition of Equation (4.3) to the resulting vibration of Equation (4.24) gives the following equation:

$$\begin{aligned} &\sum_{n=-\infty}^{\infty} \frac{d^2}{dx^2} X_n(0) e^{jn(\theta+\alpha)} = 0 \\ &\therefore \ \frac{d^2 X_n(0)}{dx^2} = 0 \end{aligned} \tag{4.27}$$

Applying the boundary condition of Equation (4.4) to the resulting vibration of Equation (4.24) gives the following equation:

$$2EI\sum_{n=-\infty}^{\infty}\frac{d^3}{dx^3}X_n(\tfrac{l}{2})e^{jn(\theta+\alpha)}=m_a\sum_{n=-\infty}^{\infty}X_n\left(\tfrac{l}{2}\right)\left(-n^2\omega^2\right)e^{jn(\theta+\alpha)}+K_1\sum_{n=-\infty}^{\infty}\{X_n(\tfrac{l}{2})-S_n\}e^{jn(\theta+\alpha)}+f(z_{l/2}) \tag{4.28}$$

where $f(z_{l/2})$ is the restoring force applied by the nonlinear supporting spring; the restoring force has the characteristics indicated in Figure 4.3, and these can be expressed in the three regions:

$$\left.\begin{array}{lll} f(z_{l/2})=K_1z+K_2\left(z_{l/2}-e_0\right) & :-\dfrac{\theta_0}{2}\le\theta\le\dfrac{\theta_0}{2} & :\text{Interva I} \\ f(z_{l/2})=K_1z & :\dfrac{\theta_0}{2}\le\theta\le\pi-\dfrac{\theta_0}{2},\quad \pi+\dfrac{\theta_0}{2}\le\theta\le 2\pi-\dfrac{\theta_0}{2} & :\text{Interval II} \\ f(z_{l/2})=K_1z+K_2\left(z_{l/2}+e_0\right) & :\pi-\dfrac{\theta_0}{2}\le\theta\le\pi+\dfrac{\theta_0}{2} & :\text{Interval III} \end{array}\right\} \tag{4.29}$$

In addition, the nonlinear portion of the restoring force $g(\theta)$ shown in Figure 4.4(c) is expressed as follows:

$$\left.\begin{array}{lll} g(\theta)=K_2\left(z_{l/2}-e_0\right) & :-\dfrac{\theta_0}{2}\le\theta\le\dfrac{\theta_0}{2} & :\text{Interva I} \\ g(\theta)=0 & :\dfrac{\theta_0}{2}\le\theta\le\pi-\dfrac{\theta_0}{2},\quad \pi+\dfrac{\theta_0}{2}\le\theta\le 2\pi-\dfrac{\theta_0}{2} & :\text{Interval II} \\ g(\theta)=K_2\left(z_{l/2}+e_0\right) & :\pi-\dfrac{\theta_0}{2}\le\theta\le\pi+\dfrac{\theta_0}{2} & :\text{Interval III} \end{array}\right\} \tag{4.30}$$

The period of the nonlinear restoring force $g(\theta)$ of Equation (4.30) can be considered to be equal to the period of the resulting vibration waveform. Thus, it can be expanded into a complex Fourier series as follows:

$$g(\theta)=\sum_{n=-\infty}^{\infty}c_ne^{jn\theta}=\frac{a_0}{2}+\sum_{n=1}^{\infty}\left(a_n\cos n\theta+b_n\sin n\theta\right) \tag{4.31}$$

Substituting Equation (4.31) into Equation (4.28) gives the following equation:

$$\frac{d^3X_n(\frac{l}{2})}{dx^3}=\frac{-n^2m_a\omega^2}{2EI}X_n(\tfrac{l}{2})+\frac{K_1}{2EI}X_n(\tfrac{l}{2})-\frac{K_1S_n}{2EI}+\frac{C_n}{2EIe^{jn\alpha}} \tag{4.32}$$

Applying Equation (4.25) to Equation (4.17) gives the following equation:

$$\begin{aligned} &X(0) = A_n + C_n = s_n \\ &\therefore \quad A_n + C_n = s_n \end{aligned} \tag{4.33}$$

Differentiating Equation (4.17) and introducing Equation (4.27) gives the following equation:

$$\begin{aligned} &\frac{d^2 X_n(0)}{dx^2} = (A_n - C_n)\,\lambda_n{}^2 = 0 \\ &\therefore \quad A_n = C_n \end{aligned} \tag{4.34}$$

Substituting Equations (4.33) and (4.34) into Equation (4.17) and differentiating gives the following equations:

$$X_n(x) = B_n \sinh \lambda_n x + D_n \sin \lambda_n x + \frac{s_n}{2}\left(\cosh \lambda_n x + \cos \lambda_n x\right) \tag{4.35}$$

$$\frac{dX_n(x)}{dx} = \left\{B_n \cosh \lambda_n x + D_n \cos \lambda_n x + \frac{s_n}{2}\left(\sinh \lambda_n x - \sin \lambda_n x\right)\right\}\lambda_n \tag{4.36}$$

$$\frac{d^2 X_n(x)}{dx^2} = \left\{B_n \sinh \lambda_n x - D_n \sin \lambda_n x + \frac{s_n}{2}\left(\cosh \lambda_n x - \cos \lambda_n x\right)\right\}\lambda_n{}^2 \tag{4.37}$$

$$\frac{d^3 X_n(x)}{dx^3} = \left\{B_n \cosh \lambda_n x - D_n \cos \lambda_n x + \frac{s_n}{2}\left(\sinh \lambda_n x + \sin \lambda_n x\right)\right\}\lambda_n{}^3 \tag{4.38}$$

Applying Equation (4.26) to Equation (4.36) gives the following equation:

$$B_n \cosh\frac{\lambda_n l}{2} + D_n \cos\frac{\lambda_n l}{2} = -\frac{S_n}{2}\left(\sinh\frac{\lambda_n l}{2} - \sin\frac{\lambda_n l}{2}\right) \tag{4.39}$$

Applying Equation (4.32) to Equation (4.38) gives the following equation:

$$\begin{aligned} &B_n(\cosh\frac{\lambda_n l}{2}-\frac{K_1}{2EI\lambda_n^3}\sinh\frac{\lambda_n l}{2})-D_n(\cos\frac{\lambda_n l}{2}+\frac{K_1}{2EI\lambda_n^3}\sin\frac{\lambda_n l}{2}) \\ &=-\frac{S_n}{2}(\sinh\frac{\lambda_n l}{2}+\sin\frac{\lambda_n l}{2})+\frac{K_1-n^2m_a\omega^2}{2EI\lambda_n^3}\frac{S_n}{2}(\cosh\frac{\lambda_n l}{2}+\cos\frac{\lambda_n l}{2})-\frac{K_1S_n}{2EI\lambda_n^3}+\frac{C_n}{2EIe^{jn\alpha}\lambda_n^3} \end{aligned} \tag{4.40}$$

Solving Equations (4.39) and (4.40), the coefficients of Equation (4.17) are determined as follows:

$$\left.\begin{aligned} A_n &= C_n = \frac{1}{2}s_n \\ B_n &= \frac{\left\{\begin{aligned}&\left(\cosh\frac{\lambda_n l}{2}\cos\frac{\lambda_n l}{2}-2\cos\frac{\lambda_n l}{2}-\sinh\frac{\lambda_n l}{2}\sin\frac{\lambda_n l}{2}+1\right)\kappa\frac{24}{l^3\lambda_n^3} \\ &-\mu\frac{\lambda_n l}{2}\left(\cosh\frac{\lambda_n l}{2}\cos\frac{\lambda_n l}{2}-\sinh\frac{\lambda_n l}{2}\sin\frac{\lambda_n l}{2}+1\right)-2\cos\frac{\lambda_n l}{2}\sinh\frac{\lambda_n l}{2}\end{aligned}\right\}}{2\Delta_n}s_n+\frac{c_n\cos\frac{\lambda_n l}{2}}{2EI{\lambda_n}^3\Delta_n e^{jn\alpha}} \\ D_n &= \frac{\left\{\begin{aligned}&-\left(\cosh\frac{\lambda_n l}{2}\cos\frac{\lambda_n l}{2}-2\cosh\frac{\lambda_n l}{2}-\sinh\frac{\lambda_n l}{2}\sin\frac{\lambda_n l}{2}+1\right)\kappa\frac{24}{l^3\lambda_n^3} \\ &+\mu\frac{\lambda_n l}{2}\left(\cosh\frac{\lambda_n l}{2}\cos\frac{\lambda_n l}{2}-\sinh\frac{\lambda_n l}{2}\sin\frac{\lambda_n l}{2}+1\right)+2\cosh\frac{\lambda_n l}{2}\sin\frac{\lambda_n l}{2}\end{aligned}\right\}}{2\Delta_n}s_n-\frac{c_n\cosh\frac{\lambda_n l}{2}}{2EI{\lambda_n}^3\Delta_n e^{jn\alpha}} \end{aligned}\right\} \tag{4.41}$$

where

$$\kappa=\frac{K_1}{k} \tag{4.42}$$

where k of Equation (4.42) is the spring constant of the beam and expressed as follows:

$$k=\frac{48EI}{l^3} \tag{4.43}$$

And Δ_n is expressed as follows:

$$\Delta_n = \left(\kappa\frac{24}{l^3\lambda_n^3} - \mu\frac{\lambda_n l}{2}\right)\left(\cosh\frac{\lambda_n l}{2}\sin\frac{\lambda_n l}{2} - \cos\frac{\lambda_n l}{2}\sinh\frac{\lambda_n l}{2}\right) + 2\cosh\frac{\lambda_n l}{2}\cos\frac{\lambda_n l}{2} \tag{4.44}$$

Substituting B_n and D_n of Equation (4.41) into Equation (4.35) gives the following equation:

$$\begin{aligned} X_n(\tfrac{l}{2}) = \frac{s_n}{\Delta_n}&\left\{\begin{aligned}&\cosh\frac{\lambda_n l}{2} + \cos\frac{\lambda_n l}{2} + \left(\kappa\frac{24}{l^3\lambda_n^3} - \mu\frac{\lambda_n l}{2}\right)\sin^2\frac{\lambda_n l}{2}\sinh\frac{\lambda_n l}{2}\\ &+ \kappa\frac{24}{l^3\lambda_n^3}\left(\sin\frac{\lambda_n l}{2}\cosh\frac{\lambda_n l}{2} - \cos\frac{\lambda_n l}{2}\sinh\frac{\lambda_n l}{2}\right)\end{aligned}\right\}\\ &+ \frac{c_n}{2EI{\lambda_n}^3\Delta_n e^{jn\alpha}}\left(\sinh\frac{\lambda_n l}{2}\cos\frac{\lambda_n l}{2} - \cosh\frac{\lambda_n l}{2}\sin\frac{\lambda_n l}{2}\right)\end{aligned} \tag{4.45}$$

Equation (4.45) is simplified as follows:

$$X_n(\tfrac{l}{2}) = s_n(N_n + 1) + \frac{M_n c_n}{k e^{jn\alpha}} \tag{4.46}$$

where

$$M_n = \frac{24}{{\lambda_n}^3 l^3 \Delta_n}\left(\sinh\frac{\lambda_n l}{2}\cos\frac{\lambda_n l}{2} - \cosh\frac{\lambda_n l}{2}\sin\frac{\lambda_n l}{2}\right) \tag{4.47}$$

$$\begin{aligned} N_n = \frac{1}{\Delta_n}&\left\{\cosh\frac{\lambda_n l}{2} + \cos\frac{\lambda_n l}{2} + \left(\kappa\frac{24}{l^3\lambda_n^3} - \mu\frac{\lambda_n l}{2}\right)\sin^2\frac{\lambda_n l}{2}\sinh\frac{\lambda_n l}{2}\right.\\ &\left.+ \kappa\frac{24}{l^3\lambda_n^3}\left(\sin\frac{\lambda_n l}{2}\cosh\frac{\lambda_n l}{2} - \cos\frac{\lambda_n l}{2}\sinh\frac{\lambda_n l}{2}\right)\right\} - 1\end{aligned} \tag{4.48}$$

(4) Derivation of Non-Dimensional Equations

Equation for the resulting vibration $z_{l/2}/e_0$, the phase lag angle α, the excitation

amplitude ratio f_1/e_0 and the non-dimensional nonlinear restoring force $g(\theta)/k\Gamma$ are the same equation in Chapter 3 because the switching-over conditions is the same. Therefore, derivation process is omitted, and these equations are shown as follows.

(i) Non-Dimensional Resulting Vibration $z_{1/2}/e_0$

$$\frac{z_{1/2}}{e_0}=\frac{\sum_{n=1,3,5,\cdots}^{\infty}\left\{\left(N_n u_n\frac{1-M_1x_1}{N_1}+M_n x_n\right)\cos n\theta+\left(N_n v_n\frac{1-M_1x_1}{N_1}+M_n y_n\right)\sin n\theta\right\}}{\sum_{n=1,3,5,\cdots}^{\infty}\left(N_n u_n\frac{1-M_1x_1}{N_1}+M_n x_n\right)\cos\frac{n\theta_0}{2}} \tag{4.49}$$

(ii) Phase Lag Angle α

$$\alpha=\tan^{-1}\left[\left\{M_1y_1+\sum_{n=3,5,7,\cdots}^{\infty}\left(N_n v_n\frac{1-M_1x_1}{N_1}+M_n y_n\right)\frac{\sin\frac{n\theta_0}{2}}{\sin\frac{\theta_0}{2}}\right\}\Big/\left(1-M_1x_1\right)\right] \tag{4.50}$$

(iii) Excitation Amplitude Ratio f_1/e_0

$$\frac{f_1}{e_0}=\frac{1}{\cos\alpha}\frac{\frac{1-M_1x_1}{N_1}}{\sum_{n=1,3,5,\cdots}^{\infty}\left(N_n u_n\frac{1-M_1x_1}{N_1}+M_n x_n\right)\cos\frac{n\theta_0}{2}} \tag{4.51}$$

(iv) Non-Dimensional Nonlinear Restoring Force $g(\theta)/k\Gamma$

$$\frac{g(\theta)}{k\Gamma}=\sum_{n=1,3,5,\cdots}^{\infty}\left(x_n\cos n\theta+y_n\sin n\theta\right) \tag{4.52}$$

(5) Determination of Non-Dimensional Fourier Coefficients x_n and y_n

Equations (4.49), (4.50), (4.51) and (4.52) can all be determined by using the three

independent parameters of the frequency ratio Ω, the phase lag angle α and the dwell phase angle θ_0 in zones I and III and non-dimensional Fourier coefficients x_n and y_n. Therefore, once x_n and y_n (n=1,3,5, $\cdots$) are known, the resulting displacement ratio $z_{l/2}/e_0$, the corresponding excitation amplitude ratio f_1/e_0 and the phase lag angle α can be found from Equations (4.49), (4.51) and (4.50). The non-dimensional Fourier coefficients x_n and y_n must be determined such that the condition of piecewise linear characteristics of nonlinear part of the restoring force is satisfied. The nonlinear portion of the restoring force $g(\theta)$ shown in Figure 4.4(c) is expressed in Equation (4.30), and piecewise linear characteristics of the nonlinear part of the restoring force is the same in Chapter 3. Furthermore, assumed harmonic resonance vibration shape in Figure 4.4 is the same in Chapter 3. As a result, the infinite dimensionless linear simultaneous equations are the same form. Therefore, derivation process is omitted and the infinite dimensionless linear simultaneous equations are shown as follows:

$$\left.\begin{aligned} x_m - \sum_{n=1,3,5,\cdots}^{\infty}\left(A_{mn}x_n - B_{mn}x_1\right) &= \sum_{n=1,3,5,\cdots}^{\infty} I_{mn} \\ y_m - \sum_{n=1,3,5,\cdots}^{\infty}\left(C_{mn}y_n - D_{mn}x_1\right) &= \sum_{n=1,3,5,\cdots}^{\infty} J_{mn} \end{aligned}\right\} \tag{4.53}$$

4.1.2 Analysis of Stability Criterion

(1) Characteristics of System and Variational Equation

Here, stability analysis is carried out for a periodic solution of a nonlinear vibration system. The system is a simply-supported beam having an attached mass and connected with a nonlinear spring at mid-span. Equation of motion of analytical system is expressed in Equation (4.1):

$$\rho A \frac{\partial^2 z}{\partial t^2} + EI \frac{\partial^4 z}{\partial x^4} = -\rho A \frac{\partial^2 q}{\partial t^2}$$

And boundary conditions are expressed as follows:

$$\left.\begin{aligned} & z\big|_{x=0} = 0 \\ & \left.\frac{d^2 z}{dx^2}\right|_{x=0} = 0 \\ & \left.\frac{dz}{dx}\right|_{x=l/2} = 0 \\ & EI \left.\frac{d^3 z}{dx^3}\right|_{x=l/2} = m_a \frac{\partial^2 y}{\partial t^2} + f\left(z_{l/2}\right) \end{aligned}\right\} \tag{4.54}$$

where the restoring force $f(z_{l/2})$ is shown in Equation (4.29):

$$f\left(z_{l/2}\right) = \begin{cases} K_1 z_{l/2} + K_2 (z_{l/2} - e_0) & ; z \geq e_0 \quad \text{Region I} \\ K_1 z_{l/2} & ; -e_0 \leq z \leq e_0 \quad \text{Region II} \\ K_1 z_{l/2} + K_2 \left(z_{l/2} + e_0\right) & ; z \leq -e_0 \quad \text{Region III} \end{cases}$$

The boundary conditions are changed by the displacement at mid-point of the beam. And thus, eigenvalues are defined in these regions. The angular frequency ω_i of a simply-supported beam is expressed by:

$$\left.\begin{aligned}&\text{Angular frequancy} \;:\; \omega_i = \frac{(\beta_i l)^2}{l^2}\sqrt{\frac{EI}{\rho A}}\\&\text{Frequency equation} \;:\; \sin\beta l = 0\\&\beta_1 l = \pi,\quad \beta_2 l = 2\pi,\quad \beta_3 l = 3\pi,\cdots\end{aligned}\right\} \tag{4.55}$$

The boundary conditions in each region are expressed as follows:

(i) Simply-Supported Beam Connected with a Linear Spring (Spring Constant K_1+K_2) at Mid-Span in Region I, III

$$\left.\begin{aligned}&z\big|_{x=0} = 0\\&\left.\frac{d^2z}{dx^2}\right|_{x=0} = 0\\&\left.\frac{dz}{dx}\right|_{x=l/2} = 0\\&2EI\left.\frac{d^3z}{dx^3}\right|_{x=l/2} = m_a\frac{\partial^2 y}{\partial t^2} + K_1 z_{l/2} + K_2(z_{l/2} \pm e_0)\end{aligned}\right\} \tag{4.56}$$

(ii) Simply-Supported Beam Connected with a Linear Spring (Spring Constant K_1) at Mid-Span in Region II

$$\left.\begin{aligned}&z\big|_{x=0} = 0\\&\left.\frac{d^2z}{dx^2}\right|_{x=0} = 0\\&\left.\frac{dz}{dx}\right|_{x=l/2} = 0\\&2EI\left.\frac{d^3z}{dx^3}\right|_{x=l/2} = m_a\frac{\partial^2 y}{\partial t^2} + K_1 z_{l/2}\end{aligned}\right\} \tag{4.57}$$

The angular frequency in region I and III is determined by the frequency equation containing the spring constant ratio $\kappa_2=(K_1+K_2)/k$ and the mass ratio $\mu=m_a/m_b$, and expressed as

follows:

$$\left.\begin{aligned}&\text{Angular frequency} \quad : \quad \omega_i^{\mathrm{I}} = \omega_i^{\mathrm{III}} = \frac{\left(\beta_i^{\mathrm{I,III}} l\right)^2}{l^2}\sqrt{\frac{EI}{\rho A}} \\ &\text{Frequency equation} \quad : \quad \mu\beta_i^{\mathrm{I,III}} l + \frac{48}{(\beta^{\mathrm{I,III}} l)^3}\kappa_2 = \frac{4}{\tan\dfrac{\beta^{\mathrm{I,III}} l}{2} - \tanh\dfrac{\beta^{\mathrm{I,III}} l}{2}}\end{aligned}\right\} \tag{4.58}$$

The angular frequency in region II is determined by the frequency equation containing the spring constant ratio $\kappa_1 = K_1 / k$ and the mass ratio $\mu = m_a / m_b$, and expressed as follows:

$$\left.\begin{aligned}&\text{Angular frequency} \quad : \quad \omega_i^{\mathrm{II}} = \frac{\left(\beta_i^{\mathrm{II}} l\right)^2}{l^2}\sqrt{\frac{EI}{\rho A}} \\ &\text{Frequency equation} \quad : \quad \mu\beta_i^{\mathrm{II}} l + \frac{48}{(\beta_i^{\mathrm{II}} l)^3}\kappa_1 = \frac{4}{\tan\dfrac{\beta_i^{\mathrm{II}} l}{2} - \tanh\dfrac{\beta_i^{\mathrm{II}} l}{2}}\end{aligned}\right\} \tag{4.59}$$

For simplicity, symbol I, II and III indicating the displacement region is expressed by ι after that:

(2) Mode Equation and Variational Equation

A mode function has orthogonality in each of the regions and it is derived by using Galerkin method. A general solution for Equation of motion (4.1) is assumed as follows:

$$z^{(\iota)}(x,t) = \sum_{i=1}^{\infty} X_i^{(\iota)}(x) \cdot T_i^{(\iota)}(t) \tag{4.60}$$

Substituting (4.60) into Equation (4.1) gives the following equation:

$$\sum_{i=1}^{\infty}\left\{\left(\frac{\mathrm{d}^2 T_i^{(\iota)}}{\mathrm{d}t^2} + \frac{EI}{\rho A}\frac{\dfrac{\mathrm{d}^4 X_i^{(\iota)}}{\mathrm{d}x^4}}{X_i^{(\iota)}} \cdot T_i^{(\iota)}\right) \cdot X_i^{(\iota)}\right\} = -\frac{\mathrm{d}^2 q}{\mathrm{d}t^2} \tag{4.61}$$

Here, the following equation can be obtained about mode function:

$$\frac{EI}{\rho A}\frac{\dfrac{\mathrm{d}^4 X_i^{(t)}}{\mathrm{d}x^4}}{X_i^{(t)}} = \left(\omega_i^{(t)}\right)^2 \tag{4.62}$$

Equation (4.61) is transformed by using Equation (4.62):

$$\sum_{i=1}^{\infty}\left\{\left(\frac{\mathrm{d}^2 T_i^{(t)}}{\mathrm{d}t^2} + \left(\omega_i^{(t)}\right)^2 T_i^{(t)}\right)\cdot X_i^{(t)}\right\} = -\frac{\mathrm{d}^2 q}{\mathrm{d}t^2} \tag{4.63}$$

Multiplying Equation (4.63) by mode functions X_i and integrating over the period (0, l) gives the following mode equation:

$$\frac{\mathrm{d}^2 T_i^{(t)}}{\mathrm{d}t^2} + \left(\omega_i^{(t)}\right)^2 T_i^{(t)} = -\frac{\int_0^l X_i^{(t)}\mathrm{d}x}{\int_0^l \left(X_i^{(t)}\right)^2 \mathrm{d}x}\frac{d^2 q(t)}{dt^2} \tag{4.64}$$

The resulting vibration in distributed parameter systems can be expressed by summation of normal modes. Therefore, when all mode coordinates are stable, the system is also stable. Alternatively, if only one mode is unstable, the system is unstable.

The phase angle is expressed in Equation (4.23):

$$\theta = \omega t - \alpha$$

The frequency ratio based on the first order natural angular frequency of a simply-supported beam is expressed as follows:

$$\frac{\omega}{\omega_1} = \Omega \tag{4.65}$$

The natural angular frequency ratio based on the first order natural angular frequency of a simply-supported beam is expressed as follows:

$$\frac{\omega_i^{(\iota)}}{\omega_1} = \left(\frac{\beta_i^{(\iota)} l}{\beta_1 l} \right)^2 = \Omega_i^{(\iota)} \tag{4.66}$$

Substituting Equations (4.23), (4.65) and (4.66) into Equation (4.64) gives the following equation:

$$\frac{\mathrm{d}^2 T_i^{(\iota)}(\theta)}{\mathrm{d}\theta^2} + \left(\frac{\Omega_i^{(\iota)}}{\Omega} \right)^2 T_i(\theta) = -\frac{\int_0^l X_i^{(\iota)} \mathrm{d}x}{\int_0^l \left(X_i^{(\iota)} \right)^2 \mathrm{d}x} \frac{\mathrm{d}^2 q(\theta)}{\mathrm{d}\theta^2} \tag{4.67}$$

The periodic solution for Equation (4.67) is expressed by T_{0i} and the variation in the vibratory displacement is expressed by ξ_i, and the following relation is obtained:

$$T_i(\theta) = T_{0i}(\theta) + \xi_i(\theta) \tag{4.68}$$

Substituting Equation (4.68) into Equation (4.67) gives the following equation:

$$\frac{\mathrm{d}^2}{\mathrm{d}\theta^2} \left(T_{0i} + \xi_i \right) + \left(\frac{\Omega_i^{(\iota)}}{\Omega} \right)^2 \left(T_{0i} + \xi_i \right) = -\frac{\int_0^l X_i^{(\iota)} \mathrm{d}x}{\int_0^l \left(X_i^{(\iota)} \right)^2 \mathrm{d}x} \frac{\mathrm{d}^2 q(\theta)}{\mathrm{d}\theta^2} \tag{4.69}$$

where the periodic solution T_{0i} also satisfies the equation of motion:

$$\frac{\mathrm{d}^2}{\mathrm{d}\theta^2} T_{0i} + \left(\frac{\Omega_i^{(\iota)}}{\Omega} \right)^2 T_{0i} = -\frac{\int_0^l X_i^{(\iota)} \mathrm{d}x}{\int_0^l \left(X_i^{(\iota)} \right)^2 \mathrm{d}x} \frac{\mathrm{d}^2 q(\theta)}{\mathrm{d}\theta^2} \tag{4.70}$$

Subtracting Equation (4.70) from (4.69), the variational equation is obtained as follows:

$$\frac{\mathrm{d}^2\xi_i}{\mathrm{d}\theta^2}+\left(\frac{\Omega_i^{(\prime)}}{\Omega}\right)^2\xi_i=0 \tag{4.71}$$

Equation (4.71) is the periodic function with the period 2π and called Hill's equation.

(3) Hill's Equation and Stability Criterion

Equation (4.71) is transformed into simultaneous equations as follows:

$$\left.\begin{aligned}\frac{\mathrm{d}\xi_i}{\mathrm{d}\theta}&=\dot{\xi}_i\\ \frac{\mathrm{d}\dot{\xi}_i}{\mathrm{d}\theta}&=-r_i^{(\prime)}\xi_i\\ r_i^{(\prime)}&=\left(\frac{\Omega_i^{(\prime)}}{\Omega}\right)^2\end{aligned}\right\} \tag{4.72}$$

Equation (4.72) is transformed into the following expression by using the solution vector $\boldsymbol{\xi_i}$ and coefficient matix **W**:

$$\left.\begin{aligned}&\dot{\boldsymbol{\xi}}_i=\mathbf{W}\boldsymbol{\xi}_i\\ &\dot{\boldsymbol{\xi}}_i=\begin{bmatrix}\dfrac{\mathrm{d}\xi_i}{\mathrm{d}\theta}\\ \dfrac{\mathrm{d}\dot{\xi}_i}{\mathrm{d}\theta}\end{bmatrix},\ \mathbf{W}=\begin{bmatrix}0 & 1\\ -r_i^{(\prime)} & 0\end{bmatrix},\ \boldsymbol{\xi}_i=\begin{bmatrix}\xi_i\\ \dot{\xi}_i\end{bmatrix}\end{aligned}\right\} \tag{4.73}$$

where the fundamental solution matrix (Wronski Matrix) for Equation (4.73) is

$$\boldsymbol{\Xi}_i(\theta)=\begin{bmatrix}\xi_{i1}(\theta) & \xi_{i2}(\theta)\\ \dfrac{d\xi_{i1}(\theta)}{d\theta} & \dfrac{\xi_{i2}(\theta)}{d\theta}\end{bmatrix},\quad \det\boldsymbol{\Xi}_i\neq 0 \tag{4.74}$$

Here, the fundamental period of the periodic solution is *T*, and the following relation can be obtained by Floquet's theorem:

$$\boldsymbol{\Xi}_i(\theta+T)=\boldsymbol{\Xi}_i(\theta)\cdot\mathbf{C}_i \tag{4.75}$$

where $\mathbf{C}_i$ is a constant matrix and expressed as follows:

$$\mathbf{C}_i=\begin{bmatrix} c_{i11} & c_{i12} \\ c_{i21} & c_{i22} \end{bmatrix},\ \det\mathbf{C}_i\neq 0 \tag{4.76}$$

The eigenvalues of the matrix $\mathbf{C}_i$ of Equation (4.76) are multipliers λ_{i1} and λ_{i2}. These are the solutions of the following equation:

$$\det[\mathbf{C}_i-\lambda_i\mathbf{I}]=\begin{vmatrix} c_{i11}-\lambda_i & c_{i12} \\ c_{i21} & c_{i22}-\lambda_i \end{vmatrix}=0 \tag{4.77}$$

Generally, the following equation holds for a fundamental solution matrix of homogenous linear equation (Sato, 1969):

$$\det\boldsymbol{\Xi}(\theta)=\det\boldsymbol{\Xi}(\theta_0)\cdot\exp\left[\int_{\theta_0}^{\theta}\{\,\mathrm{tr}\mathbf{W}(s)\,\}ds\right] \tag{4.78}$$

The unit matrix is chosen to be the initial condition of the fundamental solution matrix:

$$\boldsymbol{\Xi}_i(\theta_{\mathrm{ini}})=\begin{bmatrix} \xi_{i1}(\theta_{\mathrm{ini}}) & \xi_{i2}(\theta_{\mathrm{ini}}) \\ \dot{\xi}_{i1}(\theta_{\mathrm{ini}}) & \dot{\xi}_{i2}(\theta_{\mathrm{ini}}) \end{bmatrix}=\begin{bmatrix} 1 & 0 \\ 0 & 1 \end{bmatrix}=\mathbf{I} \tag{4.79}$$

Summing on-diagonal element of the matrix **W** of Equation (4.73),

$$\mathrm{tr}[\mathbf{W}]=0 \tag{4.80}$$

Thus using the equations (4.78) and (4.79),

$$\det\boldsymbol{\Xi}_i(\theta)=\det\boldsymbol{\Xi}_i(\theta_{\mathrm{ini}})=1 \tag{4.81}$$

By Floquet's theorem of Equation (4.75),

$$\det \boldsymbol{\Xi}_i(\theta + T) = \det \boldsymbol{\Xi}_i(\theta) \det \mathbf{C}_i \tag{4.82}$$

Therefore

$$\det \mathbf{C}_i = 1 \tag{4.83}$$

Equation (4.75) by Floquet's theorem is transformed as follows:

$$\mathbf{C}_i = \boldsymbol{\Xi}_i^{-1}(\theta_{\text{ini}}) \cdot \boldsymbol{\Xi}_i(\theta_{\text{ini}} + T) = \boldsymbol{\Xi}_i(\theta_{\text{ini}} + T) = \begin{bmatrix} \xi_{i1}(\theta_{\text{ini}} + T) & \xi_{i2}(\theta_{\text{ini}} + T) \\ \dot{\xi}_{i1}(\theta_{\text{ini}} + T) & \dot{\xi}_{i2}(\theta_{\text{ini}} + T) \end{bmatrix} \tag{4.84}$$

The multipliers λ_{i1} and λ_{i2} are derived from Equations (4.77) and (4.84):

$$\left.\begin{aligned} \lambda_i &= \frac{c_{i11} + c_{i22}}{2} \pm \sqrt{\left(\frac{c_{i11} + c_{i22}}{2}\right)^2 - 1} \\ c_{i11} &= \xi_{i1}(\theta_{\text{ini}} + T), \quad c_{i22} = \dot{\xi}_{i2}(\theta_{\text{ini}} + T) \end{aligned}\right\} \tag{4.85}$$

Summing on-diagonal element of the matrix $\mathbf{C}_i$ after the fundamental period gives the following equation:

$$A_i = c_{i11} + c_{i22} = \xi_{i1}(\theta_{\text{ini}} + T) + \dot{\xi}_{i2}(\theta_{\text{ini}} + T) \tag{4.86}$$

The product of the two multipliers λ_{i1} and λ_{i2} is calculated as follows:

$$\lambda_{i1} \cdot \lambda_{i2} = 1 \tag{4.87}$$

In the case where a periodic solution is stable, the multipliers λ_{i1} and λ_{i2} satisfy the following equation:

$$|\lambda_{i1}| \le 1,\ |\lambda_{i2}| \le 1 \tag{4.88}$$

In addition, Equation (4.87) is also considered; the stability criterion is expressed as follows:

$$|\lambda_{i1}| = |\lambda_{i2}| = 1 \tag{4.89}$$

The stability criterion of Equation (4.89) can be rewritten as follows by using A_i:

$$\left.\begin{array}{ll} \text{i)} & |A_i| > 2 \quad \text{A periodic solution is unstable} \\ \text{ii)} & |A_i| = 2 \quad \text{A periodic solution is neutral} \\ \text{iii)} & |A_i| < 2 \quad \text{A periodic solution is stable} \end{array}\right\} \tag{4.90}$$

The stable periodic solution is expressed by S_i, unstable one is expressed by U_i and neutral one is expressed by N_i, and Equation (4.90) is transformed to the following expression:

$$\left.\begin{array}{l} |A_i| < 2,\ T_i \in S_i \\ |A_i| > 2,\ T_i \in U_i \\ |A_i| = 2,\ T_i \in N_i \end{array}\right\} \tag{4.91}$$

Therefore

$$\left.\begin{array}{l} S_i = \left\{ T_i \,\middle|\, |A_i| < 2 \right\} \\ U_i = \left\{ T_i \,\middle|\, |A_i| > 2 \right\} \\ N_i = \overline{S}_i \cap \overline{U}_i = \left\{ T_i \,\middle|\, |A_i| = 2 \right\} \end{array}\right\} \tag{4.92}$$

Stable region S of the analysis system is intersection for stable region of mode coordinate and unstable region U is union for unstable region of mode coordinate. And neutral region N is defined as intersection for complement of S and U.

$$\left.\begin{aligned} S &= \bigcap_{i=1}^{\infty} S_i = \bigcap_{i=1}^{\infty} \left\{ z / e_0 \middle| |A_i| < 2 \right\} \\ U &= \bigcup_{i=1}^{\infty} U_i = \bigcup_{i=1}^{\infty} \left\{ z / e_0 \middle| |A_i| > 2 \right\} \\ N &= \overline{S} \cap \overline{U} \neq \begin{cases} \bigcap_{i=1}^{\infty} N_i \\ \bigcup_{i=1}^{\infty} N_i \end{cases} \end{aligned}\right\} \tag{4.93}$$

(4) Expression of Real Number A_i

The stability criterion is set up in the above analysis. Here, the real number A_i of Equation (4.86) is derived by determining the fundamental solutions after the fundamental period. The fundamental solutions for Equation (4.71) can be solved by inosculating method. The fundamental solutions $\xi_{i1}(\theta)$ and $\xi_{i2}(\theta)$ satisfy the initial conditions of Equation (4.79), which are shown as follows:

$$\xi_{i1}(\theta = 0): \xi_{i1}(0) = 1, \ \dot{\xi}_{i1}(0) = 0 \tag{4.94}$$

$$\xi_{i2}(\theta = 0): \xi_{i2}(0) = 0, \ \dot{\xi}_{i2}(0) = 1 \tag{4.95}$$

Here, independent variables shown in Figure 4.5 are applied as follows:

$$\theta_{\mathrm{A}} = \theta - \frac{\theta_0}{2} \tag{4.96}$$

$$\theta_{\mathrm{B}} = \theta_{\mathrm{A}} - \pi + \theta_0 \tag{4.97}$$

$$\theta_{\mathrm{C}} = \theta_{\mathrm{B}} - \theta_0 \tag{4.98}$$

$$\theta_{\mathrm{D}} = \theta_{\mathrm{C}} - \pi + \theta_0 \tag{4.99}$$

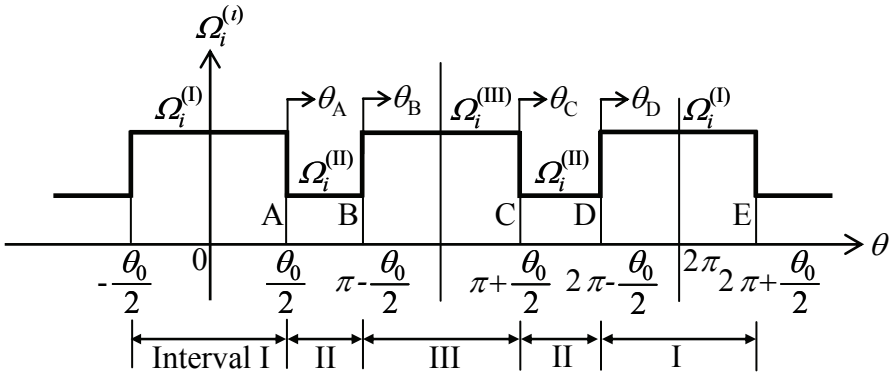

Figure 4.5 Angular frequency ratios

(i) In the case of the Fundamental Solution ξ_{i1}

(a) In the interval AB

Since Equation (4.71) is the second order differential equation, the solution is assumed as follows:

$$\left.\begin{aligned}\xi_{i1}(\theta_\mathrm{A}) &= C_{\mathrm{A}1}^{(i)}\cos\frac{\Omega_i^{\mathrm{II}}}{\Omega}\theta_\mathrm{A} + S_{\mathrm{A}1}^{(i)}\sin\frac{\Omega_i^{\mathrm{II}}}{\Omega}\theta_\mathrm{A}\\ \dot{\xi}_{i1}(\theta_\mathrm{A}) &= -\frac{\Omega_i^{\mathrm{II}}}{\Omega}C_{\mathrm{A}1}^{(i)}\sin\frac{\Omega_i^{\mathrm{II}}}{\Omega}\theta_\mathrm{A} + \frac{\Omega_i^{\mathrm{II}}}{\Omega}S_{\mathrm{A}1}^{(i)}\cos\frac{\Omega_i^{\mathrm{II}}}{\Omega}\theta_\mathrm{A}\end{aligned}\right\} \tag{4.100}$$

Applying the initial condition of Equation (4.94) to the fundamental solution of Equation (4.100) gives the following equations:

$$\left.\begin{aligned}\xi_{i1}(\theta_\mathrm{A}) &= \cos\frac{\Omega_i^{\mathrm{II}}}{\Omega}\theta_\mathrm{A}\\ \dot{\xi}_{i1}(\theta_\mathrm{A}) &= -\frac{\Omega_i^{\mathrm{II}}}{\Omega}\sin\frac{\Omega_i^{\mathrm{II}}}{\Omega}\theta_\mathrm{A}\end{aligned}\right\} \tag{4.101}$$

(b) In the interval BC

Since Equation (4.71) is the second order differential equation, the solution is assumed as follows:

$$\left.\begin{aligned}\xi_{il}(\theta_{\mathrm{B}}) &= C_{\mathrm{Bl}}^{(i)}\cos\frac{\Omega_i^{\mathrm{III}}}{\Omega}\theta_{\mathrm{B}} + S_{\mathrm{Bl}}^{(i)}\sin\frac{\Omega_i^{\mathrm{III}}}{\Omega}\theta_{\mathrm{B}} \\ \dot{\xi}_{il}(\theta_{\mathrm{B}}) &= -\frac{\Omega_i^{\mathrm{III}}}{\Omega}C_{\mathrm{Bl}}^{(i)}\sin\frac{\Omega_i^{\mathrm{III}}}{\Omega}\theta_{\mathrm{B}} + \frac{\Omega_i^{\mathrm{III}}}{\Omega}S_{\mathrm{Bl}}^{(i)}\cos\frac{\Omega_i^{\mathrm{III}}}{\Omega}\theta_{\mathrm{B}}\end{aligned}\right\} \tag{4.102}$$

Applying the initial condition of Equation (4.94) and the relation of (4.97) to the fundamental solution of Equation (4.102) gives the following equations:

$$\begin{aligned}&\xi_{il}(\theta_{\mathrm{B}}=0) = \xi_{il}(\theta_{\mathrm{A}}=\pi-\theta_0) = C_{\mathrm{Bl}}^{(i)} = \cos\left\{\frac{\Omega_i^{\mathrm{II}}}{\Omega}(\pi-\theta_0)\right\} \\ &\dot{\xi}_{il}(\theta_{\mathrm{B}}=0) = \dot{\xi}_{il}(\theta_{\mathrm{A}}=\pi-\theta_0) = \frac{\Omega_i^{\mathrm{III}}}{\Omega}S_{\mathrm{Bl}}^{(i)} = -\frac{\Omega_i^{\mathrm{II}}}{\Omega}\sin\left\{\frac{\Omega_i^{\mathrm{II}}}{\Omega}(\pi-\theta_0)\right\}, \quad S_{\mathrm{Bl}}^{(i)} = -\frac{\Omega_i^{\mathrm{II}}}{\Omega_i^{\mathrm{III}}}\sin\left\{\frac{\Omega_i^{\mathrm{II}}}{\Omega}(\pi-\theta_0)\right\}\end{aligned} \tag{4.103}$$

(c) In the interval CD

Since Equation (4.71) is the second order differential equation, the solution is assumed as follows:

$$\left.\begin{aligned}\xi_{il}(\theta_{\mathrm{C}}) &= C_{\mathrm{Cl}}^{(i)}\cos\frac{\Omega_i^{\mathrm{II}}}{\Omega}\theta_{\mathrm{C}} + S_{\mathrm{Cl}}^{(i)}\sin\frac{\Omega_i^{\mathrm{II}}}{\Omega}\theta_{\mathrm{C}} \\ \dot{\xi}_{il}(\theta_{\mathrm{C}}) &= -\frac{\Omega_i^{\mathrm{II}}}{\Omega}C_{\mathrm{Cl}}^{(i)}\sin\frac{\Omega_i^{\mathrm{II}}}{\Omega}\theta_{\mathrm{C}} + \frac{\Omega_i^{\mathrm{II}}}{\Omega}S_{\mathrm{Cl}}^{(i)}\cos\frac{\Omega_i^{\mathrm{II}}}{\Omega}\theta_{\mathrm{C}}\end{aligned}\right\} \tag{4.104}$$

Applying the initial condition of Equation (4.94) and the relation of (4.98) to the fundamental solution of Equation (4.104) gives the following equations:

$$\begin{aligned}&\xi_{il}(\theta_{\mathrm{C}}=0) = \xi_{il}(\theta_{\mathrm{B}}=\theta_0) = C_{\mathrm{Cl}}^{(i)} = C_{\mathrm{Bl}}^{(i)}\cos\frac{\Omega_i^{\mathrm{III}}}{\Omega}\theta_0 + S_{\mathrm{Bl}}^{(i)}\sin\frac{\Omega_i^{\mathrm{III}}}{\Omega}\theta_0 \\ &\dot{\xi}_{il}(\theta_{\mathrm{C}}=0) = \dot{\xi}_{il}(\theta_{\mathrm{B}}=\theta_0) = \frac{\Omega_i^{\mathrm{II}}}{\Omega}S_{\mathrm{Cl}}^{(i)} = -\frac{\Omega_i^{\mathrm{III}}}{\Omega}C_{\mathrm{Bl}}^{(i)}\sin\frac{\Omega_i^{\mathrm{III}}}{\Omega}\theta_0 + \frac{\Omega_i^{\mathrm{III}}}{\Omega}S_{\mathrm{Bl}}^{(i)}\cos\frac{\Omega_i^{\mathrm{III}}}{\Omega}\theta_0 \\ &S_{\mathrm{Cl}}^{(i)} = -\frac{\Omega_i^{\mathrm{III}}}{\Omega_i^{\mathrm{II}}}C_{\mathrm{Bl}}^{(i)}\sin\frac{\Omega_i^{\mathrm{III}}}{\Omega}\theta_0 + \frac{\Omega_i^{\mathrm{III}}}{\Omega_i^{\mathrm{II}}}S_{\mathrm{Bl}}^{(i)}\cos\frac{\Omega_i^{\mathrm{III}}}{\Omega}\theta_0\end{aligned} \tag{4.105}$$

(d) In the interval DE

Since Equation (4.71) is the second order differential equation, the solution is assumed as follows:

$$\left.\begin{aligned}\xi_{i1}(\theta_{\mathrm{D}}) &= C_{\mathrm{D1}}^{(i)}\cos\frac{\Omega_i^{\mathrm{I}}}{\Omega}\theta_{\mathrm{D}} + S_{\mathrm{D1}}^{(i)}\sin\frac{\Omega_i^{\mathrm{I}}}{\Omega}\theta_{\mathrm{D}} \\ \dot{\xi}_{i1}(\theta_{\mathrm{D}}) &= -\frac{\Omega_i^{\mathrm{I}}}{\Omega}C_{\mathrm{D1}}^{(i)}\sin\frac{\Omega_i^{\mathrm{I}}}{\Omega}\theta_{\mathrm{D}} + \frac{\Omega_i^{\mathrm{I}}}{\Omega}S_{\mathrm{D1}}^{(i)}\cos\frac{\Omega_i^{\mathrm{I}}}{\Omega}\theta_{\mathrm{D}}\end{aligned}\right\} \tag{4.106}$$

Applying the initial condition of Equation (4.94) and the relation of (4.99) to the fundamental solution of Equation (4.106) gives the following equations:

$$\begin{aligned}&\xi_{i1}(\theta_{\mathrm{D}}=0) = \xi_{i1}(\theta_{\mathrm{C}}=\pi-\theta_0) = C_{\mathrm{D1}}^{(i)} = C_{\mathrm{C1}}^{(i)}\cos\left\{\frac{\Omega_i^{\mathrm{II}}}{\Omega}(\pi-\theta_0)\right\} + S_{\mathrm{C1}}^{(i)}\sin\left\{\frac{\Omega_i^{\mathrm{II}}}{\Omega}(\pi-\theta_0)\right\} \\ &\dot{\xi}_{i1}(\theta_{\mathrm{D}}=0) = \dot{\xi}_{i1}(\theta_{\mathrm{C}}=\pi-\theta_0) = \frac{\Omega_i^{\mathrm{I}}}{\Omega}S_{\mathrm{D1}}^{(i)} = -\frac{\Omega_i^{\mathrm{II}}}{\Omega}C_{\mathrm{C1}}^{(i)}\sin\left\{\frac{\Omega_i^{\mathrm{II}}}{\Omega}(\pi-\theta_0)\right\} + \frac{\Omega_i^{\mathrm{II}}}{\Omega}S_{\mathrm{C1}}^{(i)}\cos\left\{\frac{\Omega_i^{\mathrm{II}}}{\Omega}(\pi-\theta_0)\right\} \\ &S_{\mathrm{D1}}^{(i)} = -\frac{\Omega_i^{\mathrm{II}}}{\Omega_i^{\mathrm{I}}}C_{\mathrm{C1}}^{(i)}\sin\left\{\frac{\Omega_i^{\mathrm{II}}}{\Omega}(\pi-\theta_0)\right\} + \frac{\Omega_i^{\mathrm{II}}}{\Omega_i^{\mathrm{I}}}S_{\mathrm{C1}}^{(i)}\cos\left\{\frac{\Omega_i^{\mathrm{II}}}{\Omega}(\pi-\theta_0)\right\}\end{aligned} \tag{4.107}$$

(ii) In the case of Fundamental Solution ξ_{i2}

(a) In the interval AB

Since Equation (4.71) is the second order differential equation, the solution is assumed as follows:

$$\left.\begin{aligned}\xi_{i2}(\theta_{\mathrm{A}}) &= C_{\mathrm{A2}}^{(i)}\cos\frac{\Omega_i^{\mathrm{II}}}{\Omega}\theta_{\mathrm{A}} + S_{\mathrm{A2}}^{(i)}\sin\frac{\Omega_i^{\mathrm{II}}}{\Omega}\theta_{\mathrm{A}} \\ \dot{\xi}_{i2}(\theta_{\mathrm{A}}) &= -\frac{\Omega_i^{\mathrm{II}}}{\Omega}C_{\mathrm{A2}}^{(i)}\sin\frac{\Omega_i^{\mathrm{II}}}{\Omega}\theta_{\mathrm{A}} + \frac{\Omega_i^{\mathrm{II}}}{\Omega}S_{\mathrm{A2}}^{(i)}\cos\frac{\Omega_i^{\mathrm{II}}}{\Omega}\theta_{\mathrm{A}}\end{aligned}\right\} \tag{4.108}$$

Applying the initial condition of Equation (4.95) to the fundamental solution of Equation (4.108) gives the following equations:

$$\left.\begin{aligned}\xi_{i2}(\theta_{\mathrm{A}}) &= \frac{\Omega}{\Omega_i^{\mathrm{II}}}\sin\frac{\Omega_i^{\mathrm{II}}}{\Omega}\theta_{\mathrm{A}} \\ \dot{\xi}_{i2}(\theta_{\mathrm{A}}) &= \cos\frac{\Omega_i^{\mathrm{II}}}{\Omega}\theta_{\mathrm{A}}\end{aligned}\right\} \tag{4.109}$$

(b) In the interval BC

Since Equation (4.71) is the second order differential equation, the solution is assumed as follows:

$$\left.\begin{aligned}\xi_{i2}(\theta_{\mathrm{B}}) &= C_{\mathrm{B2}}^{(i)}\cos\frac{\Omega_i^{\mathrm{III}}}{\Omega}\theta_{\mathrm{B}} + S_{\mathrm{B2}}^{(i)}\sin\frac{\Omega_i^{\mathrm{III}}}{\Omega}\theta_{\mathrm{B}} \\ \dot{\xi}_{i2}(\theta_{\mathrm{B}}) &= -\frac{\Omega_i^{\mathrm{III}}}{\Omega}C_{\mathrm{B2}}^{(i)}\sin\frac{\Omega_i^{\mathrm{III}}}{\Omega}\theta_{\mathrm{B}} + \frac{\Omega_i^{\mathrm{III}}}{\Omega}S_{\mathrm{B2}}^{(i)}\cos\frac{\Omega_i^{\mathrm{III}}}{\Omega}\theta_{\mathrm{B}}\end{aligned}\right\} \tag{4.110}$$

Applying the initial condition of Equation (4.95) and the relation of (4.97) to the fundamental solution of Equation (4.110) gives the following equations:

$$\begin{aligned}&\xi_{i2}(\theta_{\mathrm{B}}=0) = \xi_{i2}(\theta_{\mathrm{A}}=\pi-\theta_0) = C_{\mathrm{B2}}^{(i)} = \frac{\Omega}{\Omega_i^{\mathrm{II}}}\sin\left\{\frac{\Omega_i^{\mathrm{II}}}{\Omega}(\pi-\theta_0)\right\} \\ &\dot{\xi}_{i2}(\theta_{\mathrm{B}}=0) = \dot{\xi}_{i2}(\theta_{\mathrm{A}}=\pi-\theta_0) = \frac{\Omega_i^{\mathrm{III}}}{\Omega}S_{\mathrm{B2}}^{(i)} = \cos\left\{\frac{\Omega_i^{\mathrm{II}}}{\Omega}(\pi-\theta_0)\right\}, \quad S_{\mathrm{B2}}^{(i)} = -\frac{\Omega}{\Omega_i^{\mathrm{III}}}\cos\left\{\frac{\Omega_i^{\mathrm{II}}}{\Omega}(\pi-\theta_0)\right\}\end{aligned} \tag{4.111}$$

(c) In the interval CD

Since Equation (4.71) is the second order differential equation, the solution is assumed as follows:

$$\left.\begin{aligned}\xi_{i2}(\theta_{\mathrm{C}}) &= C_{\mathrm{C2}}^{(i)}\cos\frac{\Omega_i^{\mathrm{II}}}{\Omega}\theta_{\mathrm{C}} + S_{\mathrm{C2}}^{(i)}\sin\frac{\Omega_i^{\mathrm{II}}}{\Omega}\theta_{\mathrm{C}} \\ \dot{\xi}_{i2}(\theta_{\mathrm{C}}) &= -\frac{\Omega_i^{\mathrm{II}}}{\Omega}C_{\mathrm{C2}}^{(i)}\sin\frac{\Omega_i^{\mathrm{II}}}{\Omega}\theta_{\mathrm{C}} + \frac{\Omega_i^{\mathrm{II}}}{\Omega}S_{\mathrm{C2}}^{(i)}\cos\frac{\Omega_i^{\mathrm{II}}}{\Omega}\theta_{\mathrm{C}}\end{aligned}\right\} \tag{4.112}$$

Applying the initial condition of Equation (4.95) and the relation of (4.98) to the fundamental

solution of Equation (4.112) gives the following equations:

$$\left.\begin{aligned}
&\xi_{i2}(\theta_{\mathrm{C}}=0)=\xi_{i1}(\theta_{\mathrm{B}}=\theta_0)=C_{\mathrm{C2}}^{(i)}=C_{\mathrm{B2}}^{(i)}\cos\frac{\Omega_i^{\mathrm{III}}}{\Omega}\theta_0+S_{\mathrm{B2}}^{(i)}\sin\frac{\Omega_i^{\mathrm{III}}}{\Omega}\theta_0\\
&\dot{\xi}_{i2}(\theta_{\mathrm{C}}=0)=\dot{\xi}_{i1}(\theta_{\mathrm{B}}=\theta_0)=\frac{\Omega_i^{\mathrm{II}}}{\Omega}S_{\mathrm{C2}}^{(i)}=-\frac{\Omega_i^{\mathrm{III}}}{\Omega}C_{\mathrm{B2}}^{(i)}\sin\frac{\Omega_i^{\mathrm{III}}}{\Omega}\theta_0+\frac{\Omega_i^{\mathrm{III}}}{\Omega}S_{\mathrm{B2}}^{(i)}\cos\frac{\Omega_i^{\mathrm{III}}}{\Omega}\theta_0\\
&S_{\mathrm{C2}}^{(i)}=-\frac{\Omega_i^{\mathrm{III}}}{\Omega_i^{\mathrm{II}}}C_{\mathrm{B2}}^{(i)}\sin\frac{\Omega_i^{\mathrm{III}}}{\Omega}\theta_0+\frac{\Omega_i^{\mathrm{III}}}{\Omega_i^{\mathrm{II}}}S_{\mathrm{B2}}^{(i)}\cos\frac{\Omega_i^{\mathrm{III}}}{\Omega}\theta_0
\end{aligned}\right\} \tag{4.113}$$

(d) In the interval DE

Since Equation (4.71) is the second order differential equation, the solution is assumed as follows:

$$\left.\begin{aligned}
&\xi_{i2}(\theta_{\mathrm{D}})=C_{\mathrm{D2}}^{(i)}\cos\frac{\Omega_i^{\mathrm{I}}}{\Omega}\theta_{\mathrm{D}}+S_{\mathrm{D2}}^{(i)}\sin\frac{\Omega_i^{\mathrm{I}}}{\Omega}\theta_{\mathrm{D}}\\
&\dot{\xi}_{i2}(\theta_{\mathrm{D}})=-\frac{\Omega_i^{\mathrm{I}}}{\Omega}C_{\mathrm{D2}}^{(i)}\sin\frac{\Omega_i^{\mathrm{I}}}{\Omega}\theta_{\mathrm{D}}+\frac{\Omega_i^{\mathrm{I}}}{\Omega}S_{\mathrm{D2}}^{(i)}\cos\frac{\Omega_i^{\mathrm{I}}}{\Omega}\theta_{\mathrm{D}}
\end{aligned}\right\} \tag{4.114}$$

Applying the initial condition of Equation (4.95) and the relation of (4.99) to the fundamental solution of Equation (4.114) gives the following equations:

$$\left.\begin{aligned}
&\xi_{i2}(\theta_{\mathrm{D}}=0)=\xi_{i2}(\theta_{\mathrm{D}}=\pi-\theta_0)=C_{\mathrm{D2}}^{(i)}=C_{\mathrm{C2}}^{(i)}\cos\left\{\frac{\Omega_i^{\mathrm{II}}}{\Omega}(\pi-\theta_0)\right\}+S_{\mathrm{C2}}^{(i)}\sin\left\{\frac{\Omega_i^{\mathrm{II}}}{\Omega}(\pi-\theta_0)\right\}\\
&\dot{\xi}_{i2}(\theta_{\mathrm{D}}=0)=\dot{\xi}_{i2}(\theta_{\mathrm{D}}=\pi-\theta_0)=\frac{\Omega_i^{\mathrm{I}}}{\Omega}S_{\mathrm{D2}}^{(i)}=-\frac{\Omega_i^{\mathrm{II}}}{\Omega}C_{\mathrm{C2}}^{(i)}\sin\left\{\frac{\Omega_i^{\mathrm{II}}}{\Omega}(\pi-\theta_0)\right\}+\frac{\Omega_i^{\mathrm{II}}}{\Omega}S_{\mathrm{C2}}^{(i)}\cos\left\{\frac{\Omega_i^{\mathrm{II}}}{\Omega}(\pi-\theta_0)\right\}\\
&S_{\mathrm{D2}}^{(i)}=-\frac{\Omega_i^{\mathrm{II}}}{\Omega_i^{\mathrm{I}}}C_{\mathrm{C2}}^{(i)}\sin\left\{\frac{\Omega_i^{\mathrm{II}}}{\Omega}(\pi-\theta_0)\right\}+\frac{\Omega_i^{\mathrm{II}}}{\Omega_i^{\mathrm{I}}}S_{\mathrm{C2}}^{(i)}\cos\left\{\frac{\Omega_i^{\mathrm{II}}}{\Omega}(\pi-\theta_0)\right\}
\end{aligned}\right\} \tag{4.115}$$

The stability criterion is shown in equation (4.90) and the real number A_i is expressed as follows:

$$A_i=\xi_1(2\pi)+\dot{\xi}_2(2\pi) \tag{4.116}$$

Substituting Equations (4.106) and (4.114) into Equation (4.116) and setting $\theta_{\mathrm{D}}=\theta_0$ gives the real number A_i as follows:

$$\begin{aligned} A_i &= \xi_{i1}(\theta_D=\theta_0)+\dot{\xi}_{i2}(\theta_D=\theta_0) \\ &= C_{\mathrm{D1}}^{(i)}\cos\frac{\Omega_i^{\mathrm{I}}}{\Omega}\theta_0+S_{\mathrm{D1}}^{(i)}\sin\frac{\Omega_i^{\mathrm{I}}}{\Omega}\theta_0-\frac{\Omega_i^{\mathrm{I}}}{\Omega}C_{\mathrm{D2}}^{(i)}\sin\frac{\Omega_i^{\mathrm{I}}}{\Omega}\theta_0+\frac{\Omega_i^{\mathrm{I}}}{\Omega}S_{\mathrm{D2}}^{(i)}\cos\frac{\Omega_i^{\mathrm{I}}}{\Omega}\theta_0 \end{aligned} \tag{4.117}$$

The stability criterion is shown in equation (4.90):

i) $|A_i|>2$ A periodic solution is unstable
ii) $|A_i|=2$ A periodic solution is neutral
iii) $|A_i|<2$ A periodic solution is stable

4.1.3 Calculation

The steady state periodic solutions were calculated based on the theoretical analysis results in the main resonance region. The excitation vibrations were chosen as two waves as an example of a periodic excitation with an arbitrary function shown in Figure 4.6.

Harmonic wave in Figure 4.6 (a)

$$q(\theta) = \cos\theta \tag{4.118}$$

Combined wave in Figure 4.6 (b)

$$q(\theta) = \cos\theta + 0.3\sin 3\theta \tag{4.119}$$

The resulting vibration is expressed by non-dimensional Fourier coefficients x_n, y_n which are determined by the infinite dimensionless linear simultaneous equations containing the independent parameters. Therefore, if the independent parameters are given, the non-dimensional Fourier coefficients x_n, y_n are determined, and the resulting vibration can be calculated. A calculation method for obtaining periodic solutions is the same for chapter 3, and the independent parameters and the non-dimensional Fourier coefficients are calculated similarly. Calculated independent parameters are substituted into Equation (4.117), and the real

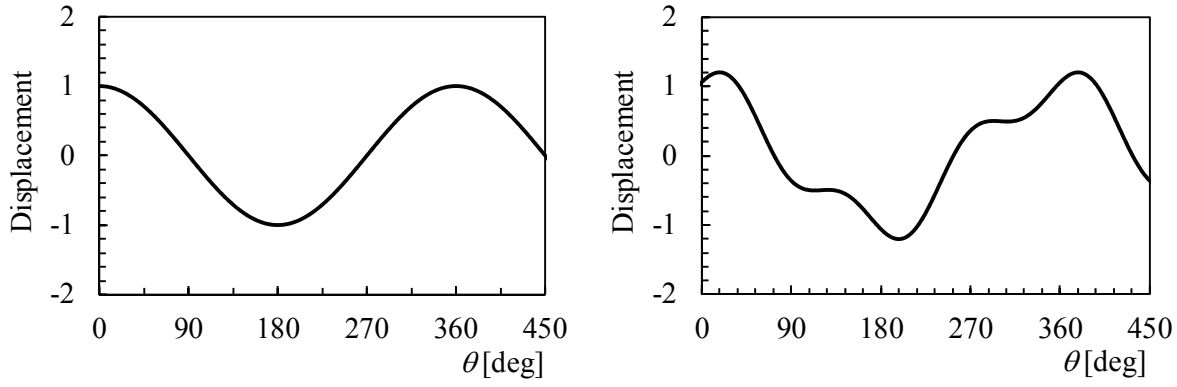

(a) $q(\theta)=\cos\theta$ (b) $q(\theta)=\cos\theta+0.3\sin 3\theta$

Figure 4.6 Exciting vibration wave

number A_i is obtained. Thus, substituting the real number A_i into the stability criterion of Equation (4.90), stability of a periodic solution is analyzed. Above steps are repeated, resonance curves distinguished from unstable branches are constructed. Strictly, it is needed that mode number of Equation (4.93) is considered to infinite order in the case of analyzing lumped parameter systems. Alternatively, this analytical model is simply-supported-beam having an attached mass connected with a nonlinear spring at mid-span, and the main resonance is only analyzed. In addition, the exciting vibration is the combined wave contained high harmonic wave whose angular frequency is more than three times higher than the fundamental one, but the third natural angular frequency of the analytical system is more than six times higher than the first one. Therefore, in calculation, the first order vibration mode is only adopted.

4.2 Experiment

Two experimental apparatus using coil springs and permanent magnets were built to embody the analytical model in Figure 4.2 and carried out to verify the analysis results.

4.2.1 Experiment by Using Coil Springs (Piecewise Linear Restoring Force)

Figure 4.7 is a diagram of the apparatus for observing steady state vibrations in a beam satisfying the equation of motion of Equation (4.1) and having piecewise linear restoring force. Table 4.1 provides the dimensions for the experimental beam and springs. The test beam (plate thickness: 0.5 mm, width: 12.8 mm) was made of spring steel. The beam was assumed to be a piecewise linear system; to model this, the linear spring ④ was connected to the beam in parallel with the collided spring ③ with a gap e_0, to create a system with a spring constant that satisfies the property indicated by the solid line. Beam ⑤ was connected to a linear spring ④ fixed to frame ② was simply supported at both ends with adjacent supporting springs ④ (coil springs) whose near ends were separated from the linear spring ③ by symmetric gaps e_0 and whose far ends were fixed to frame ②. A response vibration occurred in the beam under the excitation vibration. Once the displacement of the beam midpoint exceeded distance e_0, the beam collided with the supporting springs ③. At this time, the displacement input vibration caused a reciprocating movement of frame ② on the foundation ① via the linear ball bearing,

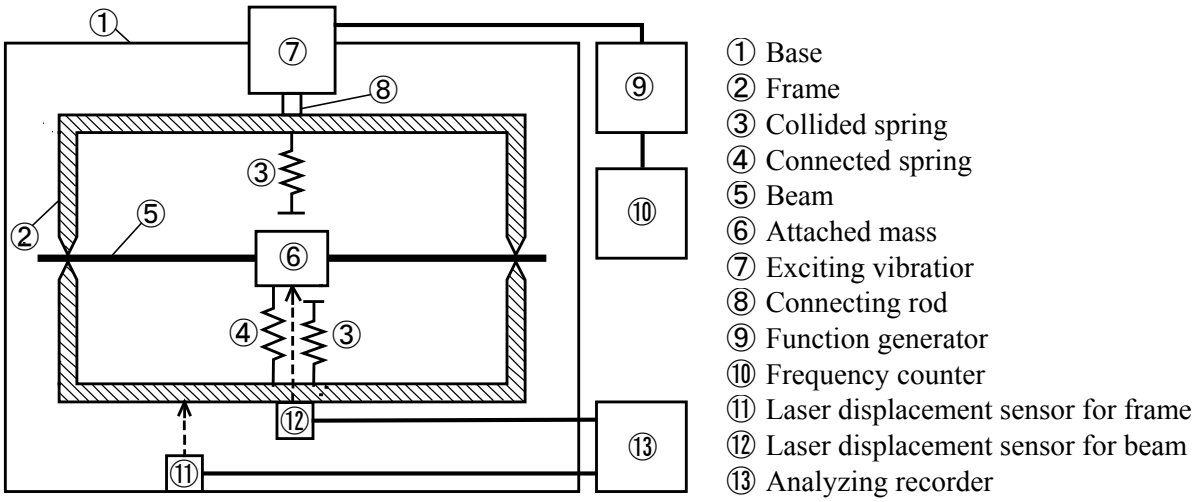

Figure 4.7 Sketch of the experiment apparatus

Table 4.1 Mechanical properties of parts used in experiment

Element	Symbol	Numerical value	
Length of the beam	l	415×10^{-3}	[m]
Cross section of the beam	A	8.67×10^{-6}	[m^2]
Attached mass	m_a	24×10^{-3}	[kg]
Mass of the beam	m_b	28.8×10^{-3}	[kg]
Density of the beam	ρ	7740	[kg/m^3]
Second moment of area for the beam	I	0.213×10^{-8}	[m^4]
Young's modulus of the beam	E	177×10^{9}	[Pa]
Spring constant of the beam	k	25.3	[N/m]
Clearance	e_0	5.0×10^{-3}	[m]
Connected spring constant	K_1	23.52	[N/m]
Collided spring constant	K_2	49.03	[N/m]

acting to cause a periodic excitation displacement vibration of the beam ⑤. A connecting rod ⑧ fixed to the foundation ① was connected to the exciting vibrator ⑦. The displacement vibration caused by the exciting vibrator ⑦ was set by the frequency counter ⑩ connected to the function generator ⑨. Friction with the floor had little effect on the frame ② from during vibration, so that this factor could be neglected. The excitation displacement was measured with a laser displacement sensor ⑪ and the resulting vibration was measured with another laser displacement sensor ⑫ mounted on the frame. The analog outputs from the sensors were stored on an analyzing recorder ⑬.

4.2.2 Experiment by Using Permanent Magnets (Nonlinear Restoring Force)

Figure 4.8 is a diagram of the apparatus for observing steady state vibrations in a beam satisfying the equation of motion of Equation (4.1) and having nonlinear restoring force. Figure 4.9 is a photograph of the apparatus. Basic component of the experimental apparatus is the same of one by using coil springs. Table 4.2 provides the dimensions for the experimental beam and magnets. In Figure 4.10, a red line shows the characteristics of the restoring force by the permanent magnets, and blue lines shows it approximated by a piecewise linear. In calculation, the blue lines are selected to give equal areas between the red line and blue lines below the curve and between the red line and blue lines above the curve. Table 4.3 provides the characteristics of the restoring force approximated by piecewise linear function.

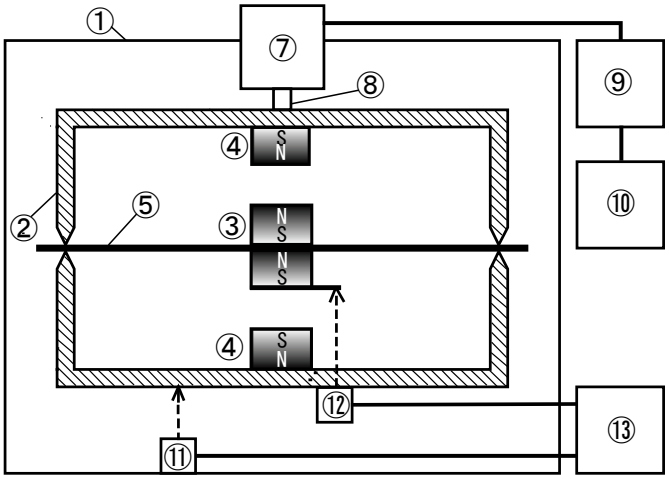

① Base
② Frame
③ Permanent magnet attached beam
④ Permanent magnet attached frame
⑤ Beam
⑦ Exciting vibratior
⑧ Connecting rod
⑨ Function generator
⑩ Frequency counter
⑪ Laser displacement sensor for frame
⑫ Laser displacement sensor for beam
⑬ Analyzing recorder

Figure 4.8 Sketch of the experiment apparatus

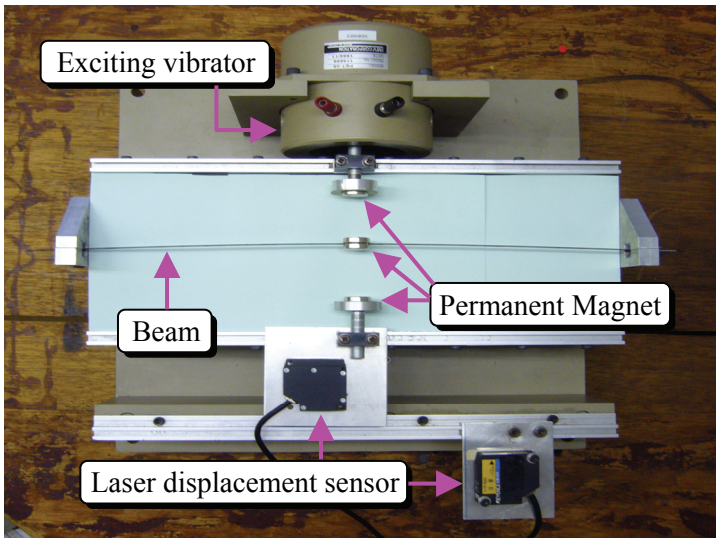

Figure 4.9 Photograph of the experiment apparatus

Table 4.2 Mechanical properties of parts used in experiment

Element	Symbol	Numerical value	
Length of the beam	l	415×10^{-3}	[m]
Cross section of the beam	A	8.67×10^{-6}	[m^2]
Attached mass (Magnet)	m_a	14.1×10^{-3}	[kg]
Mass of the beam	m_b	28.8×10^{-3}	[kg]
Density of the beam	ρ	7740	[kg/m^3]
Second moment of area for the beam	I	0.213×10^{-8}	[m^4]
Young's modulus of the beam	E	177×10^{9}	[Pa]
Spring constant of the beam	k	25.3	[N/m]
Surface inductive flux of the permanent magnet	G	1790	[G]

Table 4.3 Characteristics of the restoring force approximated by piecewise linear

Element	Symbol	Numerical value	
Coefficient of restoring force for linear region	K_1	44.3	[N/m]
Coefficient of restoring force for nonlinear region	K_2	53.13	[N/m]
Clearance	e_0	6.0×10^{-3}	[m]

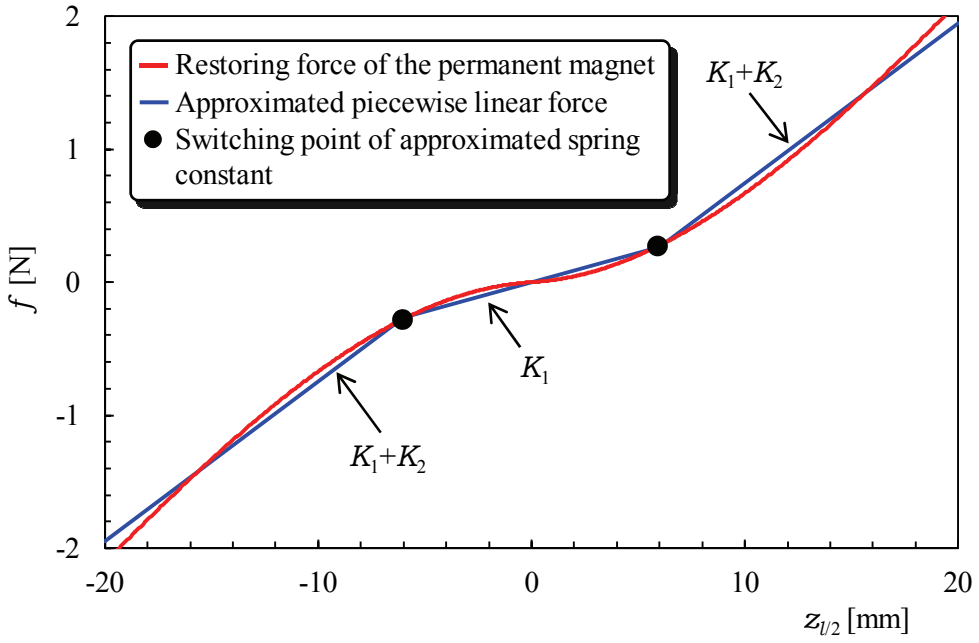

Figure 4.10 Restoring force of the permanent magnet

4.3 The Results of Theoretical Calculation and Experiment

4.3.1 Comparison of Theoretical Calculation Results with Experimental Results

(1)Using Coil Springs (Piecewise Linear Restoring Force)

Figure 4.11 shows the resonance curve for comparing the theoretical calculation results with experimental results excited by the harmonic excitation [$q(t)=\cos\omega t$] in Figure 4.6(a). The solid line shows theoretical calculation results. The black solid line represents stable branches and the red solid line represents unstable ones distinguished by the stability analysis. These results show quite a good agreement. An elbow in the resonance curve was apparent when the maximum vibration amplitude at the beam midpoint entered the nonlinear region (marked with ●), beyond which the curve bent sharply to the right, indicating prominent nonlinear behavior. The results in the physical model (open circles ○) show a jump to the lower line of linear vibrations when the vibration frequency ratio exceeded a value of $\Omega \approx 1.69$ as Ω was being increased. No results were obtained in the nonlinear region in the physical model at

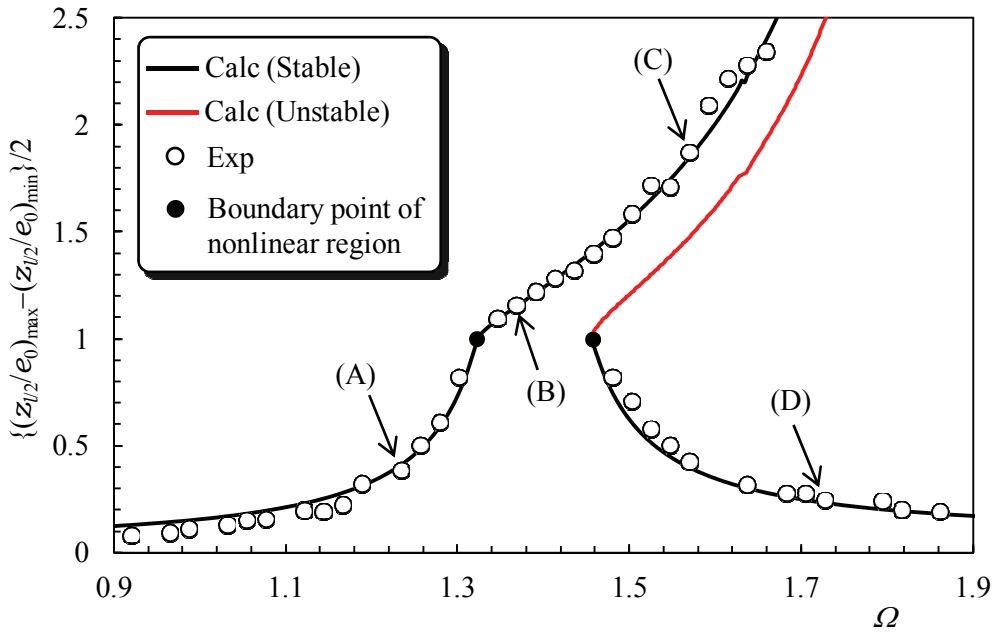

{ $q(t)=\cos\omega t$, $K_1/k=0.93$, $K_2/k=1.94$, $f_1/e_0=0.10$, $\mu=0.83$ }

Figure 4.11 Resonance curves for comparing theoretical calculation results with experimental results

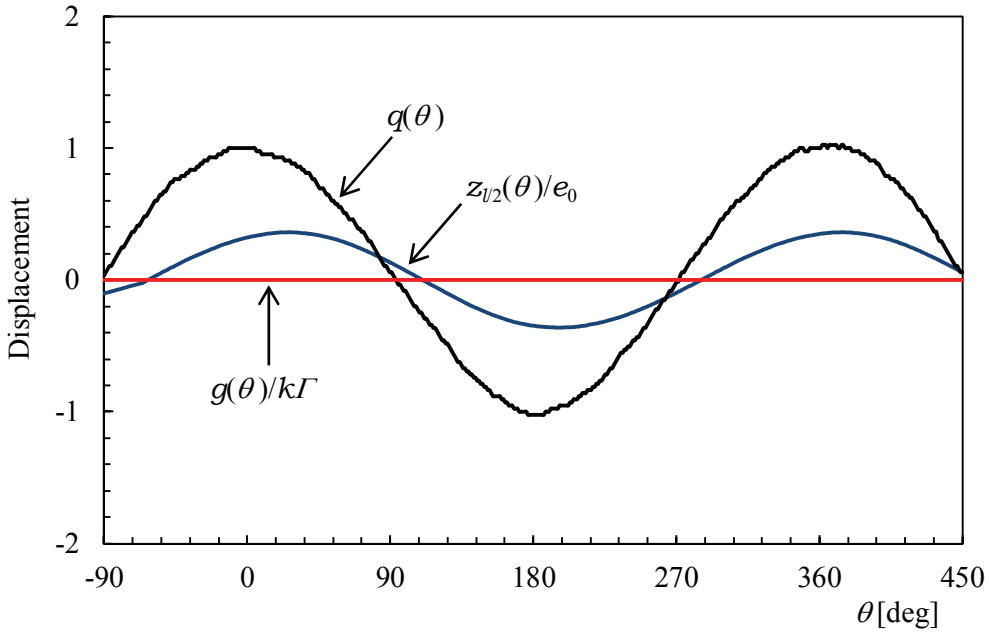

(a) Experimental result

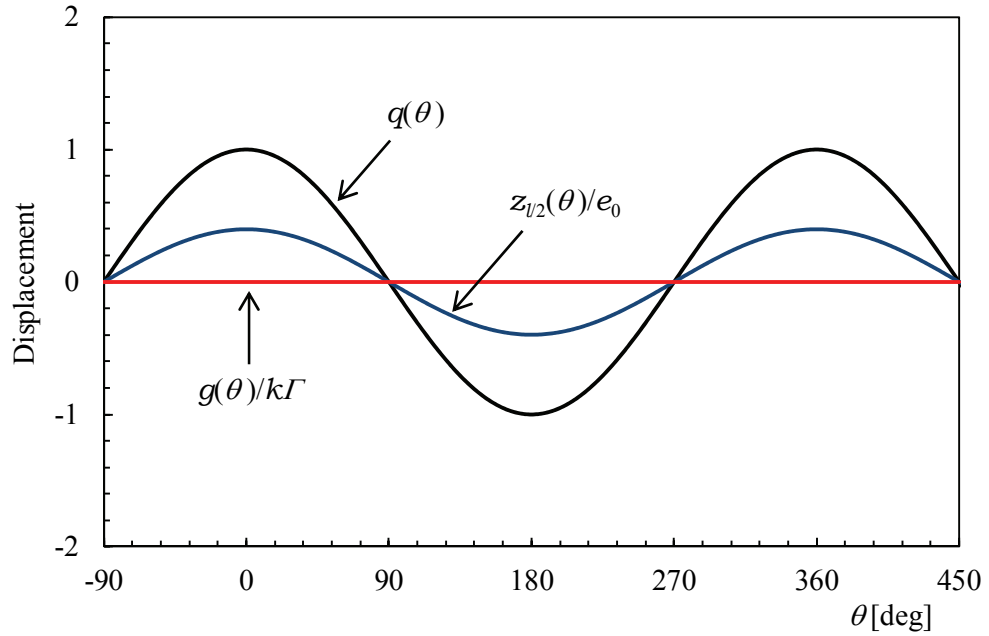

(b) Theoretical calculation result

Figure 4.12 The comparison of experimental result with theoretical calculation result at point A (Ω=1.23) in Figure 4.11

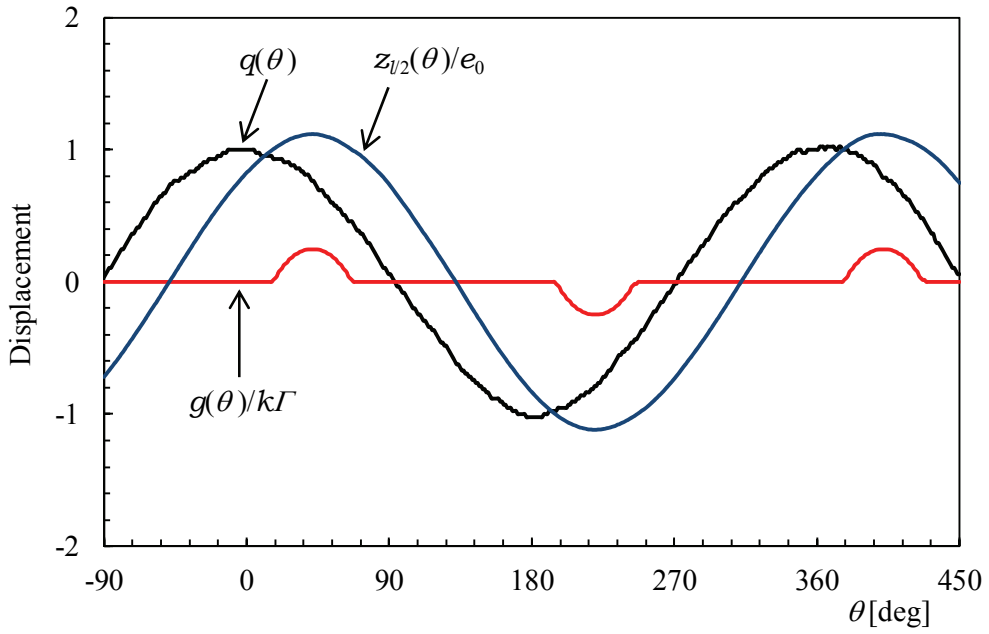

(a) Experimental result

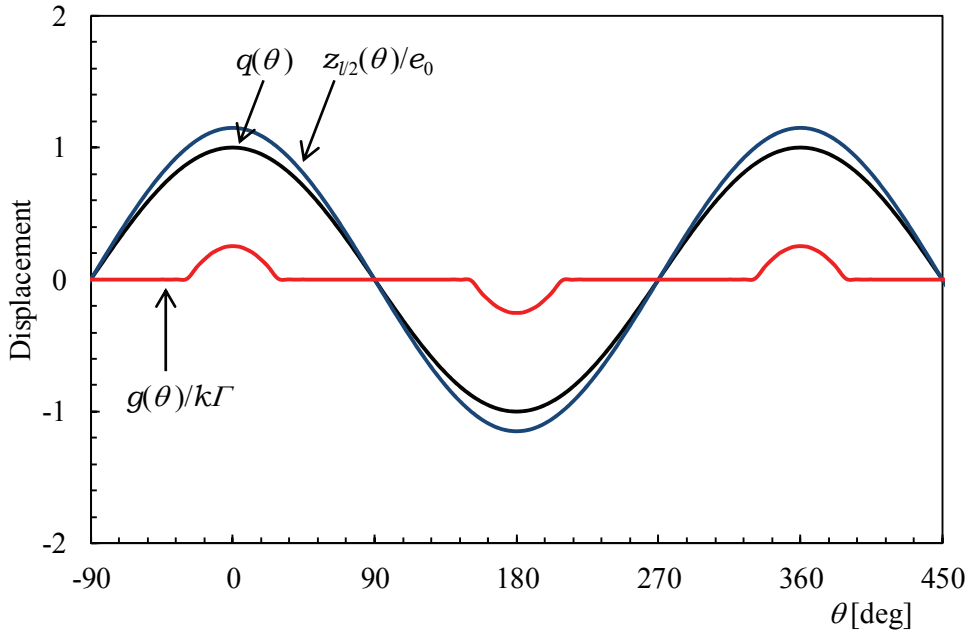

(b) Theoretical calculation result

Figure 4.13 The comparison of experimental result with theoretical calculation result at point B (Ω=1.37) in Figure 4.11

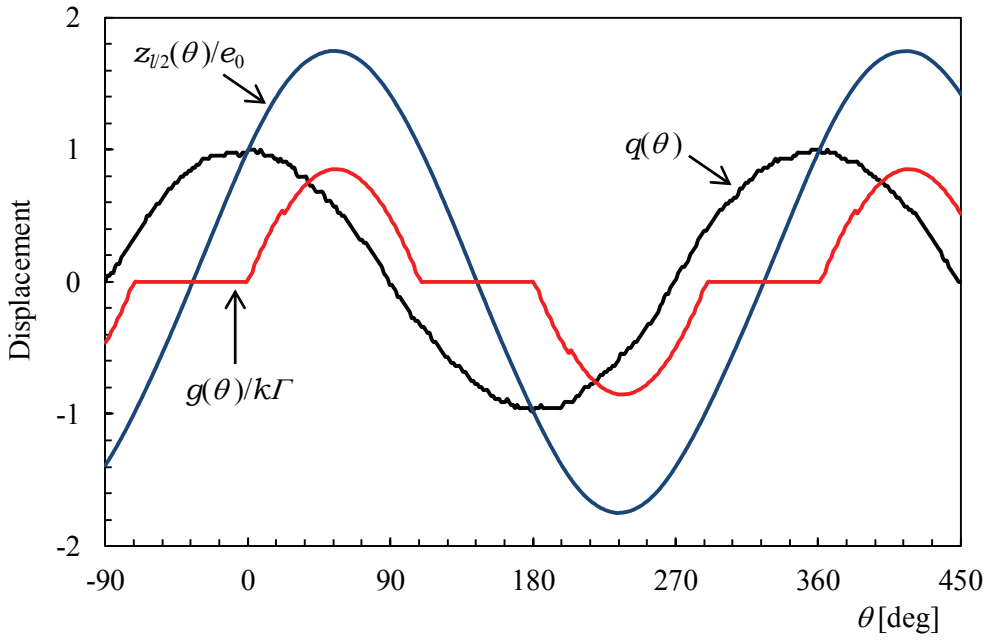

(a) Experimental result

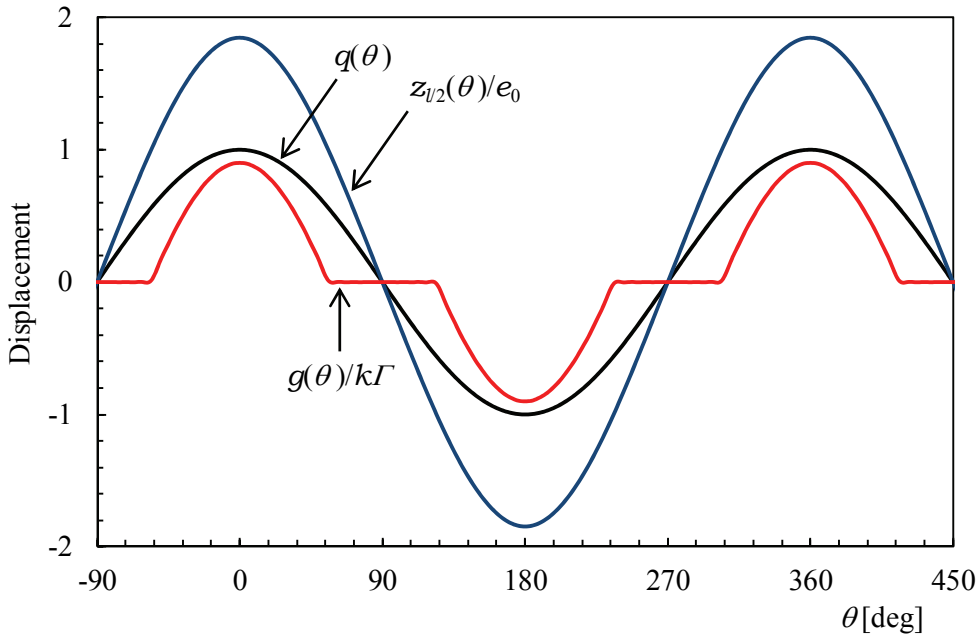

(b) Theoretical calculation result

Figure 4.14 The comparison of experimental result with theoretical calculation result at point C (Ω=1.57) in Figure 4.11

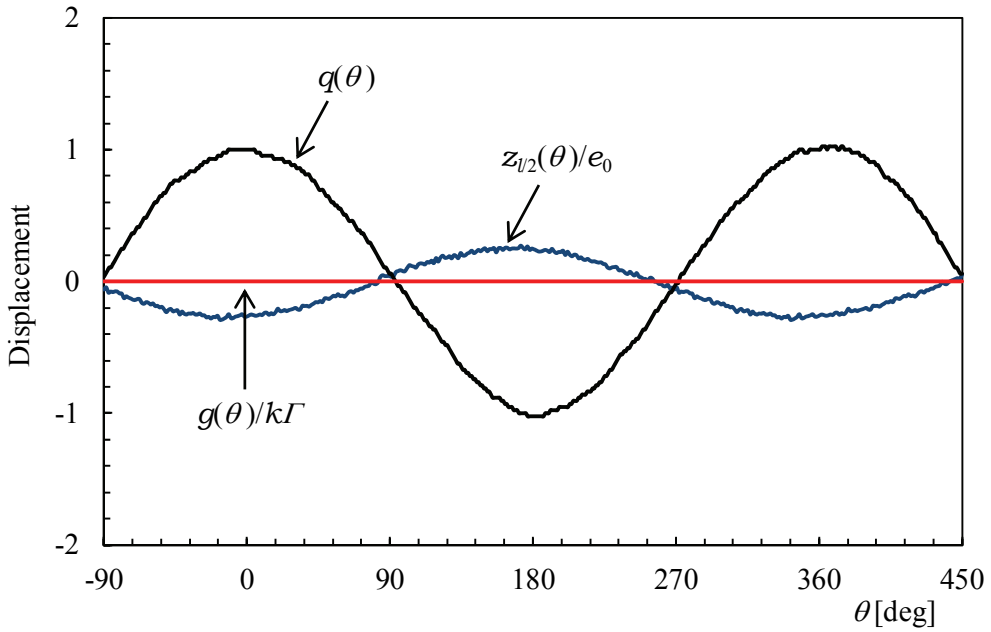

(a) Experimental result

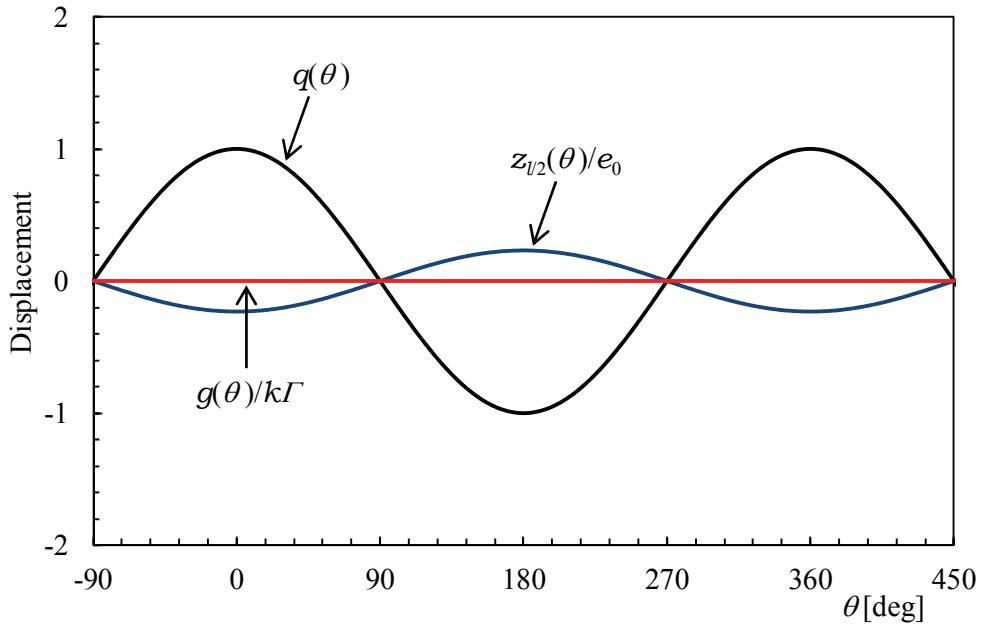

(b) Theoretical calculation result

Figure 4.15 The comparison of experimental result with theoretical calculation result at point D (Ω=1.73) in Figure 4.11

higher values of Ω. This was because damping was not considered in the analytical model, while in the physical model there was damping due to air resistance, internal friction in the material and friction at the beam supports. Conversely, when the frequency was being reduced, there was a corresponding jump in the results in the physical model to the upper curve representing resonance near the value of $\Omega \approx 1.48$.

Figures 4.12-4.15 present comparisons of the experimental results with theoretical calculation ones for the waveforms of the resulting displacement ratio $z(\theta)/e_0$ and the nonlinear part of restoring force $g(\theta)/k\Gamma$ under the excitation $q(\theta)$ at points A, B, C and D on the resonance curve in Figure 4.11. The amplitudes of these predicted values show good agreement between the experimental and theoretical calculation models, but the phase lag of the experimental model waveform was about 60º behind the phase lag of the numerical model $z(\theta)/e_0$, with respect to the excitation $q(\theta)$ in Figures 4.13 and 4.14. This discrepancy was attributed to the effects of damping terms and delay in the action of the restoring force in the supporting spring, which were not accounted for in the theoretical analysis used to develop Equation (4.1).

(2)Using Permanent Magnets (Nonlinear Restoring Force)

Figure 4.16 shows the resonance curve for comparing the theoretical calculation results with experimental results excited by the harmonic excitation [$q(t)=\cos\omega t$] in Figure 4.6(a). The nonlinear restoring force of the experimental model was generated by the permanent magnets. In calculation results, this nonlinear restoring force was approximated by the piecewise linear shown in Figure 4.10. The experimental results (○ symbols) and theoretical calculations agreed reasonably well. In the physical model, jumping phenomena occurred as is the case with using coil springs.

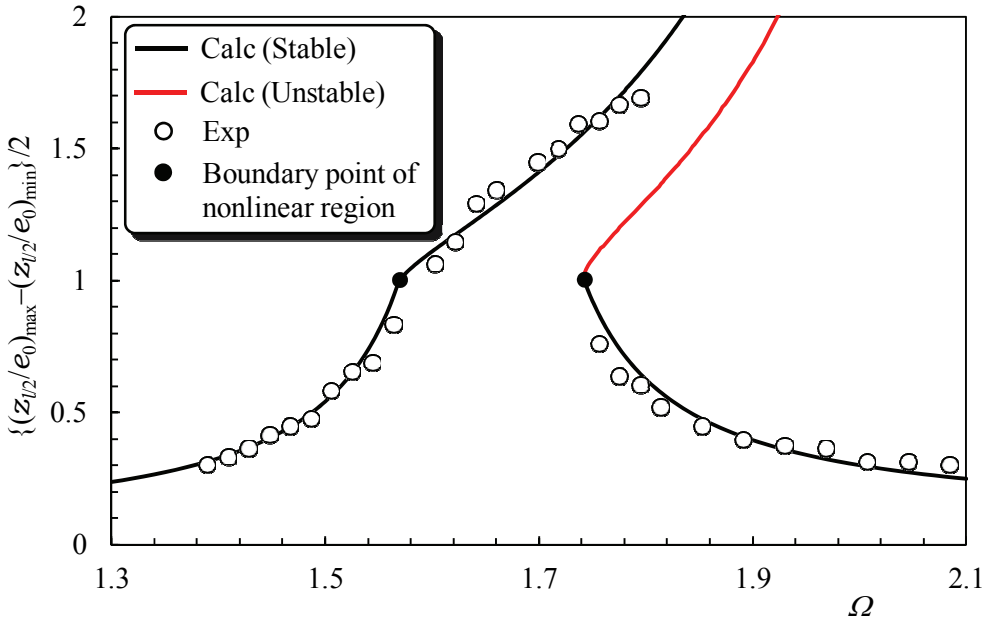

{ $q(t)=\cos\omega t$, $K_1/k=1.75$, $K_2/k=2.1$, $f_1/e_0=0.083$, $\mu=0.49$ }

Figure 4.16 Resonance curves for comparing theoretical calculation results with experimental results

4.3.2 Example of Theoretical Calculations

The steady state periodic solutions were calculated based on the theoretical analysis results in the harmonic resonance region. The calculations were carried out for the combined wave given in Figure 4.6(b), as an example of excitation by a function of arbitrary period. The symbols ● in the figure indicate the boundary between before and after the amplitude of the beam center was sufficiently great for the beam to collide with the support spring whose constant was K_2 (the nonlinear region).

Figure 4.17 shows resonance curves when the spring constant ratio K_2/k is held parameter. The stability analysis was also carried out, and stable branches were distinguished from unstable ones on the resonance curves. Black solid lines represent stable branches and red solid lines represent unstable ones. The spring constant ratio K_2/k expresses the magnitude of the nonlinearity of the supporting spring; when the resonance curve enters the nonlinear region, it bends, and the greater K_2/k is, the more the resonance curve bends to the right.

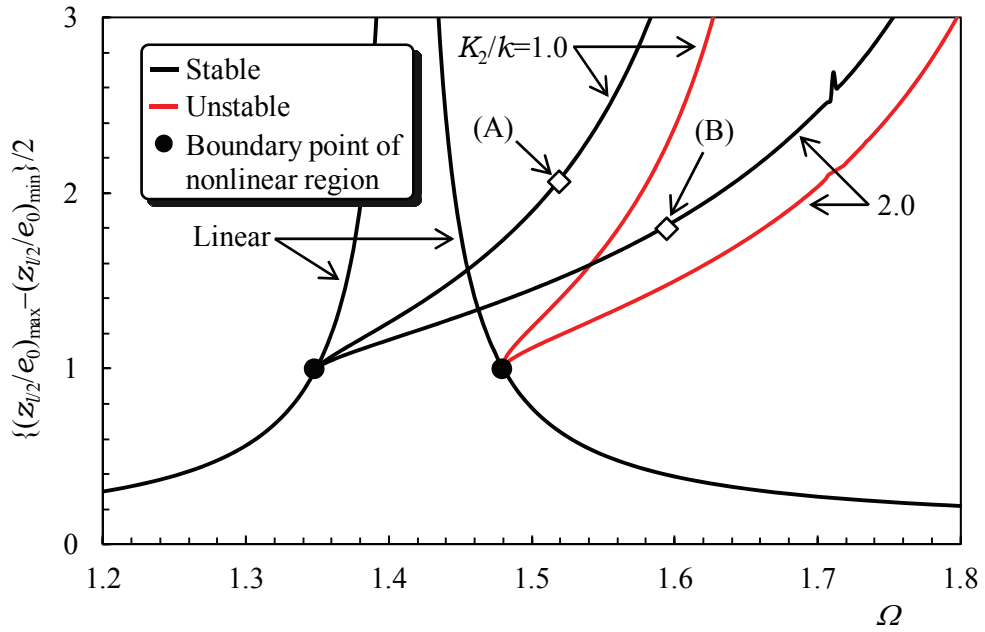

{ $q(t)=\cos\omega t+0.3\sin 3\omega t$, $K_1/k=1.0$, $f_1/e_0=0.1$, $\mu=1.0$ }

Figure 4.17 Resonance curves in the case where nonlinearity K_2/k is parameter

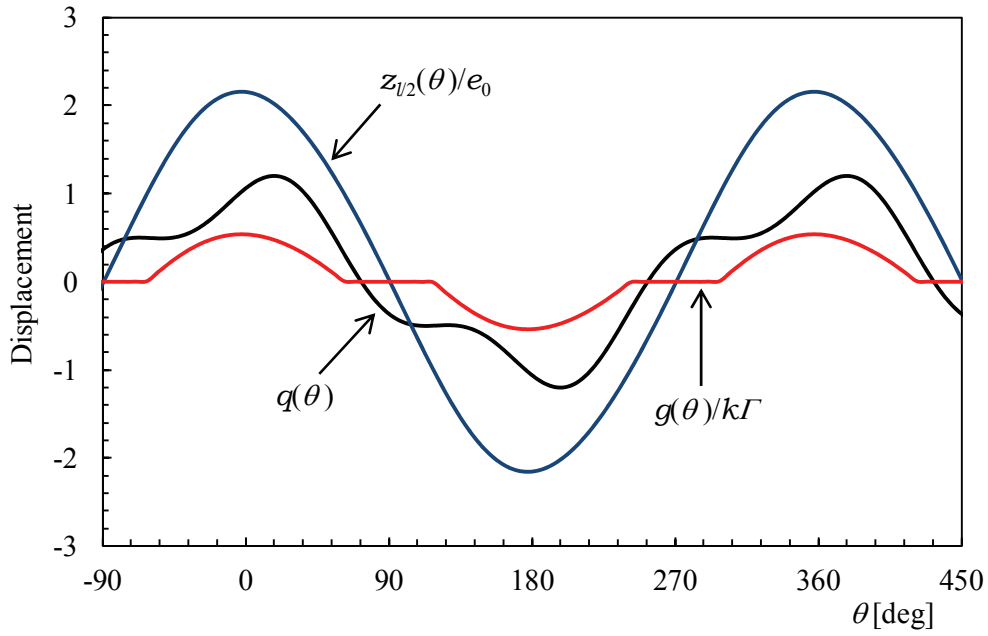

(a) Point A (Ω=1.53)

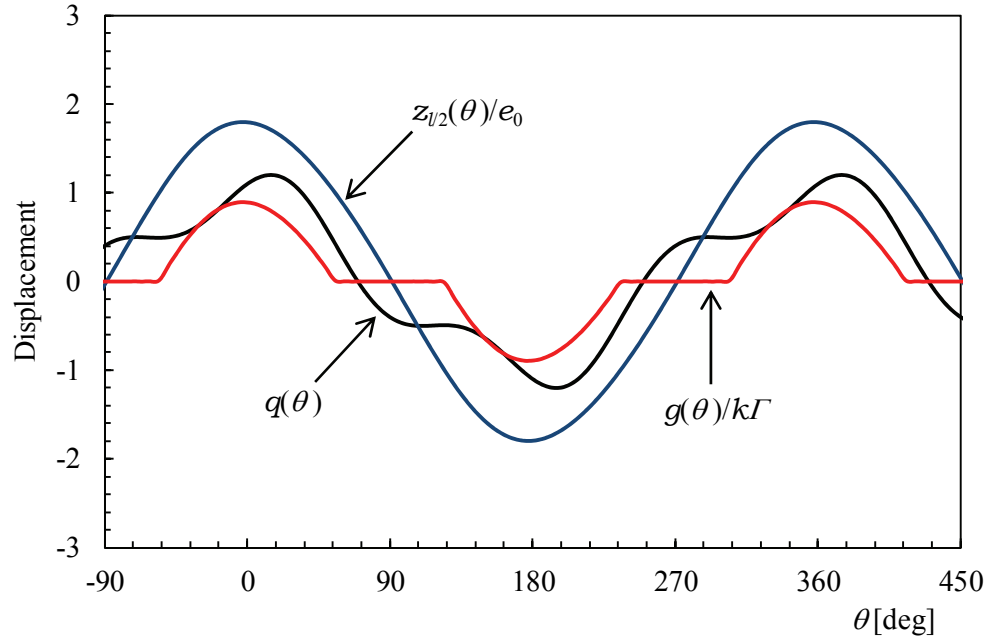

(b) Point B (Ω=1.59)

Figure 4.18 Waveforms of displacement excitation, resulting vibration and nonlinear part of restoring force in Figure 4.18

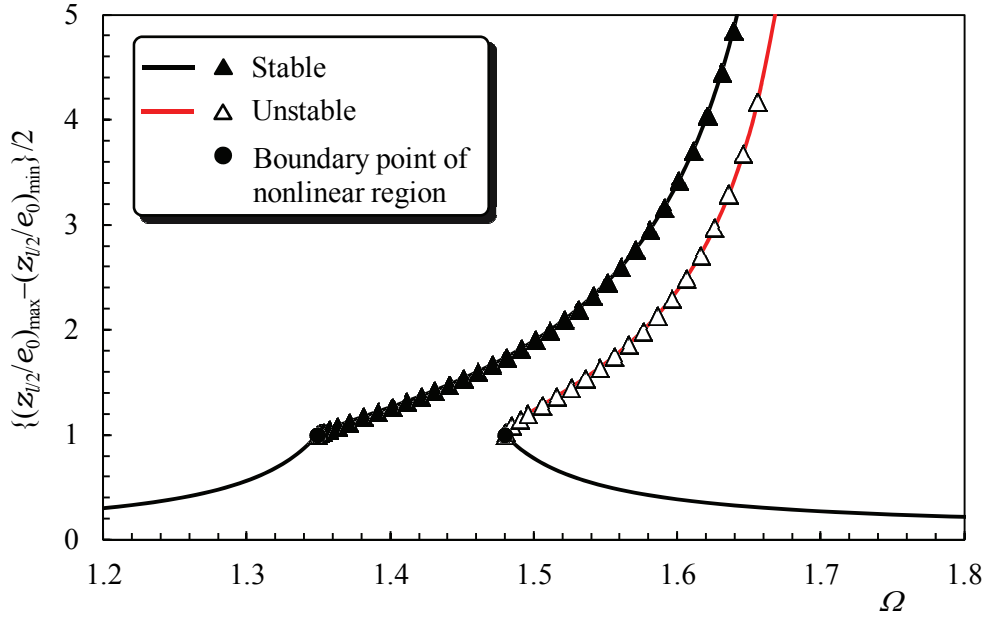

(a) Resonance curve

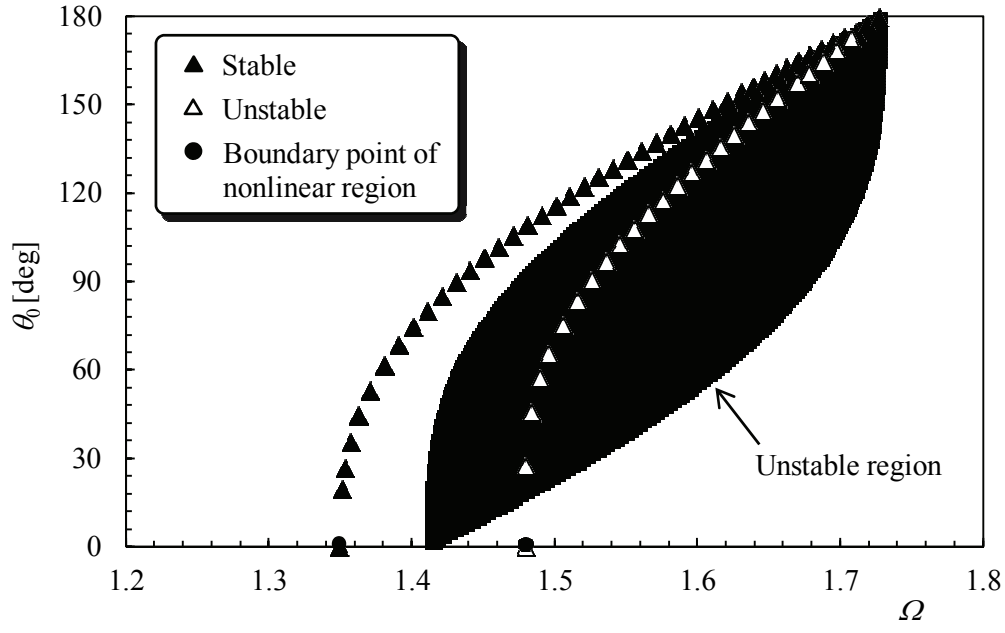

(b) Stability chart

$\{q(t)=\cos\omega t+0.3\sin 3\omega t,\ K_1/k=1.0,\ K_2/k=1.0,\ f_1/e_0=0.1,\ \mu=1.0\}$

Figure 4.19 Resonance curve and stability chart in the case of nonlinearity $K_2/k=1.0$

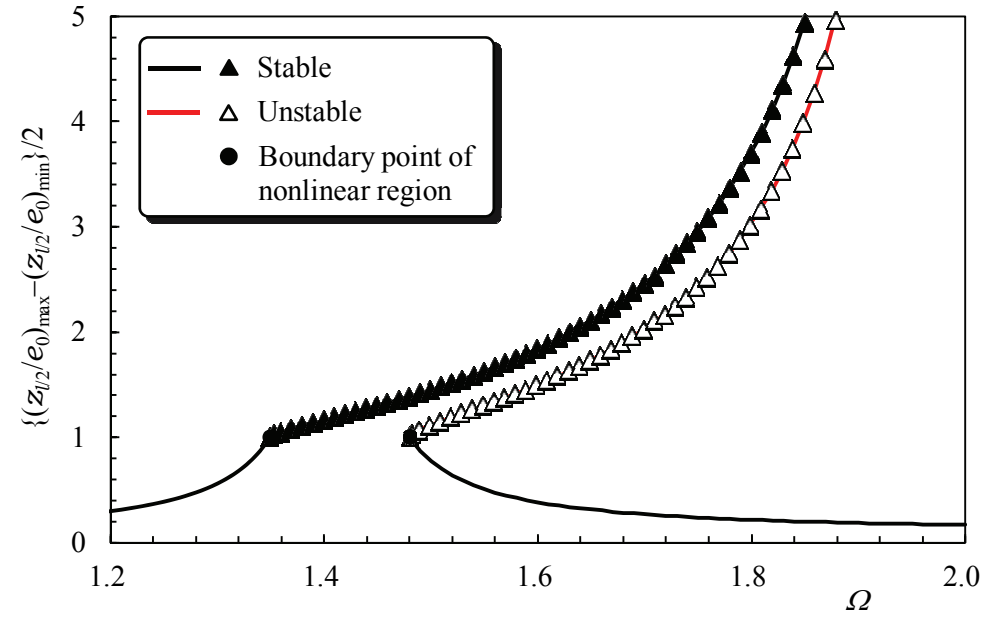

(a) Resonance curve

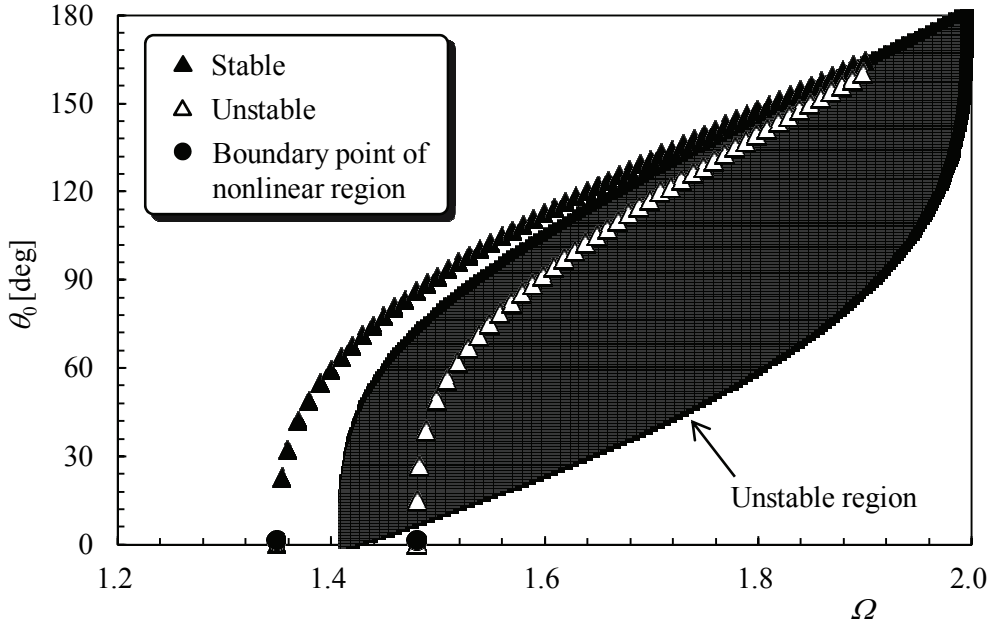

(b) Stability chart

$\{q(t)=\cos\omega t+0.3\sin 3\omega t,\ K_1/k=1.0,\ K_2/k=2.0,\ f_1/e_0=0.1,\ \mu=1.0\}$

Figure 4.20 Resonance curve and stability chart in the case of nonlinearity $K_2/k=2.0$

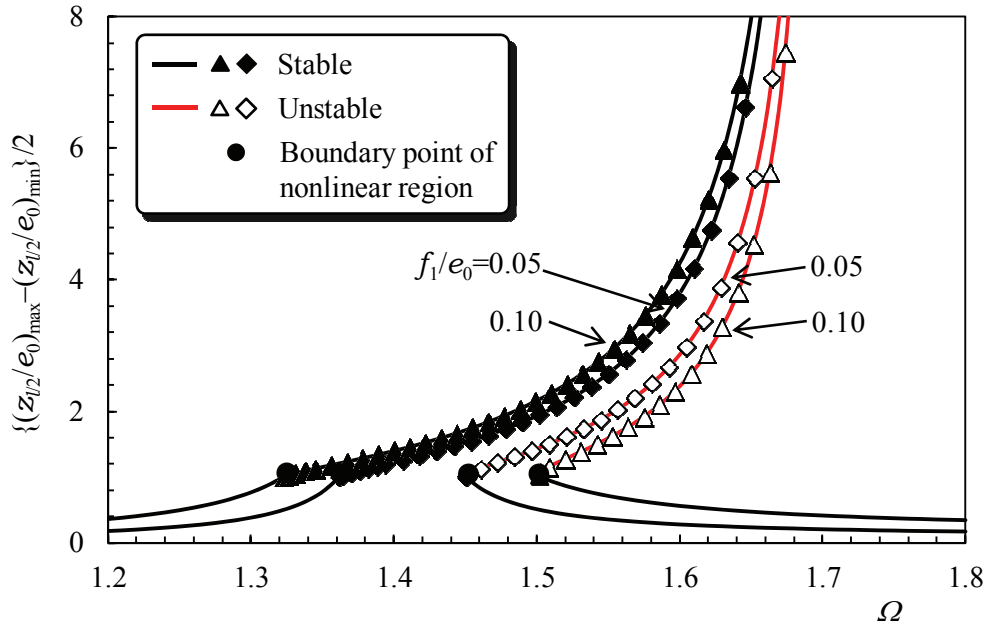

(a) Resonance curves

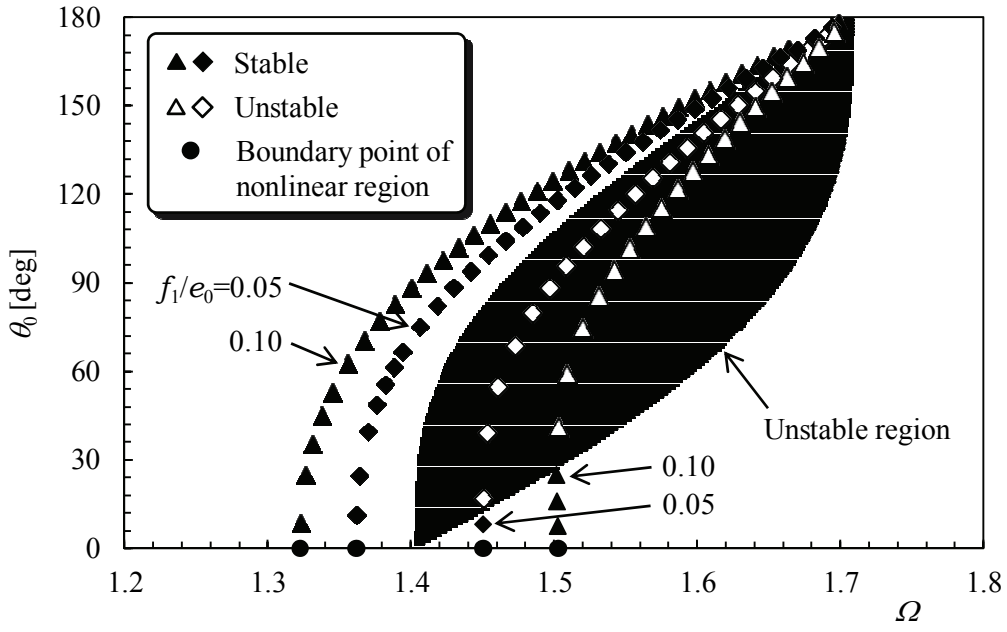

(b) Stability charts

$\{q(t)=\cos\omega t+0.3\sin 3\omega t,\ K_1/k=1.0,\ K_2/k=2.0,\ \mu=0\}$

Figure 4.21 Resonance curves and stability chart in the case where excitation amplitude ratio f_1/e_0 is parameter

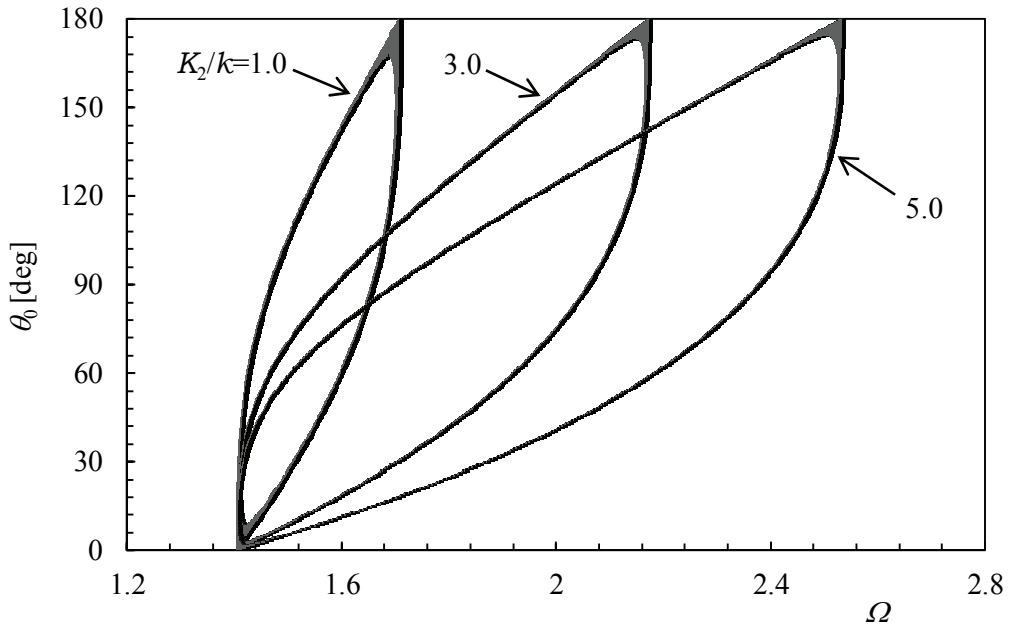

$\{K_1/k=1.0,\ \mu=0\}$

Figure 4.22 Stability chart in the case where nonlinearity K_2/k is parameter

Figures 4.18 presents theoretical calculation results for the waveform of the resulting displacement ratio $z_{l/2}(\theta)/e_0$ and the nonlinear part of restoring force $g(\theta)/k\Gamma$ under the excitation $q(\theta)$ at points A and B on the resonance curve in Figure 4.17. Points A and B lie on the left of the resonance curve, thus resulting vibration is the same phase with respect to the excitation $q(\theta)$.

Figure 4.19(a) shows the resonance curve in the case of nonlinearity $K_2/k=1.0$. Figure 4.19(b) shows the stability chart to distinguish the stable branches from the unstable ones of the resonance curve. This stability chart corresponds to the resonance curve in figure 4.19(a). The "islands" painted by black in the stability chart are unstable regions, while points in the exterior region represent stability. When the restoring force is provided by a hardened spring ($K_2>0$), the insular areas sloped upwards to the right. The displacement of the beam center subjected to exciting vibration exceeds to clearance, it is showed resonance curve tilts to the right towards. The symbols (▲, △) are common in Figures 4.19(a) and (b), and the symbol ▲ means stable periodic solution, the symbol △ means unstable one. All of the periodic solutions on the left

side of the resonance curve exist outside of the “island” area in the stability chart, and periodic solutions are all stable. Most of the periodic solutions on the right side of the resonance curve exist inside of the “island” area in the stability chart. While, not all periodic solutions are unstable, but a few periodic solutions are stable on the right side of the resonance curve at $\Omega \fallingdotseq 1.48$.

Figure 4.20(a) shows the resonance curve in the case of nonlinearity $K_2/k=2.0$. Figure 4.20 (b) shows the stability chart corresponding to the resonance curve. The resonance curve is more rightward compared with Figure 4.19(a). In Figure 4.20(b), stability region at $\Omega \fallingdotseq 1.48$ is smaller than Figure 4.19(b). Because the nonlinearity is large, unstable region expands and more tilts to rightward.

Figure 4.21(a) shows resonance curves in which the excitation amplitude ratio f_1/e_0 has been parameterized. Figure 4.21(b) shows the stability chart corresponding to the resonance curves. The symbols (◆, ◇) indicate the theoretical calculation results in the case of excitation amplitude ratio $f_1/e_0=0.05$, and the symbols (▲, △) indicate ones in the case of $f_1/e_0=0.1$. The symbols (◆, ▲) means stable periodic solutions and the symbols (◇, △) means unstable ones. The greater f_1/e_0 is, the wider the extent of the resonance region, and periodic solutions back away from unstable region. Therefore, stable periodic solutions increase on the right side of the resonance curve.

Figure 4.22 shows the stability charts in which the nonlinearity K_2/k has been parameterized. The greater nonlinearity K_2/k, unstable region expands and "island" tilts to rightward.

4.4 Summary

This chapter investigated the stability of a periodic solution for a simply-supported-beam as an example of distributed parameter systems connected to a nonlinear spring replaced with a model of a symmetric piecewise linear system. The following results were obtained:

(1) An analytical model was constructed of a simply-supported-beam as an example of distributed parameter systems connected to a nonlinear spring at the midpoint of the beam span. This nonlinear restoring force was approximated by a symmetrical piecewise linear system in lateral bending. The Fourier series method was applied to the steady state forced vibration under an excitation having an arbitrary period and a theoretical solution was derived for the resulting vibration.

(2) The stability of the steady state periodic solutions was investigated by a variational equation. An analytical procedure for examining the effects of minute perturbations on the steady state solution of the equation of motion in modal coordinate was proposed, based on incorporating a variational equation. The stability criterion for periodic solutions in harmonic resonance was derived.

(3) Theoretical calculations were performed based on the results of the analysis in (1). The resonance curves were created using the parameters K_2/k (spring constant ratio) and f_1/e_0 (excitation amplitude ratio) and the effects of several factors on the output characteristics were revealed. The waveform of the resulting vibration in the periodic solution and the nonlinear portion of the restoring force were found.

(4) Stability analysis carried out based on the results of the analysis in (2), and the stability charts were constructed. These charts were applied for the resonance curves, and stable branches were distinguished from unstable ones.

(5) Experiments were performed to check the analytical results for the resonance curve and the waveform of the resulting vibration, the nonlinear portion of the restoring force. And the calculated results were shown to agree well with the experimental ones. This analytical method was confirmed to be effective.

(6) This is a general method for handling excitations with arbitrary periods. It was also shown that, once this analytical method has been established, it is possible to find a solution and distinguish stable solutions from unstable ones, regardless of the magnitude of the parameters.

Chapter 5
Conclusions

5.1 Summary

This thesis was aimed at clarifying resonance phenomena theoretically for piecewise linear systems subjected to periodic excitation. The primary results of this study can be summarized as follows.

In chapter 1, the objectives and background for the thesis were described and its composition was shown.

In chapter 2, as an example of lumped parameter systems, the response vibration in a single-degree-of-freedom mass-spring-damper system with an asymmetrical piecewise linear restoring force and excited by a periodic displacement using arbitrary functions was analyzed. In order to clarify harmonic, superharmonic, and subharmonic resonances for the piecewise linear system, the resulting vibrations were analyzed by the Fourier series method. In this analysis, the waveform of the restoring force was not limited to being symmetric around the maximum point through the introduction of two parameters for every instance of collision, and exact solutions were derived. Analysis of the stability criterion was also performed for periodic solutions using a variational equation in order to investigate the consequences of a minute perturbation on the steady state vibration predicted by a periodic solution for the original equation of motion. The steady state periodic solutions were calculated based on the results of a theoretical analysis, and the resonance curves and stability charts were constructed. The calculation results showed the effects of the damping ratio, the stiffness of clamped spring, clearance, and the amplitude of forced vibration on the resonance curves. An experiment and a numerical simulation using the fourth-order Runge–Kutta method were also performed to verify the results of the theoretical analysis. Comparing the theoretical results with the experimental and numerical simulation ones, these were shown that they showed a fairly good agreement.

In chapter 3, as an example of distributed parameter systems, the response vibration in an Euler–Bernoulli beam with a symmetrical piecewise linear restoring force excited by periodic displacement with arbitrary functions was analyzed. In this model, the position on the beam that was subjected to the symmetrical piecewise linear restring force can be arbitrarily chosen. In

other words, the case of two springs clamped symmetrically at an arbitrary distance above and below the beam and at an arbitrary position along the beam was analyzed. In order to clarify the main resonance of the system, the resulting vibration was analyzed by using the Fourier series method, and a theoretical solution was derived. Calculations were performed based on the theoretical analysis and resonance curves were constructed. The calculation results showed the effects of the stiffness of the clamped spring, collision position, clearance, and the amplitude of forced vibration on the resonance curves. An experiments was also carried out to verify the results of the theoretical analysis. The experimental results were in good agreement with the theoretical predictions.

In chapter 4, a stability analysis method was proposed for the periodic steady state solution in an Euler–Bernoulli beam with a symmetrical piecewise linear restoring force excited by a periodic displacement using arbitrary functions. The proposed method employed a variational equation to investigate the consequences of a minute perturbation on the steady state vibration in modal coordinates. These perturbations were added by a periodic solution for the modal equation of motion. Conditional equations for the stability criterion for a periodic steady state solution were shown. Calculations were performed on the basis of the theoretical results, and stability charts were constructed. These charts were then used to examine resonance curves given by the theoretical analysis results, and the stable periodic solutions were distinguished from the unstable ones. Experiments were also carried out to verify the theoretical analysis results. Comparing the theoretical results with the experimental ones, it was shown that they showed a fairly good agreement.

As mentioned above, this thesis clarified resonance phenomena theoretically for lumped and distributed parameter systems having a piecewise linear restoring force subjected to periodic excitation. The Fourier series method was applied to obtain a theoretical solution for the resulting vibration with no limitations on the exciting forced vibration. Furthermore, the steady state periodic solutions were calculated based on the results of theoretical analysis, and resonance curves were calculated using several design parameters. As a result, the effects of each of these parameters on the resonance were numerically shown.

5.2 Recommendations for Future Research

In this thesis, it was shown that the Fourier series method is effective for piecewise linear systems, and resonance phenomena for lumped and distributed parameter systems having piecewise linear restoring force were clarified. However, in order to establish a design method for a real structure having clearance, clarifying more details of resonance phenomena in distributed parameter systems is needed. Furthermore, the Fourier series method has possibility for applying a transient response vibration. Therefore, it is recommended to investigate a transient response and steady state vibrations for harmonic, superharmic, subharmonic and ultra-subharmonic resonance in distributed parameter systems with structural and external damping by the Fourier series method.

Bibliography

Suzuki, K., Aoki, S. and Ohyama, T., 1987, Dynamic Response Analysis of the Piping System Considering Nonlinear Characteristics of Support : 1st Report, Influence of Gap of Support, *Transactions of the Japan Society of Mechanical Engineers, Series C*, Vol.53, No.490, pp.1141-1146.

The Japan Society of Mechanical Engineers, 1996, *The Machines and Industrial Equipments Damage due to the Southern Hyogo-prefecture Earthquake*, pp.123, Tokyo, Maruzen Co., Ltd.

Kuroda, T. et al., 1980, Experimental Seismic Study on 600MWe CANDU Using Full-Scale Partial Models, *B4 CNS 1st Annual Conference Montreal*.

Kusamoto, D., Yasuda, Y., Watanabe, K., Kimura, H. and Hoshino, A., 2006, Toyota's New Six-Speed Automatic Transaxle U660E for FWD Vehicles, *SAE Technical Paper Series*, 2006-01-0847.

Doyle, G. and Faulkner, L., 1982, Torsional Vibrations in a Mechanical Drive, *SAE Technical Paper Series*, 821029.

Harris, C. M., 1996, *Shock and Vibration Handbook, Fourth Edition*, pp.4.1-4.47, NewYork, McGraw-Hill Co., Inc.

.

Nayrfeh, A. H. and Mook, D. T., 1979, *Nonlinear Oscillations*, NewYork, John Wiley & Sons, Inc.

Yamamoto, T., Yasuda, K. and Nagasaka, I., Ultra-Subharmonic Oscillations in a Nonlinear Vibratory System, *Bulletin of the Japan Society of Mechanical Engineers,* Vol.19, No.138, pp.1442-1447.

The Japan Society of Mechanical Engineers, 2007, *Dynamics of Nonlinear Systems*, pp.23-46, Tokyo, Corona Publishing Co., Ltd.

Urabe, S., 1969, Galerkin's Procedure for Nonlinear Periodic Systems, *Archive for Rational Mechanics and Analysis*, Vol.20, No.2, pp.120-152.

Maezawa, S., 1960, Steady Forced Vibration of Unsymmetrical Piecewise-Linear System (1st Report, Explanation of Analytical Procedure), *Transactions of the Japan Society of Mechanical Engineers,* Vol.26, No.167, pp.884-900.

Kumano, H. and Maezawa, S., 1982, Forced Vibrations in an Unsymmetric Piecewise-Linear System Excited by General Periodic Force Functions (2nd Report, The Analysis up to the 4th Order Superharmonic Resonance by Means of the Method of Convergency Improvement), *Bulletin of the Japan Society of Mechanical Engineers,* Vol.25, No.206, pp.1289-1298.

Choi, Y. S. and Noah, S. T., 1988, Forced Periodic Vibration of Unsymmetric Piecewise-Linear Systems, *Journal of Sound and Vibration*, Vol.121, No.1, pp.117-126.

Wong, C. W., Zhang, W. S. and Lau, S. L., 1991, Periodic Forced Vibration of Unsymmetrical Piecewise-Linear Systems by Incremental Harmonic Balance Method, *Journal of Sound and Vibration*, Vol.149, No.1, pp.91-105.

Aoki, S. and Watanabe, T., 1995, Forced Vibration Analysis of Cantilever Beam with Unsymmetrical Stop, *Transactions of the Japan Society of Mechanical Engineers, Series C*, Vol.61, No.588, pp.3190-3195.

Yoshitake, Y., Sueoka, A., Hiyoshi, M. and Takeuchi, N., 1995, Nonlinear Vibrations of a Two-Degrees-of-Freedom System with Clearance (Harmonic Vibration, Higher-Harmonic Vibration, Chaos and Hyper-Chaos), *Transactions of the Japan*

Society of Mechanical Engineers, Series C, Vol.61, No.591, pp.4123-4130.

Wang, Y., 1995, Dynamics of Unsymmetric Piecewise-Linear/Non-Linear Systems Using Finite Elements in Time, *Journal of Sound and Vibration*, Vol.185, No.1, pp.155-170.

Shintani, M., Miyaki, T., Ohta, H. and Takada, H., 1998, Study on Analytical Model of Nonlinear Vibration with Gap under Random Vibration, *Transactions of the Japan Society of Mechanical Engineers, Series C*, Vol.64, No.620, pp.1141-1147.

Maruyama, S., Kato, T., Nagai, K. and Yamaguchi, T., 2006, Experiments on Chaotic Vibrations of a Cantilevered Beam under Vibroimpact, *Transactions of the Japan Society of Mechanical Engineers, Series C*, Vol.72, No.719, pp.2073-2079.

Sato, J., 1968, *Linear Ordinary Differential Equation (in Japanese)*, p.140, Tokyo, Diamond, Inc.

Maezawa, S., 1969, *Nonlinear Ordinary Differential Equation (in Japanese)*, p.113, Tokyo, Diamond, Inc.

Acknowledgement

I would like to express my sincere gratitude to my supervisor, Professor Takuya YOSHIMURA of the Department of Mechanical Engineering, Tokyo Metropolitan University, for his guidance, patience and support throughout this study.

I would like to thank Professor Masami OKADA of the Department of Mathematics and Information Science, Tokyo Metropolitan University, Associate Professor Toshiki OGUCHI of the Department of Mechanical Engineering, Tokyo Metropolitan University and Professor Keisuke KAMIYA of the Department of Mechanical Engineering, Aichi Institute of Technology, for their suggestions and encouragement that make my research of great achievement.

I would like to thank Professor emeritus Hiroyuki KUMANO of Tokyo Metropolitan University for providing me this precious study opportunity and continuous advice and support. Without him, I would not be a researcher.

I would like to thank my father Hisao and my mother Setsumi for their endless love, understanding, support, encouragement and sacrifice throughout my life.

Finally, I would like to express my deepest gratitude to my wife Yukari. Without your love and support, this work would not have been possible.